MEASURED AND PREDICTED ROTORDYNAMIC COEFFICIENTS AND STATIC PERFORMANCE OF A ROCKER-PIVOT TILT PAD BEARING IN LOAD-ON-PAD AND LOAD-BETWEEN-PAD CONFIGURATIONS

A Thesis

by

CLINT RYAN CARTER

Submitted to the Office of Graduate Studies of
Texas A&M University
in partial fulfillment of the requirements for the degree of

MASTER OF SCIENCE

August 2007

Major Subject: Mechanical Engineering

MEASURED AND PREDICTED ROTORDYNAMIC COEFFICIENTS AND STATIC PERFORMANCE OF A ROCKER-PIVOT TILT PAD BEARING IN LOAD-ON-PAD AND LOAD-BETWEEN-PAD CONFIGURATIONS

A Thesis

by

CLINT RYAN CARTER

Submitted to the Office of Graduate Studies of
Texas A&M University
in partial fulfillment of the requirements for the degree of

MASTER OF SCIENCE

Approved by:

Chair of Committee,	Dara W. Childs
Committee Members,	John Vance
	Stuart Scott
Head of Department,	Dennis O'Neal

August 2007

Major Subject: Mechanical Engineering

ABSTRACT

Measured and Predicted Rotordynamic Coefficients and Static Performance of a Rocker-Pivot Tilt Pad Bearing in Load-On-Pad and Load-Between-Pad Configurations.

(August 2007)

Clint Ryan Carter, B.S., Texas A&M University

Chair of Advisory Committee: Dr. Dara W. Childs

This thesis presents the static and dynamic performance data for a 5 pad tilting pad bearing in both the load-on-pad (LOP) and the load-between-pad (LBP) configurations over a variety of different loads and speeds. The bearing tested was an Orion Advantage with direct lubrication exhibiting these specifications: 5 pads, .282 preload, 60% offset, 57.87° pad arc angle, 101.587 mm (3.9995 in) rotor diameter, .1575 mm (.0062 in) diametrical clearance, 60.325 mm (2.375 in) pad length.

Dynamic tests were performed over a range of frequencies to observe any frequency effects on the dynamic stfffnesses. It was found that under most test conditions the direct real part of the dynamic stiffnesses could be approximated as quadratic functions of the excitation frequency. This frequency dependency is caused by pad inertia, pad flexibility, and fluid inertia. The observed frequency dependency can be accounted for with the addition of an added mass matrix to the conventional [K][C] matrix model to produce a frequency independent [K][C][M] model. This method eliminates the often debated question over whether a stability analysis should be performed at the running speed or at the first natural frequency. Substantially large added mass terms in the loaded direction were found that approached 60 kg. Some conditions for the LBP bearing exhibited unloaded direct mass coefficients that were at or near zero, which would lead to a frequency dependent [K][C] model to be used instead. The whirl frequency ratio was found to be zero at all test conditions.

Static data were also recorded which included pad temperatures, attitude angle, eccentricity, static stiffness and power loss. Some cross coupling in the form of deviation from the loaded axis was evident from the locus plots; however, the cross coupled stiffness coefficients were found to be very small relative to the direct stiffness coefficients.

Both static and dynamic experimental results were compared to theoretical predictions via a bulk flow analysis. Most parameters were modeled well including the static eccentricity ε_o and

dynamic direct stiffness coefficients K_{xx} and K_{yy}, which were slightly over predicted. However, the direct damping coefficients C_{xx} and C_{yy} were significantly over predicted.

ACKNOWLEDGEMENTS

I am heavily indebted to Dr. Childs for his guidance, patience and unending support throughout my undergraduate and graduate studies here at A&M. Unanimous among his students is their admiration and gratitude towards Dr. Childs, as I can think of no other professor I would rather work under.

I sincerely appreciate Dresser-Rand and Orion Corporation for donating the bearing for my research and the TRC for their financial support of the Turbomachinery Laboratory. My thanks also go out to Adnan Al-Ghasem for his immense help during my graduate work. Bader Jughaiman and Eric Hensley also deserve recognition for their efforts to make this research possible. Special thanks are in order for Stephen Phillips, who hired me as a student worker for Dr. Childs and set my career on the path to success. Last but certainly not least, I certainly could not have accomplished so much at the TurboLab without the advice of Eddie Denk and his employees.

TABLE OF CONTENTS

Page

LIST OF FIGURES

Page

Page

Page

Page

Page

LIST OF TABLES

Page

Page

Page

NOMENCLATURE

$\boldsymbol{A_{ij}}$	Fourier transforms for the measured stator acceleration. (e.g. A_{ij} is the acceleration in "j" direction, due to an excitation force in the "i" direction) [L/t^2]
C_{ij}	Direct and cross-coupled damping coefficients [F.t/L]
ΔC_{ij}	Uncertainty of direct and cross-coupled damping coefficients [F.t/L]
C_b	Radial bearing clearance [L]
c_p	Lubricant specific heat [F.L/(M.t)]
D	Bearing diameter [L]
$\boldsymbol{D_{ij}}$	Fourier transforms for the measured stator relative motion [L]
e_x e_y	Bearing equilibrium position in the x and y directions [L]
$\boldsymbol{F_{ij}}$	Fourier transforms for the measured stator force [F]
F_s	Static force applied by pneumatic loader [F]
f_{bx} f_{by}	Bearing reaction force component in the x,y direction respectively [F]
f_{x} f_{y}	Measured excitation force component in the x,y direction [F]
$\boldsymbol{H_{ij}}$	Direct and cross-coupled dynamic stiffnesses [F/L]
$\boldsymbol{j}$	Imaginary unit, $\sqrt{-1}$ [-]
K_{ij}	Direct and cross-coupled stiffness coefficients [F/L]
ΔK_{ij}	Uncertainty of direct and cross-coupled stiffness coefficients [F/L]
L	Pad length [L]
M_s	Mass of the stator [M]
M_{ij}	Direct and cross-coupled added-mass coefficients [M]
ΔM_{ij}	Uncertainty of added-mass coefficients [M]
P	Bearing unit load ($\frac{F_s}{LD}$) [F/L^2]
$\dot{Q}$	Bearing oil supply flow rate [L^3/t]
R	Bearing radius [L]
Re	Reynolds number, $\mathrm{Re} = \frac{\rho C_b R \omega}{\mu}$ [-]
r^2_{ij}	Square of the correlation coefficient [-]
S	Sommerfeld number, $S = \frac{\mu N L D}{W}\left(\frac{R}{C_b}\right)^2$ [-]
T_{in}	Oil inlet temperature [T]
T_{out}	Oil outlet temperature (NDE) [T]
$\ddot{x}_s$ $\ddot{y}_s$	Absolute acceleration of the stator in the x,y direction [L/t^2]
Δx Δy	Relative motion between the rotor and the stator in the x,y directions [L]
ε	Static Eccentricity ratio [-]
ϕ	Attitude angle measured from the $+y$ axis to the $+x$ axis [Angle]

Λ	Square of the excitation frequency, Ω^2 [$(1/t)^2$]
ρ	Lubricant density [M/L^3]
μ	Lubricant viscosity [$F.t/L^2$]
ω	Running speed of rotor [1/t]
Ω	Excitation frequency of stator [1/t]

Subscripts

x,y	*x* and *y* direction (defined in Fig. 9)
i,j	*x,y*

Abbreviations

rpm	Revolutions per minute
DE, NDE	Drive end, non-drive end
TP	Tilting-pad

INTRODUCTION

Tilting pad journal bearings have long been the bearing of choice for high speed turbomachines. The inherent design of the bearing gives it substantial advantages over conventional journal bearings. This design differentiates from a conventional bearing by the fact that it has been divided up into multiple sections that are allowed to move freely and independently from the others. Fig. 1 below shows one such tilt pad bearing that has been divided into four sections which are called pads. One side of the pad is in close contact with the journal where hydrodynamic fluid film lubrication takes place while the opposite side of the pad rotates freely via a pivot which transfers the fluid film forces from the pad to the housing. The pad pivot has several important advantages. Because the pad can pivot, it is forgiving and tolerant to misalignment unlike a conventional bearing. However, perhaps the most important feature is the ability of the pad to rotate to an equilibrium position in which the fluid forces are equal on both sides of the bearing pivot. This means that the equivalent pad fluid film force is transferred directly through the pivots which are all arranged to coincide with the center of journal. All fluid film forces are thereby directed to the journal center, which allows a level of stability not matched by other bearing types. The concentration of forces at the journal center alleviates all cross coupled stiffness effects that are responsible for rotor instabilities. However, all tilt pad journal bearings exhibit a small amount of cross coupled stiffness due to tolerance stack ups and slight misalignment from the manufacturing process.

This thesis follows the style and format of the ASME Journal of Tribology.

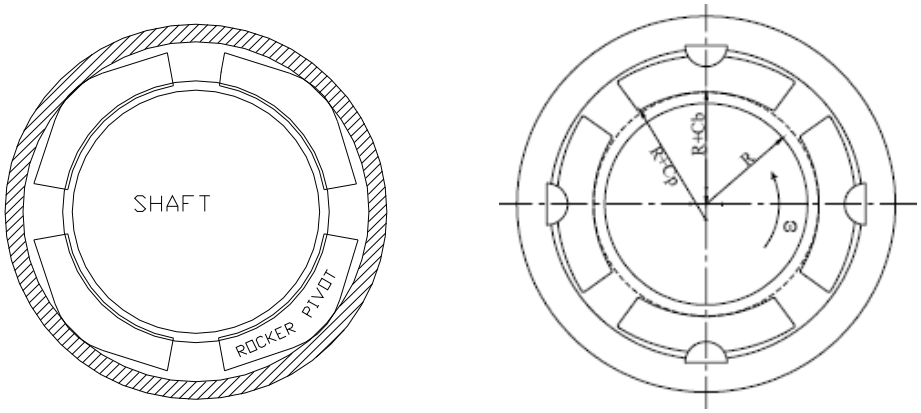

(a) (b)

Fig. 1 Rocker pivot (a) and spherical seat (b) type tilt pad bearing [1, 2]

Tilt pad bearings are also very versatile because they can be tailored to meet a variety of different needs. This versatility comes from the numerous parameters that can be adjusted that are not available with other types of bearings. Fig. 2 (a) below shows a sectional view of the shaft and pivot. This figure shows that the machined radius of the pad is larger than that of the shaft. This is necessary to establish the hydrodynamic wedge effect which provides needed lift and stiffness to the bearing by drawing fluid in between the two surfaces. The amount of stiffness can be changed by altering the radius of the shaft and pivot as well as the clearance. All of these parameters are quantified in a number known as "preload" with the definition given below:

$$\text{Preload} = 1 - \frac{C_b}{C_p}$$

where C_b is the bearing clearance and C_p is the pad clearance and:

$$C_b = R_b - R_s \quad , \quad C_p = R_p - R_s$$

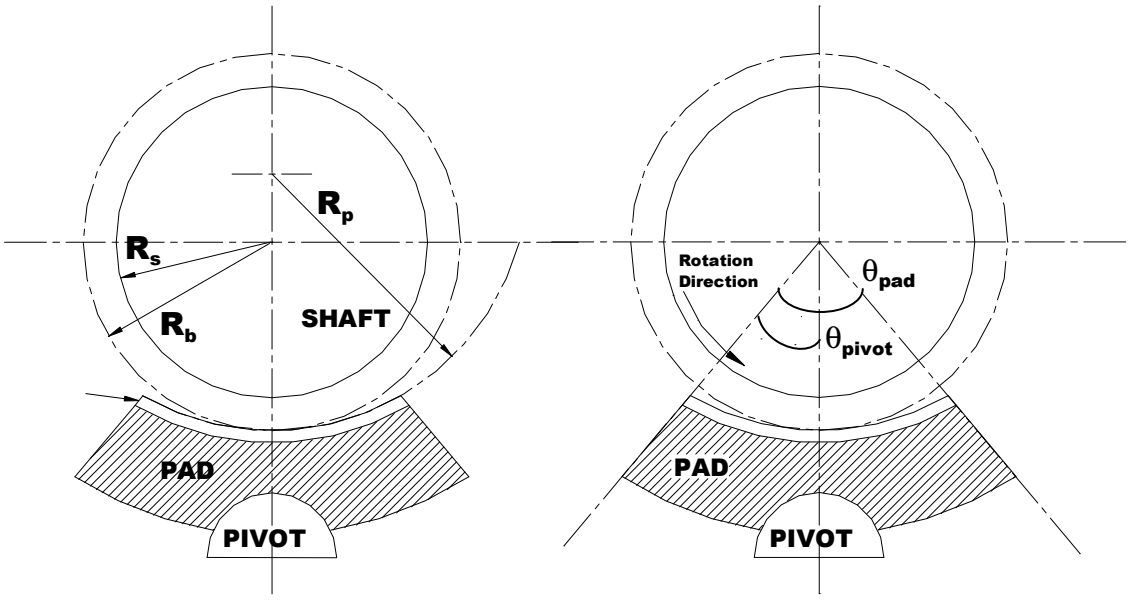

(a) (b)

Fig. 2 Pad preload (a) and offset (b) diagrams [1]

Generally an increase in preload will increase the stiffness of the bearing while decreasing the damping. A positive preload indicates a wedge shaped surface and is used in almost all tilt pad bearings. Of course the clearance can also be adjusted. An increase in bearing clearance will be accompanied by a loss of stiffness but an increase in damping.

Another important adjustment comes from what is referred to as "pad offset" which is displayed in Fig. 2 (b). Offset simply describes where the pivot is located relative to the leading edge of the pad and is defined as:

$$\text{Pivot Offset} = \frac{\theta_{pivot}}{\theta_{pad}}$$

An offset of .5 indicates that the pivot is located in the middle of the pad, equally spaced from the leading and trailing edges of the pad. A .5 or 50% offset is commonly seen since the bearing can perform equally well regardless of the rotor direction of rotation. Bearings with offsets ranging from .5 to .6 are also used to obtain better bearing performance but work best when rotated in one direction only. Work by DeCamillo [3] showed that these bearings will not be

damaged if rotated in the reverse direction, however pad temperatures were shown to rise significantly.

In addition to the methods mentioned above for altering performance the bearing may also be run in either a load-on-pad (LOP) or load-between-pad (LBP) configuration. The LOP setup is commonly used on high speed light rotors where extra stability is required and is accomplished by the stiffness asymmetry of the LOP condition. The LBP setup is more likely to be seen in applications that require the higher load capacity and damping afforded the LBP configuration.
The last major design issue affecting performance comes from the design of the pivot itself. Many different types of pivots exist, some of which are listed in Table 1 taken from Kirk and Reedy [4].

Table 1 Common Pivot Types for Tilting Pad Bearings [4]

Type	Description	Type of contact for light load (heavy load)
A	Sphere on a flat plate	Point (circular)
B	Sphere in a sphere	Point (circular)
C	Sphere in a cylinder	Point (noncircular)
D	Cylinder in a cylinder	Line (rectangle)
E	General curvature	Point (noncircular)

Kirk and Reedy performed research into what effect the stiffness and damping of the pivot had on the effective damping of the bearing. They found that some pivot designs had fairly low structural stiffness which, when coupled in series with the fluid film stiffness, lowered the overall stiffness of the bearing substantially. The conclusion from his study was that pivot stiffness can play a large role in the performance of the bearing.

A major concern for bearing designers of turbomachines is finding the appropriate stiffness and damping coefficients for each bearing to accurately model the entire rotordynamic system. The fluid film will in effect be approximated by a series of springs and dampers. Fig. 3 below shows a journal bearing modeled with the 8 reduced stiffness and damping coefficients identified by Barret [5].

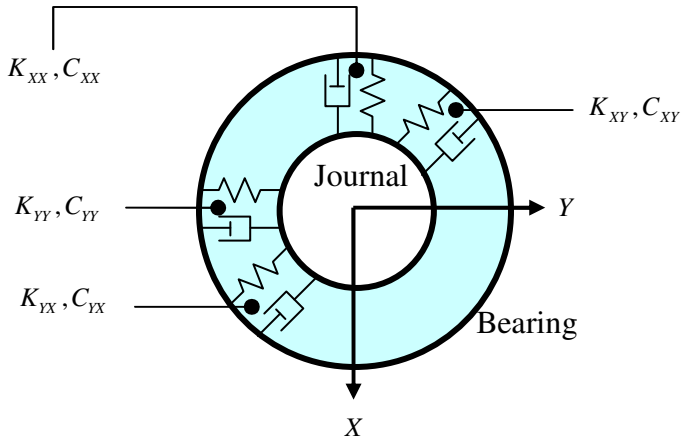

Fig. 3 Spring and damper equivalent of bearing fluid film [6]

The design of this test bearing is unique in that it uses a special wedge shaped leading edge on the pads that has a groove for the application of cool lubricant. This design was pioneered by Ball and Byrne [7] for Orion Corporation and is shown in Fig. 4. The wedge shape of the leading edge is called a "flow director" and has the purpose of wiping and redirecting hot carryover oil away from the cool oil injected into the leading edge via the "leading edge groove". Also called the "Advantage", this pad should run cooler than other designs by avoiding mixing of the hot and cool oil, leading to improved stiffness and damping due to the higher viscosity of the cooler lubricating oil. However, given that the oil inlet groove is located on the leading edge of the pad, these bearings should not be run in the reverse rotation direction.

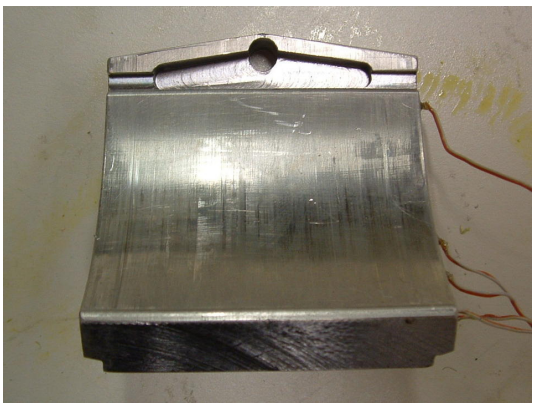

Fig. 4 Orion leading edge groove pad

LITERATURE REVIEW

The first major publication addressing the issue of stiffness and damping coefficients was published by Lund [8] in his ground breaking 1964 paper, *Spring and Damping Coefficients for the Tilting Pad Journal Bearing*. In this paper Lund calculates the stiffness and damping of a single fixed non rotational pad and then sums the contributions from each pad to find the combined effect of the pad assembly. Likewise, this procedure is now referred to as "Lund's Pad Assembly Method". As a result, Lund was able to plot stiffness and damping design curves that had no cross coupling effects once pad inertia was neglected. This was significant because it showed for the first time the stability advantages that were inherent in the design of tilt pad bearings.

Lund's design curves do not take into account frequency dependency and for many years the common assumption was that the coefficients should be calculated at the synchronous frequency. This assumption was used by many researchers and designers including Shapiro and Colsher [9] and Nicholas [10]. However after Nicholas [10] published a work in which he assumed that the vibrating frequency of the tilt pads were synchronous Lund stated that it was mathematically incorrect to use a synchronous frequency in a stability calculation and that the damped natural frequency should instead be used [11]. This controversy led to a new string of research into answering the question of what frequency should be used when performing stability analyses.

Several studies have been performed in the investigation of the frequency dependency of the rotordynamic coefficients of tilt pad bearings. Parsell et al. [12] first explored the concept of frequency dependency with a theoretical analysis of a 5 pad tilt pad bearing in both the load-on and load-between pad configurations. They derived a set of equations that produced reduced tilt-pad dynamic coefficients in terms of the entire set of dynamic coefficients. They set out to answer the question of whether or not synchronously derived coefficients were sufficient for a stability analysis or if frequency dependency would have to be accounted for. Their results showed that for a zero preloaded bearing the stiffness coefficients dropped greatly with increasing frequency and that the damping coefficients would rise from being negative and become more positive with increased excitation. The effect was reduced with preloaded bearings, but even so his work set the stage for experimental work to verify his findings.

One of the first experimental investigations of the phenomenon was conducted by Ha and Yang [13]. They performed experiments on a 5 pad tilt pad bearing with a 300mm journal in the load-on pad configuration. Tests were conducted at speeds ranging from 1.2 to 3.6 krpm and under two load conditions of 5 and 10 kN. The bearing was excited at frequencies that varied from .6 to .9 times running speed to observe the effects of frequency on the bearing coefficients. They found a slight decrease in the stiffness coefficients as well as a slight increase in the damping coefficients with increasing frequency. The results were limited by the low speeds, loads and amplitudes of shaking available for testing but were significant because they gave the first real indication of frequency dependency and gave evidence for the work of Parsell.

Ikeda et al. [14] performed tests of a large 580mm (20.8in) diameter 4 pad tilt pad bearing in the LBP configuration. Aside from its larger size the bearing design was similar to the one tested in this thesis, both being made by Orion Corp and having the same wedge shaped leading edge groove to facilitate direct lubrication. The bearing was modified however to have a Rayleigh step machined into the unloaded pads to preload them and reduce vibration. Synchronous excitation testing was done to obtain stiffness and damping coefficients. In their results they found that the direct stiffness coefficients increased linearly with Sommerfeld number but that the stiffnesses were over predicted by their bearing code based upon Reynolds equation. The damping coefficients remained almost constant regardless of loading or speed condition which contrasted greatly with the predicted damping, which grew linearly with increasing Sommerfeld number.

Two recent investigations into the frequency dependency of rotordynamic coefficients have been undertaken by Al-Ghasem [1] and Rodriguez and Childs [15] at the Texas A&M Turbolab. Al-Ghasem tested a 116.8 mm (4.6 inch) pad flex pad bearing in the load-between pad configuration to obtain rotordynamic coefficients and observe frequency effects. The bearing was tested for a range of speeds from 4-12krpm with excitation up to 300 Hz. In his results he found direct real dynamic stiffness coefficients that were highly dependent upon the frequency of excitation. These stiffnesses decreased rapidly with increasing frequency. Similar results were seen in his theoretical bulk flow analysis of the bearing using XLTRC^2 which also predicted large frequency dependent stiffnesses. He attributed this predicted frequency dependency to the reduction in degrees of freedom from two degrees of freedom per pad to just two for the entire assembly. To address the issue of the frequency dependent stiffnesses, Al-Ghasem introduced a mass term that produced frequency independent coefficients. This mass

term was quite significant at 32 kg, which could have implications for the critical speeds of light rotors.

Rodriguez and Childs [15] also performed tests on the same bearing but in a load-on-pad condition. Similar frequency dependent stiffnesses were found and accounted for with frequency independent mass terms which approached 40 kg. Both a bulk-flow and Reynolds equation analysis was performed. The bulk flow was found to be more capable of predicting the frequency dependent stiffnesses after the 1x frequency (running speed) due to its ability to account for inertial affects that cause a decrease in the dynamic stiffnesses with frequency. Up to running speed however there was little difference between the analysis methods. While the predictions modeled the experimental stiffnesses well up to running speed, further increases in frequency led to an over prediction of the dynamic stiffnesses.

In 2001 Wygant [16] performed experimental testing on a five pad tilt pad bearing with a L/D ratio of .75, journal diameter of 70 mm, a clearance of 113 μm, and a 50% offset. In his research he varied the pad preload, pad pivot mechanism, and excitation frequency in both the LOP and LBP configurations to find the effect of each on the bearing performance. The preload was varied from -.333 to +.5 with results showing that increasing the amount of positive preload led to increases in stiffness and decreases in the dynamic damping coefficients. Both rocker-back and spherical seat pad pivots were also examined, with the spherical seat pivots showing considerable cross coupling effects while the rocker-back pads displayed no statistically significant cross coupled stiffness coefficients. Lastly, Wygant examined the effect of variable frequency excitation on the stiffness and damping coefficients. Generally he found the direct stiffness coefficients to decrease with increasing frequency and the direct damping coefficients were found to increase. However, the test bearing was excited at only 3 frequencies, .5x, 1x, and 2x as opposed to the 25 frequencies available with the test rig of Rodriguez and Childs. Wygant also tested the bearing at loads (approximately 690 kPa (100 psi) max) and speeds (2250 rpm max) which were much lower than common practice for a bearing of its size.

Dmochowski [17] conducted variable excitation (20-300Hz) testing of a 99mm five pad tilt pad bearing in a load-between pad configuration under moderate loads. He found that the stiffnesses decreased with excitation but found no change in the damping coefficients with frequency. Dmochowski also ran a theoretical computer code to verify his experimental results. His code, based on Lund's assembly method, took into account thermoelastic deformation, frequency effects, and pad pivot stiffness and damping using pivot equations from Kirk and

Reedy [4]. The code was able to model the experimental results with good agreement. On the other hand a similar but lightly loaded bearing was modeled in his code which surprisingly predicted a slight increase in bearing stiffness and a large drop in damping with excitation frequency.

The concept of frequency dependent coefficients is not limited to tilt-pad or flex-pad journal bearings. Many other bearing and seal types, with both gas and fluid film lubrication exhibit this phenomenon. Al-Jughaiman [18] tested a 117.1 mm diameter pressure dam bearing which showed a large decrease in stiffness coefficients with increasing excitation frequency. Graviss [19] found significant frequency dependency in a set of grooved annular oil seals and Childs [20] tested an low stiffness annular honeycomb gas seal that showed a loss of stiffness at higher frequencies. Reinhardt and Lund [21] showed that Reynolds numbers as small as 10^2 can lead to significant inertial effects even though the flow is still entirely laminar. The subsequent added mass can cause significant errors when estimating critical speeds on short, light weight rotors.

There is a wealth of information on the static performance of tilting pad bearings, which include pad temperatures, locus plots, and power loss among others. Pad temperatures for various tilting pad bearings have been examined by Edney and Mellinger [22] In their tests, several flooded and direct lube tilt pad bearings were run in a steam turbine while thermocouples imbedded in the pads recorded temperature data vs. speed. They noticed that as speed increased so did the pad temperatures. However once shaft speeds approached 12 to 14 krpm they saw the pad temperatures abruptly decrease unexpectedly while the power loss greatly increased. They concluded that this phenomenon was caused by a transition in the fluid film from laminar to turbulent flow which causes an increase in the heat transfer from the pads to the cooler oil surrounding the pads.

TEST RIG DESCRIPTION

Testing Apparatus

The testing apparatus shown below in Fig. 5 was designed by Kaul [23] and implemented by Kaul and Culotta [24] Detailed information regarding the design of this test rig can be found in Kaul [23]. Originally designed to test oil seals this test rig has been readily adapted to test a variety of components including pressure dam, tilt pad and flex pad bearings.

The rig is constructed so that the bearing or seal is placed at the center of the rotor which is supported on both ends by hybrid ceramic ball bearings that are lubricated with a mist lube system. The bearing or seal is supported in a housing that is attached to the steel pedestals via "pitch stabilizers". The pitch stabilizers consist of 6 steel turnbuckles that are spaced at 120 degree intervals on the housing. They allow the bearing housing to move freely in the radial direction yet prevent pitch and yaw rotations and axial movement. Power is delivered to the rotor via a 65 KW (90HP) air turbine and flexible coupling. Speed can be varied from 0 to 16000 rpm. ISO VG 32 oil is supplied to the test bearing housing via a gear pump in varying quantities up to 90 liter/min. Air buffer seals are located on the inner portion of the pedestals and are used to separate the test exit oil from the mist lube inside the ball-bearing pedestals.

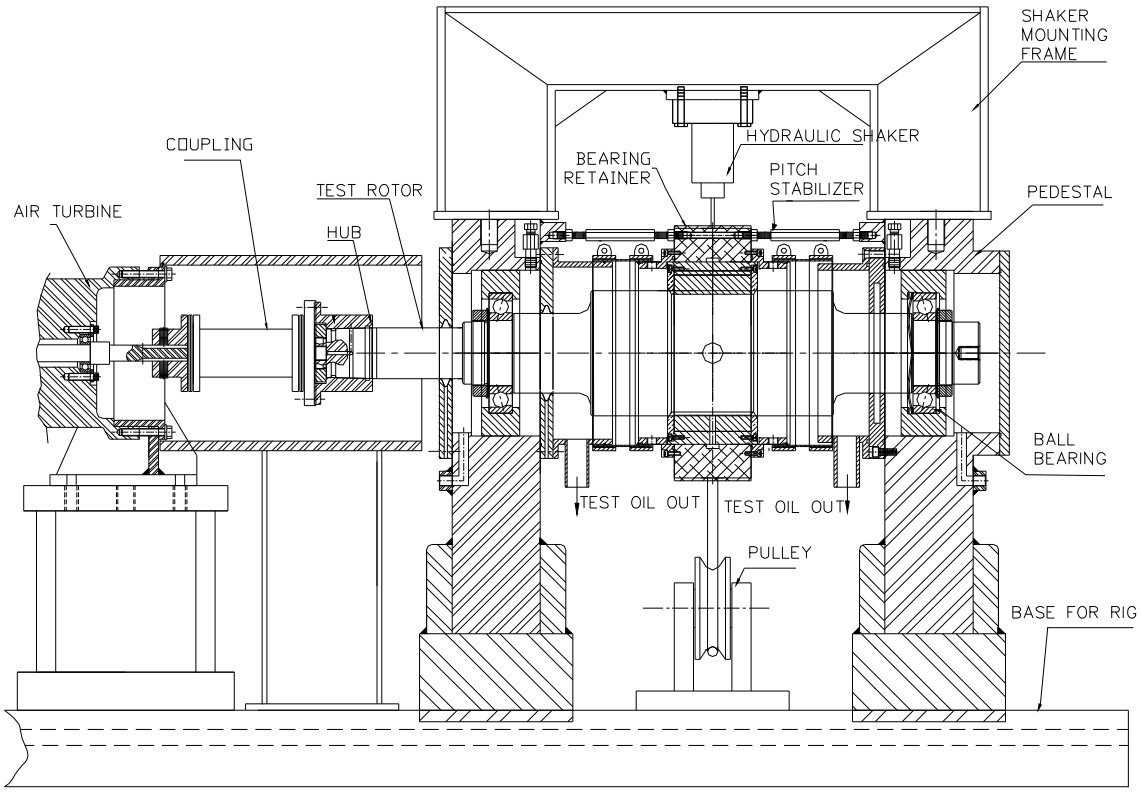

Fig. 5 Cross sectional view of test stand

Static and Dynamic Loading

Load is applied to the bearing to measure the quantities of interest, which include stiffness and damping coefficients as well as pad temperature profiles. This load comes from two different sources, namely, the hydraulic shakers mounted above the bearing housing and the pneumatic powered static loader. Both devices are shown below in Fig. 6 and Fig. 7. The static loader can apply a steady load of up to 22,000 N in the *y* direction.

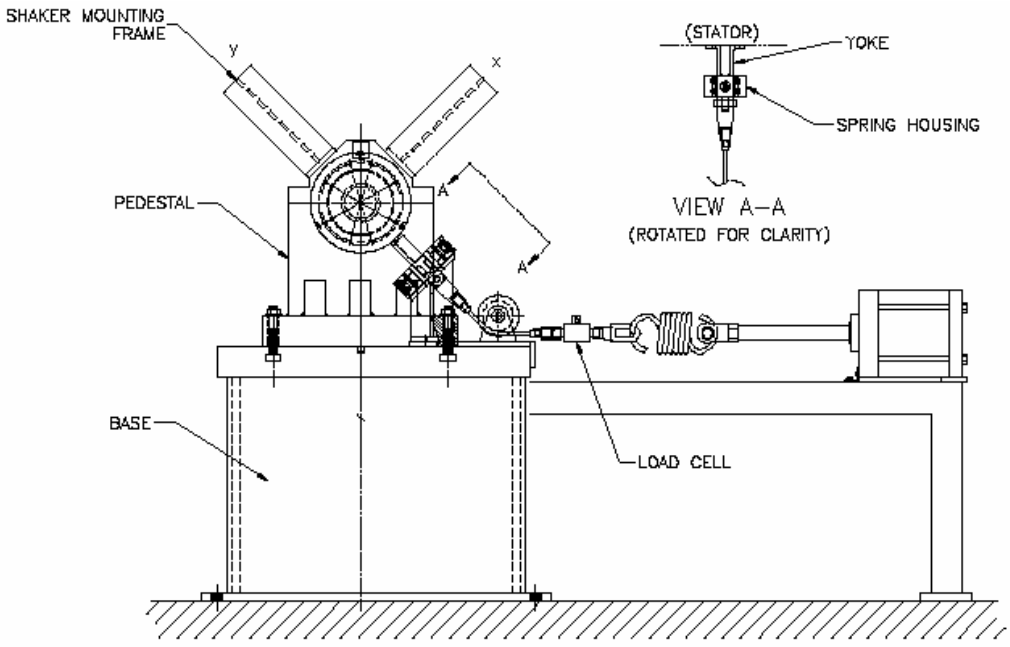

Fig. 6 Static loader setup

The hydraulic shakers are used mainly to apply a dynamic force although they can also be used to apply static loads as well. They can produce 4,450 N in tension and 11,125 N in compression for the *y* direction and 4,450 N in both compression and tension in the *x* direction. A pseudo-random waveform which includes all frequencies from 0-320 Hz in 20Hz intervals is sent to the hydraulic shakers as the input signal. The shakers will apply force to the stator via stingers to displace the housing at the desired frequencies determined in the waveform. Stingers are used to transfer force from the shaker to the bearing housing and have a long slender shape to isolate the dynamics of the bearing from the test structure. The stinger is rigidly attached to the bearing housing at one end and attached to the shaker via a load cell that is used to record the loads imposed by the shaker.

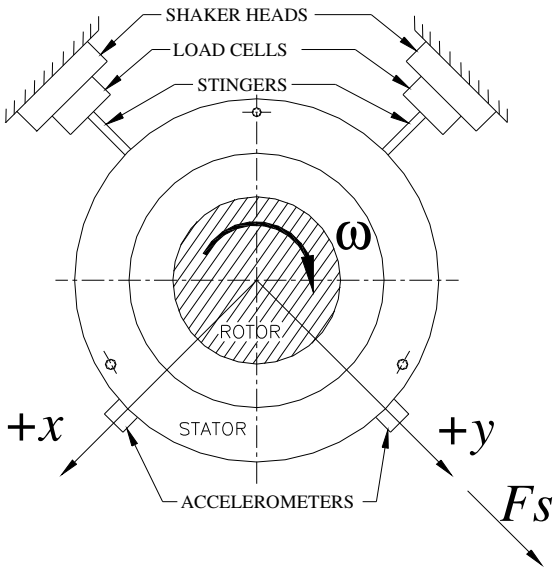

Fig. 7 Exciter head shown attached to stator via stingers and load

Instrumentation

A variety of different sensors are used to gain the necessary coefficients and static data. As can be seen in Fig. 7 two piezoelectric accelerometers are attached to the bearing housing to record absolute accelerations induced by the shakers. A series of eddy current proximity probes are placed in the *x* and *y* axis of the bearing housing to measure displacement of the bearing relative to the rotor. Two probes are place in a plane at the drive end and two more are placed in a parallel plane at the non-drive end. Because measurements are taken in two parallel planes, both the pitch and yaw of the stator housing can be measured. Before testing, all pitch and yaw is removed to ensure that the bearing is centered properly.

Pad temperatures are also monitored via embedded thermocouples that are installed just below the babbit surface of the pad. A detailed layout of the thermocouple probes can be found in the figures on page 35 and 64. Other instrumentation includes thermocouples that are installed in the bearing housing to monitor the oil inlet temperature as well as oil exit temperatures. Fluid pressure probes also measure oil inlet and exit pressures.

Test Bearing

The bearing tested is an Orion five-pad rocker back tilting pad bearing with a 60% pivot offset. Lubrication is applied directly to the pad via a leading edge groove (LEG) which is shown in Fig. 8.

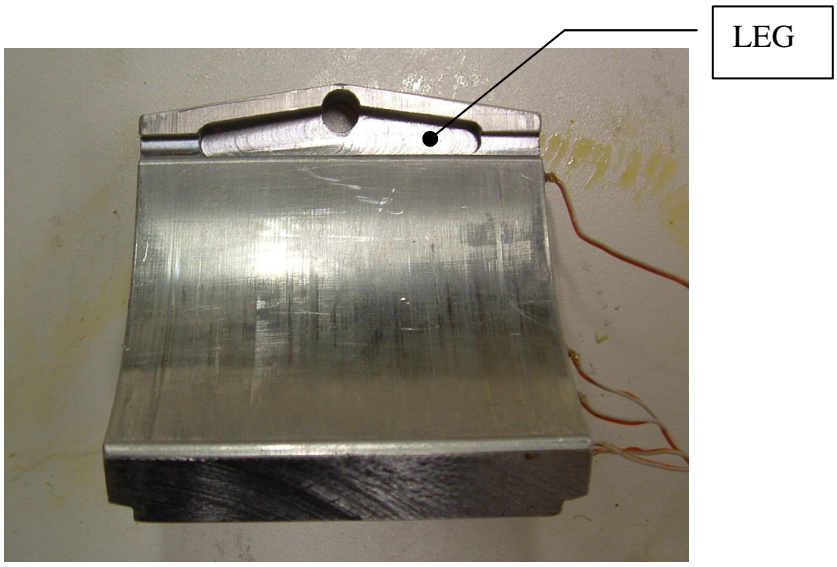

Fig. 8 Photo of leading edge groove

Because the lubricant is applied directly, mixing of the lubricant should be kept to a minimum which will result in lower pad temperatures and improved stiffness and damping coefficients. Table 2 and Fig. 9 shown below give a detailed description of the bearing.

Table 2 Bearing Design Specifications

Number of pads	5
Configuration	LBP
Pad arc angle	57.87˚
Pivot offset	60%
Rotor Diameter	101.587 mm (3.9995 in)
Pad axial length	60.325 mm (2.375 in)
Diametrical pad clearance	.221 mm (.0087 in)
Diametrical bearing clearance	.1575 mm (.0062 in)
Preload	.282
Radial pad clearance (C_p)	.1105 mm (.00435 in)
Radial bearing clearance (C_b)	.0792 mm (.00312 in)
Pad polar inertia	0.000249 kgm^2
Pad mass	.44 kg (.96 lbm)
Lubricant type	ISO VG32

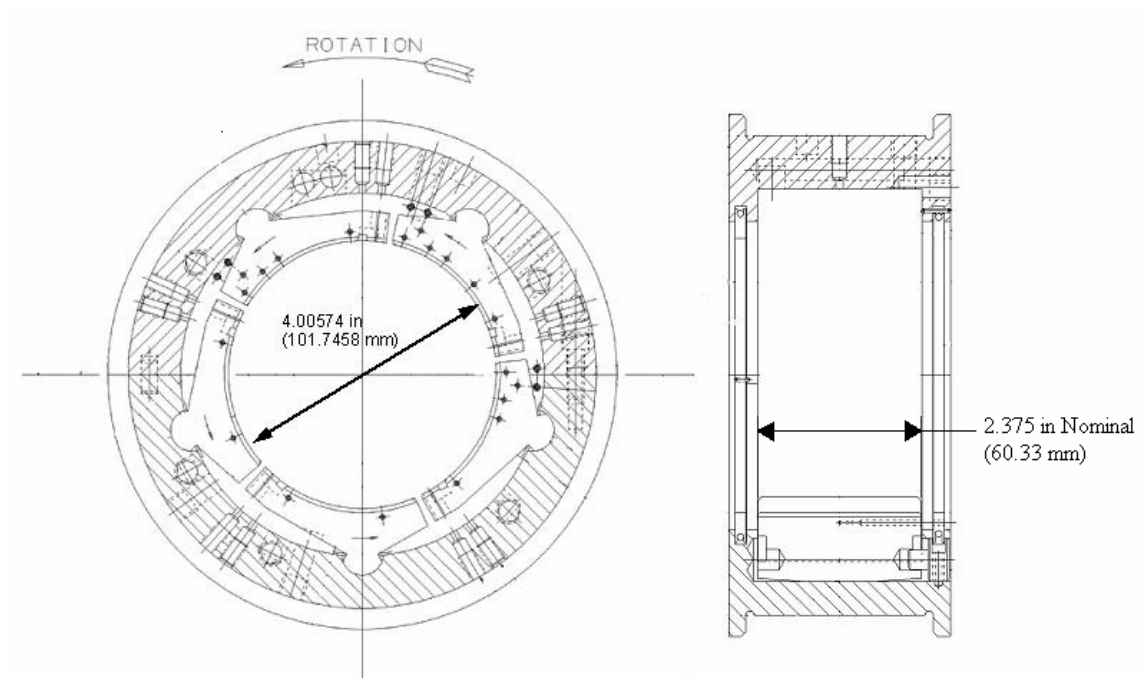

Fig. 9 Bearing cross sectional views

EXPERIMENTAL PROCEDURE

Static Testing Procedures

Testing is performed under a variety of different combinations of load and speed so that the effects of each may be known. Table 3 below lists the various conditions in which the bearing was tested. These conditions vary from 4,000 rpm and 345 kPa to 13,000 rpm and 3101 kPa.

Table 3 Test Matrix

	Oil Flow (L/min)	Unit Load (psi) kPa				
		345(50)	1034(150)	1723(250)	2412(350)	3101(450)
4000 RPM	12.5	X	X	X	X	NA
7000 RPM	20.8	X	X	X	X	X
10000 RPM	20.8	X	X	X	X	X
13000 RPM	30.3	X	X	X	X	X

Before testing can begin, the position of the bearing relative to the shaft must be found. This task is accomplished by the use of a "bump test". A bump test is used to find the center of the bearing and is carried out by moving the bearing housing to the extreme positions in both the *x* and *y* directions using the zonic shakers. The min and max voltages associated with the subsequent proximity probe readings are averaged, and that average voltage is then associated with the bearing being centered. As the bearing housing moves off center, the voltages increase or decrease with a linear voltage that is converted into eccentricity.

Once the position of the bearing is found with the bump test, the rotor is taken up to the desired speed. After the oil flow rate is set, a load is applied via the static loader. At this point, the test rig is allowed to run until a steady state condition has been reached in regards to bearing temperatures and rotor speed. The following data are taken during a static test:

1) Static position data giving the eccentricity of the bearing.
2) Pad temperature
3) Oil inlet and exit temperatures
4) Force applied by the static loader
5) Shaft speed
6) Oil flow rate

Static Performance Indicators

There are many different indicators of the static performance characteristics. One of the most important parameters is the eccentricity ratio. This ratio is found by using a locus plot, one of which is shown below in Fig. 10, which illustrates the position of the bearing relative to the clearance. The eccentricity ratio can be used in conjunction with the amount of static load to indicate the stiffness and load carrying capacity of the bearing.

Eccentricity is defined by:

$$\varepsilon_{x0} = \frac{e_x}{C_P} \quad \textbf{(1)}$$

$$\varepsilon_{y0} = \frac{e_x}{C_P} \quad \textbf{(2)}$$

$$\varepsilon_0 = \sqrt{\varepsilon_x{}^2 + \varepsilon_y{}^2} \quad \textbf{(3)}$$

Once the eccentricity ratio is found, another important parameter can be obtained, the attitude angle. The attitude angle is important because it can indicate the amount of cross-coupling inherent in the bearing. Large attitude angles are indicative of substantial amounts of cross coupling and are shown as large position deviations from the loaded axis on the Loci plot. Attitude angle is defined by:

$$\phi = \tan^{-1}\left(\frac{\varepsilon_{xo}}{\varepsilon_{yo}}\right)\frac{180}{\pi} \quad \textbf{(4)}$$

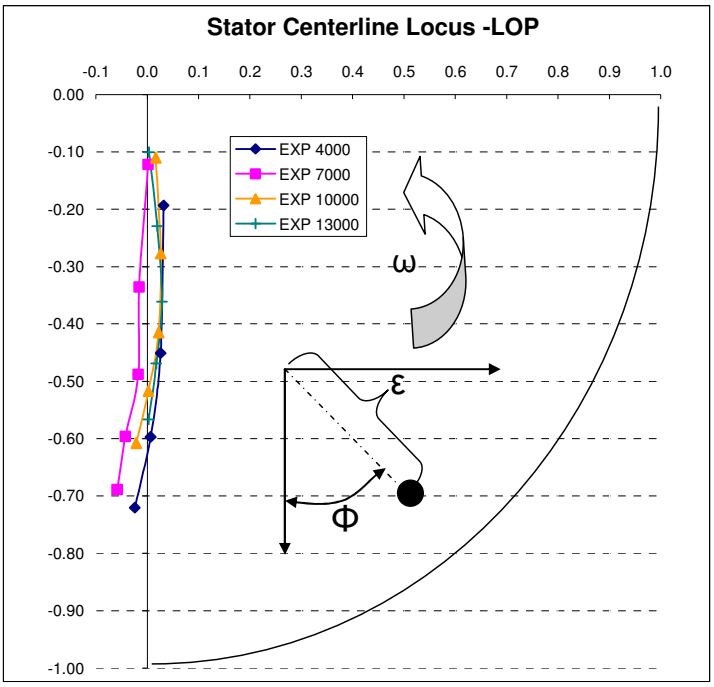

Fig. 10 Physical meaning of attitude angle and eccentricity ratio for a given locus plot

Power Loss is another important static parameter. A good approximation of the power loss is made by measuring the energy of the lubricant entering and exiting the bearing. By recording the temperature of the inlet and exit oil, an energy balance can be performed in which it is assumed that all of the energy used to shear the lubricant is carried out of the bearing by the lubricant in the form of heat. This heat generation is assumed to be equal to the power loss and is defined below in Eq. (5) where $\dot{Q}$ is equal to the volumetric flow rate in m^3/s, ρ is the density of the lubricant in kg/m^3, and C_P and T represent the heat capacity in $J/(kg.°K)$ and temperature in degree Kelvin. Equations 6 and 7 are used to calculate the temperature dependent values of specific heat and density for the given lubricant (ISO VG 32).

$$P = \dot{Q}(\rho_e C_{pe} T_e - \rho_i C_{pi} T_i) \quad \textbf{(5)}$$

$$C_p = 3.627T + 811.75 \quad (J/kg.°K) \quad \textbf{(6)}$$

$$\rho = -0.6616T + 1064 \quad (kg/m^3) \quad \textbf{(7)}$$

Dynamic Testing Procedures

Each test condition in Table 3 will include a static and dynamic test. The dynamic test typically occurs immediately following the static test and is done at the same operating condition as the static test. Dynamic tests are performed when a pseudo-random waveform input signal is sent sequentially to the *x* and then *y* Zonic hydraulic shakers. This waveform contains every frequency from 20-320 Hz in 20 Hz intervals and is mechanically reproduced by the shakers as they excite the test bearing housing. The amplitude of this vibration is kept to within 5%-10% of the bearing clearance to insure linear behavior of the bearing response and is varied slightly to obtain the most repeatable results. Each *test* is made up of one *shake* in the *x* direction followed by another *shake* in the *y* direction. Each shake contains a waveform that is repeated 32 times with the data being averaged in the frequency domain. Ten tests are performed on the bearing for each test condition to perform a statistical analysis. Given this information, for each condition there are 32 X 10 =320 waveforms sent to the bearing in the *x* direction and 320 waveforms sent to the bearing in the opposing *y* direction, which allows for a high level of confidence in the results.

During a shake, the following data are recorded in the time domain:

1) Absolute acceleration of the stator in the *x* and *y* directions
2) Stator displacement relative to the rotor via *x* and *y* proximity probes
3) Forces imposed upon the stator via load cells on the shakers

Dynamic Impedance Function H_{ij}

The data collected from is used to determine the rotordynamic stiffness, damping and added mass coefficients. The process described here to determine the coefficients was taken from Childs and Hale [25] and Rouvas and Childs [26]. The equation of motion for the stator must be found first and is derived by observing the forces acting upon the stator. These forces come from both the hydraulic shakers and the fluid reaction forces in the bearing. After applying Newton's Second Law to the stator in both the *x* and *y* directions the equation of motion is:

$$M_s \begin{bmatrix} \ddot{x}_s \\ \ddot{y}_s \end{bmatrix} = \begin{bmatrix} f_x \\ f_y \end{bmatrix} - \begin{bmatrix} f_{bx} \\ f_{by} \end{bmatrix} \quad \textbf{(8)}$$

In this equation, M_s is the mass of the stator, $\ddot{x}_s$ and $\ddot{y}_s$ are the absolute stator accelerations, f_x , f_y are the forces induced by the hydraulic shakers, and f_{bx} and f_{by} are the bearing reaction forces.

The bearing reaction forces are related to the rotordynamic coefficients through Eq. (9) in which the reaction forces are modeled with stiffness [K], damping [C] and added mass matrices [M]. Each coefficient in the matrix has one of four different designations as shown on the coefficient subscript. These designations are (*xx,yy*) or (*xy,yx*) with the former representing direct and the latter representing cross-coupled coefficients.

$$-\begin{bmatrix} f_{bx} \\ f_{by} \end{bmatrix} = \begin{bmatrix} K_{xx} & K_{xy} \\ K_{yx} & K_{yy} \end{bmatrix} \begin{bmatrix} \Delta x \\ \Delta y \end{bmatrix} + \begin{bmatrix} C_{xx} & C_{xy} \\ C_{yx} & C_{yy} \end{bmatrix} \begin{bmatrix} \Delta \dot{x} \\ \Delta \dot{y} \end{bmatrix} + \begin{bmatrix} M_{xx} & M_{xy} \\ M_{yx} & M_{yy} \end{bmatrix} \begin{bmatrix} \Delta \ddot{x} \\ \Delta \ddot{y} \end{bmatrix} \quad \textbf{(9)}$$

The next step occurs when Eq. (9) is substituted into Eq. (8) to produce Eq. (10) shown below. In this equation, all of the left hand side terms as well as the Δx and Δy terms on the right hand side are directly measured either by load transducers, accelerometers, or proximity probes (Δx and Δy).

$$\begin{bmatrix} f_x - M_s \ddot{x}_s \\ f_y - M_s \ddot{y}_s \end{bmatrix} = -\begin{bmatrix} K_{xx} & K_{xy} \\ K_{yx} & K_{yy} \end{bmatrix} \begin{bmatrix} \Delta x \\ \Delta y \end{bmatrix} - \begin{bmatrix} C_{xx} & C_{xy} \\ C_{yx} & C_{yy} \end{bmatrix} \begin{bmatrix} \Delta \dot{x} \\ \Delta \dot{y} \end{bmatrix} - \begin{bmatrix} M_{xx} & M_{xy} \\ M_{yx} & M_{yy} \end{bmatrix} \begin{bmatrix} \Delta \ddot{x} \\ \Delta \ddot{y} \end{bmatrix} \quad \textbf{(10)}$$

However, a FFT must be performed on equation (10) to extract the coefficients. The FFT version is:

$$\begin{bmatrix} \boldsymbol{F_x} - M_s \boldsymbol{A_x} \\ \boldsymbol{F_y} - M_s \boldsymbol{A_y} \end{bmatrix} = -\begin{bmatrix} \boldsymbol{H_{xx}} & \boldsymbol{H_{xy}} \\ \boldsymbol{H_{yx}} & \boldsymbol{H_{yy}} \end{bmatrix} \begin{bmatrix} \boldsymbol{D_x} \\ \boldsymbol{D_y} \end{bmatrix} \quad \textbf{(11)}$$

The FFT output contains the dynamic stiffness functions H_{xx}, H_{xy}, H_{yy} and H_{yx}, which are related to the rotordynamic coefficients through:

$$\boldsymbol{H}_{ij} = K_{ij} - \Omega^2 M_{ij} + j(\Omega C_{ij}) \quad \textbf{(12)}$$

Eq. (12) shows that the $\boldsymbol{H_{ij}}$ term is composed of a real and an imaginary component. These components are defined as:

$$\mathrm{Re}(\boldsymbol{H}_{ij}) = K_{ij} - \Omega^2 M_{ij} \quad \textbf{(13)}$$

$$\mathrm{Im}(\boldsymbol{H}_{ij}) = \Omega C_{ij} \quad \textbf{(14)}$$

Equation (13) states that the stiffness and added mass coefficients are related to the real part of the dynamic stiffness function $\boldsymbol{H}_{ij}$, and Eq. (14) states that the damping coefficients are found in the imaginary part of the function $\boldsymbol{H}_{ij}$.

Equation (15) contains two equations yet has four unknown stiffness functions $\boldsymbol{H}_{ij}$, so two more equations are needed. These equations are found by shaking the stator in two directions, *x* and *y*, to create two extra independent equations to yield four equations and four unknowns as shown below.

$$\begin{bmatrix} \boldsymbol{F}_{xx} - M_s \boldsymbol{A}_{xx} & \boldsymbol{F}_{xy} - M_s \boldsymbol{A}_{xy} \\ \boldsymbol{F}_{yx} - M_s \boldsymbol{A}_{yx} & \boldsymbol{F}_{yy} - M_s \boldsymbol{A}_{yy} \end{bmatrix} = -\begin{bmatrix} \boldsymbol{H}_{xx} & \boldsymbol{H}_{xy} \\ \boldsymbol{H}_{yx} & \boldsymbol{H}_{yy} \end{bmatrix} \begin{bmatrix} \boldsymbol{D}_{xx} & \boldsymbol{D}_{xy} \\ \boldsymbol{D}_{yx} & \boldsymbol{D}_{yy} \end{bmatrix} \quad \textbf{(15)}$$

Coefficient Extraction from Impedance Function H_{ij}

Before the coefficients are extracted, note that, because each test condition is repeated ten times, each impedance function value $\boldsymbol{H}_{ij}$ is averaged over those test using Eq. (16) below.

$$\boldsymbol{H}_{ij} = \frac{\sum_{k=1}^{10} \boldsymbol{h}_{ijk}}{10} \quad \textbf{(16)}$$

As shown above in Eq. (13) the stiffness K_{ij} and added mass M_{ij} coefficients depend on the real part of the impedance function $\boldsymbol{H}_{ij}$. To find these coefficients, the real part of the dynamic stiffness function $\boldsymbol{H}_{ij}$ is plotted vs. frequency of excitation Ω. Shown below in Fig. 11 (a) is a plot of Re($\boldsymbol{H}_{xx}$) and Re($\boldsymbol{H}_{yy}$) vs. frequency. If a curve fit were drawn through each data point set, the *y*-axis intercept would define the value of stiffness coefficients K_{xx} and K_{yy}. The curvature of the fit would indicate the magnitude of the added mass coefficient M_{ij}. In this regard, the greater the curvature, the higher the added mass coefficient.

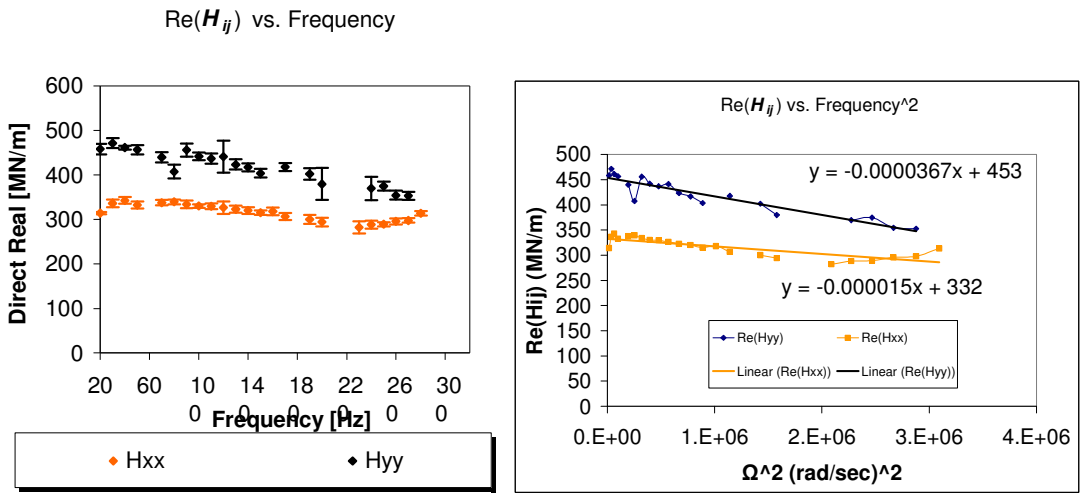

(a) (b)

Fig. 11 LOP 13000 rpm 1034 kPa direct real dynamic stiffness vs. (a) Hz, (b) Ω^2

To find the curvature and the y-intercept, the dynamic stiffnesses are plotted vs. Ω^2 as shown in Fig. 11 (b) to produce a linear relationship between impedance and frequency. A least squares linear regression fit of these data is made with the *y*-intercept and slope which are found by using equations (17) and (18) respectively.

$$b = \bar{y} - m\bar{x} \tag{17}$$

where: $\bar{x} = \frac{1}{N}\sum_{i=1}^{N} x_i$, $\bar{y} = \frac{1}{N}\sum_{i=1}^{N} y_i$, N = number of data point sets (x and y)

$$m = \frac{N\sum_{i=1}^{N} x_i y_i - \sum_{i=1}^{N} x_i \sum_{i=1}^{N} y_i}{N\sum_{i=1}^{N} x_i^{\,2} - \left(\sum_{i=1}^{N} x_i\right)^2} \tag{18}$$

The slope of the line m is equal to the amount of added mass M_{ij}, and the intercept b is equal to the stiffness coefficient K_{ij}. The equation of the line in Fig. 11 (b) gives the added mass coefficients M_{xx} = 15 kg and M_{yy} = 36.7 kg, and the stiffness coefficient values K_{xx} and K_{yy} are 332.5 MN/m and 453.4 MN/m, respectively.

Once these coefficients are determined, they can be substituted into Eq. (13), and this plotted as a curve fit of the data in Fig. 11 (a) to produce the curve fit of the data shown in Fig. 12.

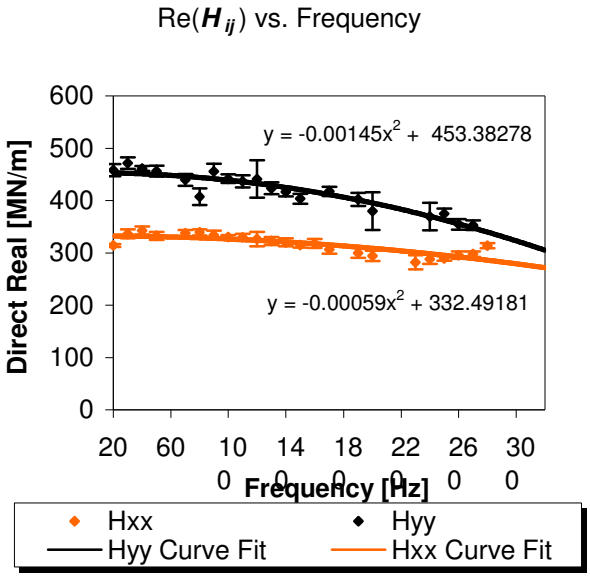

Fig. 12 Curve fit of dynamic stiffnesses

The same procedure can be applied to find the cross coupled stiffness and added mass coefficients $K_{xy}, K_{yx}, M_{xy}, M_{yx}$. Shown below in Fig. 13 (b) are the stiffness coefficients K_{xy} and K_{yx}, which are equal to 80.5 MN/m and 1.56 MN/m respectively. Added mass coefficients M_{xy} and M_{yx} are equal to -12.8 kg and -18 kg respectively.

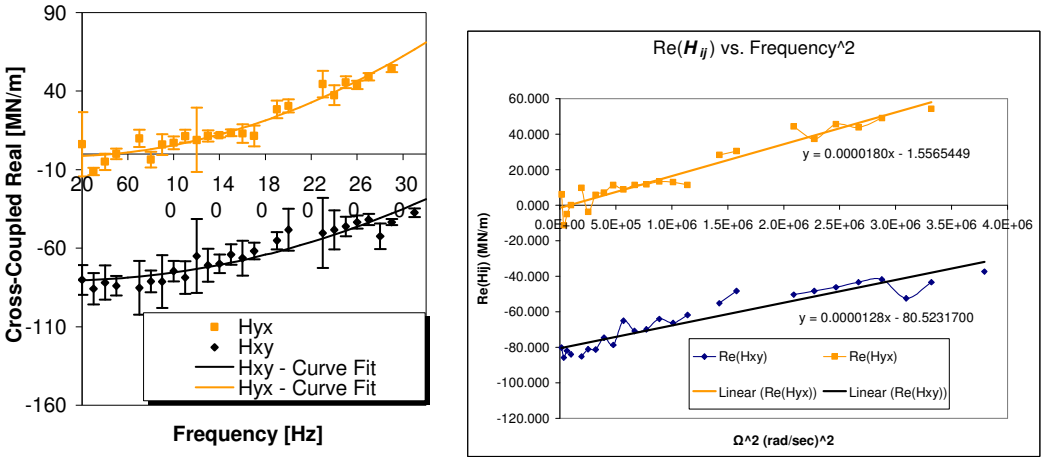

Fig. 13 LOP 13000 rpm 1034 kPa indirect real dynamic stiffness vs. (a) Hz, (b) Ω^2

Equation (14) shows that the damping coefficient C_{ij} is dependent on the imaginary part of the impedance function H_{ij} and is equal to the slope of the curve-fit. In this instance, the y intercept is not of importance. The curve fit is accomplished using equations (17) and (18) as well as the standard equation of a line. Fig. 14 below shows the linear behavior of the dynamic stiffnesses in relation to the frequency of vibration as well as the subsequent curve fit. The curve fit slope gives an estimate of the direct damping C_{xx} and C_{yy} as 226.7 $KN \cdot \sec/m$ and 204.5 $KN \cdot \sec/m$ respectively.

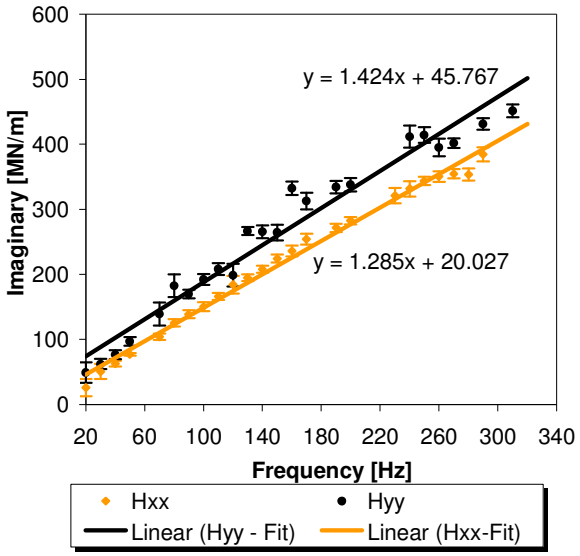

Fig. 14 Direct imaginary dynamic stiffness LOP 13000 rpm 1034 kPa

Uncertainties of Curve Fit

Each coefficient is an "estimate" of the actual value since the coefficients themselves are not directly measured and are instead derived from a series of equations. These equations listed above have an associated amount of uncertainty which is listed below and are taken from [2].

Standard Deviation of H_{ij} $$S_{ij}^{y} = \sqrt{\frac{\sum_{k=1}^{10}(h_{ijk} - H_{ij})^2}{9}}$$

Mean Square Error s^2 $$\frac{\sum_{i=1}^{N}(y_i - \hat{y}_i)^2}{N-2}$$ (y_i = curve fit data , $\hat{y}_i$ =exp data)

S_{xx} $$\sum_{i=1}^{N} x_i^2 - N\,\bar{x}^2$$ (all data points from Ω2 curve fit)

Uncertainty of the slope Δm $$t \times \sqrt{\frac{s^2}{S_{xx}}}$$

Uncertainty of the intercept Δb $$t \times \sqrt{s^2 \left(\frac{1}{N} + \frac{\bar{x}^2}{S_{xx}} \right)}$$

The “t” term listed in the above equations is a multiplicative factor which is derived by using a 95% confidence interval. This interval specifies that the value of t be equal to 1.96.

XLTRC^2 PREDICTIONS

Classic lubrication theory as applied to bearings has traditionally been based upon the Reynolds equation. The equation is reduced from the Navier Stokes equations once the temporal and convective acceleration terms are dropped. These terms can be dropped only when the flow has been determined to be laminar which the literature defines as being associated with a Reynolds number of less than 2000 [27]. However, Reinhardt and Lund [21] reported that even purely laminar flows can lead to inertial effects. They stated that Reynolds numbers as small as 10^2 can indicate substantial inertial effects at which point the Reynolds equation alone may not be enough to accurately model the performance of the bearing.

XLTFPBrg, developed by Dr. San Andres at the Texas A&M Turbomachinery Laboratory, is part of the XLTRC^2 Rotordynamics Suite. XLTFPBrg can be used to predict the behavior of flex-pad, tilting-pad, and rigid pad bearings. This package is used here to predict the dynamic and static behavior of the test bearing. The code uses the Bulk-flow governing equations which includes continuity, circumferential-momentum, axial-momentum, cross-film-momentum, and energy transport equations [28]. The code leaves an option for a pure Reynolds equation analysis that excludes the temporal and convective acceleration terms. A Reynolds equation model can only include the stiffness and damping matrices of a conventional [K][C] model and not the added-mass matrix. Past research by Rodriguez [2] and Al-Ghasan [1] has shown that the Reynolds analysis option was able to predict the large added mass terms of the experimental results due primarily to the reduction in the degrees of freedom from the initial 12 degrees (four pads time three degrees of freedom) to the two rotor degrees of freedom. The bulk-flow analysis gave comparable results to the Reynolds out to running speed, but at the higher frequencies the ability to include fluid inertia resulted in better predictions to the experimental results. Consequently they came to the conclusion that fluid and pad inertia affected the dynamic stiffnesses only at the higher excitation frequencies and had little effect up to running speed.

Table 4 below gives some insight as to why inertia terms can be expected in the results for this bearing. This table shows the maximum measured Reynolds numbers at each test speed. Most of these numbers are higher than the 10^2 threshold stated by Reinhardt and Lund. The bulk flow option was used for the predictions in this thesis in order to account for any observed inertia affects.

Table 4 LBP and LOP Maximum Reynolds Numbers

Rotor Speed (rpm)	4000	7000	10000	13000
LBP Maximum Reynolds Number	79.13678	146.9587	229.8477	307.099
LOP Maximum Reynolds Number	90.40383	171.0518	266.9884	369.4513

The input screen of XLTFPBrg is shown below in Fig. 15. To begin the process, the bearing's physical dimensions and orientation are entered along with lubricant type. Parameters that change depending on the test condition include the temperature of the inlet oil, the unit load in Newtons, and rotor speed. The program has the following analysis options that can be used depending upon the need:

1) Fluid inertia Option: The option exists to not include fluid inertia in the analysis, at which point the Reynolds equation is used to find the bearing coefficients. However, the user can include inertia by choosing the bulk-flow analysis option. The measured results as seen later will show large amounts of inertia were present, so the entire bulk flow analysis was selected.
2) Frequency Analysis Option: This option allows the bearing coefficients to be computed when the bearing is excited at a single frequency (running speed) or at multiple frequencies that are specified by the user. Because the goal of the research was to investigate frequency dependent behavior of the bearing, the multiple frequency option was selected with a frequency range of 0-320 Hz.
3) Thermal Analysis Option: Two different thermal options are available, the isothermal analysis and the adiabatic analysis. The isothermal option assumes that the lubricant film temperature remains constant across the pad circumference, and the adiabatic option assumes that no heat transfer takes place between the rotor and bearing. Because neither of these options realistically occurs in practice, both analysis were performed and compared to the measured results to see which option does the best job. Fig. 16 shows that both stiffness and damping are more reliably modeled with the adiabatic option.

XLTFPBrg Spreadsheet for Tilting, Flexure, and Rigid Pad Bearing Coefficients

Version 2.0, Copyright 1998-1999 by Texas A&M University. All rights reserved.

Title: Someya HDB, Test Bearing #11, pp. 227 TEST#9 Adia

Journal Diameter	0.101587	meters	3.9995	Fluid Inertia Option	Include Fluid Inertia		
Bearing Axial Length	0.060325	meters	2.375	It Max	199	--	
Diametral Pad Clearance	0.000221	meters	0.00624	Momentum Relaxation Factor	0.9	--	
Radial Preload Clearanc	0.000079	meters		Pressure Relaxation Factor	0.6	--	
Number of Pads	5	--		Temperature Relaxation Factor	0.9	--	
Pad Arc Length	57.87	degrees		Oil Mixing Parameter	0.7	--	
Pad Pivot Offset	0.6	--		Thermal Analysis Option	Adiabatic, Qj=Qb=0		
Bearing Type Option	Tilting Pads			Shaft Temperature	0	deg K	
Pad Inertia	0.000249	kg-m^2		Bearing Temperature	0	deg K	
Pad Stiffness	0	N-m/rad		Pad Back Temperature	0	deg K	
Pad Damping	0	N-s-m/rad		Pad Outer Radius	0	meters	
				Pad Material	Steel - 4130		
Supply Pressure	1.55E+05	N/m^2		Pad Therm Cond	43.2675666	W/(m-K)	
Supply Temperature	316.66	deg. K					

Pad Geometry Option	Use Pad Definition Table	
Lead Edge of Pad 1	7	degrees

Pad Number	Pad Lead Edge	Pad Arc Len
--	degrees	degrees
1	19.27	57.87
2	91.27	57.87
3	163.27	57.87
4	235.27	57.87
5	307.27	57.87

Selected Lubricant		
ISO 32		
Viscosity at Tsupply	0.02301467	N-s/m^2
Density at Tsupply	854.482454	kg/m^3
Compressibility	4.58E-10	m^2/N
Specific Heat	1960.36871	J/(kg-K)
Thermal Conductivity	0.13099221	W/(m-K)
Coef Therm Exp	0.00076	1/K
Temp Visc Coef	0.02929926	1/K

EccX Initial Guess	0.02	--
EccY Initial Guess	-0.4	--
Rotor Relative Roughness	0	--
Bearing Relative Roughness	0	--
Moody's Coef Amod	0.001375	--
Moody's Coef Bmod	500000	--
Moody's Coef Expo	0.33333	--
Frequency Analysis Option	Nonsynchronous Analysis	
Constant Shaft Rpm	10000	rpm

Fig. 15 Input parameters for XLTFPBrg program

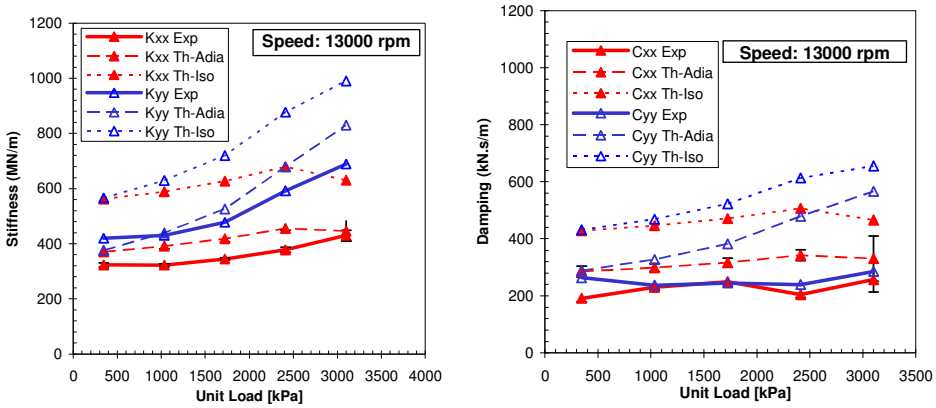

Fig. 16 LBP XLTRC^2 adiabatic and isothermal (a) stiffness and (b) damping coefficients

LBP CONFIGURATION RESULTS AND PREDICTIONS

Static Results

Loci Plots

Locus plots shown below in Fig. 17 show the change in position of the bearing due to a static load applied in the *y* direction by the pneumatic loader. Noticeable cross coupling effects are shown in Fig. 17 (a) and (b) at higher loads and low speeds, due to deviation from the y axis in the loci plots. However, at intermediate and high speeds as exhibited in Fig. 17 (c) and (d) the amount of cross coupling is low, since this deviation is kept to a minimum. Shown in Fig. 18 below are loci plots for each test speed. As expected, as the speed increased the eccentricities decreased except for the last two data points at high load for the 7000 rpm condition, at which point a sudden loss of stiffness occurred.

Predictions for each condition show almost no cross coupling effects as are expected for a tilt pad bearing. Hence, the cross coupling seen in experimental results mentioned above is not predicted from the static data. The bearing eccentricities are predicted well except for the low speed and intermediate to high load conditions as seen in Fig. 17 (a) and (b). At these conditions, the eccentricity is very much under predicted, which means the code over predicts the static stiffness of the bearing by a significant margin.

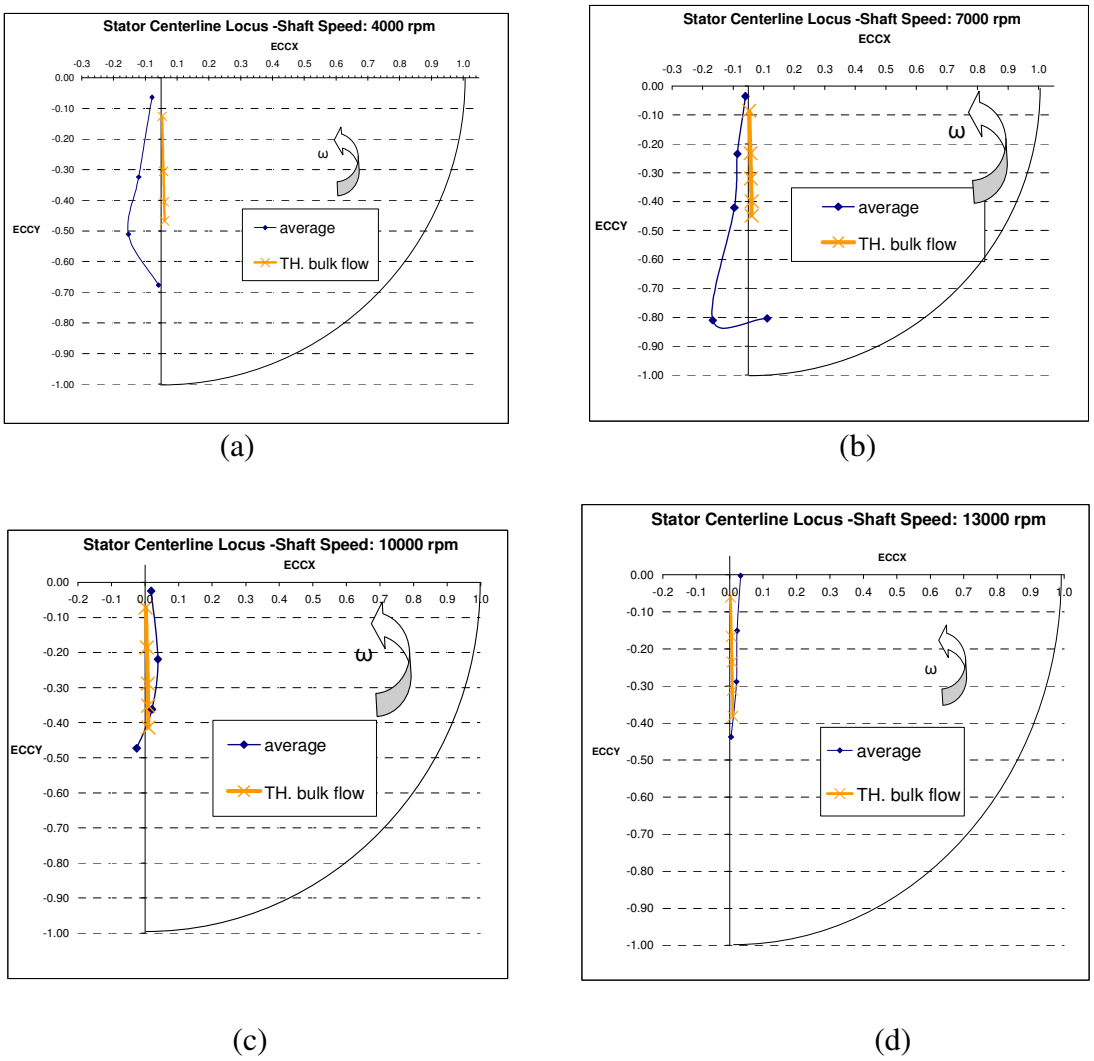

Fig. 17 LBP predicted and measured loci plots for various shaft speed: (a) 4000 rpm, (b) 7000 rpm, (c) 10000 rpm, (d) 13000 rpm

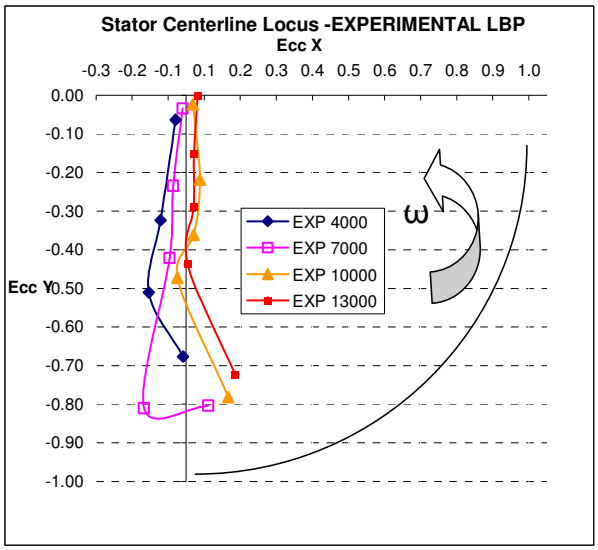

Fig. 18 LBP overall comparison of measured loci plots for different speeds

Attitude Angle

Shown below in Fig. 19 is a plot of the measured attitude angle vs. applied load. The attitude angles are highest at low loads and high speed but quickly decrease with increasing load. After passing 2000 kPa there is very little attitude angle present for all conditions. The code predicts a straight line path for the loci plots which translates into very low attitude angles at all test conditions as seen in Fig. 19 (b).

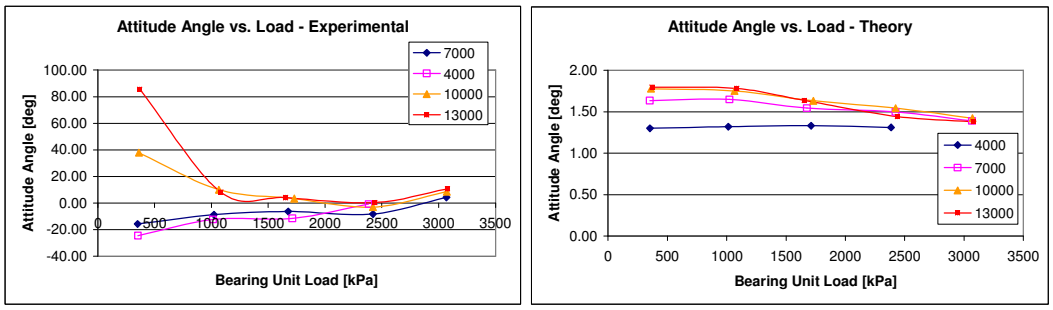

(a) (b)

Fig. 19 LBP attitude angle change with load for (a) measured test and (b) predicted XLTRC

Power Loss

Fig. 20 shows a series of plots that graph power loss versus shaft speed. Power loss is normally defined as being proportional to oil viscosity and the square of the rotor speed in which case, a parabolic relationship would be expected between the two variables. However as the oil viscosity decreases so does the power loss until a steady state is reached. As a result the following plots have a more linear than parabolic shape. While the power losses do increase linearly with speed, they are much over predicted as seen below. The relationship between power loss and unit load for various speeds is shown in Fig. 21. The plots show that power loss is not dependent upon the load, only the speed.

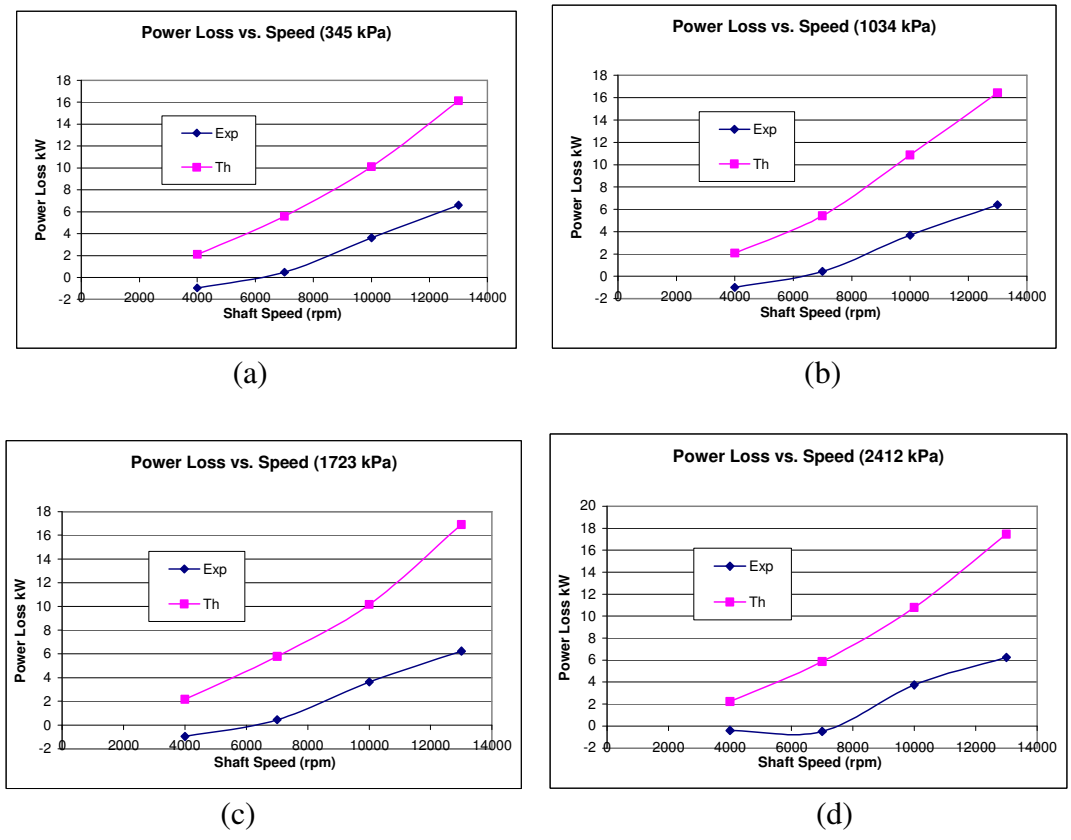

Fig. 20 LBP power loss versus shaft speed comparisons with predictions for varying loads: (a) 345 kPa, (b) 1034 kPa, (c) 1723 kPa, (d) 2412 kPa, (e) 3101 kPa

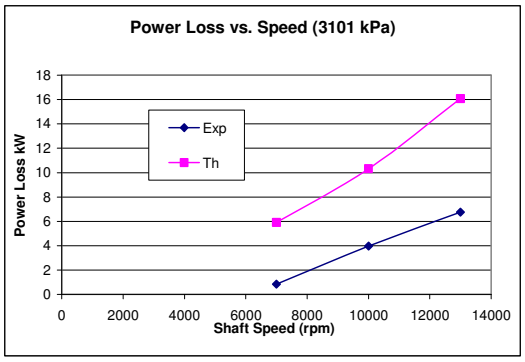

(e)

Fig. 20 "Continued"

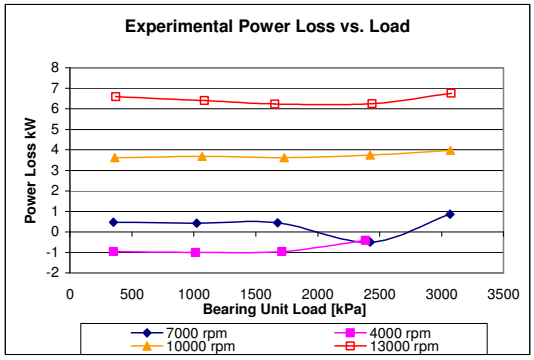

Fig. 21 LBP power loss vs. load for different shaft speeds

Pad Temperature Data

A series of thermocouples have been embedded circumferentially just under the babbit lining of each pad. There are 17 circumferential thermocouples, five of which are located on the loaded pad (pad number 1). Unfortunately, in the LBP configuration all of the leading edge thermocouples were inoperable so these temperatures were not recorded. The layout and orientation of each thermocouple is shown in Fig. 22. Those thermocouples that were not operational are grayed out.

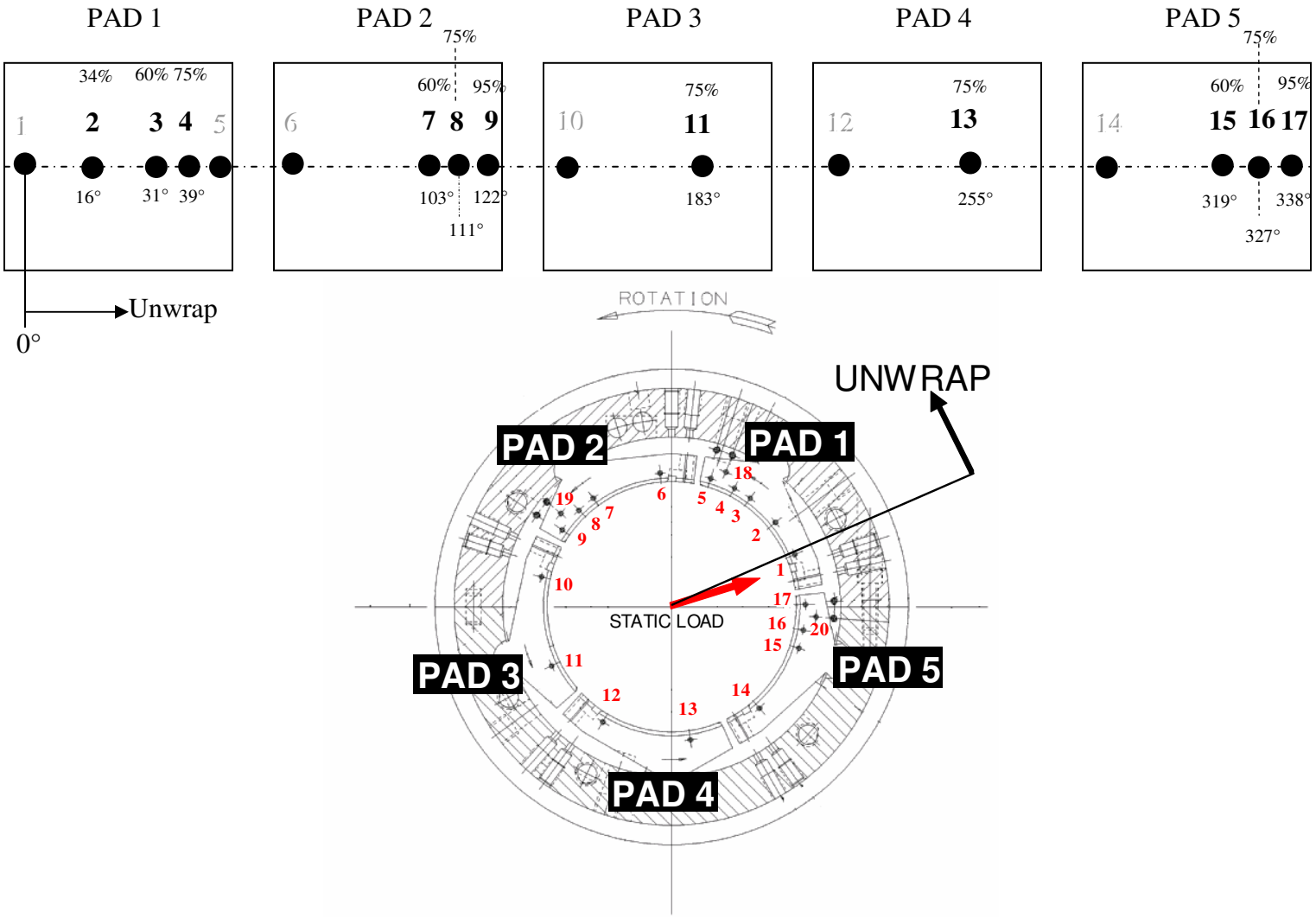

Fig. 22 LBP thermocouple layout

Displayed in Fig. 23 is the temperature circumferentially along each pad, and any changes that occur with respect to speed. As expected, the temperatures of the loaded pads, 1 and 5, are the highest, with the temperatures increasing steadily with speed. Temperatures at the leading edge were lowest, while the trailing edge was highest, reaching a maximum temperature of 91°C on pad 5. Even at this high speed and load condition (13000 rpm 2412 kPa), the pad temperatures were fairly low. The leading edge groove design seems to contribute to a lower overall temperature profile for the bearing for this loading condition.

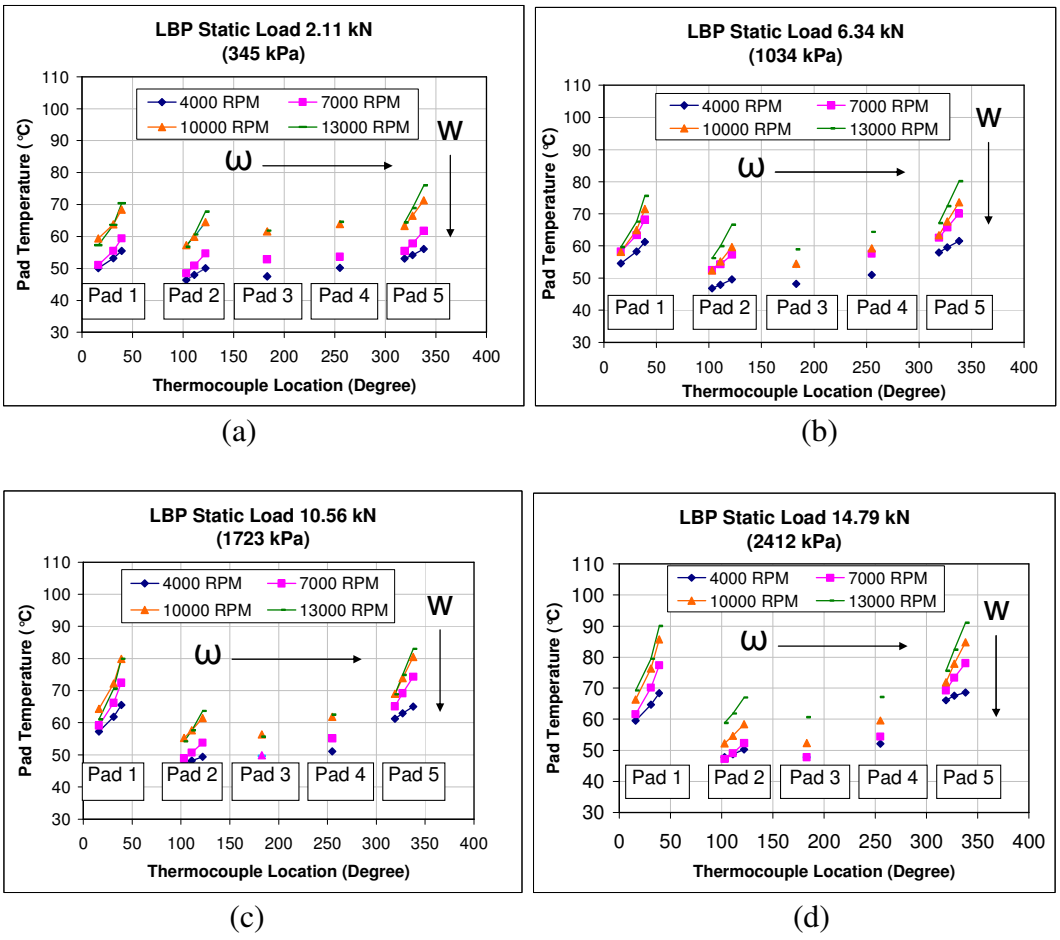

Fig. 23 LBP pad temperatures as they vary with location for load conditions of: (a) 346 kPa, (b) 1034 kPa, (c) 1723 kPa, (d) 2412 kPa

A comparison between the measured and predicted maximum bearing temperatures is shown below in Fig. 24. Both results show temperatures that rise at similar linear rates with increasing speed. Overall, the model slightly over predicts the bearing temperatures.

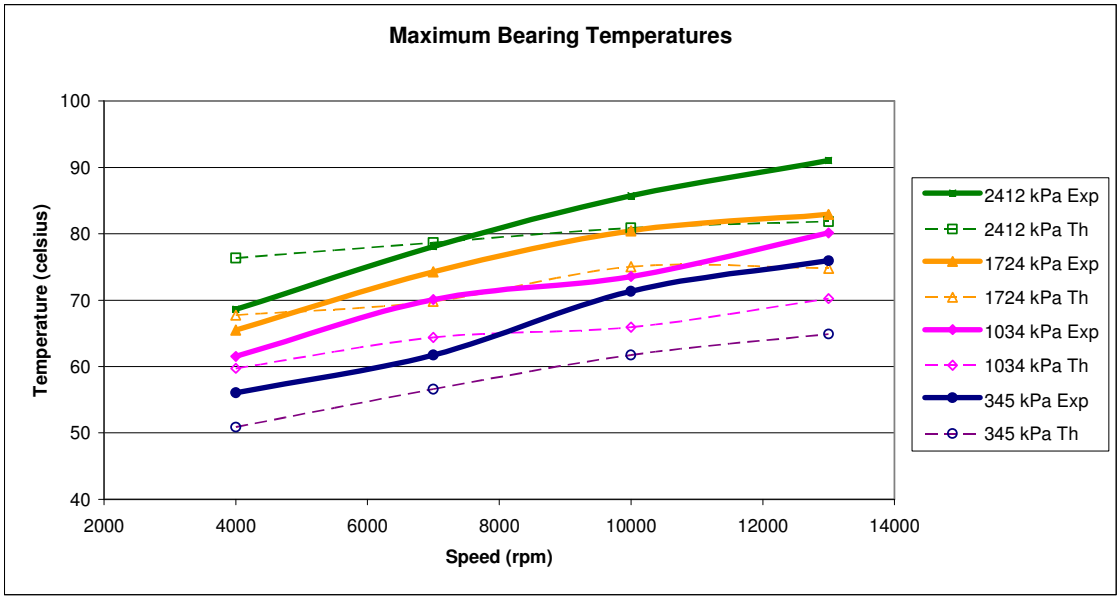

Fig. 24 LBP predicted and measured maximum bearing temperatures

Dynamic Results

Baseline Dynamic Stiffness

A baseline test is performed to find the dynamic coefficients of the structure of the test rig alone. The bearing is fitted into a steel housing that is connected to the test rig through the pitch stabilizers as well as numerous hoses. The housing has a significant mass, and the pitch stabilizers add a small amount of stiffness. The rubber hoses connected to the bearing housing will add some damping as well. When a dynamic test is performed, each one of these components will contribute to the final rotordynamic coefficients. Because we are interested only in the coefficients associated with the bearing, all of the stiffness, damping and mass from the test structure must be subtracted from the final results. This is accomplished by performing a dynamic test on the bearing at 0 rpm and without lubricant. With this “dry shake” test, the only coefficients measured will be from the test rig, which can be saved and later subtracted from the

actual bearing test. Since the test structure stiffness and damping is subtracted, only the coefficients related to the bearing are left. The results of the dry shake test are shown in Fig. 25.

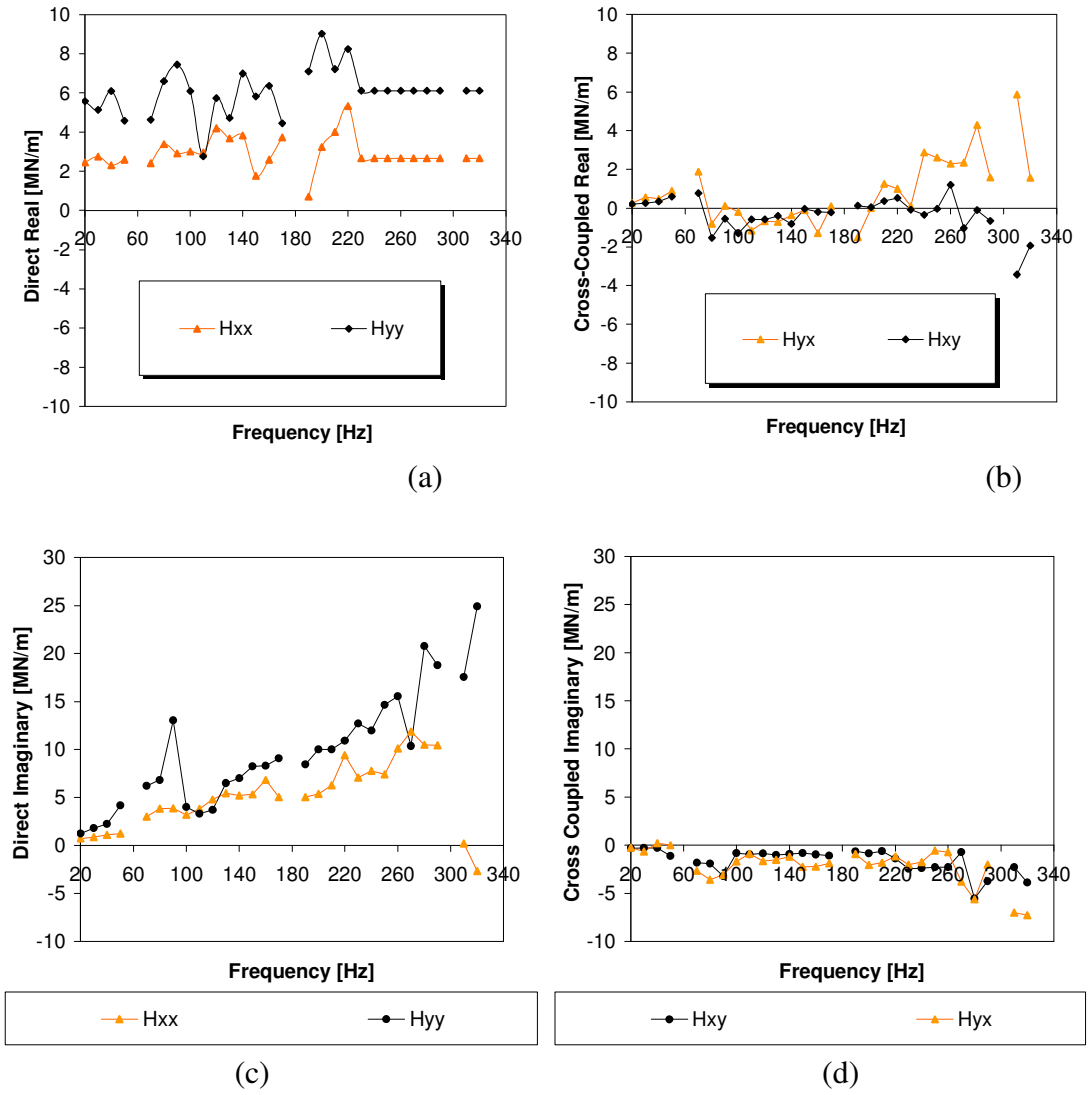

Fig. 25 LBP baseline dynamic stiffnesses for: (a) direct real, (b) cross coupled real, (c) direct imaginary, (d) cross coupled imaginary

The direct real part of the dynamic stiffness is shown in Fig. 25 (a) and is representative of the direct stiffness and added mass terms. This plot shows that the direct stiffness is fairly low where $K_{xx} = 2.57MN/m$ and $K_{yy} = 5.04MN/m$. The differences in the stiffness values for

the *x* and *y* direction are accounted for by the fact that the static loader attachment in the *y* direction produces some additional stiffness. The direct stiffness coefficients derived from Fig. 25 (c) show that the damping from the hoses, cables and support structure is minimum, with $C_{xx} = 5.21 kN..s/m$ and $C_{yy} = 6.33 kN.s/m$. Cross coupled coefficients were found to be negligible.

Test Condition Dynamic Stiffnesses

In this section, measured and predicted dynamic stiffnesses will be shown for every combination of minimum and maximum load and speed. Results for the lowest load and speed condition are shown in Fig. 26. The direct real component of the dynamic stiffnesses is shown in Fig. 26 (a). This plot shows that the stiffness coefficient K_{yy} is well modeled by the code; however the code does not model Re(H_{xx}) as well, so that K_{xx} is not predicted with the same accuracy as K_{yy}. Re(H_{yy}) decreases with an increase in frequency, which indicates a positive added mass term M_{yy} while the opposite is true with the Re(H_{xx}) dynamic stiffnesses. Re(H_{xx}) slightly increases with frequency, which indicates a negative added mass term. This negative mass term is not predicted by the code since the code is predicting the mass term to be slightly positive. Because the curvature of measured Re(H_{yy}) is larger than the predicted Re(H_{yy}), the added mass term M_{yy} will also be larger what than the theory predicted.

As seen in the loci plots in the previous section, the code does not predict any significant cross coupled stiffness, and this is also shown in the dynamic stiffnesses shown in Fig. 26 (b). The cross coupled dynamic stiffnesses Re($\boldsymbol{H_{yx}}$) increases steadily with frequency and displays a small stiffness coefficient K_{yx} and a large cross coupled mass coefficient M_{yx} due to the increasing slope. The K_{xy} and M_{xy} coefficients are both very small. It is worth noting that both cross coupled stiffness coefficients are positive, which promotes stability.

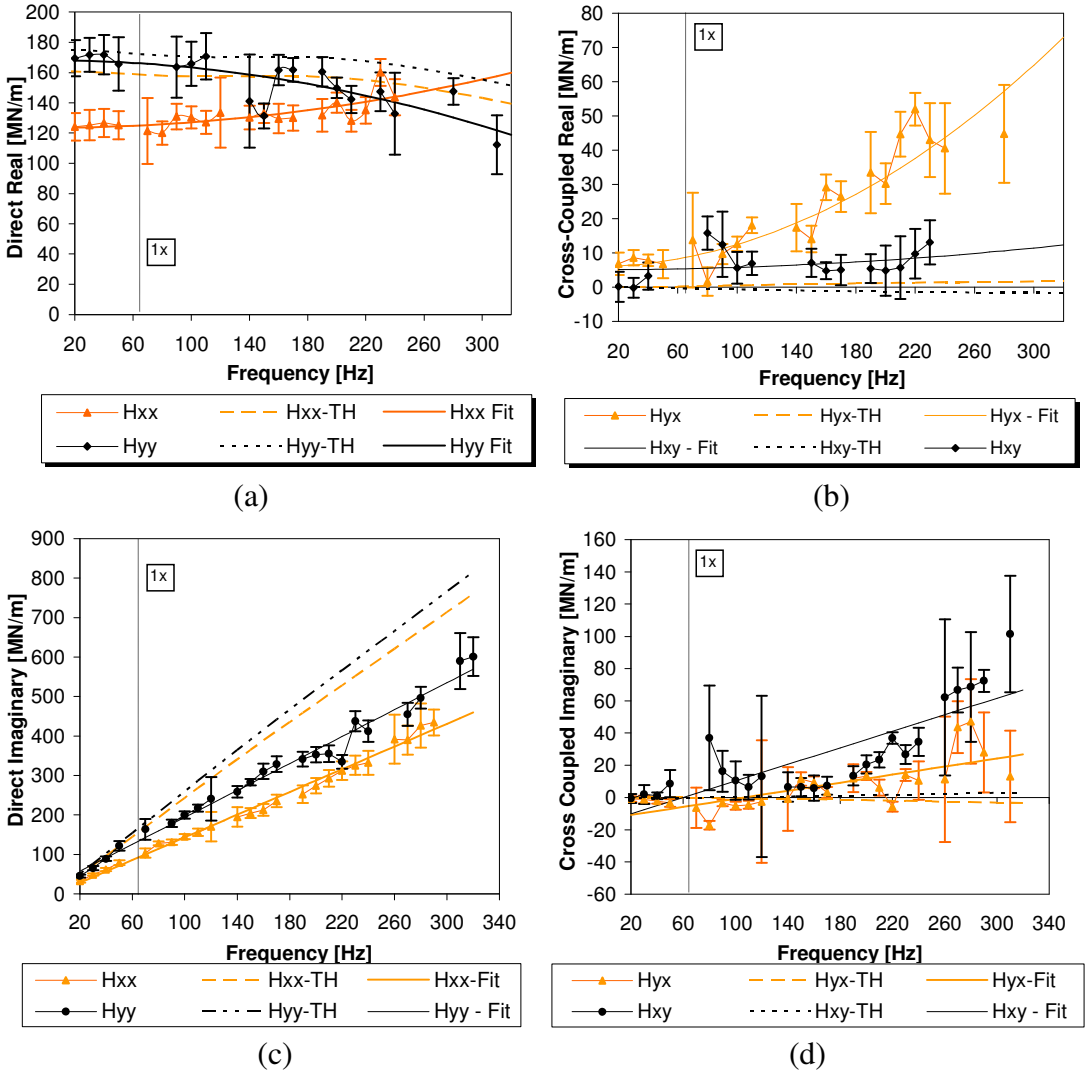

Fig. 26 LBP dynamic stiffnesses at 4000 rpm and 345 kPa for: (a) direct real, (b) cross coupled real, (c) direct imaginary, (d) cross coupled imaginary

The imaginary direct dynamic stiffnesses shown in Fig. 26 (c) increase linearly with increasing frequency as expected; however, the measured slopes are lower, which indicates that the damping is over predicted. For both experiment and prediction the loaded direction direct damping is higher than the unloaded. Cross-coupled damping of the same sign is present as seen in Fig. 26 (d), however, the amount is trivial compared to the direct terms.

The plots shown below in Fig. 27 are for the lowest speed and highest load case (4000 rpm 2412 kPa). Fig. 27 (a) shows that the direct stiffness coefficient K_{yy} is over predicted and that the coefficient K_{xx} is under predicted. Both measured dynamic stiffnesses H_{yy} and H_{xx} show negative direct added mass terms, unlike the predicted results which show some amount of positive added mass. The measured H_{yy} stiffnesses also differ from the lightly loaded condition shown in Fig. 26 because the increased loading has induced a negative added mass term M_{yy}. Overall, the direct stiffness coefficients have increased greatly compared to the 345 kPa load condition. The cross coupled stiffness coefficients have also increased over the 345 kPa condition but show the same general trend as far as mass coefficient are concerned. It should be noted that these stiffnesses remain positive for all frequencies of excitation. Imaginary cross coupled dynamic stiffnesses are shown in Fig. 27 (c), however the measured values have not changed greatly as opposed to the 345 kPa load condition. The predicted values have not kept this same trend; however, as they have continued to increase with load. Hence, the damping is not modeled well, especially in the loaded direction.

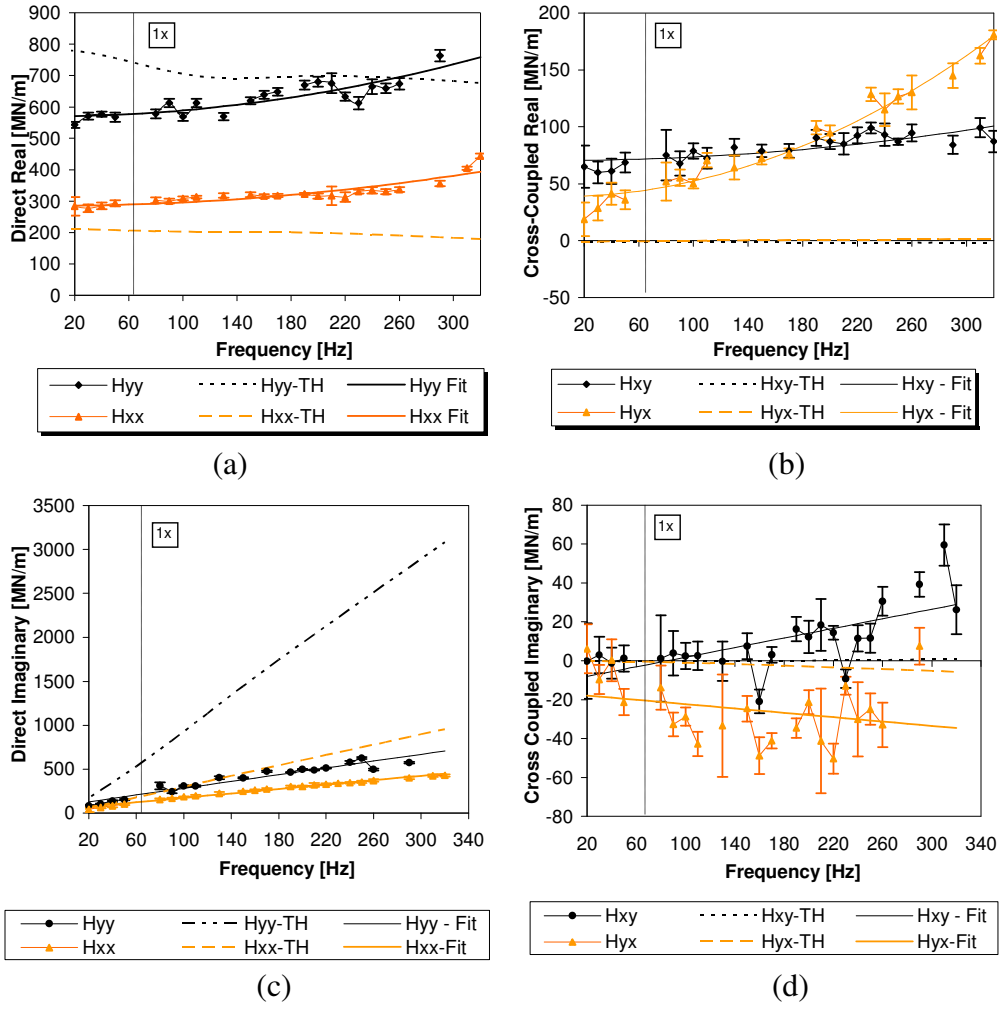

Fig. 27 LBP dynamic stiffnesses at 4000 rpm and 2412 kPa for: (a) direct real, (b) cross coupled real, (c) direct imaginary, (d) cross coupled imaginary

The dynamic stiffnesses associated with the highest speed / lowest-load condition (13000 rpm 345 kPa) are shown in Fig. 28. The measured and predicted direct stiffness coefficients have fairly good agreement, as seen in Fig. 28 (a). What the theory does not predict however is the stiffness orthotropy present in the measured results. The added mass terms are well modeled in the unloaded direction but under predicted in the loaded. Cross coupled real dynamic stiffnesses shown in Fig. 28 (b) are, as in the 4000 rpm case, not well predicted since the code does not

predict it to any great degree. The measured cross coupled real dynamic stiffnesses are of equal and opposite sign and show negative mass coefficients. Hence, the cross coupled stiffnesses are destabilizing and will be examined with a stability analysis. As shown in Fig. 28 (c), the code predicts the C_{yy} coefficients correctly but overestimates the C_{xx} coefficient.

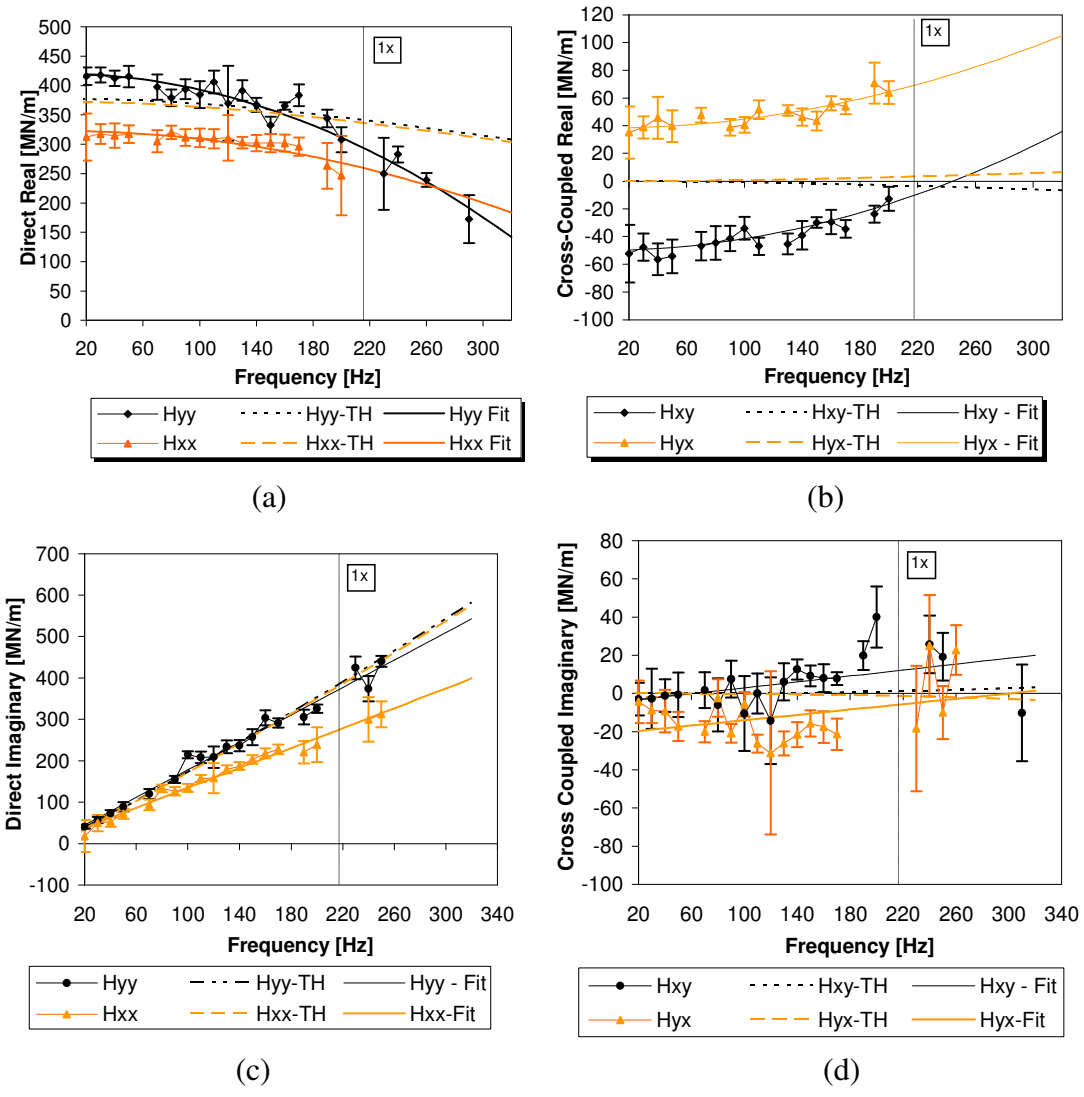

Fig. 28 LBP dynamic stiffnesses at 13000 rpm and 345 kPa for: (a) direct real, (b) cross coupled real, (c) direct imaginary, (d) cross coupled imaginary

Shown below in Fig. 29 is the highest-speed, highest-load case of 13000 rpm and 3101 kPa. The direct real dynamic stiffnesses in Fig. 29 (a) indicate that the loaded stiffness coefficient

K_{yy} is over predicted and the unloaded K_{xx} coefficient is modeled very well. The added mass coefficients are almost identical for both measured and theoretical predictions due to the similar curvatures of the stiffnesses. Some of the cross coupled stiffness coefficients and associated added mass terms were not measured well enough to comment since the uncertainties were very high. Consequently the cross coupled stiffness and mass coefficients K_{yx} and M_{yx} are not reportable at this condition. Similar problems in data repeatability were found with Re($\boldsymbol{H_{yx}}$) and the resulting C_{yx} damping term was dismissed. Overall, the damping is over predicted.

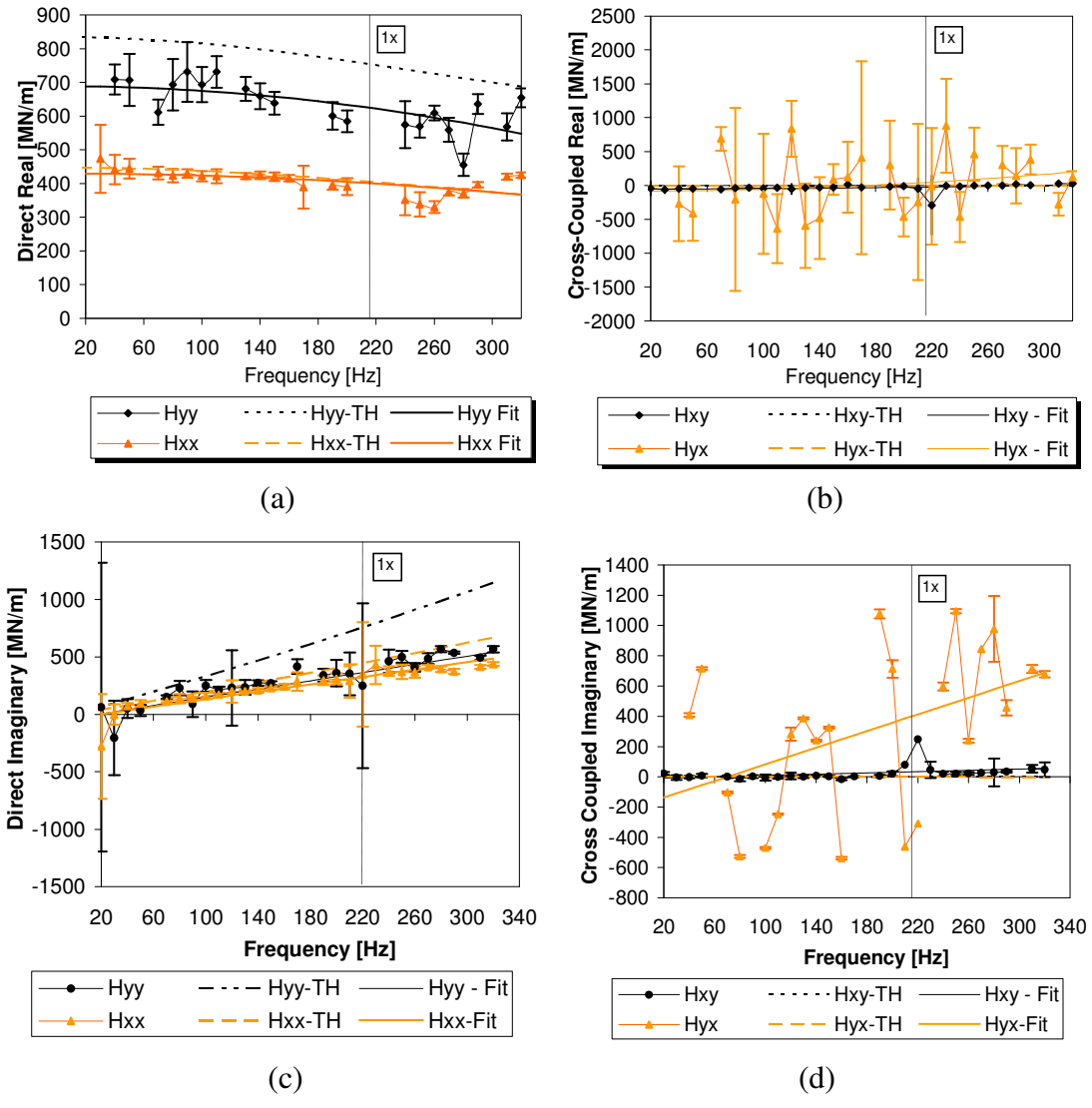

Fig. 29 LBP 13000 rpm 3101 kPa dynamic stiffnesses for: (a) direct real, (b) cross coupled real, (c) direct imaginary, (d) cross coupled imaginary

Stiffness Coefficients

Shown in Fig. 30 below is the effect of unit load on the stiffness coefficients. The plots show that the stiffness is a linear if not slightly parabolic function of unit load. The stiffness coefficient K_{yy} is well modeled at the lower loads; however, as load increases the code tends to over predict the stiffness. The unloaded stiffness coefficient K_{xx} on the other hand is well modeled at all loads for the 4000 rpm and 7000 rpm cases and slightly over predicts stiffness at the higher speeds. Stiffness orthotropy is minimum at the lower loadings but increases rapidly with load.

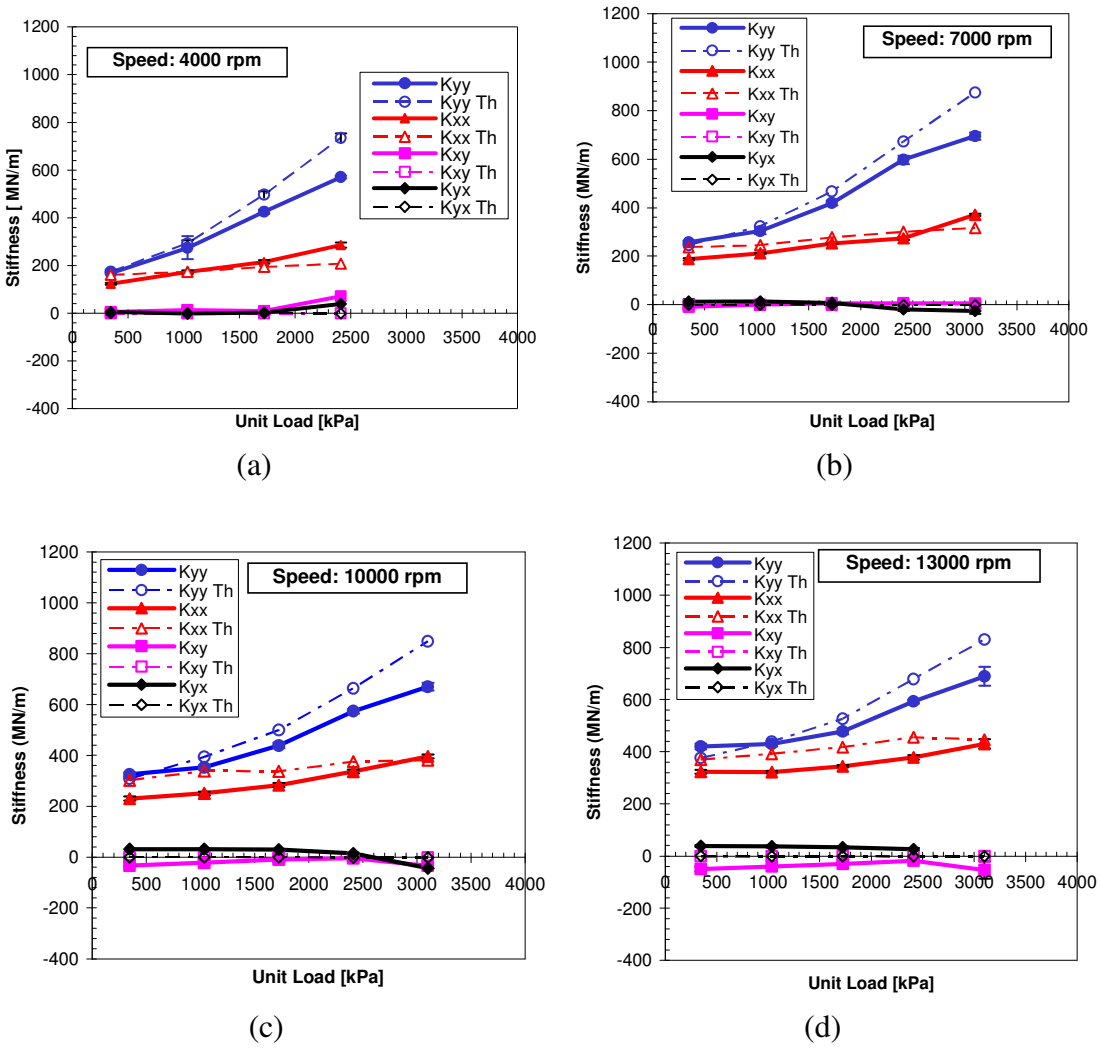

Fig. 30 LBP direct and cross coupled stiffness coefficients vs. load for varying speed: (a) 4000 rpm, (b) 7000 rpm, (c) 10000 rpm, (d) 13000 rpm

The cross coupled coefficients are all relatively small compared to the direct coefficients. However, they are generally equal and opposite to each other at the higher speeds as seen in Fig. 31. Hence, these coefficients could destabilize the bearing.

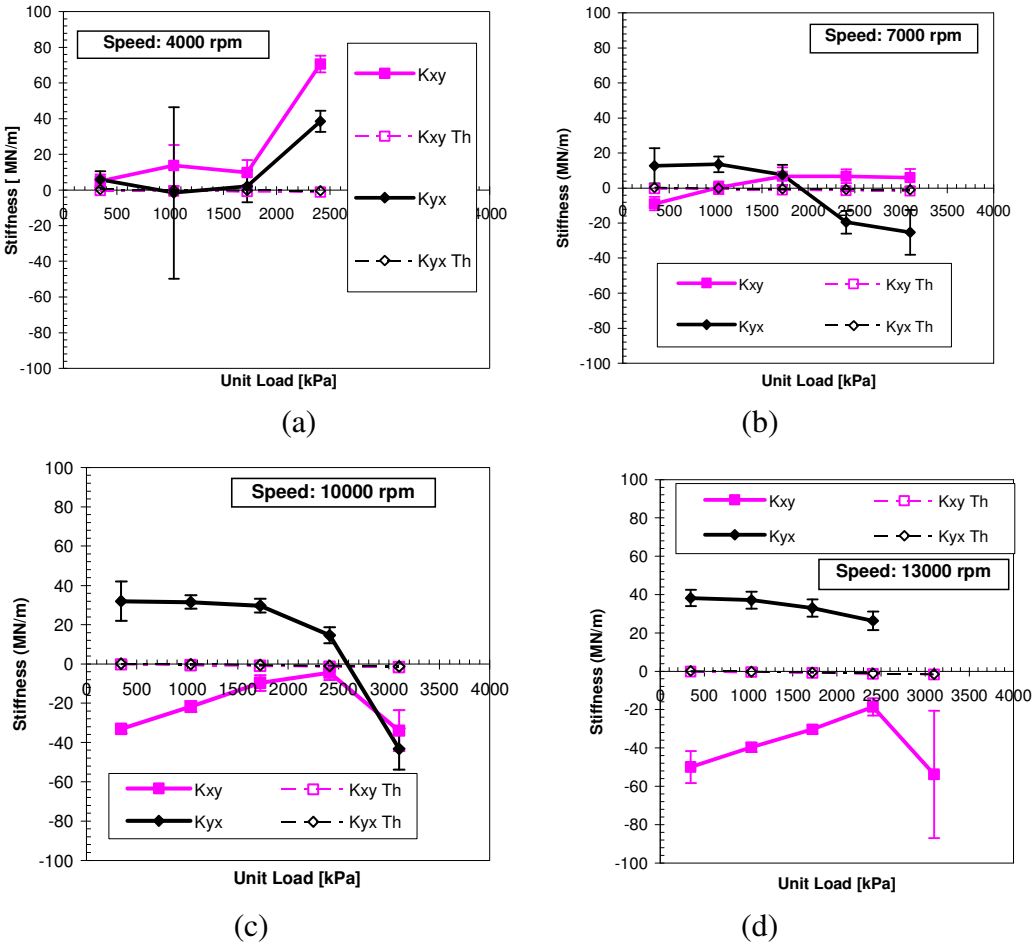

Fig. 31 LBP cross coupled stiffness coefficients vs. load for varying speed: (a) 4000 rpm, (b) 7000 rpm, (c) 10000 rpm, (d) 13000 rpm

The effect of speed on the stiffness coefficients of the bearing is shown in Fig. 32. While a linear relationship does seem to exist between the two, the effect is not as large as that observed in the previous section where unit load was the variable. Under most conditions, the direct

stiffnesses grow with increasing speed. However at the higher load conditions the stiffness coefficient K_{yy} remains constant regardless of speed.

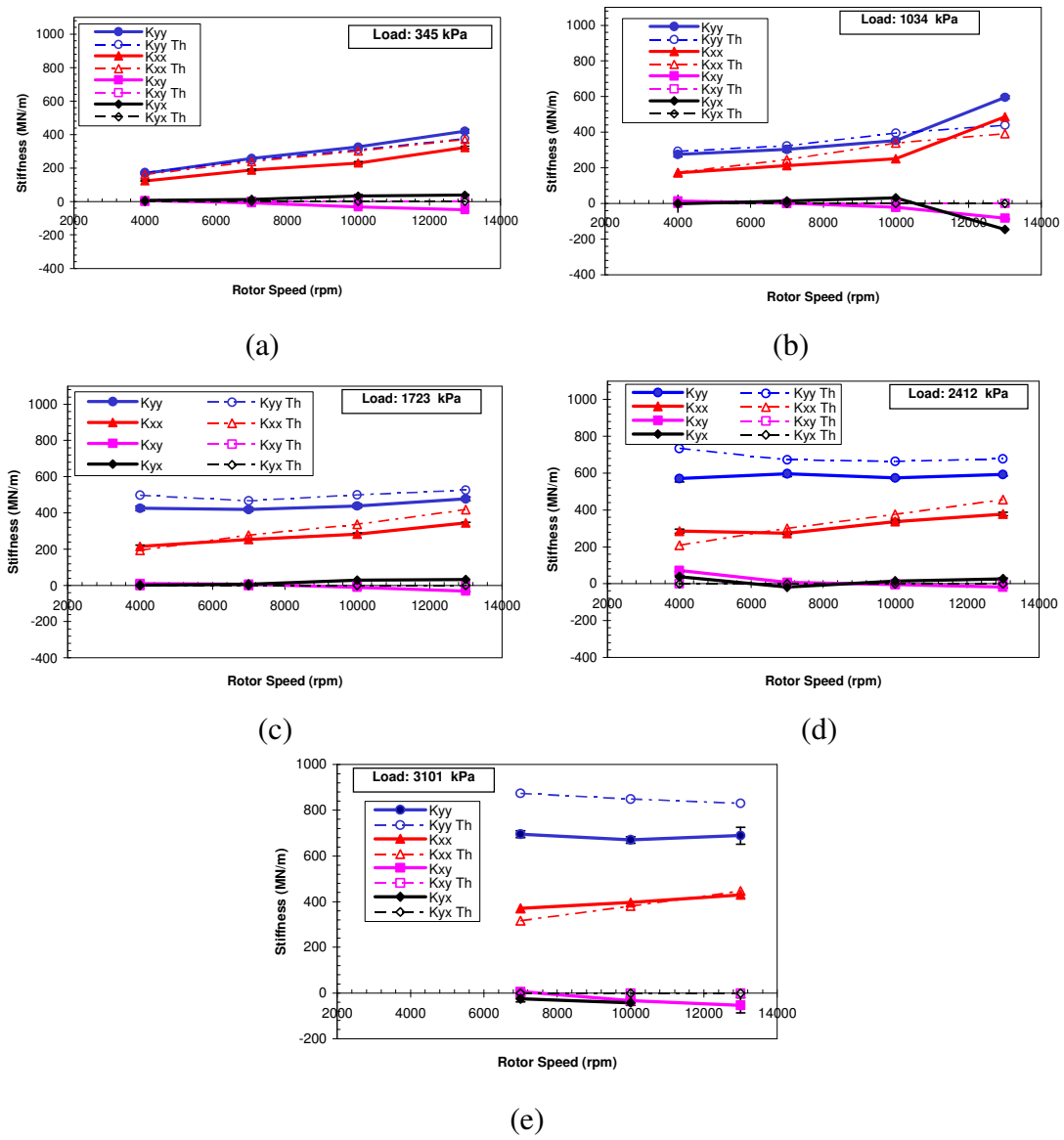

Fig. 32 LBP direct and cross-coupled stiffness coefficients vs. speed for varying load: (a) 346 kPa, (b) 1034 kPa, (c) 1723 kPa, (d) 2412 kPa, (e) 3101 kPa

The cross coupled stiffness coefficients versus speed are shown in Fig. 33.

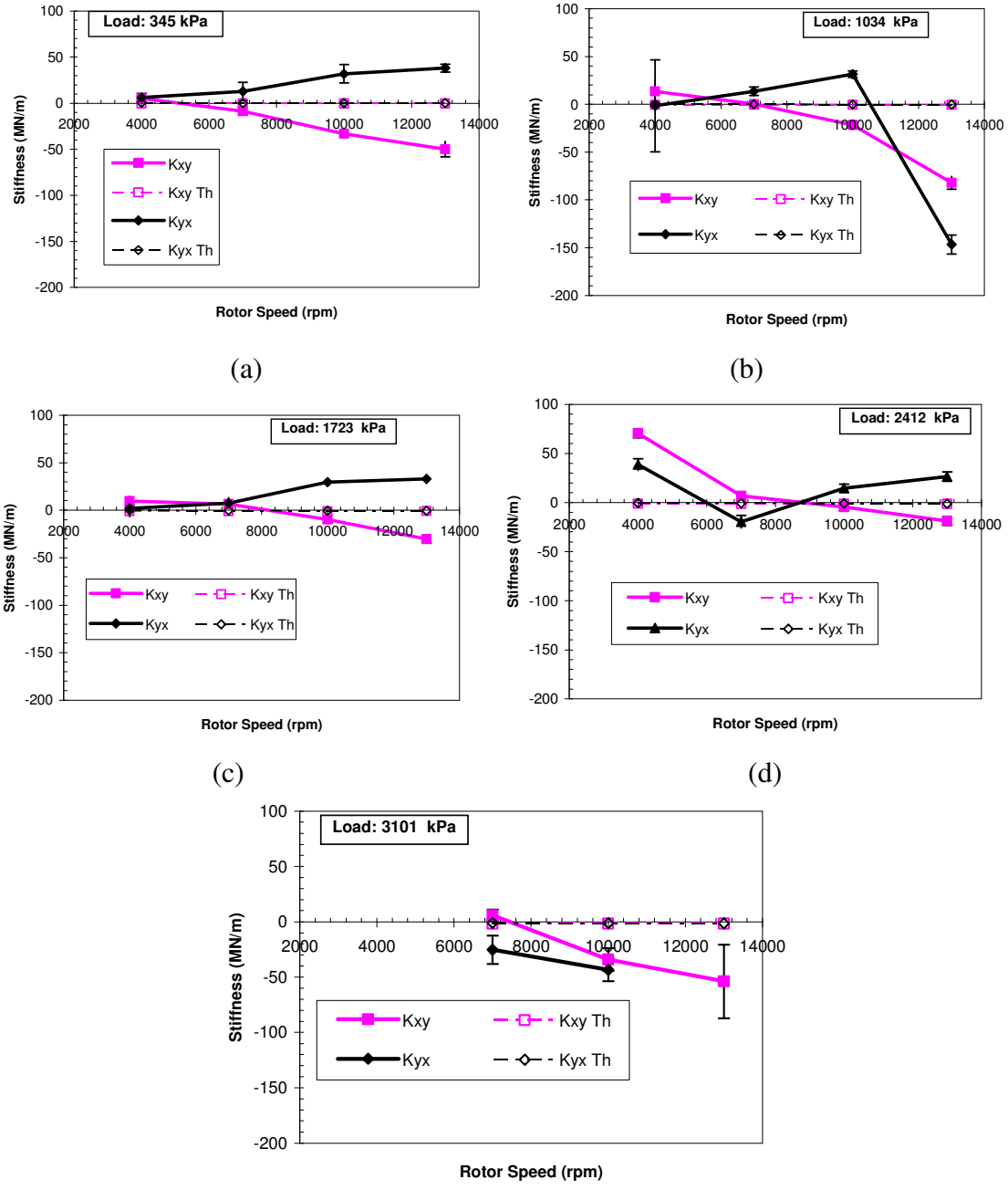

Fig. 33 LBP cross-coupled stiffness coefficients vs. speed for varying load: (a) 346 kPa, (b) 1034 kPa, (c) 1723 kPa, (d) 2412 kPa, (e) 3101 kPa

Damping Coefficients

Shown in Fig. 34 is how the damping coefficients vary with unit load for various speeds. The measured damping coefficients vary very little with load, and the cross coupled coefficients are small relative to the direct coefficients. The direct damping is modeled well at low loads; however, it is greatly over predicted with increasing load, especially in the loaded direction. However, as speed is increased the predictions became more reliable.

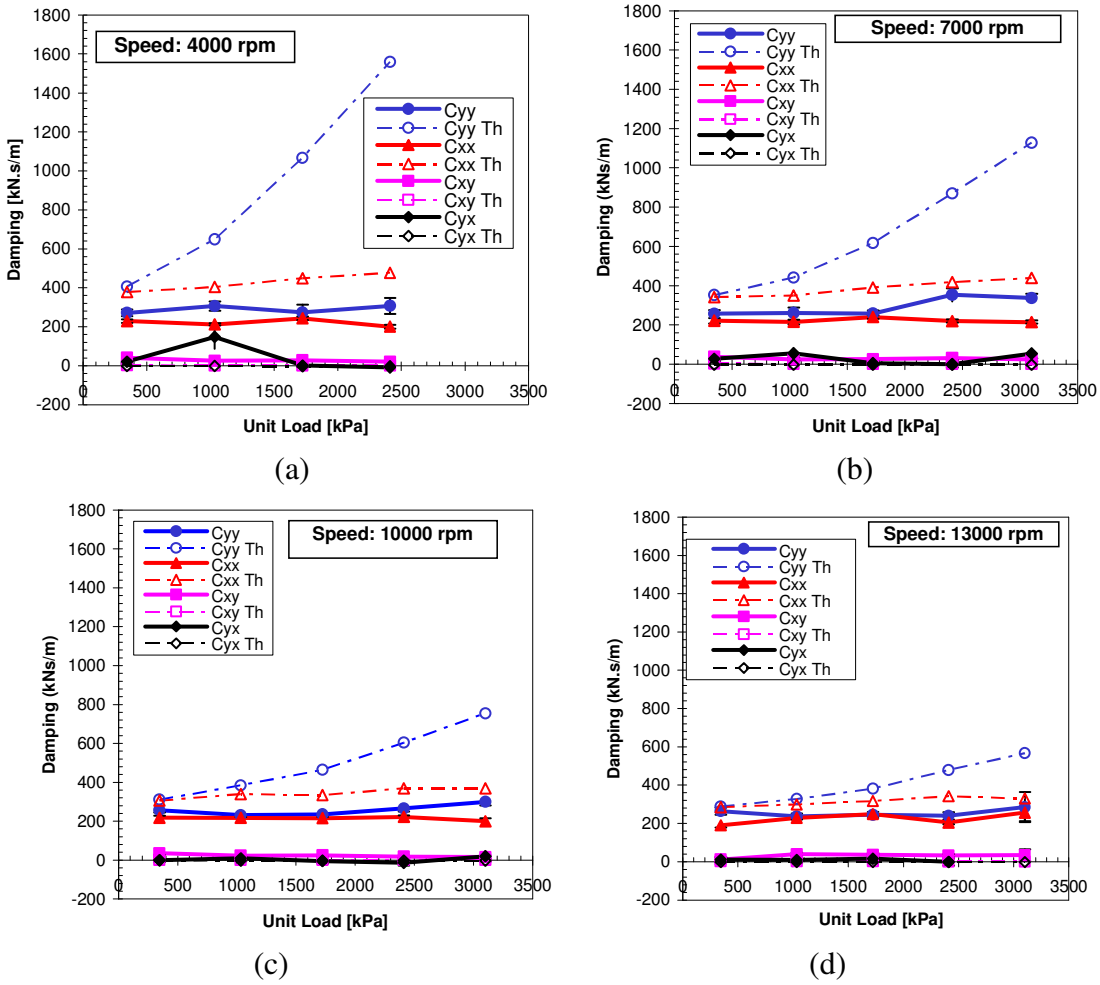

Fig. 34 LBP direct and cross coupled damping coefficients vs. load for varying speed: (a) 4000 rpm, (b) 7000 rpm, (c) 10000 rpm, (d) 13000 rpm

Cross coupled damping versus load is shown in Fig. 35. C_{xy} remains almost constant with increasing load at approximately 30 kN.s/m, while C_{yx} varies considerable with no discernable pattern.

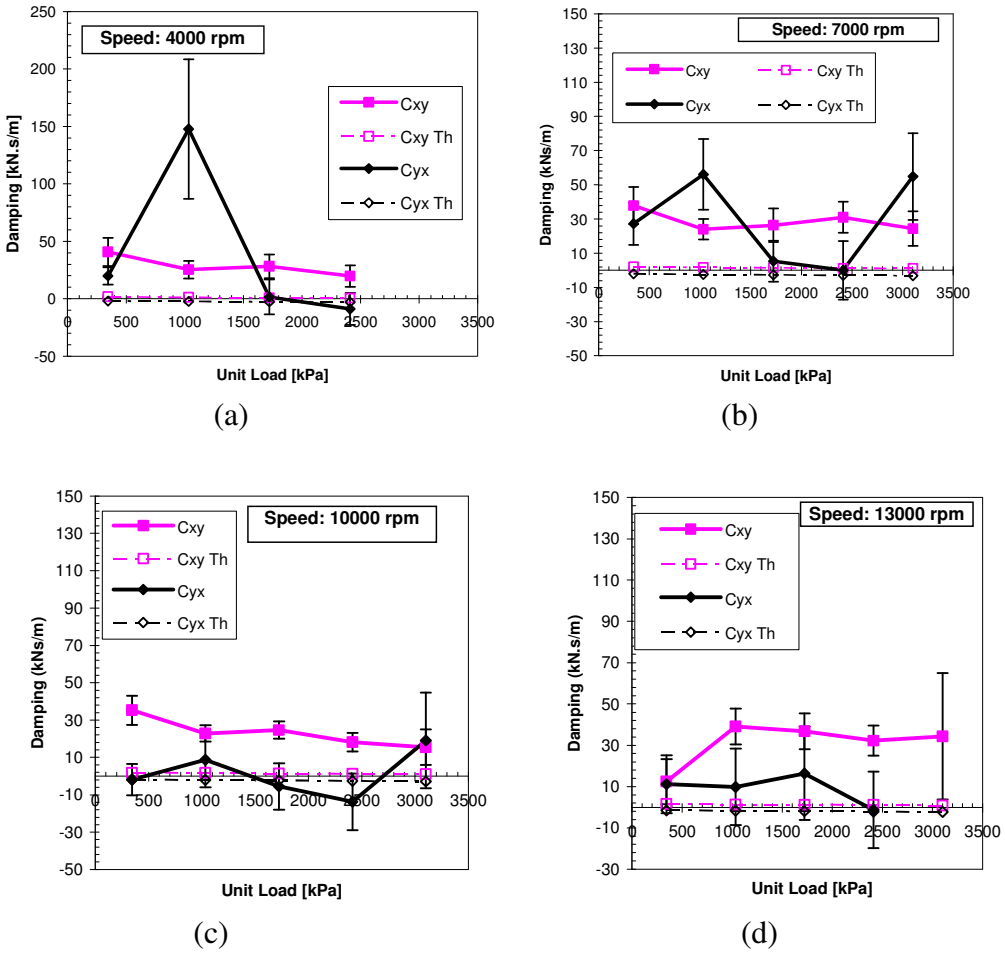

Fig. 35 LBP cross coupled damping coefficients vs. load for varying speed: (a) 4000 rpm, (b) 7000 rpm, (c) 10000 rpm, (d) 13000 rpm

Damping as a function of rotor speed is shown in Fig. 36. As with unit load, rotor speed does not seem to impact the damping coefficients to any great degree. Code predictions show good agreement at low load, but the code predicts that the damping will rise substantially as load is increased (especially at low speeds) which is not seen in the measured results.

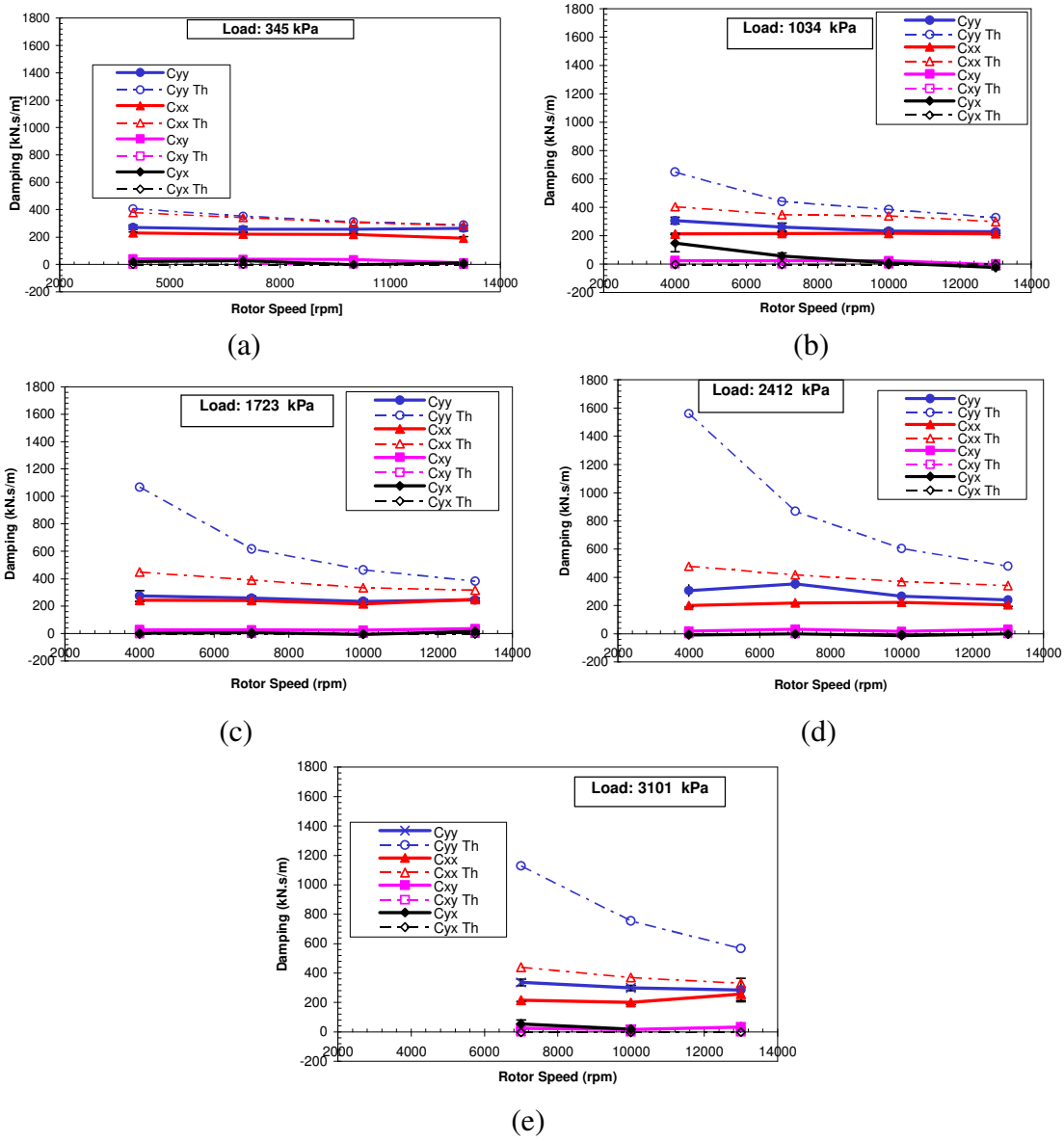

Fig. 36 LBP direct and cross-coupled damping coefficients vs. speed for varying load: (a) 346 kPa, (b) 1034 kPa, (c) 1723 kPa, (d) 2412 kPa, (e) 3101 kPa

Cross coupled damping coefficients vs. speed are shown in Fig. 37.

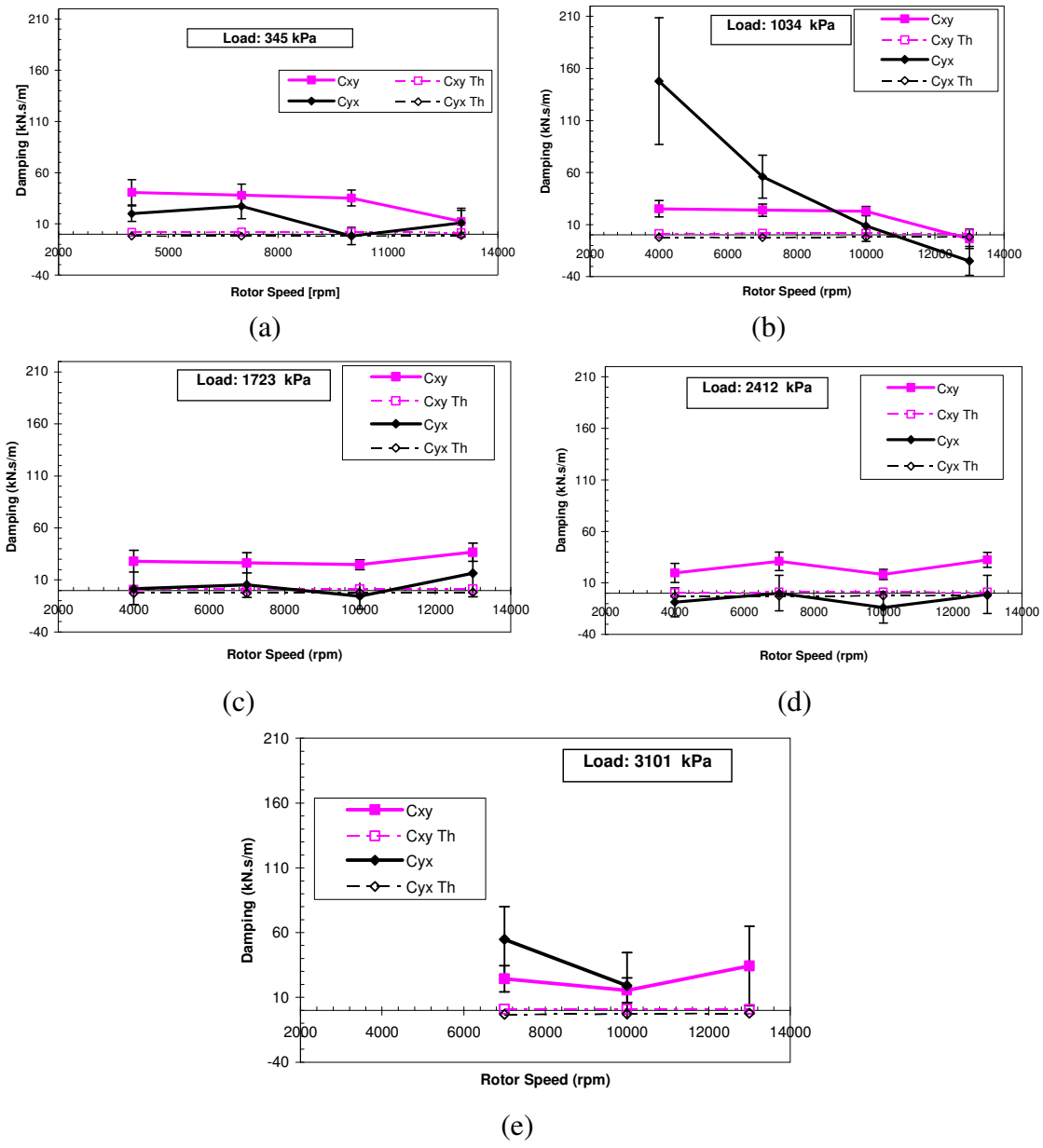

Fig. 37 LBP cross-coupled damping coefficients vs. speed for varying load: (a) 346 kPa, (b) 1034 kPa, (c) 1723 kPa, (d) 2412 kPa, (e) 3101 kPa

Mass Coefficients

Direct added mass coefficients are shown below in Fig. 38 versus unit loading. At the lowest shaft speed, all of the mass coefficients became more negative as load increased, which meant that the dynamic stiffnesses were increasing with increasing excitation frequency. However, at the other speeds there was no real change of the mass coefficient due to unit loading. It is worth noting that M_{xx} is near zero for many points at the 7 krpm and 10 krpm speeds as seen in Fig. 38 (b) and (c). At these conditions the lack of an added mass term should lead to consideration of a frequency dependent [K][C] model instead of a frequency independent [K][C][M] model.

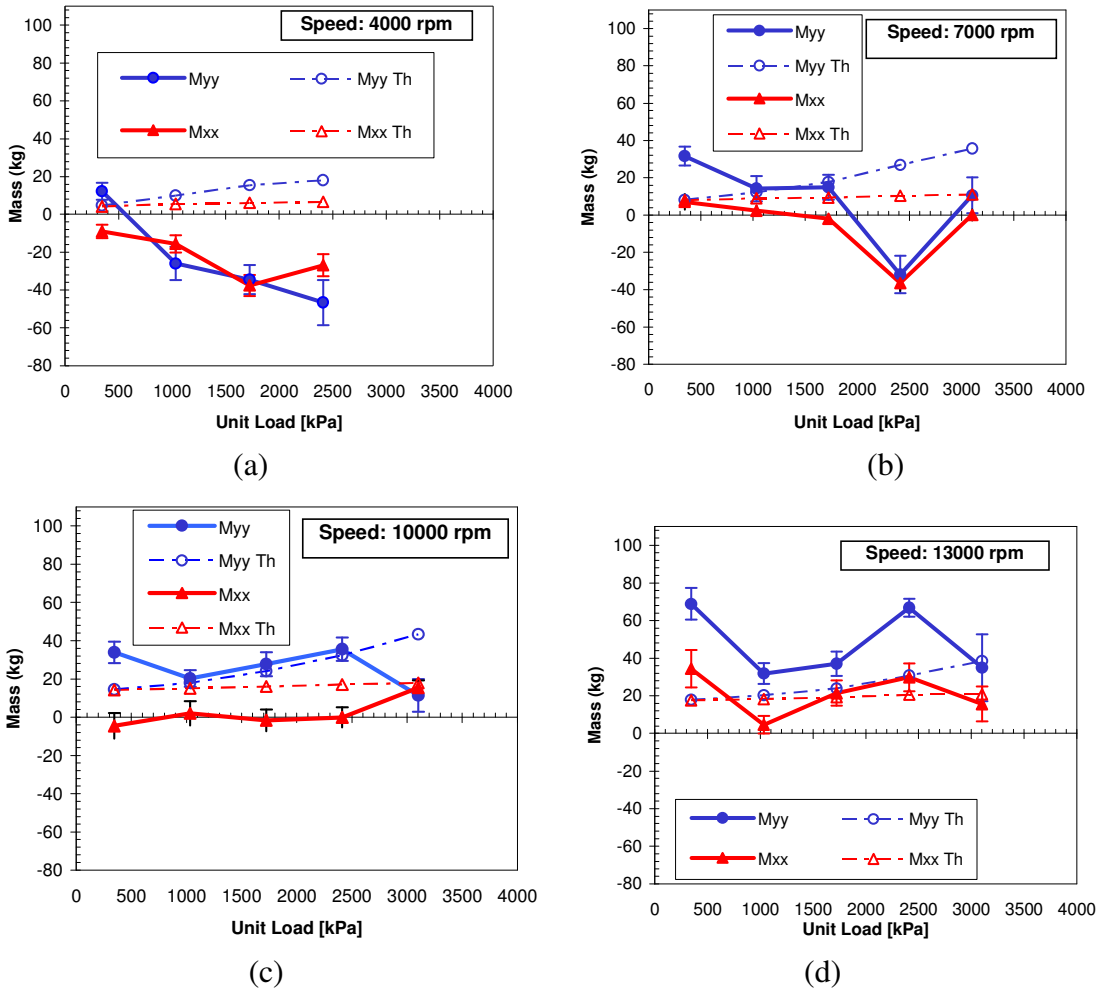

Fig. 38 LBP direct mass coefficients vs. load for varying speed: (a) 4000 rpm, (b) 7000 rpm, (c) 10000 rpm, (d) 13000 rpm

The cross coupled mass coefficients versus load are shown in Fig. 39. All of the coefficients were found to have the same negative sign, which means that stability will not be impacted. Predicted cross coupled mass coefficients generally remain negligible while the predicted direct coefficients are always positive and increase linearly with speed.

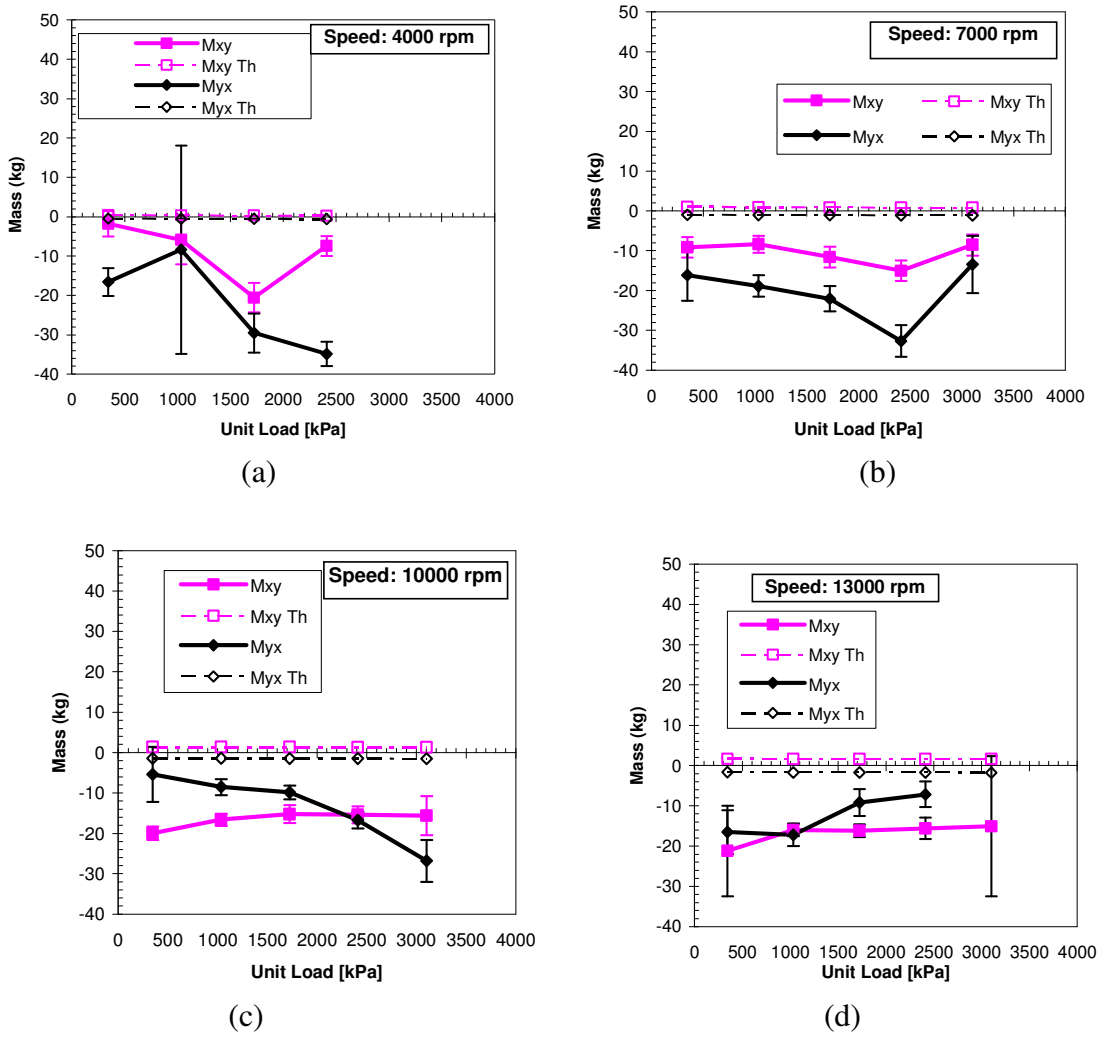

Fig. 39 LBP cross coupled mass coefficients vs. load for varying speed: (a) 4000 rpm, (b) 7000 rpm, (c) 10000 rpm, (d) 13000 rpm

The effect of rotor speed on the direct added mass coefficients is shown in Fig. 40. Rotor speed has a large affect on the direct added mass coefficients. Generally these coefficients grow more positive with speed and remain positive for almost all conditions. The coefficients M_{yy}

and M_{xx} seem to grow positive at the same rate. however the magnitude of M_{yy} remains higher than M_{xx}.

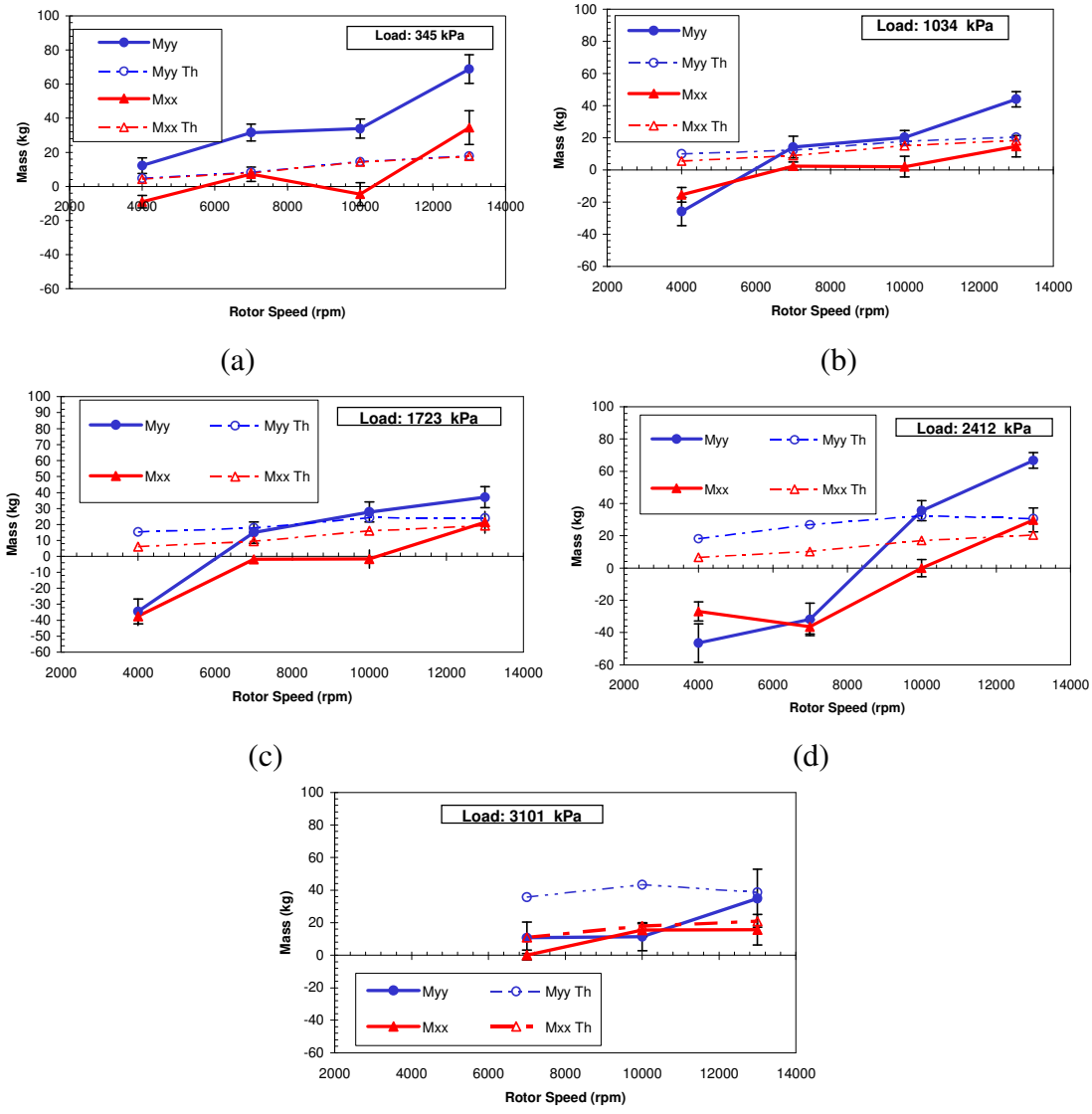

Fig. 40 LBP direct mass coefficients vs. speed for varying load: (a) 346 kPa, (b) 1034 kPa, (c) 1723 kPa, (d) 2412 kPa, (e) 3101 kPa

Fig. 41 shows the cross coupled mass coefficients versus rotor speed. As noted before, all of the coefficients are negative, with magnitudes that are generally smaller than the direct terms.

The cross coupled coefficients also show little change throughout the speed range compared to the direct terms. As stated before, since the cross coupled coefficients are all negative they should not have an impact on the stability of the bearing.

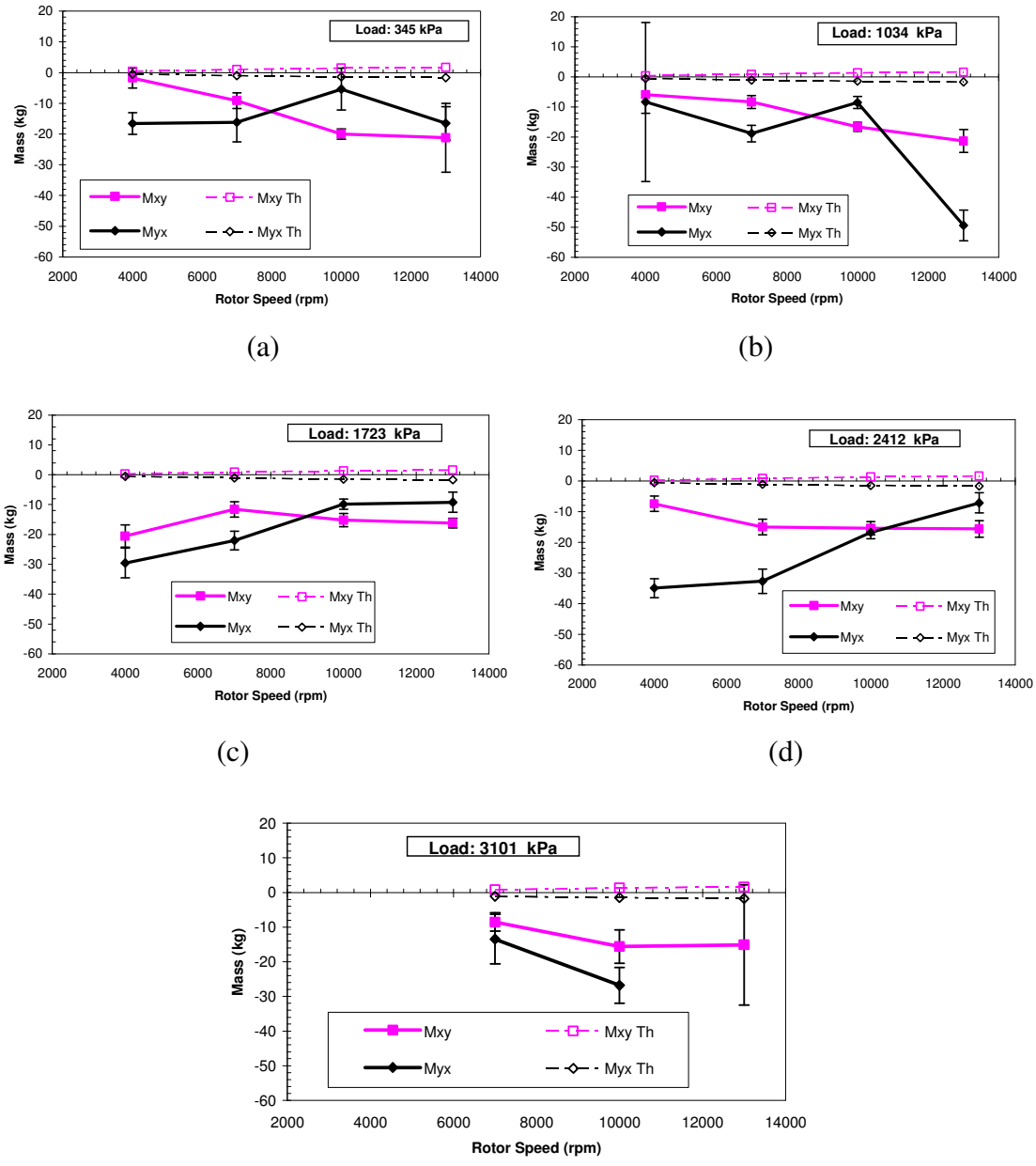

Fig. 41 LBP cross-coupled mass coefficients vs. speed for varying load: (a) 346 kPa, (b) 1034 kPa, (c) 1723 kPa, (d) 2412 kPa, (e) 3101 kPa

Static vs. Dynamic Stiffness

The plots in Fig. 42 show the relationship between dynamic and static stiffness. The dynamic stiffness was obtained during the dynamic test and is simply the stiffness coefficient obtained at the zero frequency *y* intercept. The static stiffness was obtained by plotting static load vs. bearing displacement and recording the slope of this curve at the various conditions. After the slope is found, that value is designated as the static stiffness. The plot of Fig. 42 (a) displays a good relationship between the two stiffness values at the lower loads but the dynamic stiffness becomes much higher than the static stiffness as the load continues to increase. In Fig. 42 (b) the static stiffness actually decreases with increasing load, while the dynamic stiffness increases. Most load conditions at the higher speeds show relatively good agreement between the stiffness values with the stiffness increasing linearly with load.

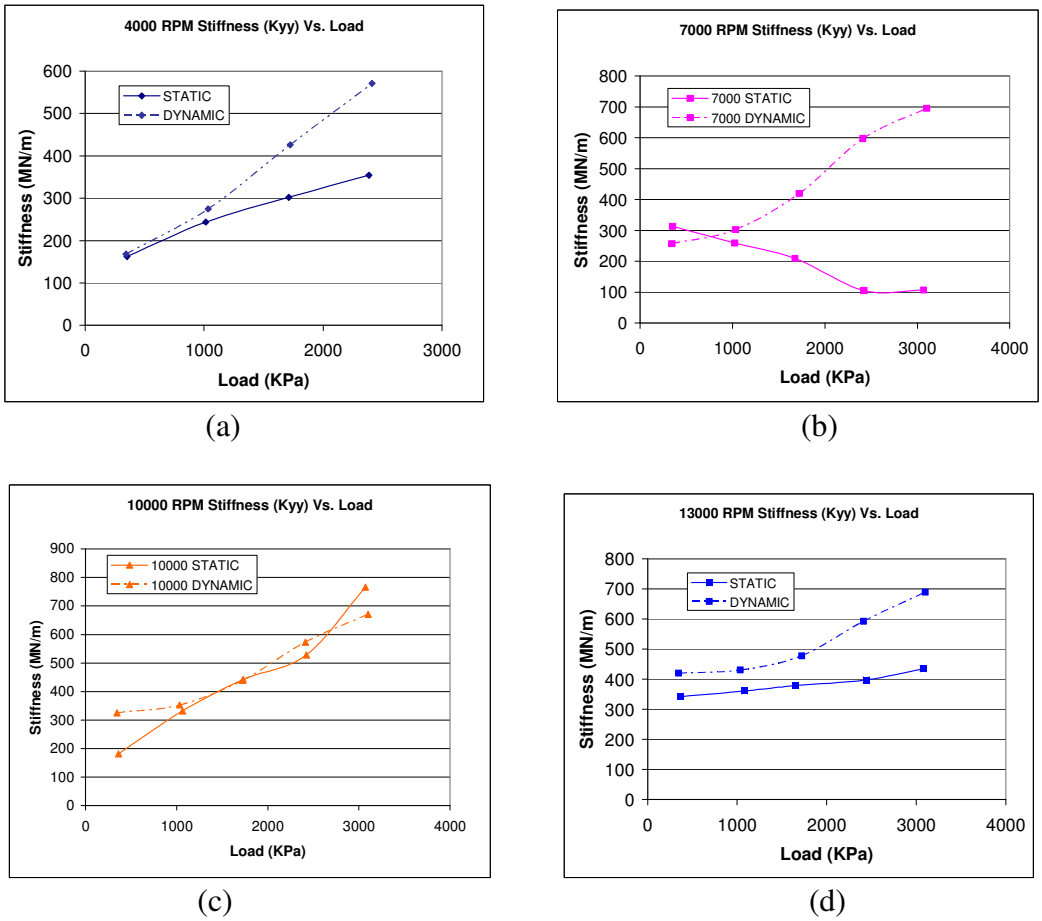

Fig. 42 LBP comparison of dynamic stiffness coefficients to static stiffness for different speeds: (a) 4000 rpm, (b) 70000 rpm, (c) 10000 rpm, (d) 13000 rpm

Whirl Frequency Ratio

The whirl frequency ratio is used to characterize the stability characteristics of a bearing. It is defined as being the ratio of the whirl frequency or processional frequency of the shaft to the rotational speed at which the rotor becomes unstable which is also called the onset speed of instability.

$$WFR = \frac{\Omega}{\Omega_{osi}} \tag{19}$$

This definition shows that the smaller the WFR, the more stable the system will be because a small WFR in effect has raised the onset speed of instability. A typical plain journal bearing will have a WFR of about .5. The WFR can be found using equations taken from the work of San Andres [29] in which the fluid inertia was included in the calculation of the WFR.

The WFR was calculated to be a pure imaginary number at all conditions. Therefore, the WFR is effectively equal to zero. In conclusion, the bearing has achieved infinite stability for all load and speed conditions.

Pad Flutter

Pad flutter data were taken to observe the dynamic behavior of both the loaded and unloaded pads. To do this, two proximity probes were installed on the pads which recorded the pad position with time as shown in Fig. 43. These data were then sent to a dynamic signal analyzer which allowed an FFT to be conducted. In Fig. 44 is a spectrum for two different operating conditions. The frequencies are fairly clean with only the synchronous motion exhibiting any significant behavior. Time traces were also recorded to analyze the magnitude of the pad displacements; however, all of these displacements were negligible. This would imply that the pad preload was sufficient to stabilize the unloaded pad.

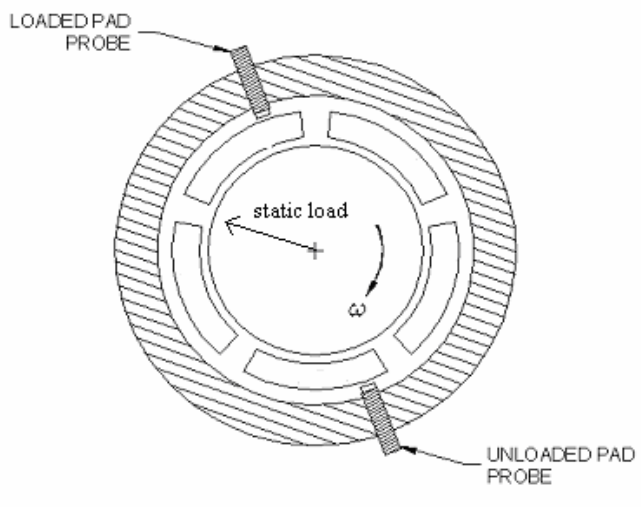

Fig. 43 LBP pad flutter probe installation

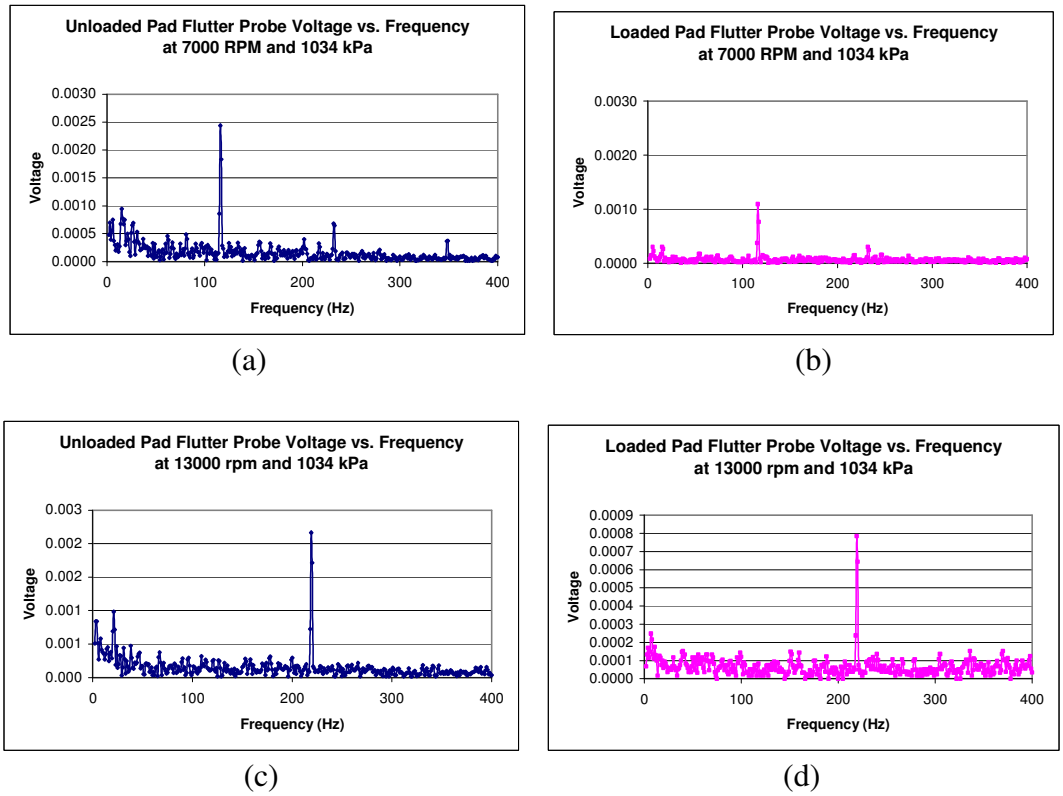

Fig. 44 LBP pad flutter voltage vs. frequency at 1034 kPa for: (a) unloaded pad 7000 rpm, (b) loaded pad 7000 rpm, (c) unloaded pad 13000 rpm, (d) loaded pad 13000 rpm

LOP CONFIGURATION RESULTS AND PREDICTIONS

Static Results

Loci Plots

The Loci plots shown in Fig. 45 show the displacement of the bearing due to the applied load. As compared to the LBP case there is very little cross coupling seen for all conditions. Also, there is almost no cross coupling present in the theoretical predictions. The maximum eccentricity reached is 70%, however, the code only predicts a 50% maximum, so the code is over predicting the stiffness.

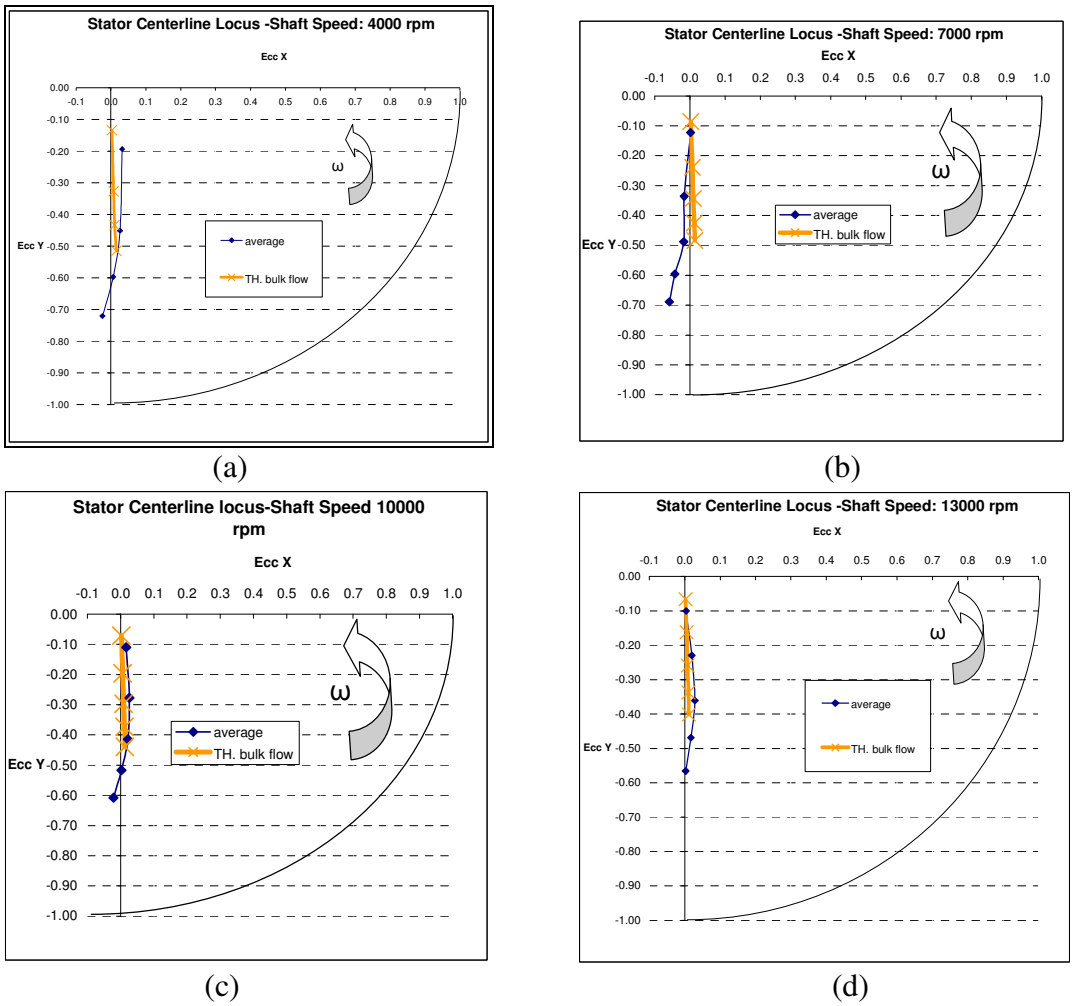

Fig. 45 LOP predicted and measured loci plots for various shaft speeds: (a) 4000 rpm, (b) 7000 rpm, (c) 10000 rpm, (d) 13000 rpm

The plot in Fig. 46 displays all of the measured loci overlaid for comparison reasons. As the speed grows, the load capacity continues to steadily increase with the 13000 rpm condition having the greatest stiffness due to its lower eccentricities.

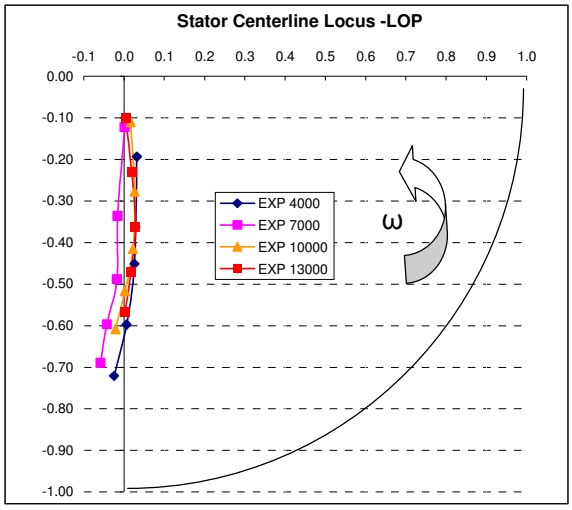

Fig. 46 LOP comparison of measured loci plots for different speeds

Attitude Angle

The attitude angle versus unit load plot is given for both measured and predicted cases in Fig. 47. The general trend of the plots, except for the 7 krpm case is that of a decreasing attitude angle with increasing bearing load. Observation of the 7krpm condition shows a slight negative increase in the attitude angle with load. Fig. 47 (b) plots the predicted attitude angle where the maximum angle is very small, only 1.75° as opposed to 10° for the measured case.

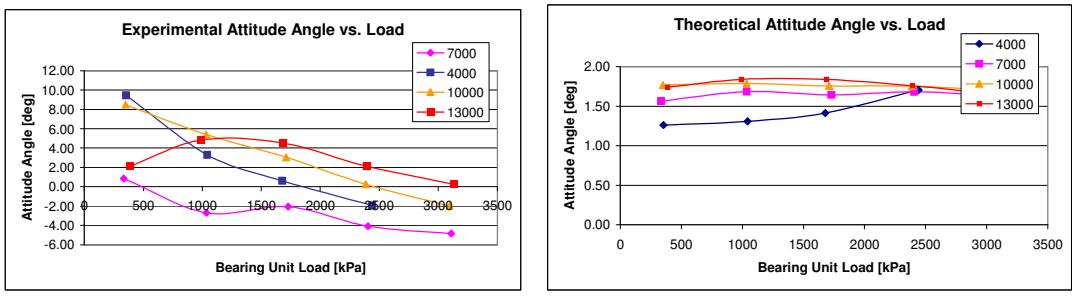

(a) (b)

Fig. 47 LOP attitude angle change with load for (a) measured test and (b) predicted XLTRC

Power Loss

Power loss versus speed is shown in Fig. 48 for the measured and predicted results. Good agreement is shown at most conditions with losses increasing linearly with speed just as in the LBP configuration. Maximum power loss is approximately 15 kW.

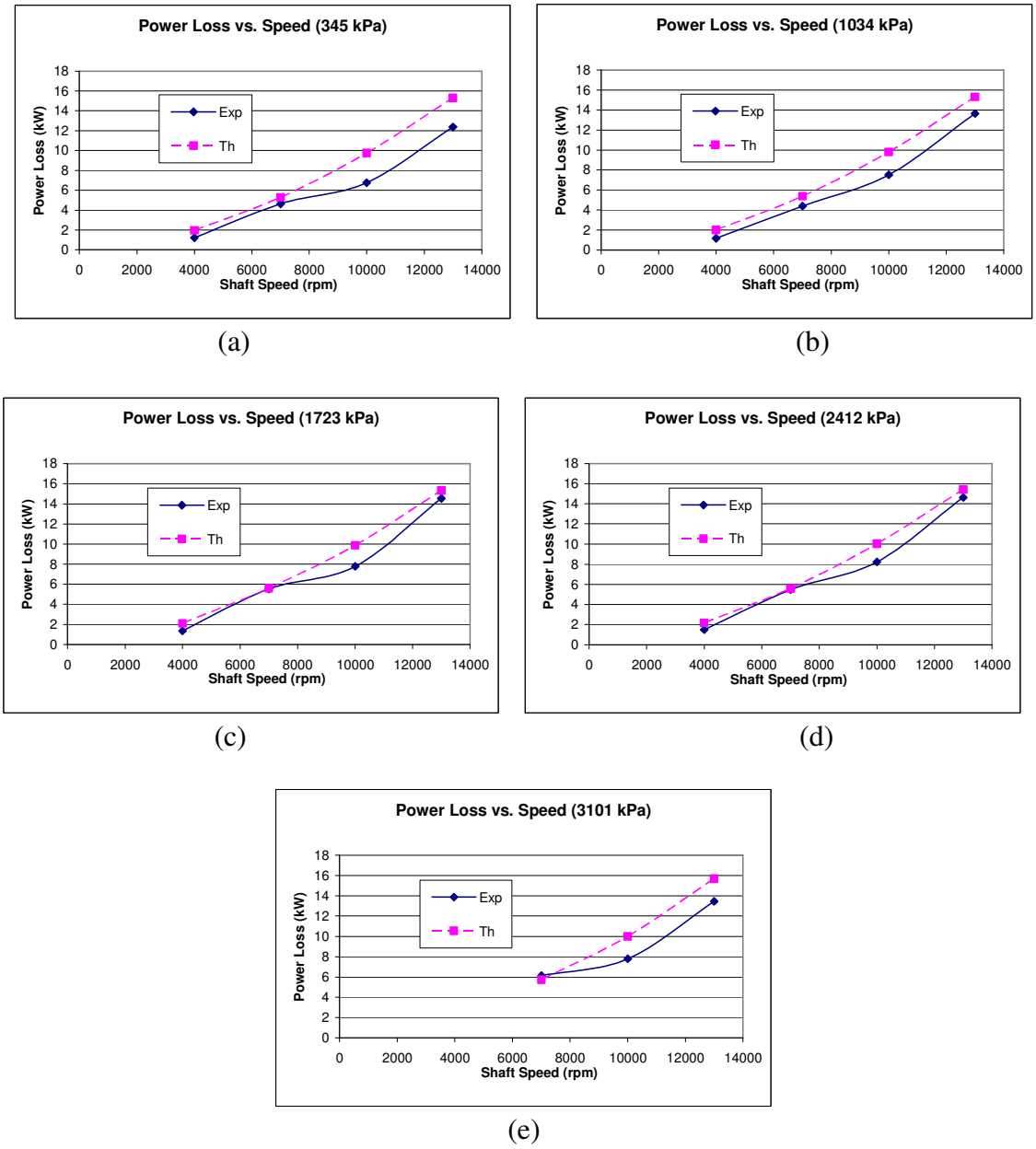

Fig. 48 LOP power loss versus shaft speed comparisons with theory for varying loads: (a) 345 kPa, (b) 1034 kPa, (c) 1723 kPa, (d) 2412 kPa, (e) 3101 kPa

Shown in Fig. 49 is a plot of power loss versus bearing unit load for each shaft speed. Power loss is a function of speed but not load.

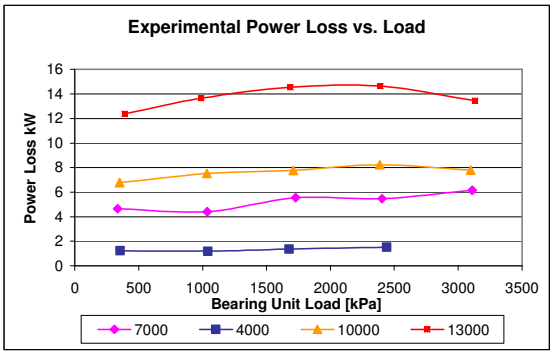

Fig. 49 LOP power loss vs. load for different shaft speeds

Pad Temperature Data

Configuration of the temperature probes is shown in Fig. 50 where the load is applied directly to pad number 1. Unlike the LBP case, all of the probes were working correctly during this test.

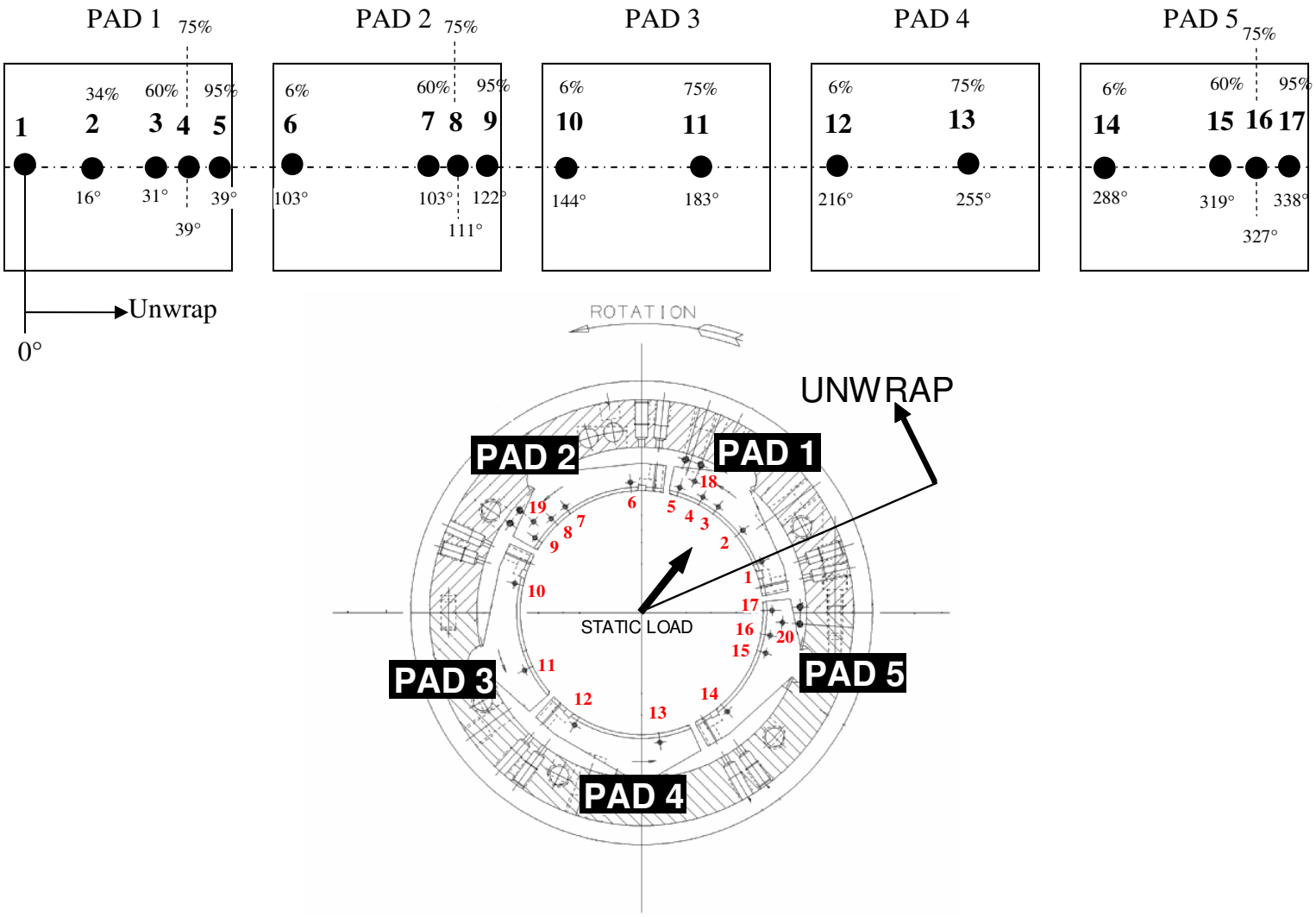

Fig. 50 LOP thermocouple layout

Temperature profiles along the pad are shown in Fig. 51 where the highest pad temperatures are associated with pad number 1 since it is under the most load. Temperatures decrease with pad number 2 and continue to fall until they increase again with pad number 5. Maximum pad temperatures appear to be slightly higher than the LBP case at 97°C.

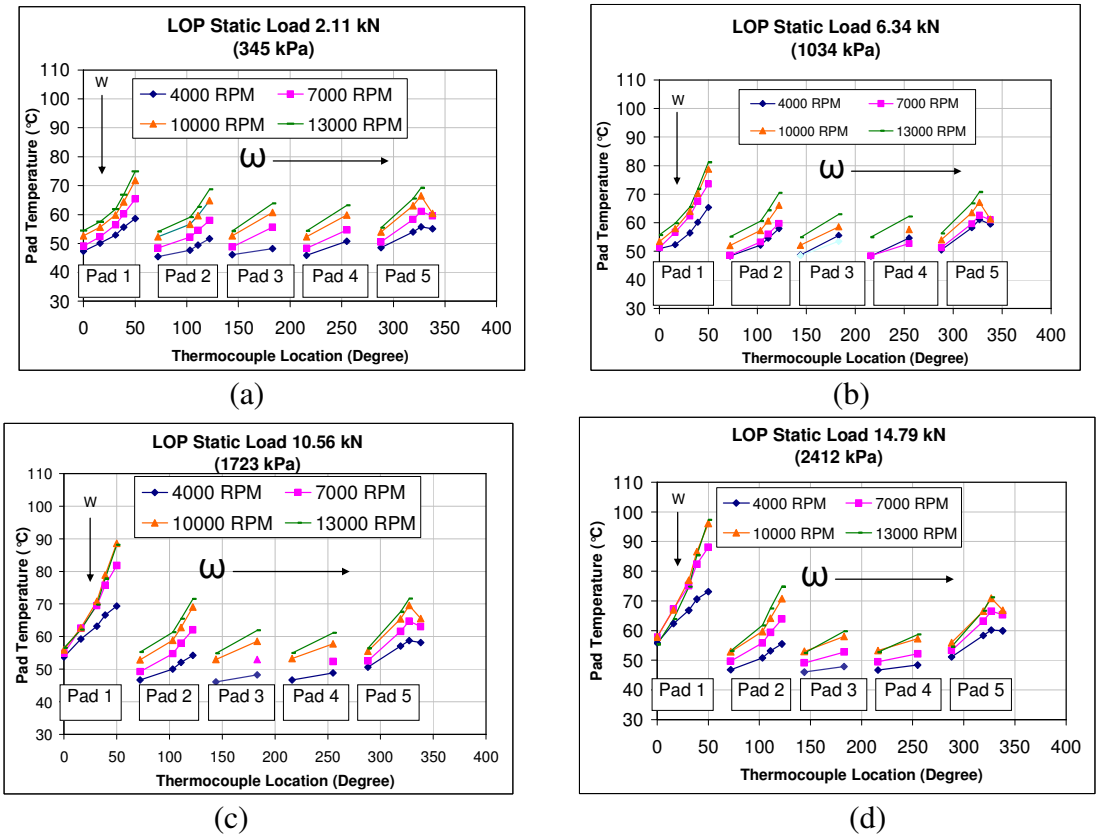

Fig. 51 LOP pad temperatures as they vary with location for load conditions of: (a) 346 kPa, (b) 1034 kPa, (c) 1723 kPa, (d) 2412 kPa, (e) 3101 kPa

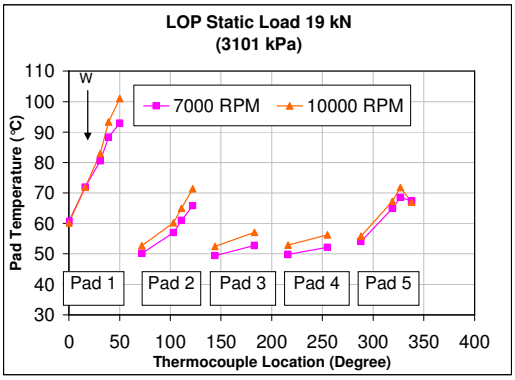

(e)

Fig. 51 "Continued"

Shown in Fig. 52 below is a comparison between the measured and predicted maximum bearing temperatures. Both results show temperatures that rise at similar rates with increasing speed. Overall, the model over predicts the bearing temperatures to a greater degree than with the LBP configuration.

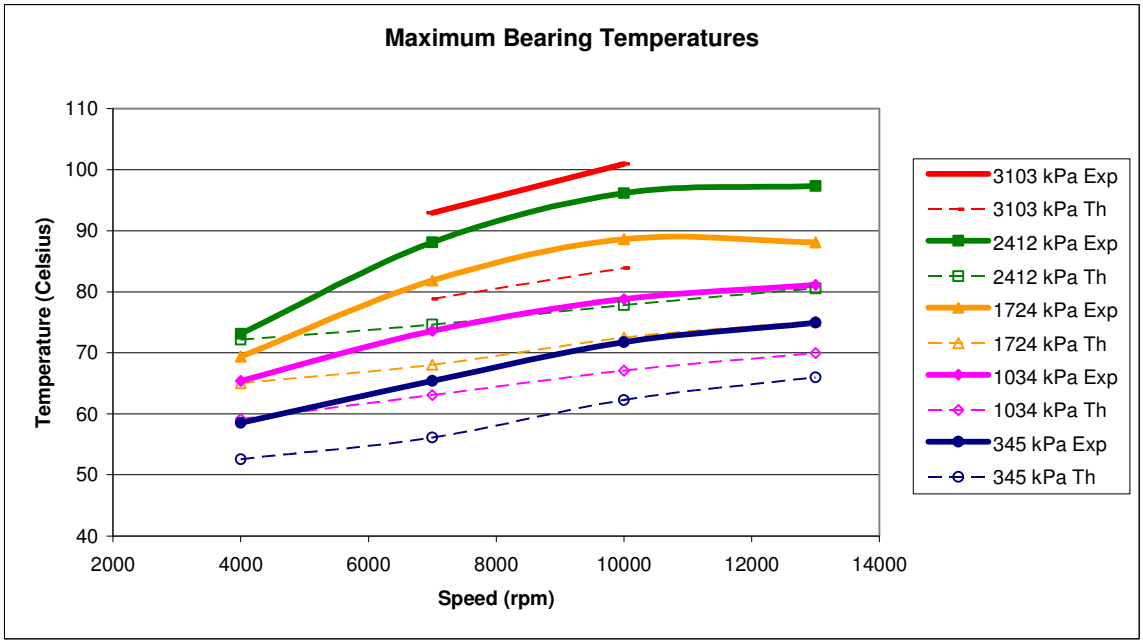

Fig. 52 LOP predicted and measured maximum bearing temperatures

Dynamic Results

Baseline Dynamic Stiffnesses

As described in the LBP section, the baseline test is performed to subtract the stiffness, damping, and added mass terms of the test rigs structure from the actual dynamic test. This step allows the coefficients of only the fluid film to be found. Shown in Fig. 53 are plots of the baseline stiffnesses once the mass of the stator has been accounted for.

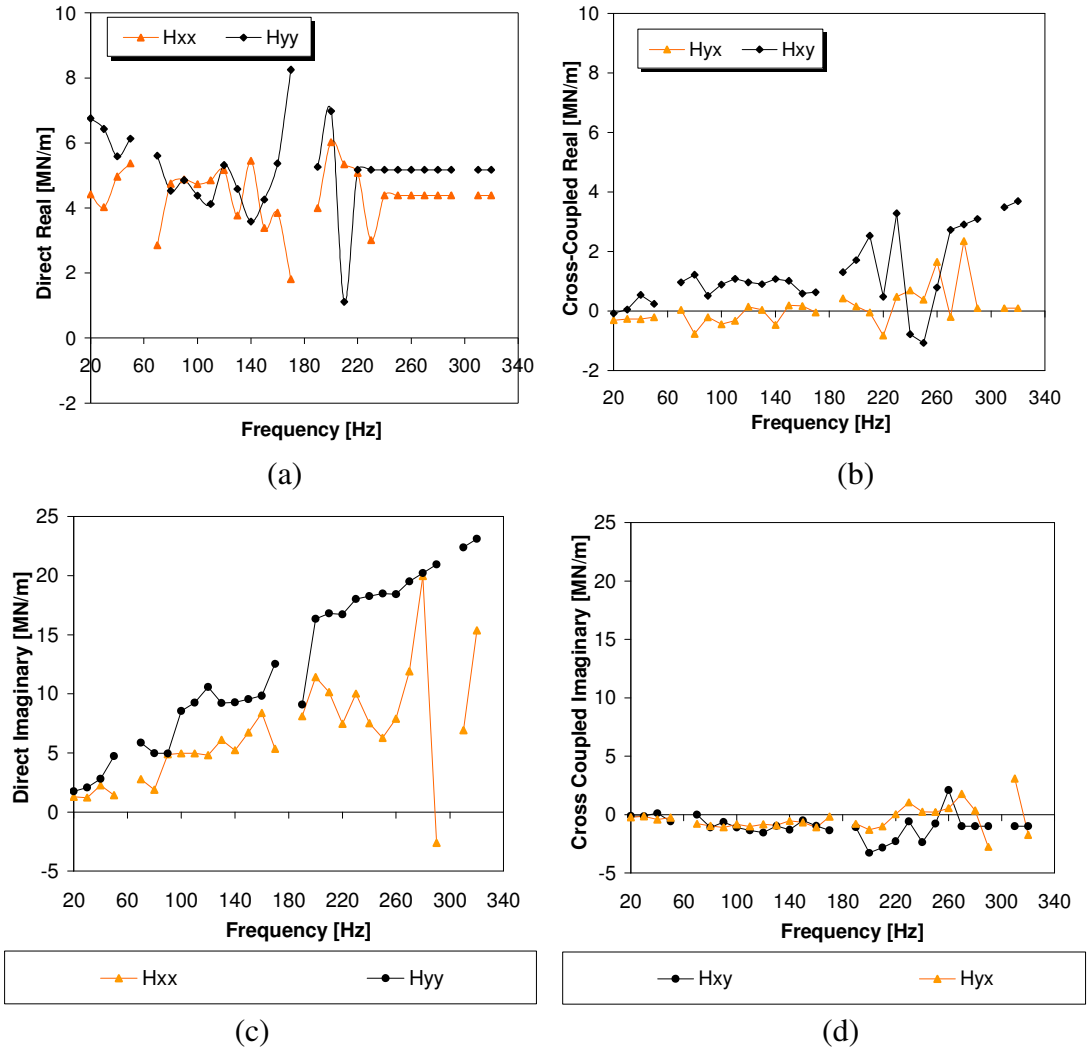

Fig. 53 LOP baseline dynamic stiffnesses for: (a) direct real, (b) cross coupled real, (c) direct imaginary, (d) cross coupled imaginary

Fig. 53 shows that the stiffness and damping due to the structure are as follows: $K_{xx} = 4.42MN/m$, $K_{yy} = 5.50MN/m$, $C_{xx} = 7.01kN.s/m$, $C_{yy} = 11.50kN.s/m$. Cross coupled terms were negligible.

Test Condition Dynamic Stiffness Coefficients

The following plots will be of the dynamic stiffness coefficients for all minimum and maximum load and speed conditions. Fig. 54 (a) plots the direct real dynamic stiffness coefficients at 4000 rpm and 345 kPa which decrease with frequency, indicating a positive added mass term. The rate of decrease however is considerably larger than that of the code, meaning the code has under predicted the added mass, more so in the loaded direction. On the other hand, the stiffness coefficients are modeled fairly well in the code with the measured coefficients being $K_{xx} = 134.24MN/m$ and $K_{yy} = 171.07MN/m$ and the prediction being equal to $K_{xx} = 152.5MN/m$ and $K_{yy} = 164.4MN/m$.

The cross coupled real stiffnesses are given in Fig. 54 (b) where the H_{yx} and H_{xy} terms lead to the same stiffness coefficients but with the H_{yx} having a considerable cross coupled added mass term and H_{yx} having none. Theoretical predictions are much the same as for the LBP condition since the cross coupled stiffness terms are negligible. Direct damping shown in Fig. 54 (c) is somewhat overstated by the theory.

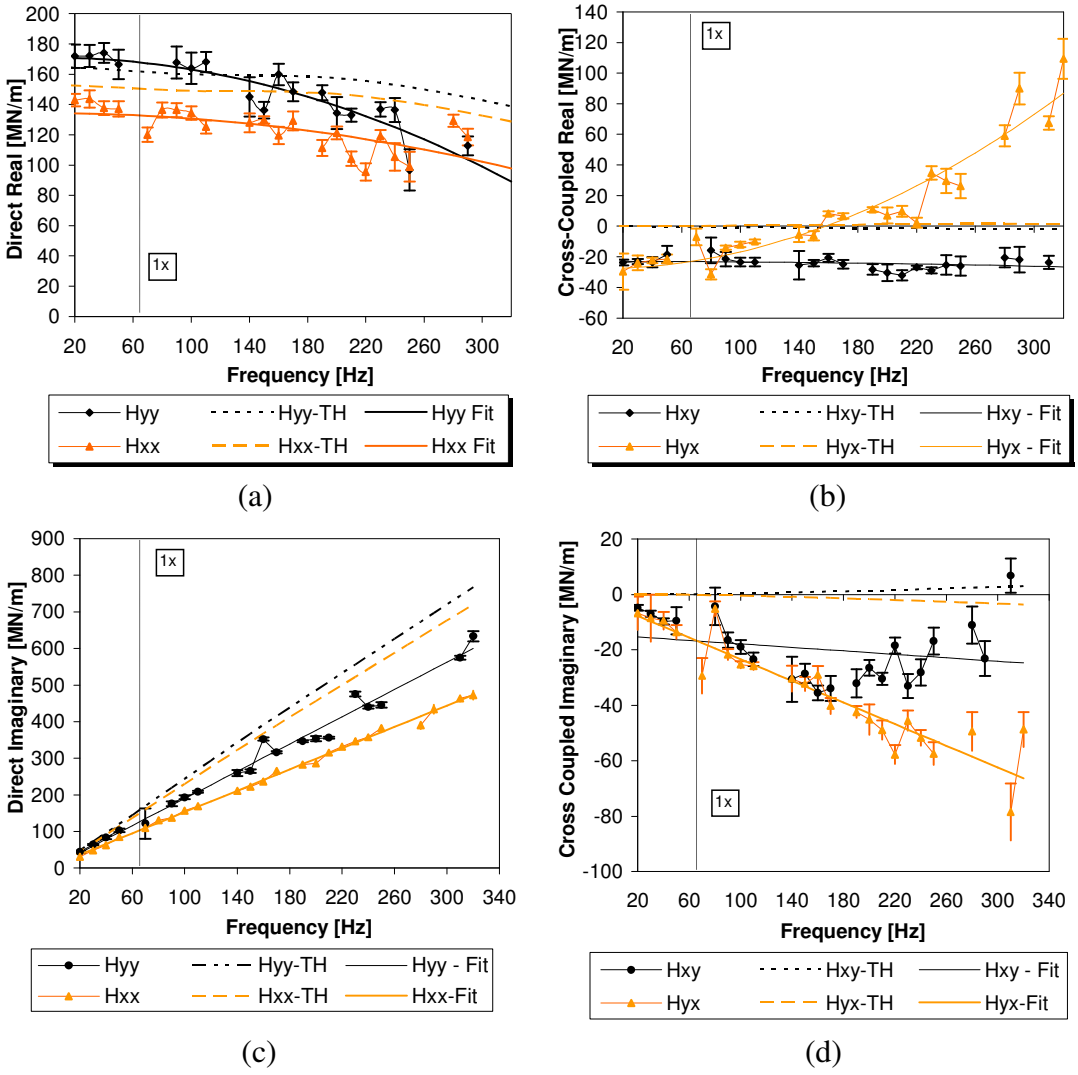

Fig. 54 LOP dynamic stiffnesses at 4000 rpm and 345 kPa for: (a) direct real, (b) cross coupled real, (c) direct imaginary, (d) cross coupled imaginary

Fig. 55 corresponds to the dynamic stiffnesses of the 4000 rpm 2412 kPa condition and is the highest load at this speed. The direct real dynamic stiffnesses exhibit very little added mass and a similar result is predicted. The direct stiffness coefficient in the loaded direction is predicted well with the measured value being $K_{yy} = 775.4MN/m$ and the prediction 664.4MN/m. However, the unloaded direction has a stiffness of $K_{xx} = 200.15MN/m$ and a predicted

stiffness of 398.4 MN/m. The increased load has caused curvature in H_{xy} and a decrease in the stiffness coefficient K_{xy} from -23 MN/m to 0 MN/m

The cross coupled dynamic stiffness Re($\boldsymbol{H_{yx}}$) has remained constant with the load increase. Some cross coupling effects are noted here in the predicted results with K_{xy} and K_{yx} both equal to -11 MN/m but not showing any added mass. Predicted and measured direct damping dynamic stiffnesses have deviated considerably with the additional loading, and the code over predicts the damping to a great degree.

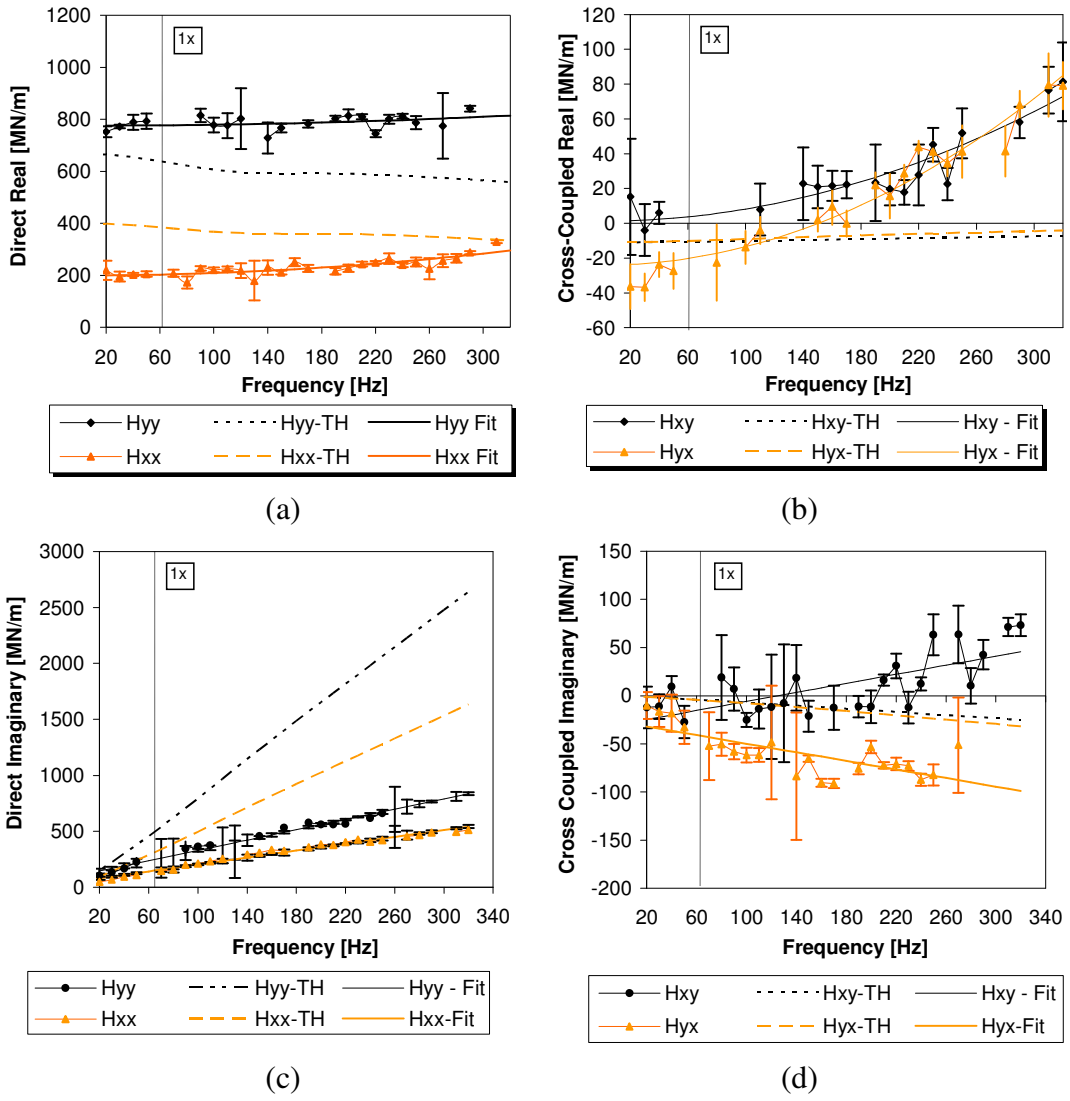

Fig. 55 LOP dynamic stiffnesses at 4000 rpm and 2412 kPa for: (a) direct real, (b) cross coupled real, (c) direct imaginary, (d) cross coupled imaginary

Fig. 56 displays the dynamic stiffnesses for the highest-speed / lowest-load condition (13000 rpm and 345 kPa). Much like the 4000 rpm speed condition, there is a considerable amount of direct added mass, particularly in the loaded direction. The amount of mass in the unloaded direction is predicted well but under predicted in the loaded direction. Predicted stiffness orthotropy present in the 4000 rpm case has disappeared at this higher speed; however, the measured results show a significantly higher stiffness in the loaded direction. Cross coupled dynamic stiffnesses shown in Fig. 56 (b) display negative added mass terms in both directions with negligible cross coupled stiffness for K_{xy}. However the K_{yx} coefficient shows a significant amount of stiffness at -91 NM/m. As shown in previous sections, the damping is well modeled at these low load conditions.

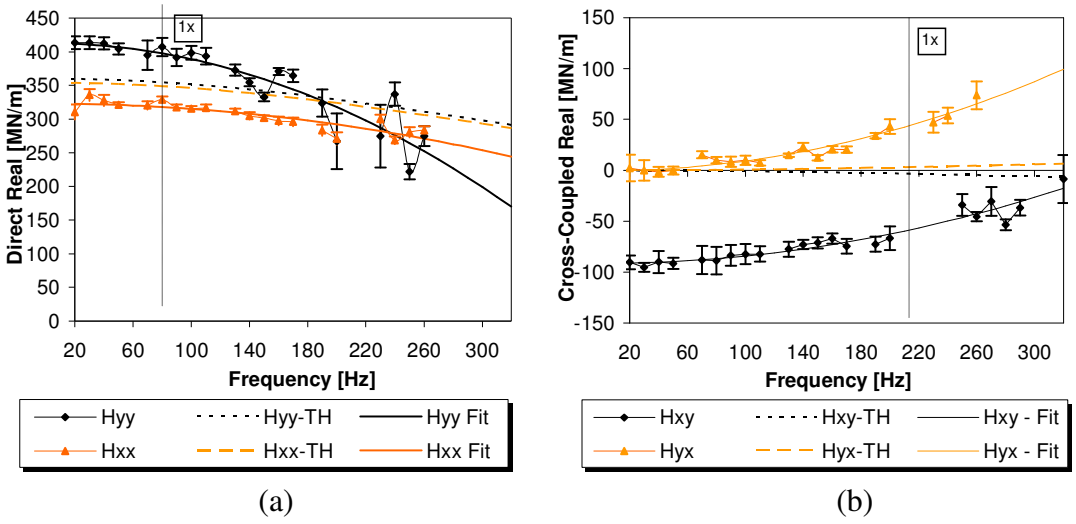

Fig. 56 LOP dynamic stiffnesses at 13000 rpm and 345 kPa for: (a) direct real, (b) cross coupled real, (c) direct imaginary, (d) cross coupled imaginary

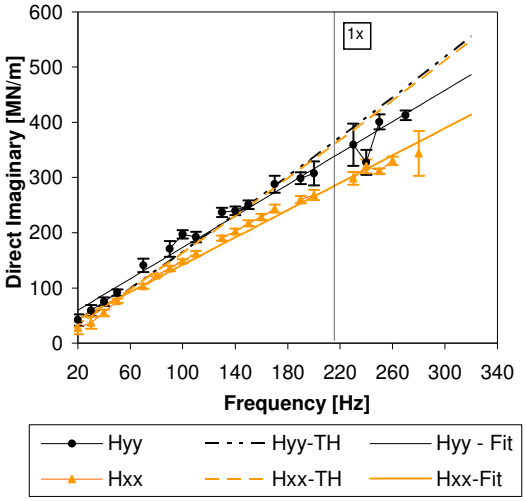

(c)

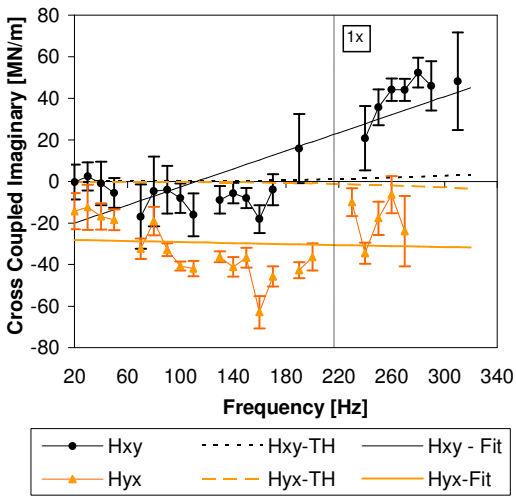

(d)

Fig. 56 "Continued"

Shown below in Fig. 57 are the measured and predicted results for the highest-speed, highest-load configuration of 13000 rpm and 3101 kPa. Fig. 57 (a) shows that the higher load increases stiffness orthotropy with $K_{xx} = 856.7MN/m$ and $K_{yy} = 413.34MN/m$. Because the dynamic stiffnesses decrease with frequency, some added mass coefficients will be present, again particularly in the loaded direction. Cross coupled stiffness coefficients can be seen in Fig. 57 (b) where $K_{xy} = K_{yx} = -41N/m$ along with negative added mass. The predicted damping coefficients are substantially higher than those measured at this condition.

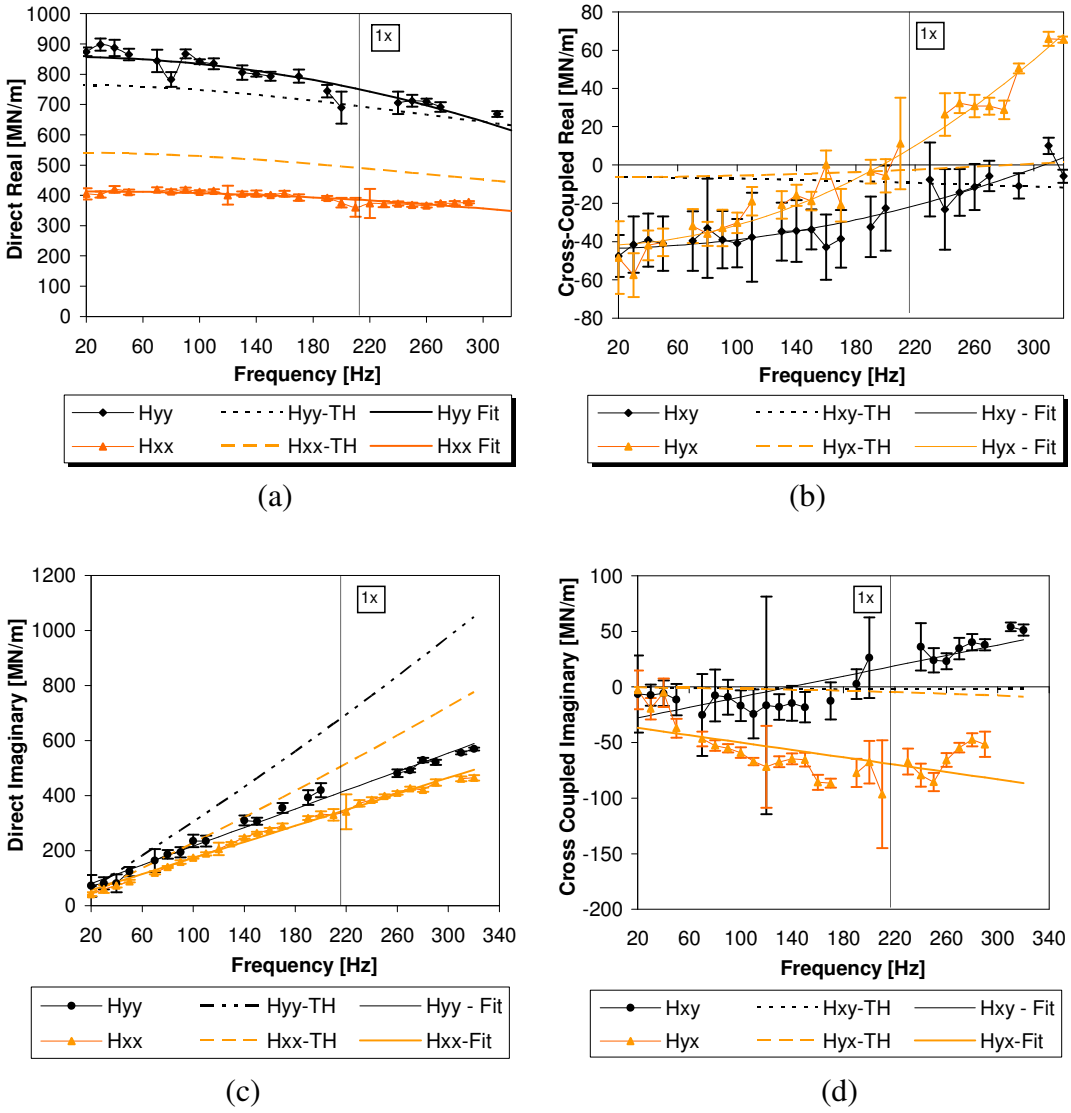

Fig. 57 LOP dynamic stiffnesses at 13000 rpm and 3101 kPa for: (a) direct real, (b) cross coupled real, (c) direct imaginary, (d) cross coupled imaginary

Stiffness Coefficients

Stiffness coefficients versus load for the various rotor speeds are represented in Fig. 58. Generally, the trend shows a linear increase in stiffness with increasing load as expected. The theoretical predictions are better at the lower loads and for the loaded-direction coefficients. Load direction coefficients increase at a much higher rate, since the unloaded coefficients do not

seem to be overly dependent on loading conditions. Stiffness orthotropy is minimal at the lower loadings but quickly increases with loading.

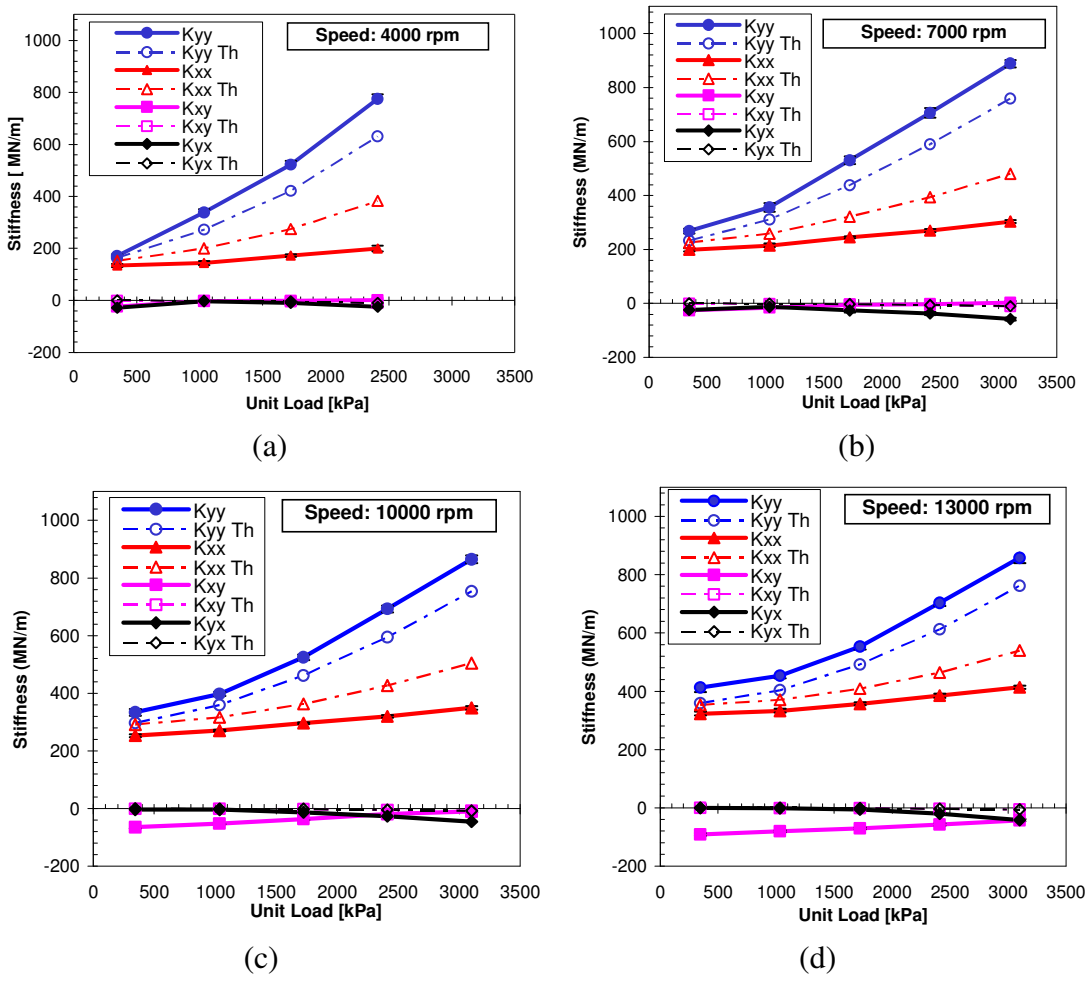

Fig. 58 LOP direct and cross coupled stiffness coefficients vs. load for varying speed: (a) 4000 rpm, (b) 7000 rpm, (c) 10000 rpm, (d) 13000 rpm

Shown in Fig. 59 are plots of cross coupled stiffness versus unit load. The cross coupled coefficient K_{yx} is negative and continues to grow more negative as load increases. In contrast, the coefficient K_{xy} (while still remaining negative) tends to become less so with increasing unit load. However, the magnitudes of the cross coupled stiffness coefficients remains small relative to the direct coefficients. Combined with the fact that the majority of the coefficients are of the same sign, these coefficients should not lead to any stability problems.

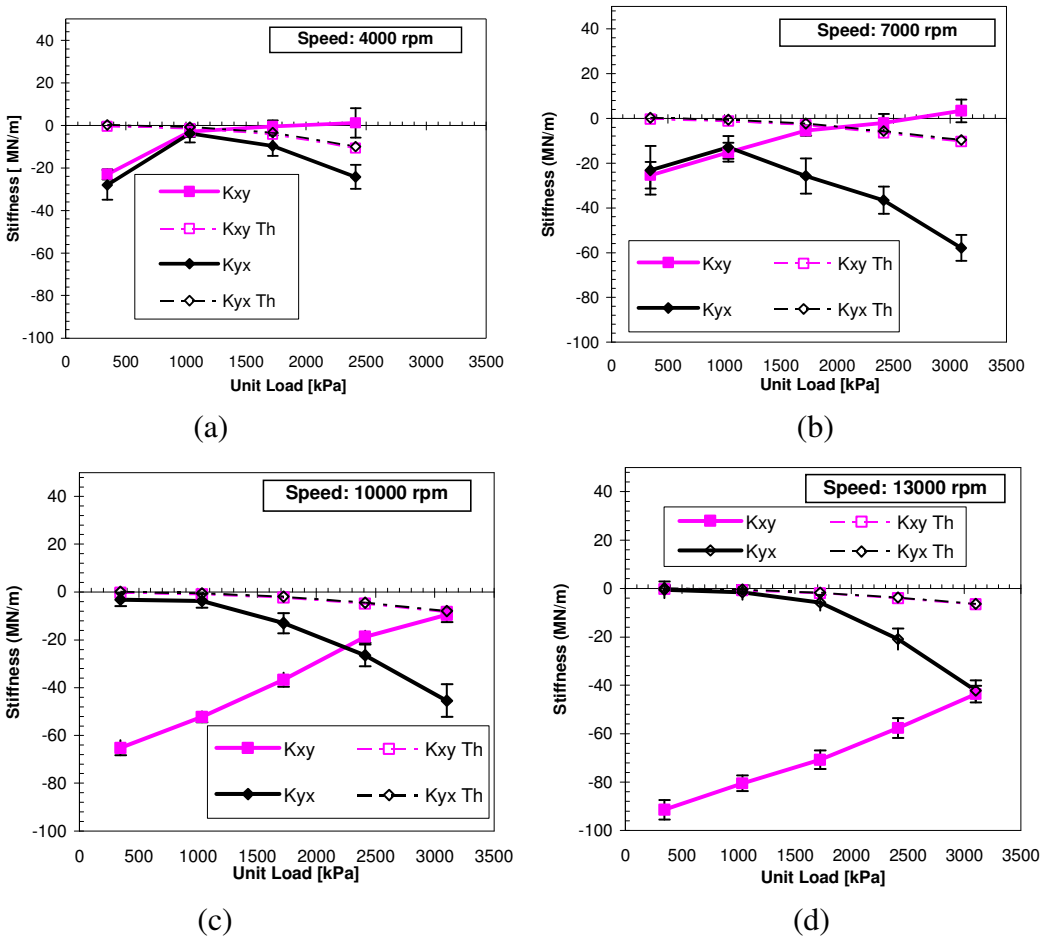

Fig. 59 LOP cross coupled stiffness coefficients vs. load for varying speed: (a) 4000 rpm, (b) 7000 rpm, (c) 10000 rpm, (d) 13000 rpm

Fig. 60 shows the stiffness coefficients vs. rotor speed. A linear relationship exists between stiffness and rotor speed (except at the higher loads for the coefficient K_{yy}) at which point there is no longer a dependency. At all conditions, the stiffness coefficients are not as dependent upon speed as upon load. Close observation reveals that the cross coupled coefficient K_{xy} tends to become slightly more negative with increasing load while K_{yx} seems to be unaffected. The predicted coefficients exhibit good correlation in the loaded direction; however, they are not as accurate in the unloaded direction.

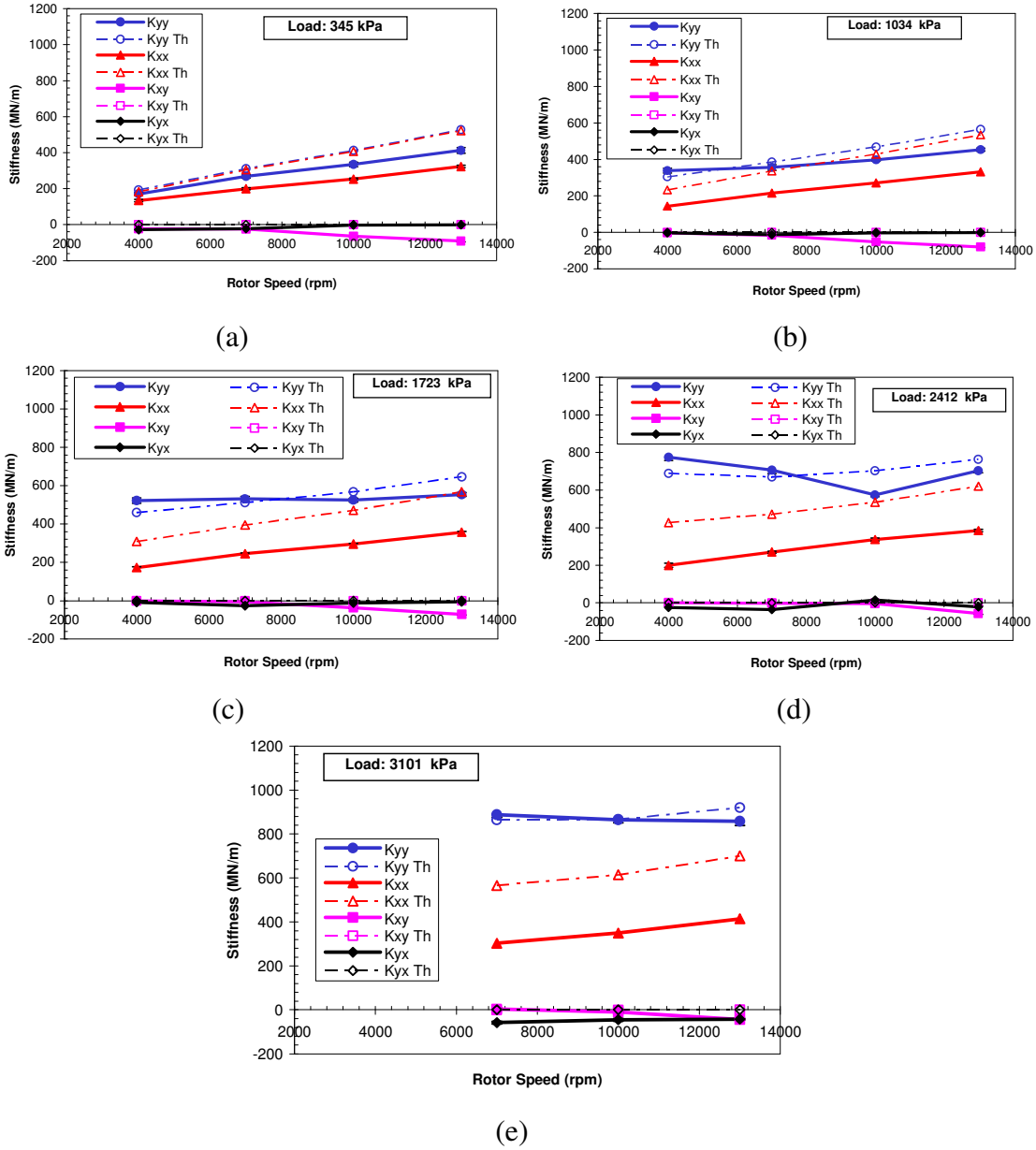

Fig. 60 LOP direct and cross-coupled stiffness coefficients vs. speed for varying loads of: (a) 346 kPa, (b) 1034 kPa, (c) 1723 kPa, (d) 2412 kPa, (e) 3101 kPa

Shown in Fig. 61 are cross coupled stiffnesses versus speed. K_{yx} does not seem to be heavily dependent upon speed changes, while K_{xy} grows more negative with increasing speed. Again, the fact that the coefficients are both negative should lead to confidence in the stability of the bearing.

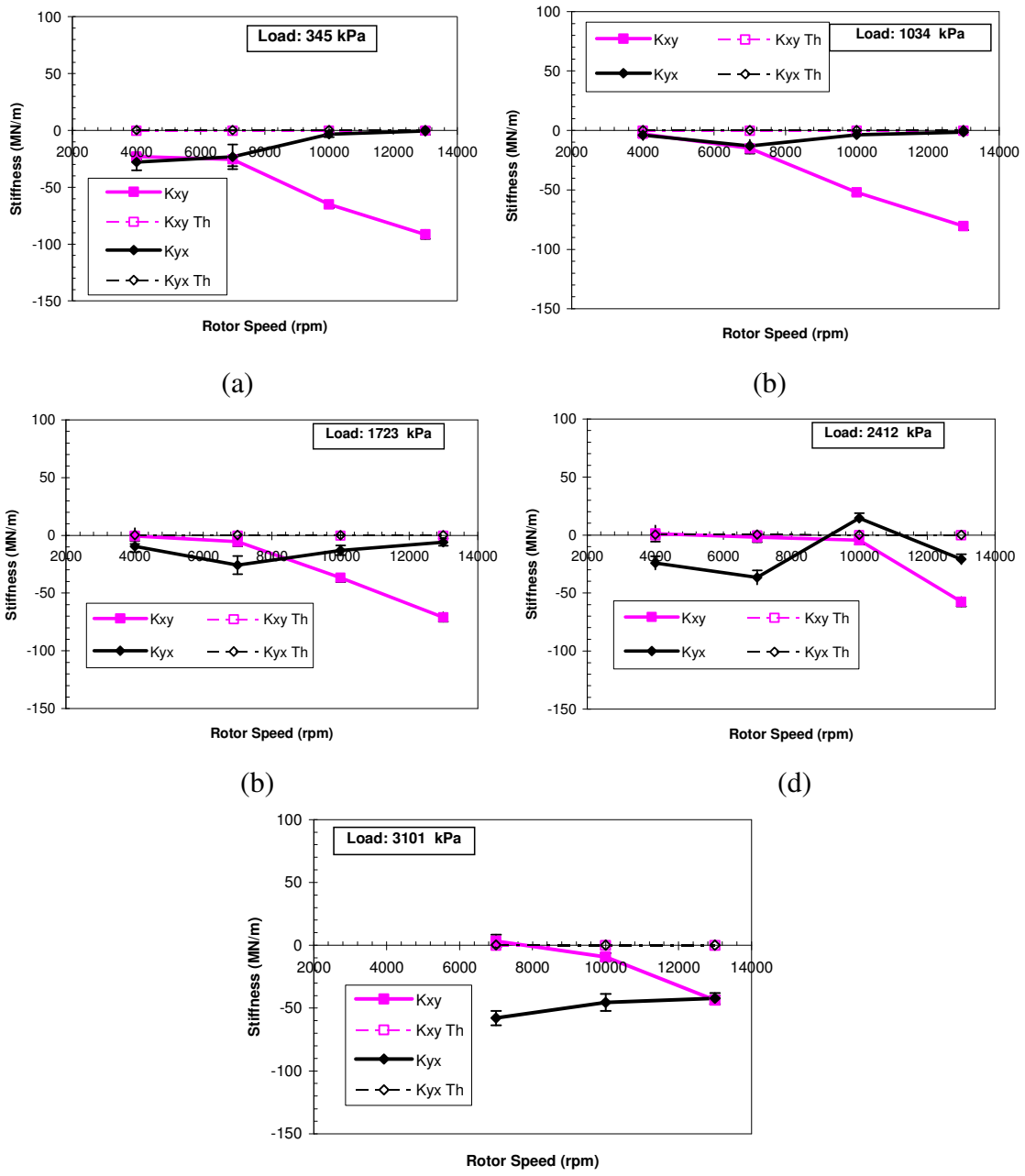

Fig. 61 LOP cross-coupled stiffness coefficients versus speed for varying loads of: (a)346 kPa, (b) 1034 kPa, (c) 1723 kPa, (d) 2412 kPa, (e) 3101 kPa

Damping Coefficients

The effect of load on the damping coefficients is shown in Fig. 62. The measured coefficients are largely unaffected by load unlike the predicted results, which show a steady increase in damping with loading. Predictions match fairly well at the lowest loads however the spread between experiment and prediction quickly rises. This difference is greatest at the lowest speed and decreases with increasing speed

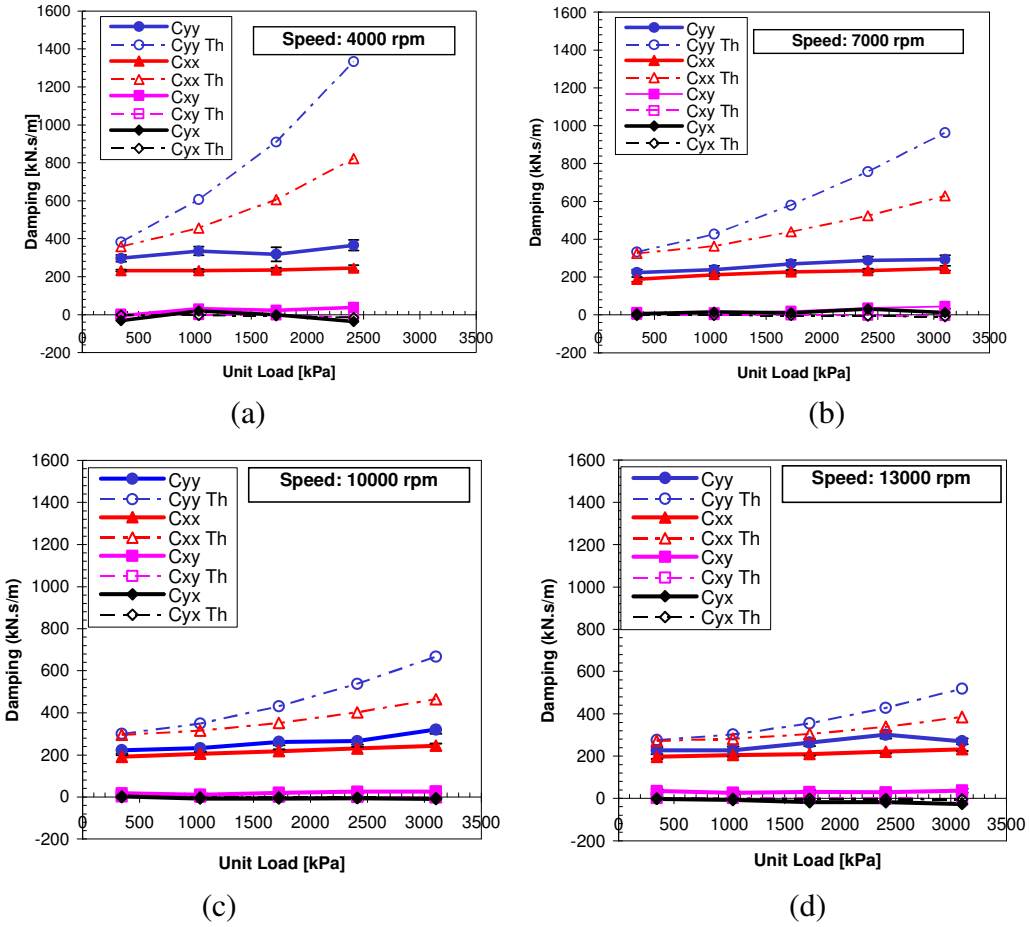

Fig. 62 LOP direct and cross coupled damping coefficients vs. load for varying speed: (a) 4000 rpm, (b) 7000 rpm, (c) 10000 rpm, (d) 13000 rpm

Fig. 63 shows the cross coupled damping coefficients versus unit load. The coefficient C_{xy} remains fairly constant and positive throughout the load range. However, C_{yx} is negative at the higher speeds while being positive at the 7 krpm speed. At the 7 krpm speed however the coefficients are fairly similar in both magnitude and sign, meaning real dissipative damping.

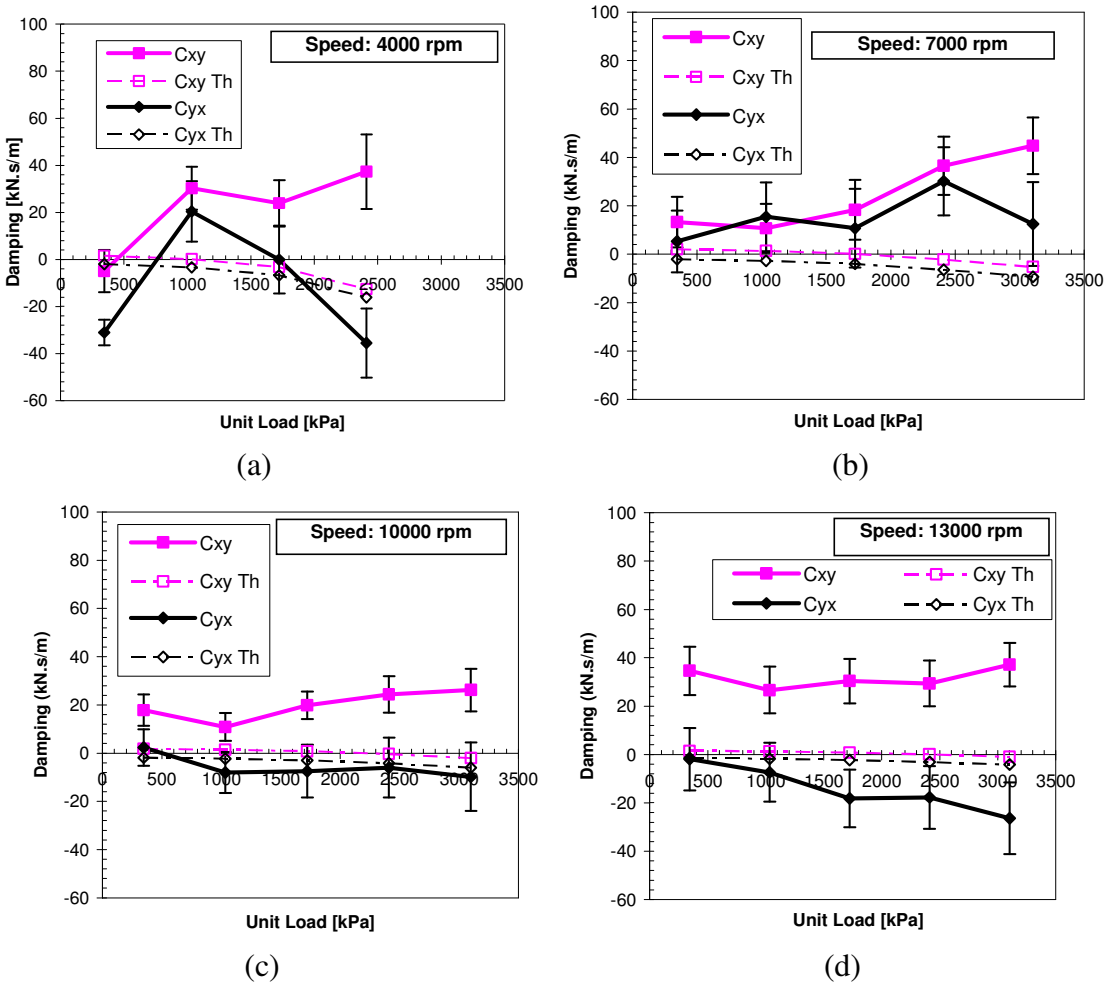

Fig. 63 LOP cross coupled damping coefficients vs. load for varying speed: (a) 4000 rpm, (b) 7000 rpm, (c) 10000 rpm, (d) 13000 rpm

Shown in Fig. 64 is the effect of speed on the damping coefficients. The measured damping is not dependent on either load or speed but is almost constant, regardless of the test condition. On the other hand, the prediction predicts a maximum amount of damping at low speed and high load and a minimum at high speed and low load.

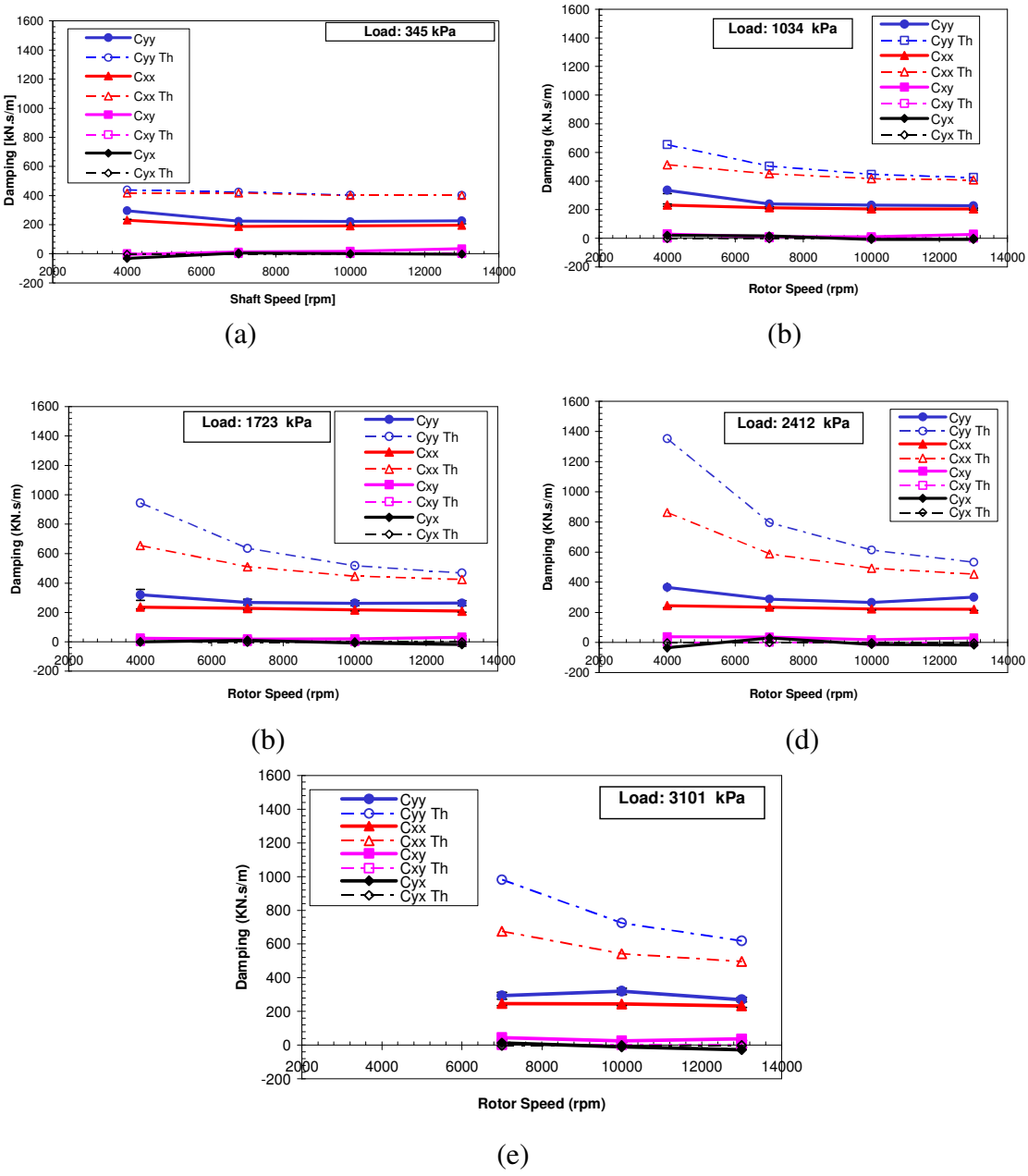

Fig. 64 LOP direct and cross-coupled damping coefficients vs. speed for varying load: (a) 346 kPa, (b) 1034 kPa, (c) 1723 kPa, (d) 2412 kPa, (e) 3101 kPa

Below in Fig. 65 are the cross coupled damping coefficients and their change with speed. Neither cross coupled coefficients are shown to have much dependence on speed, while C_{yx} seems to alternate between positive and negative values.

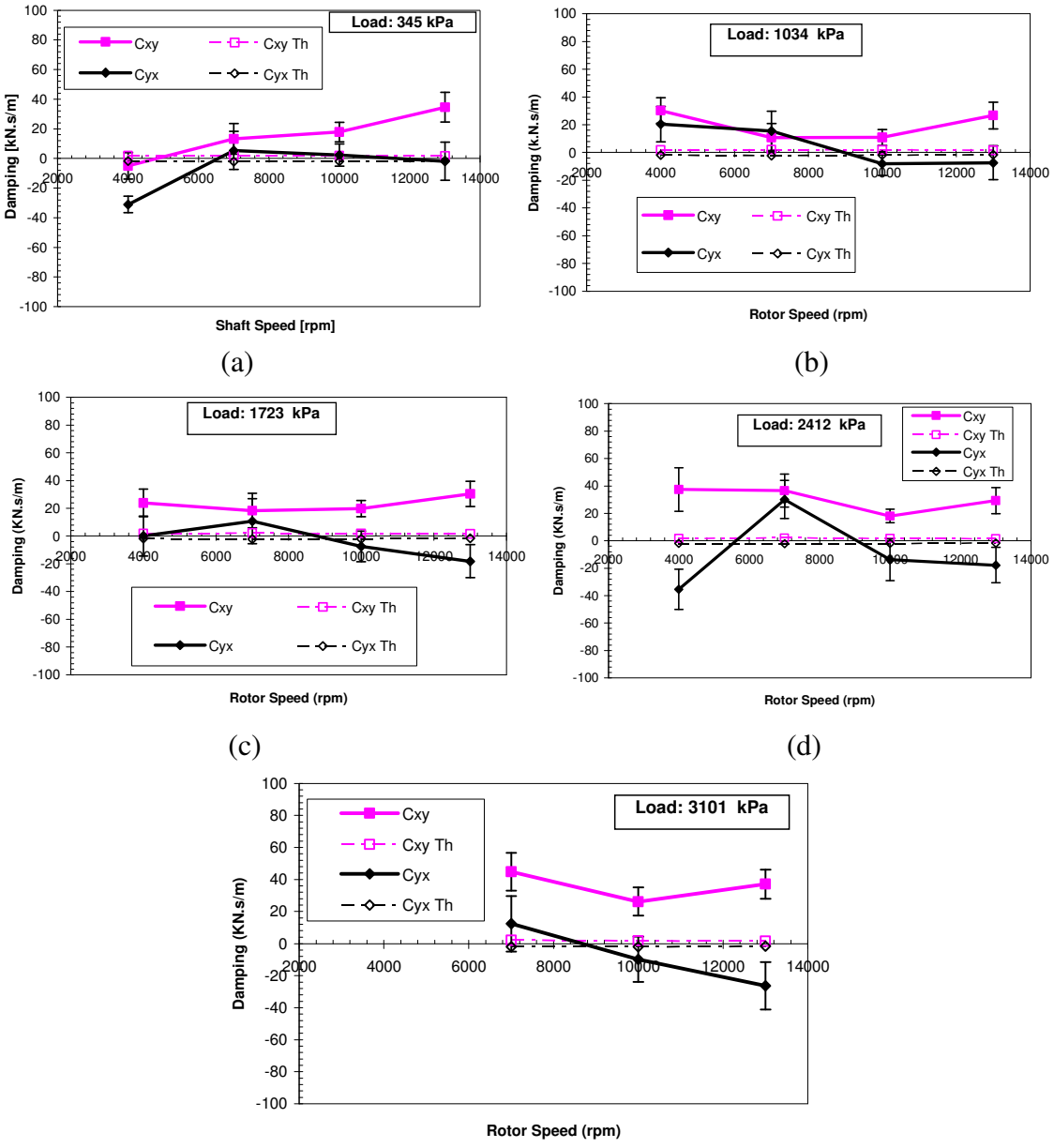

Fig. 65 LOP cross-coupled damping coefficients vs. speed for varying load: (a) 346 kPa, (b) 1034 kPa, (c) 1723 kPa, (d) 2412 kPa, (e) 3101 kPa

Mass Coefficients

Fig. 66 below shows the relationship between added mass coefficients and unit loading. The direct coefficient M_{yy} displays a behavior in which a positive added mass occurs at low load which then decreases for the low-intermediate loads and then steadily increases at higher loads resulting in a bowl shaped curve. Except for the 4 krpm case, the added mass in the loaded direction is always higher than that of the unloaded and reaches a maximum value of 60 kg at the highest speed. In contrast, the M_{xx} coefficient reaches only a third of the value of M_{yy} at approximately 20 kg. No great amount of load dependency is seen in any of the coefficients accept for M_{yy}. Generally, the theory under predicts the added mass and always predicts positive direct terms while some negative added mass was seen in the measured results at the lowest speed of 4krpm.

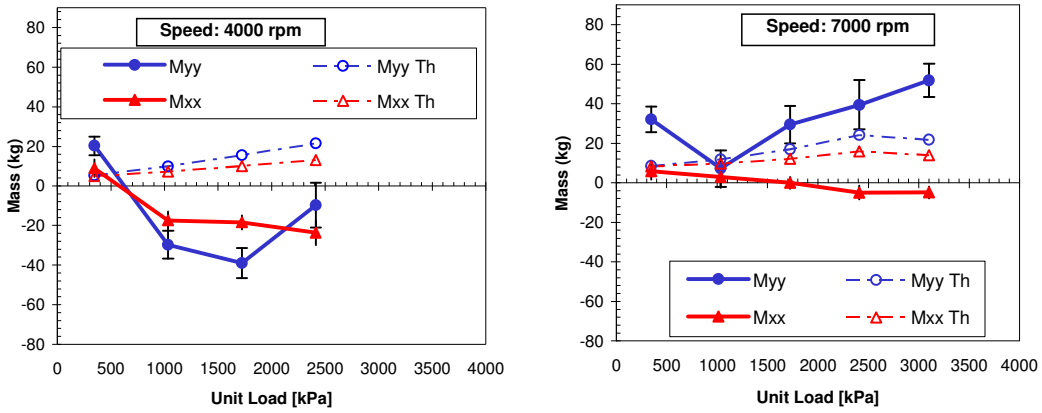

(a) (b)

Fig. 66 LOP direct mass coefficients vs. load for varying speed: (a) 4000 rpm, (b) 7000 rpm, (c) 10000 rpm, (d) 13000 rpm

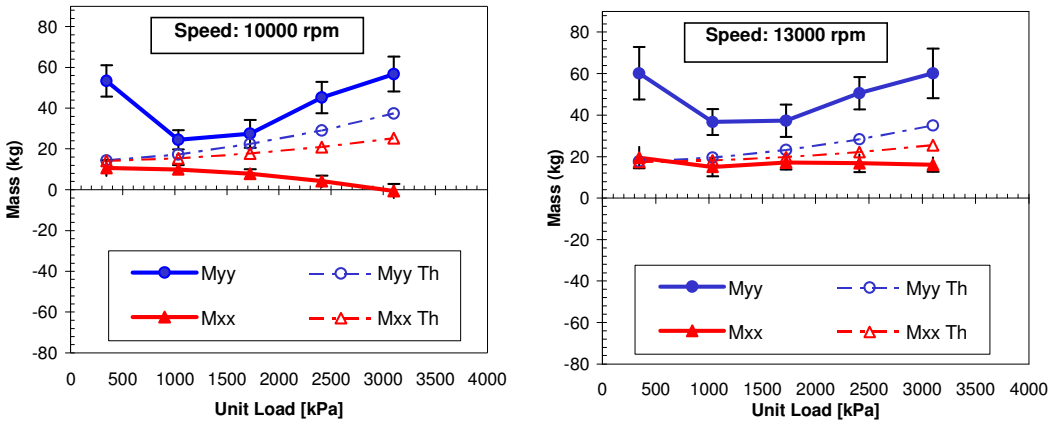

(c) (d)

Fig. 66 "Continued"

Shown in Fig. 67 are the cross coupled mass coefficients versus unit load. At the higher speeds, both cross coupled coefficients are negative, however at 7 krpm M_{xy} is found to be positive and M_{yx} is negative. Likewise, for the 4 krpm running speed, M_{xy} is slightly positive while M_{yx} is heavily negative. A stability analysis will be performed later in this thesis to determine if the opposite signs of the mass coefficients will have any impact on the stability of the bearing.

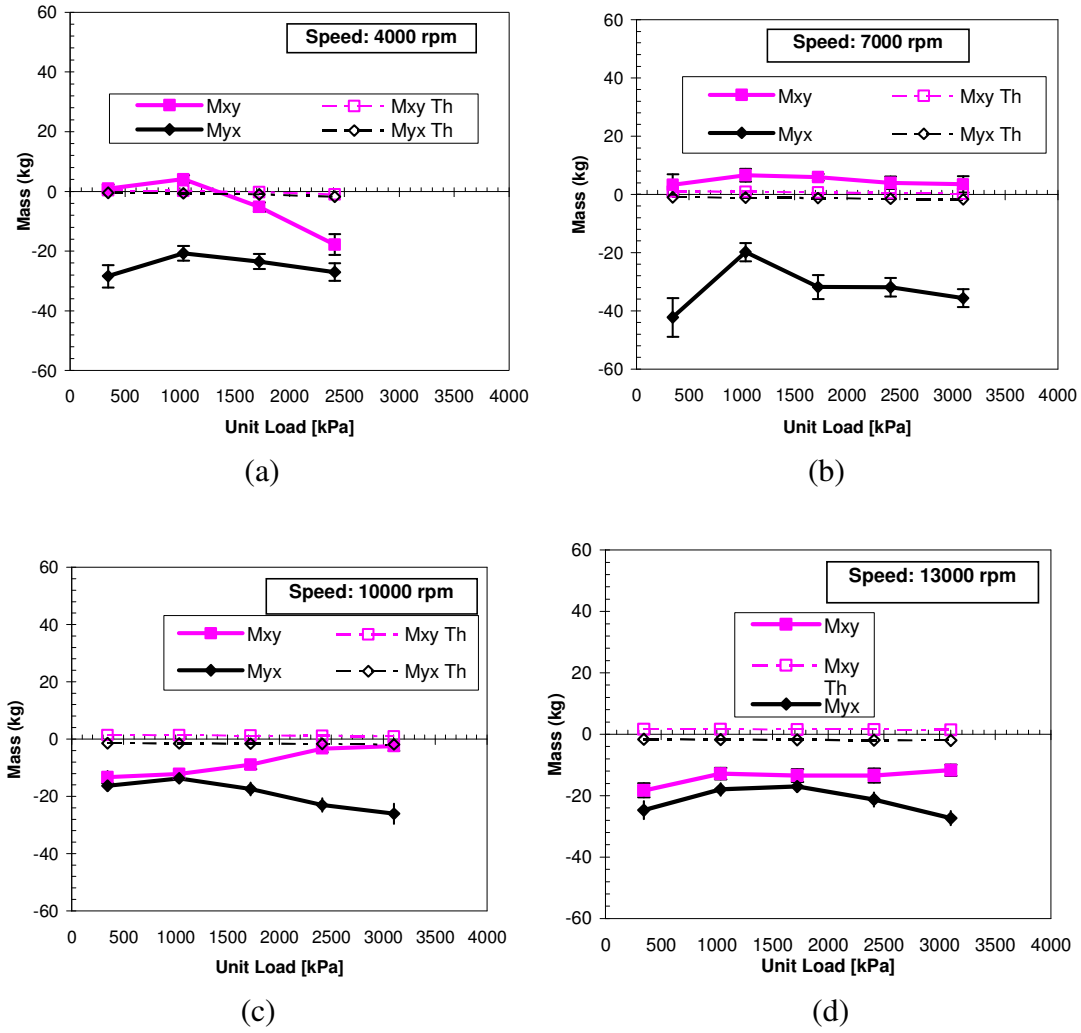

Fig. 67 LOP cross coupled mass coefficients vs. load for varying speed: (a) 4000 rpm, (b) 7000 rpm, (c) 10000 rpm, (d) 13000 rpm

Fig. 68 below displays added mass coefficients vs. shaft speed. The direct coefficient M_{yy} shows some speed dependency since it generally increases with speed. In general, the unloaded direct coefficient M_{xx} is negative at the lowest speed and continues to become more positive reaching a maximum value of 20 kg at 13 krpm. Predicted direct coefficients show little speed dependency except at the lowest speeds in the intermediate and high loads where these values are greatest but quickly drop to constant levels.

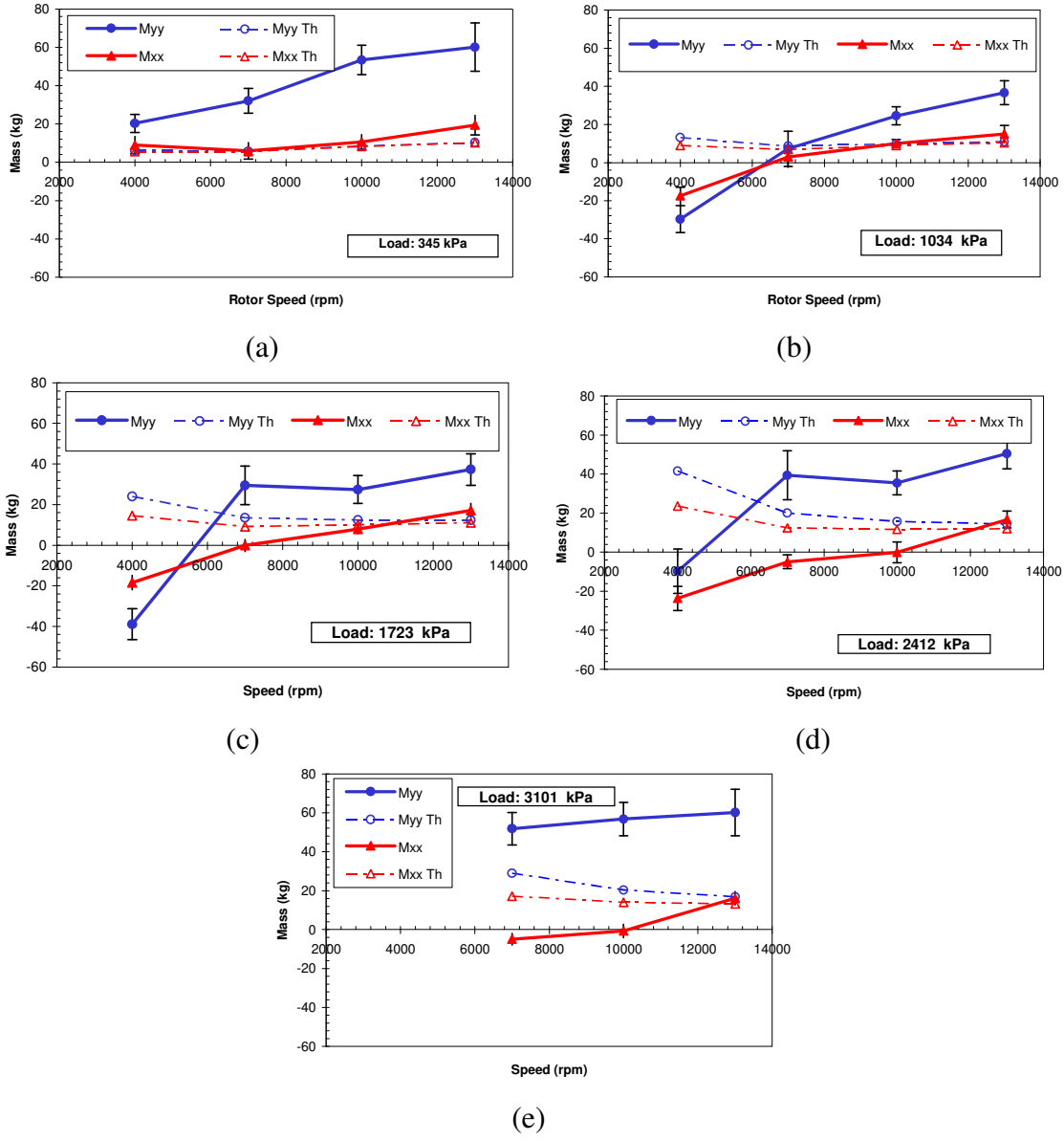

Fig. 68 LOP direct and cross-coupled mass coefficients vs. speed for varying load: (a) 346 kPa, (b) 1034 kPa, (c) 1723 kPa, (d) 2412 kPa, (e) 3101 kPa

Shown in Fig. 69 are the cross coupled mass coefficients versus speed. The lower speeds display a switch in the signs of the coefficients, while the higher speeds show only negative coefficients.

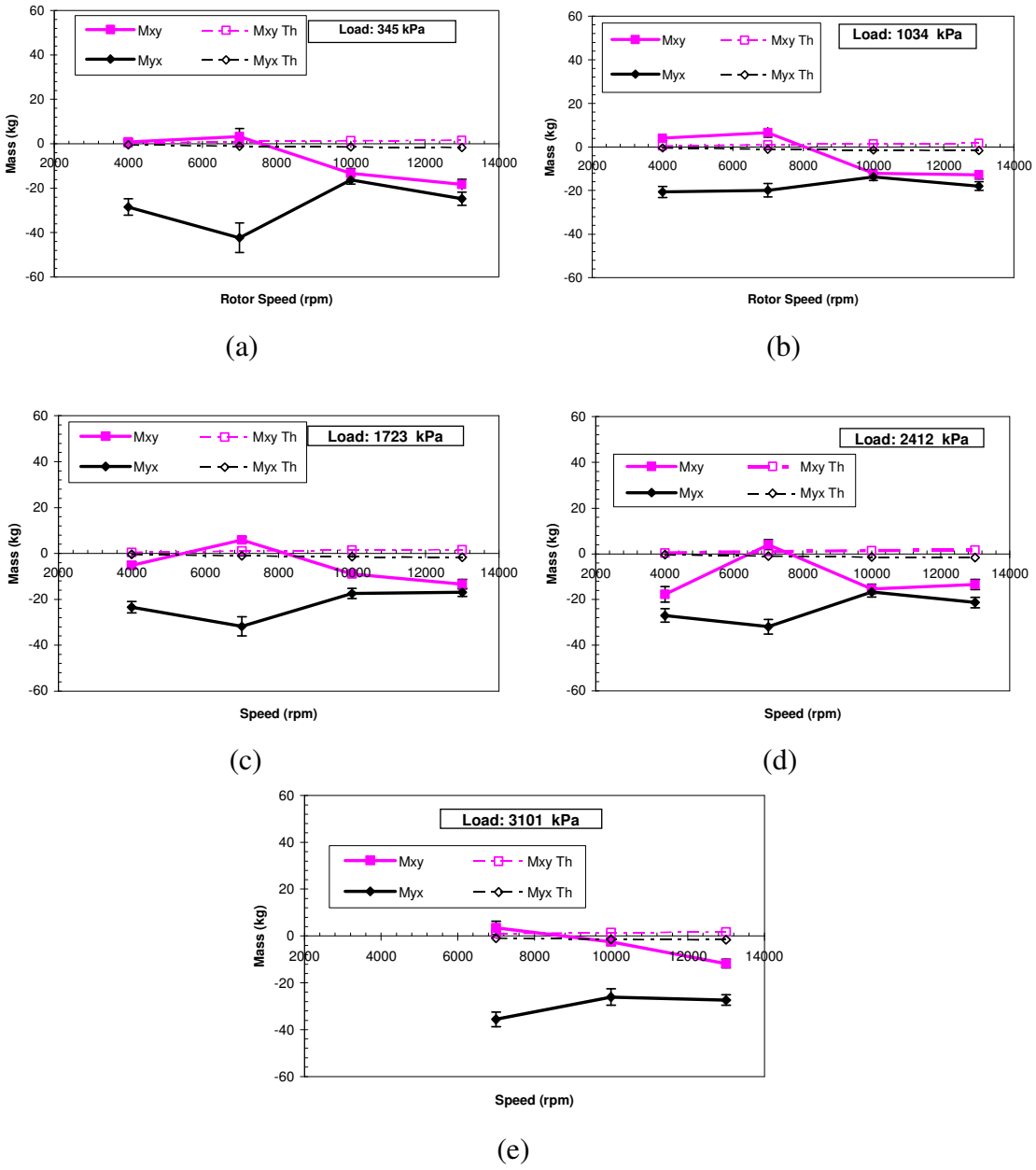

Fig. 69 LOP cross-coupled mass coefficients vs. speed for varying load: (a) 346 kPa, (b) 1034 kPa, (c) 1723 kPa, (d) 2412 kPa, (e) 3101 kPa

Static vs. Dynamic Stiffness

In Fig. 70, a comparison is shown between the static stiffness obtained using the static loader and the dynamic stiffnesses coefficients obtained during a dynamic test. Ideally the stiffnesses should be identical with both methods. The plots in Fig. 70 highlight the fact that good agreement exist until higher loads are encountered, at which point the deviation begins to grow.

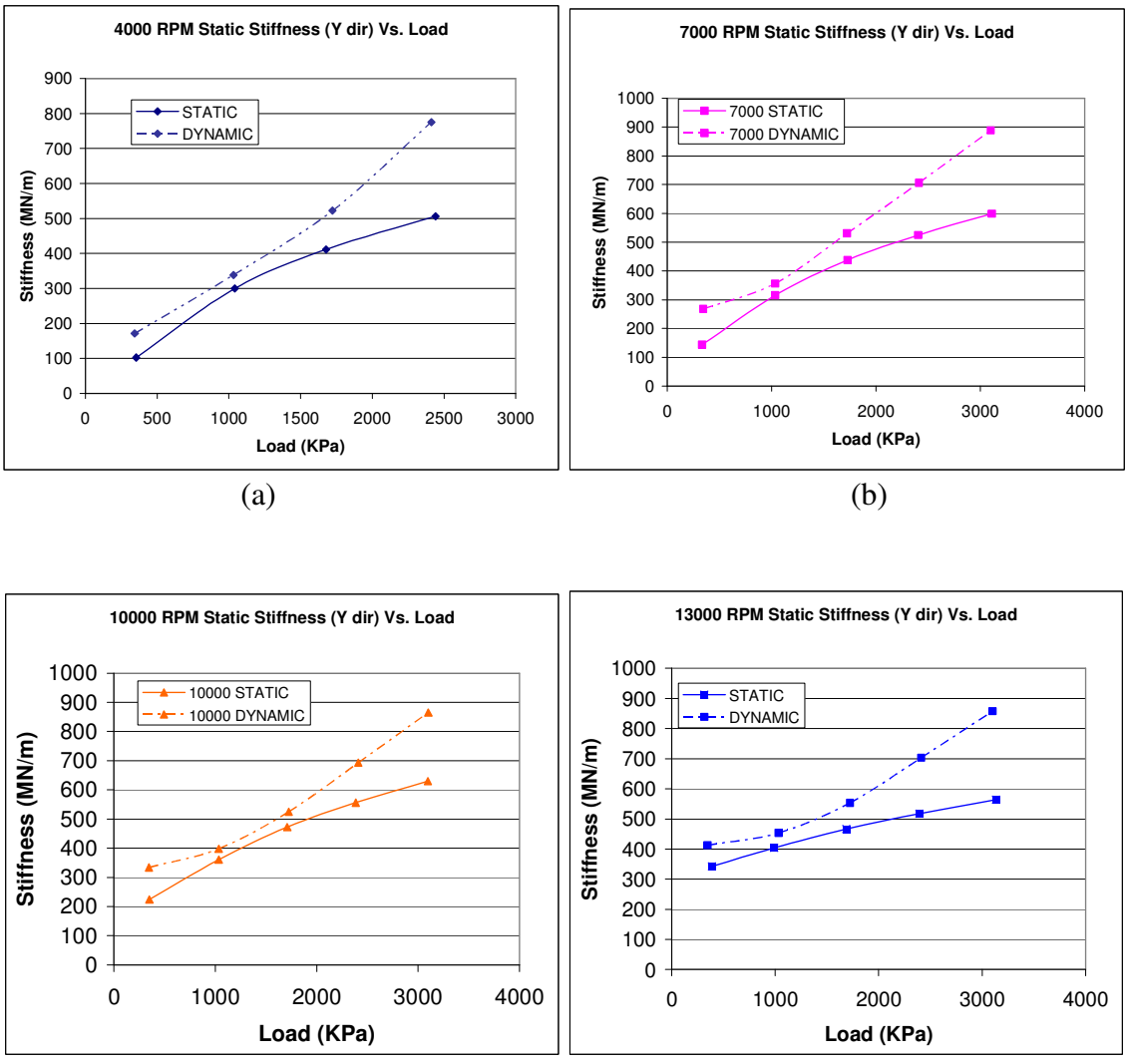

Fig. 70 LOP static and dynamic stiffness vs. load for varying shaft speeds: (a) 4000 rpm, (b) 7000 rpm, (c) 10000 rpm, (d) 13000 rpm

Whirl Frequency Ratio

As mentioned in the previous LBP section the WFR is an important indicator of stability. Similar to the LBP case, the WFR was again calculated to be an imaginary number under all conditions. The bearing has achieved infinite stability which essentially gives it a WFR of zero.

Pad Flutter

Configuration of the pad flutter probes in relation to the applied load is shown below in Fig. 71 while a frequency spectrum of the pad flutter time data is shown in Fig. 72. As displayed before in the LBP condition, only running speed and its harmonics are predominant with no substantial sub-synchronous motion exhibited.

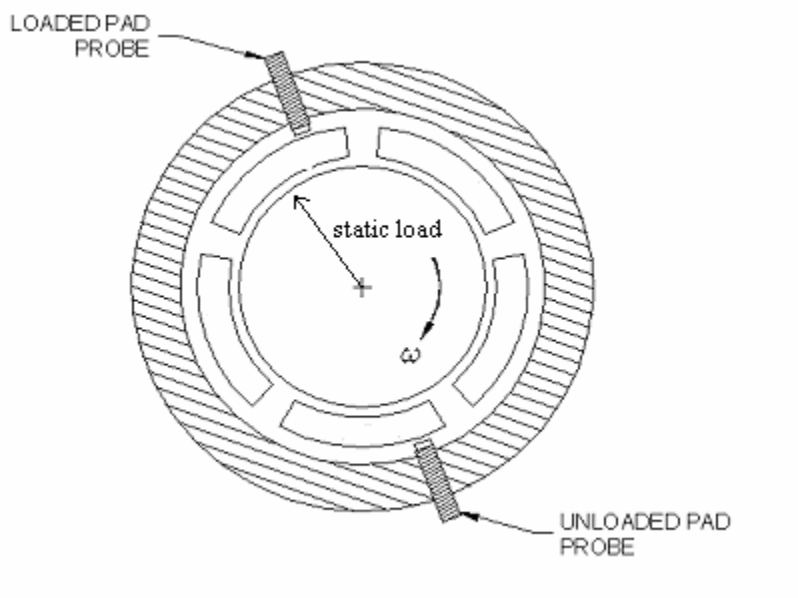

Fig. 71 LOP pad flutter probe installation

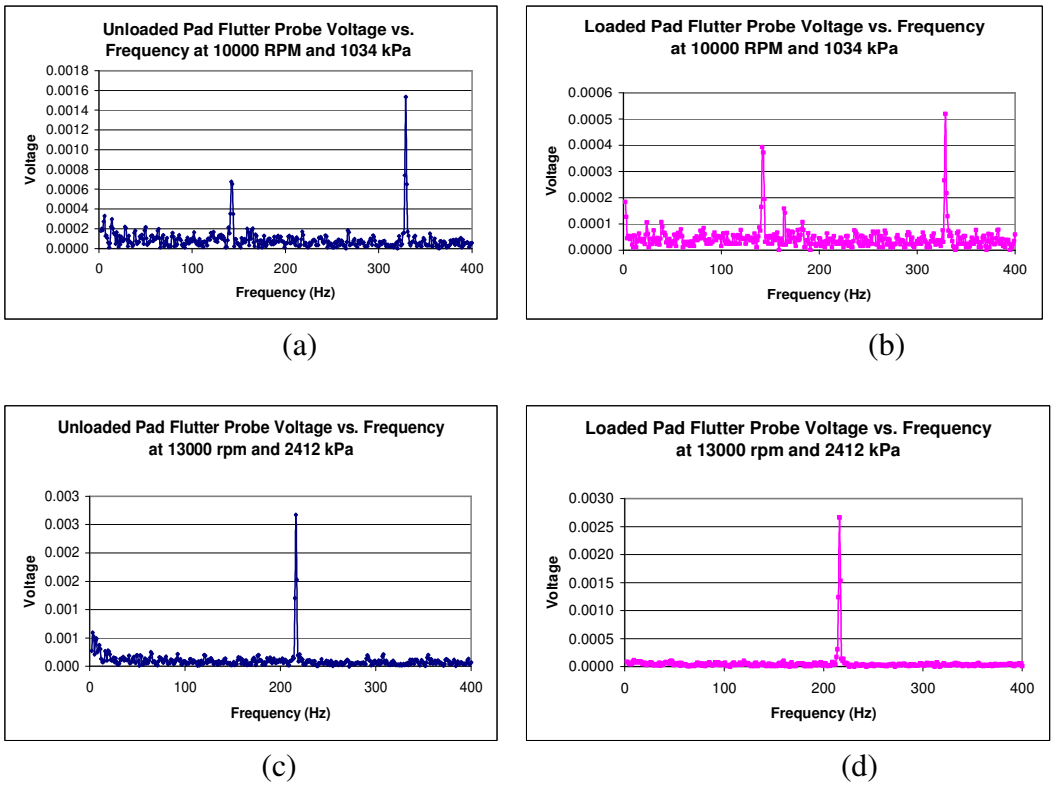

Fig. 72 LOP pad flutter voltage vs. frequency for conditions of: (a) unloaded pad 10000 rpm at 1034 kPa, (b) loaded pad 10000 rpm at 1034 kPa, (c) unloaded pad 13000 rpm at 2412 kPa, (d) loaded pad 13000 rpm at 2412 kPa

LBP AND LOP COMPARISON

This section is provided to show a comparison between some of the experimental differences between the two bearing configurations, both dynamic and static. Fig. 73 shows the locus plots for each rotor speed. The LBP bearing is seen to have a noticeably larger amount of deviation from the loaded axis at the lower speeds. At higher speeds little cross coupling is seen until the highest load is applied to the LBP bearing, at which time significant movement in the unloaded direction occurs.

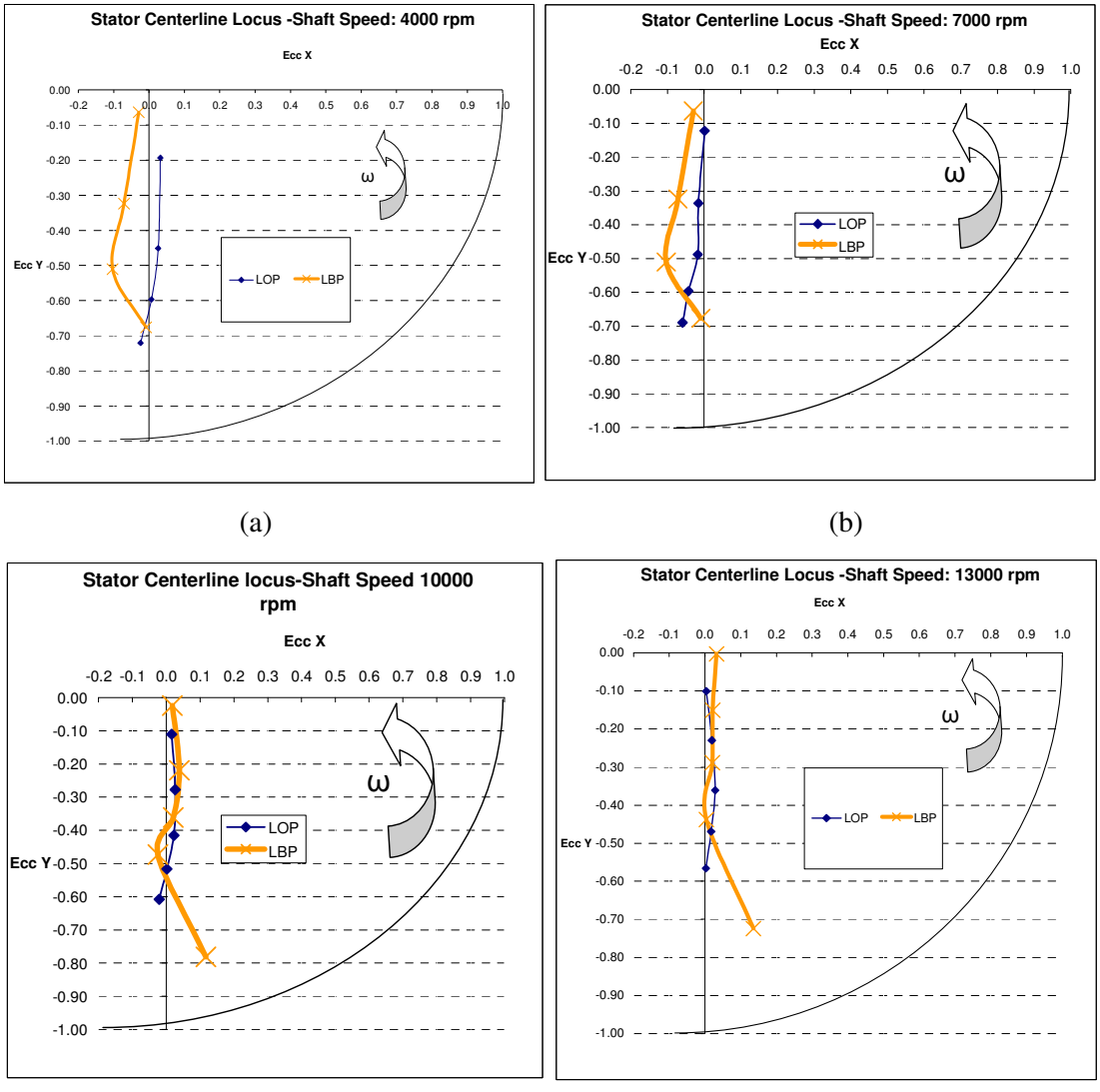

Fig. 73 Comparison of LBP and LOP loci plots

The pad temperature profiles for both bearings are shown side by side in Fig. 74. Generally for the LBP configuration, the temperature profiles are symmetric since the load is equally divided between pads one and five. This differs from the LOP case due to load being applied to only one pad. Consequently the highest temperatures are seen on this one loaded pad, with average temperatures that surpass those in the LBP bearing. However, the differences between the pad temperatures for the two bearings are small.

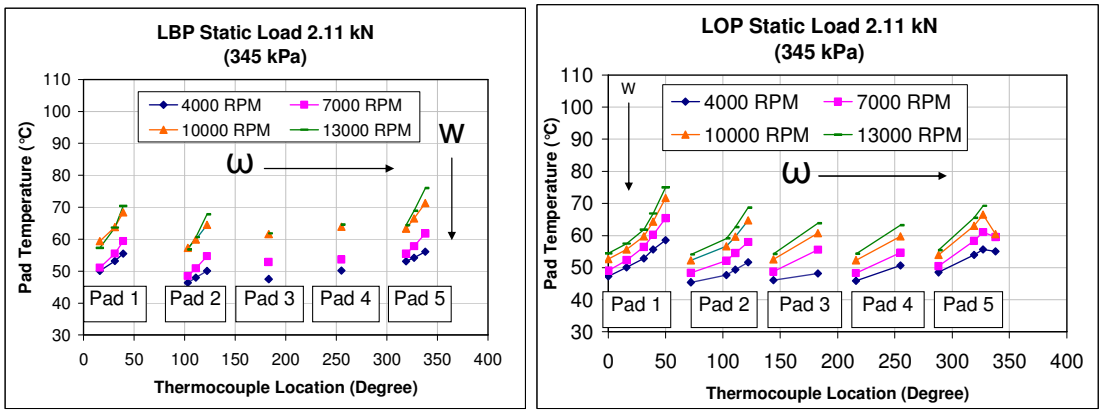

(a)

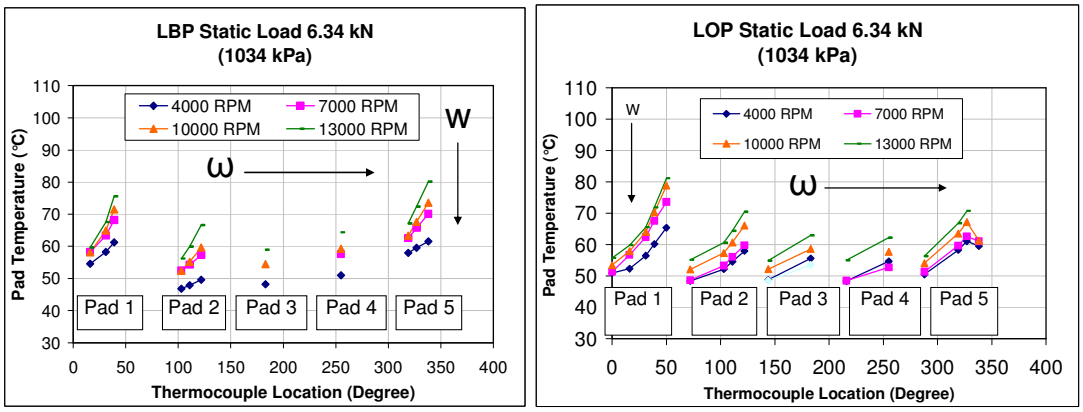

(b)

Fig. 74 Side by side comparison of LOP to LBP pad temperatures for (a) 345 kPa, (b) 1034 kPa, (c) 1723 kPa, (d) 2412 kPa

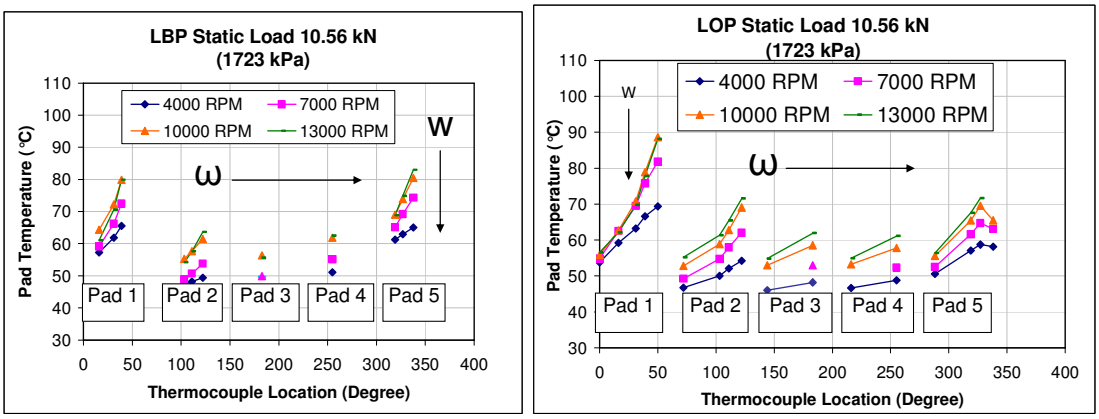

(c)

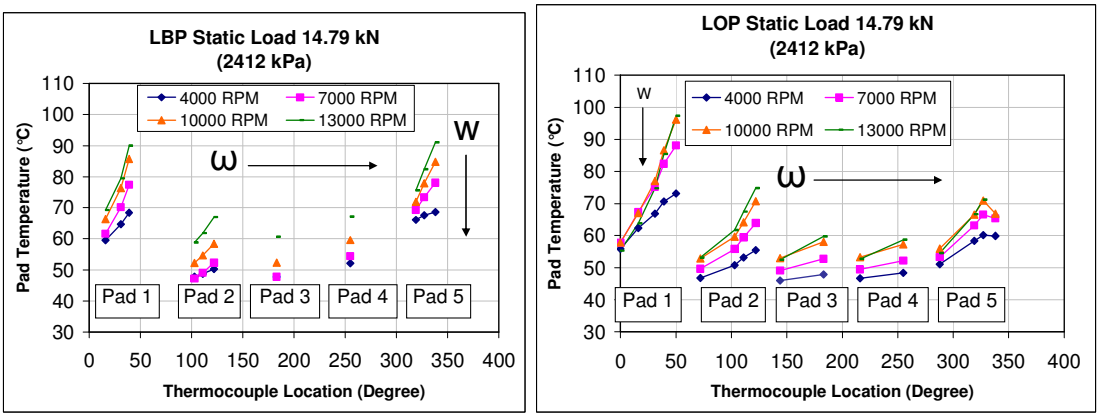

(d)

Fig. 74 "Continued"

To see the effect of the loading configuration, the stiffness coefficients resulting from both the LOP and LBP configurations can be plotted simultaneously on the same graph. Shown in Fig. 75 are the measured direct stiffness coefficients versus unit load. The plots show that the direct stiffness coefficient K_{yy} is significantly greater for the LOP condition than for the LBP condition. Little difference between the two bearings exists with the measured direct stiffness coefficient K_{xx}. Overall, the LOP bearing showed considerably more orthotropy than the LBP bearing. For the 4000 rpm maximum load condition the LOP bearing was two times more orthotropic than the LBP bearing.

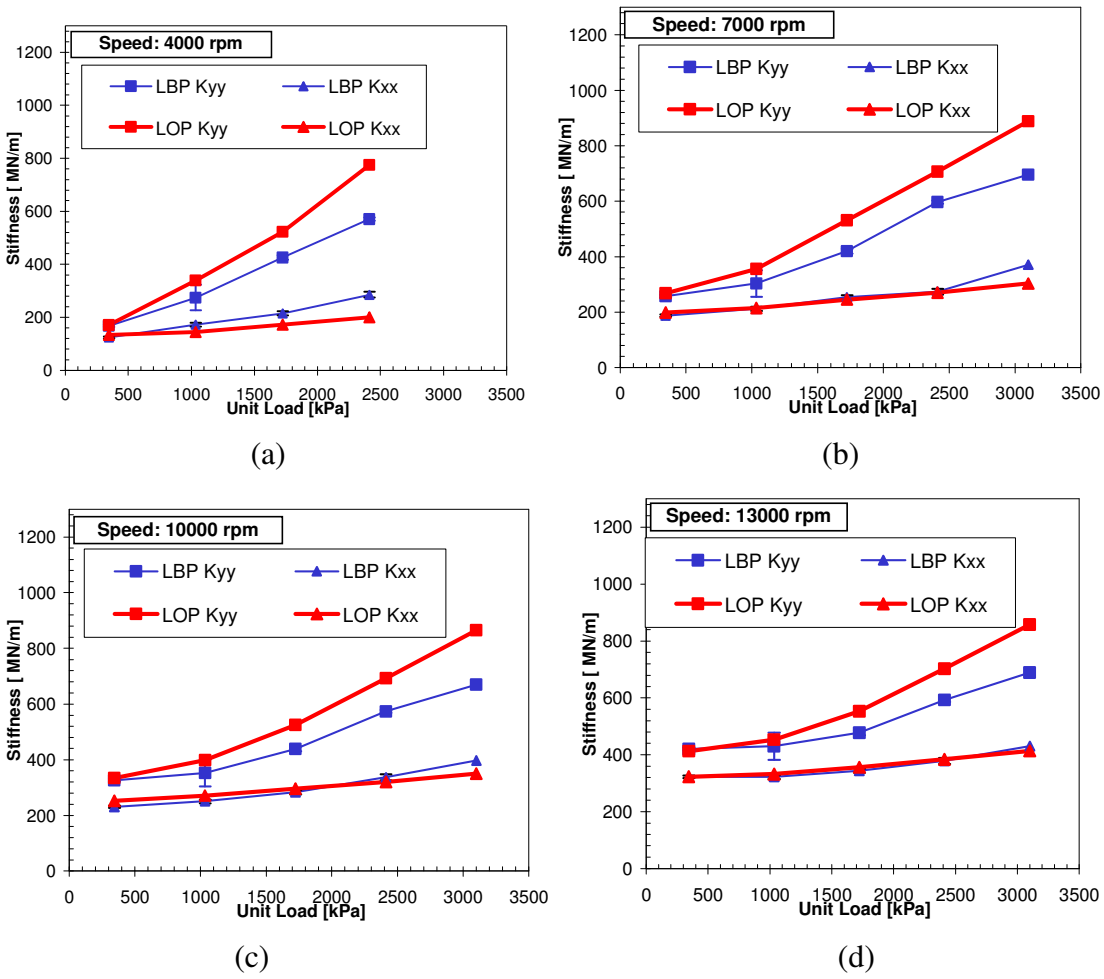

Fig. 75 LBP and LOP direct stiffness versus unit loading

Bearing damping is shown in Fig. 76. Little difference is seen between the LOP and LBP bearings in the measured damping coefficients. At the lowest speed of 4 krpm, damping is greatest from the LOP bearing direct damping term C_{yy}. The LBP direct damping coefficient C_{yy} is 10% to 15% less on average than for LOP bearing. Direct damping from the unloaded coefficient C_{xx} remains constant for both bearings, with an approximate value of 230 kN.s/m.

Generally the values of all damping coefficients remain fairly constant with increasing load, with the loaded coefficient C_{yy} maintaining a small increase over the unloaded coefficients.

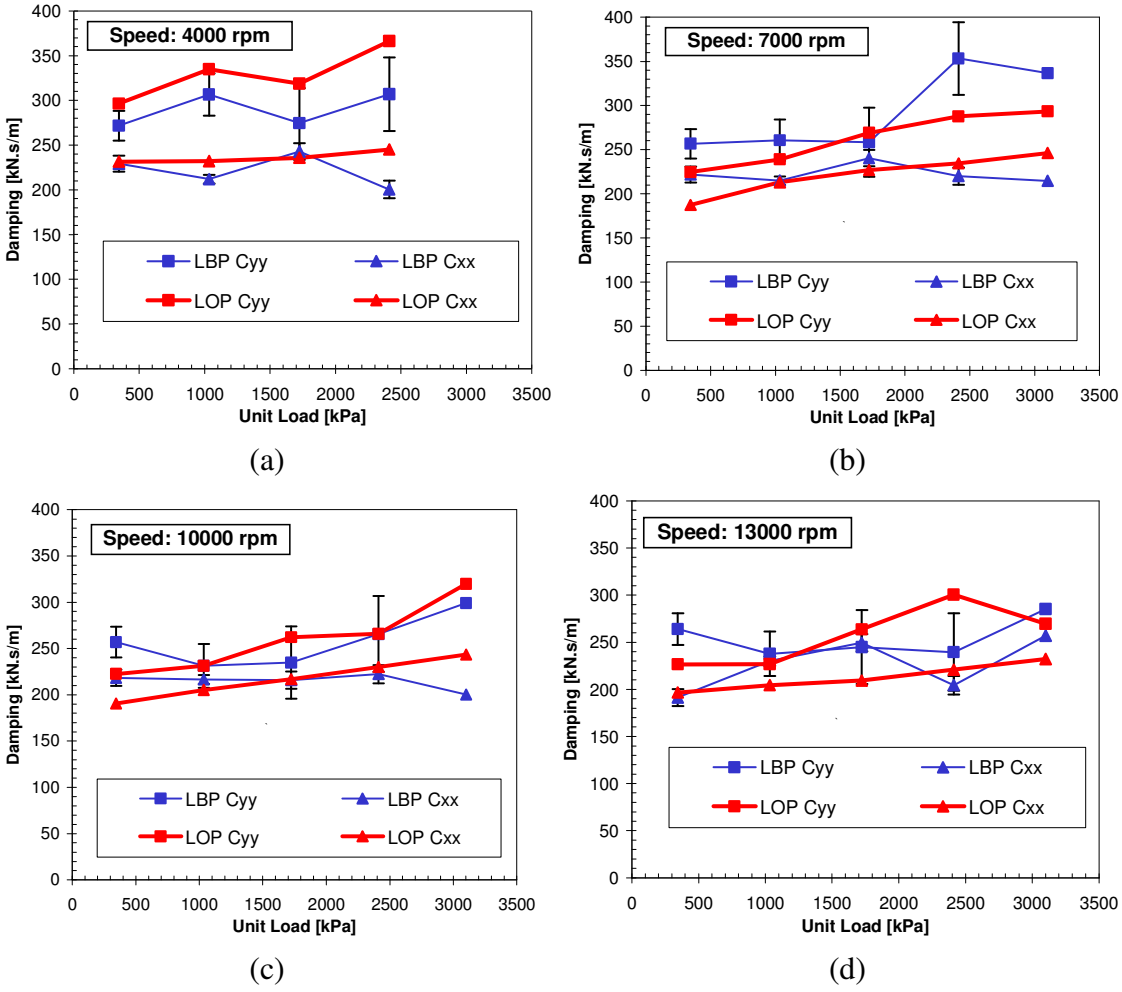

Fig. 76 LBP and LOP direct damping coefficients versus unit load

Shown in Fig. 77 are the static and dynamic stiffnesses associated with each bearing configuration. For almost all load and speed conditions, both the LOP static and dynamic stiffness are greater than those of the LBP bearing. Differences between the two bearings become more apparent as load is increased.

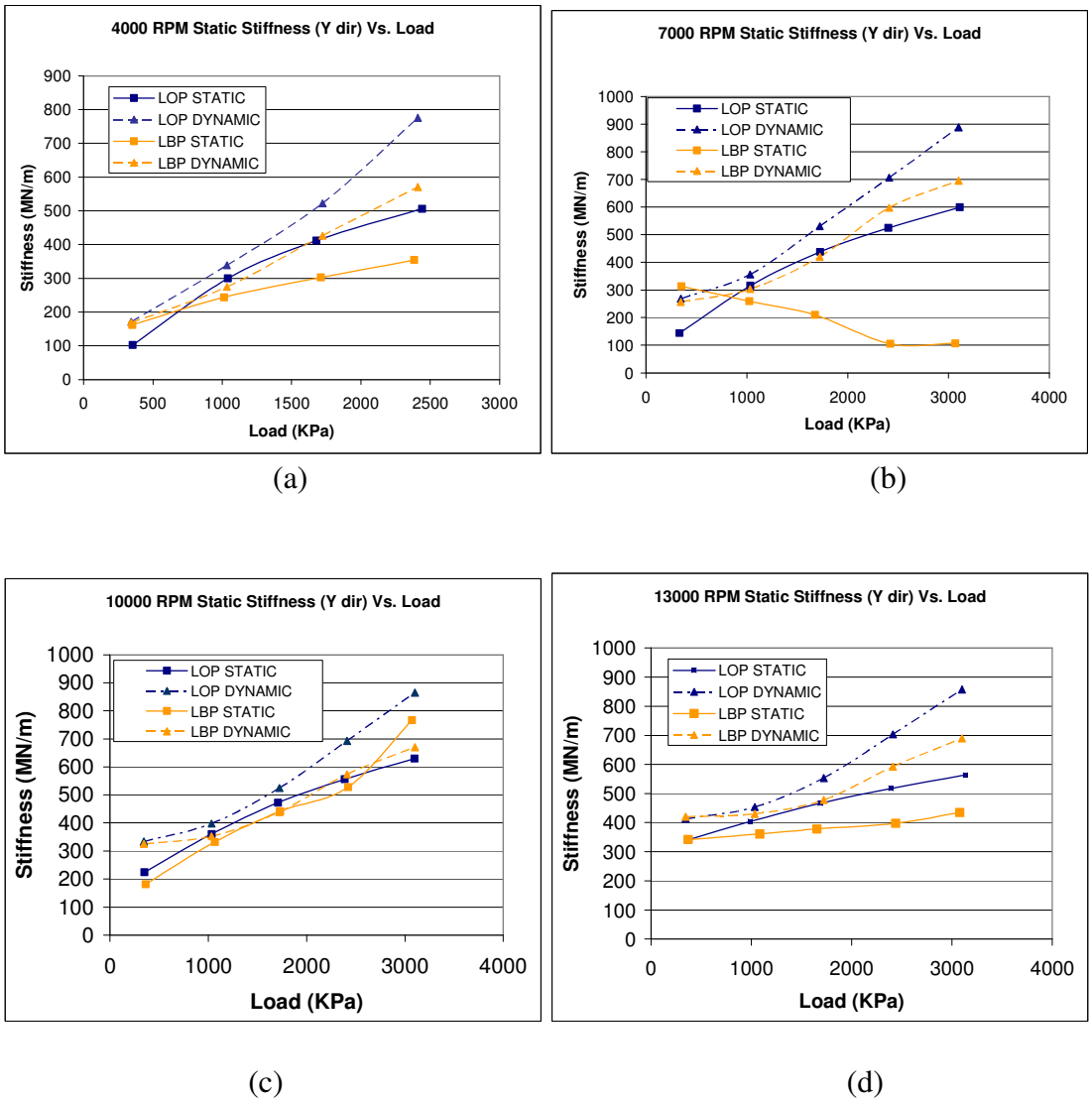

Fig. 77 Static and dynamic stiffness for LOP and LBP configurations for (a) 4 krpm, (b) 7 krpm, (c) 10 krpm, (d) 13 krpm

SUMMARY AND CONCLUSION

Dynamic Results

Rotordynamic coefficients results over a variety of speeds and loads are presented. Two different models can be chosen to define the rotordynamic bearing coefficients. If a conventional [K][C] model is chosen then the coefficients will be frequency dependent. A rotordynamic stability analysis using this model can be performed but only at the damped natural frequency, which requires iteration [15]. The other alternative is the introduction of a [K][C][M] model that eliminates the frequency dependency and the need for an iterative solution. The usage of this model eliminates the question as to what frequency the dynamic coefficients should be calculated at.

The experimental results show that most of the direct real dynamic stiffnesses can be fitted well with a quadratic equation to quantify the amount of added mass. For most test conditions the bearing can be better represented using a [K][C][M] model instead of the conventional [K][C] model. For the LBP bearing, some conditions presented unloaded added mass coefficients that were at or near zero, in which case a frequency dependent [K][C] model should be considered. With this [K][C][M] method, frequency independent coefficients can be obtained. However, bearing damping coefficients were not found to be dependent upon excitation frequency, load or speed. This result is similar to that seen by Ikeda et al. [14]. A stability analysis of the bearing in both load configurations was also performed in which it was found that the bearing has a whirl frequency ratio of zero, which means infinite stability.

Stiffness Coefficients: The direct stiffness coefficients were heavily dependent upon load, much more so than speed and increased linearly with load. Stiffness asymmetry was apparent in both the theory and tests with the theory slightly over predicting the stiffness coefficients.

Mass Coefficients: Large added mass coefficients were found that approached 60 kg. Direct coefficients in the loaded direction were significantly higher than the unloaded and were mostly speed dependent, rising steadily with speed. The coefficients were generally over predicted at lower speed and under predicted at higher. Some experimental test conditions exhibited negative added mass terms. This was especially prevalent at the 4000 krpm test condition for both the

LBP and LOP bearings. This phenomenon was not predicted by the code, which predicted a small but positive amount of added mass at this speed.

Damping Coefficients: Damping generally proves to be constant regardless of speed and load. Because of this, the damping coefficients were significantly over predicted by the code at low speeds and high load.

Static Results

Locus plots show that the static stiffness of the bearing is over predicted at lower speeds but improves with higher speed. Some cross coupling is seen in these plots in the form of deviation from the loaded axis, this is more predominant in the LBP results. Attitude angles are significant at higher speeds and low loads, but decrease to very low levels at the highest load.

Pad temperatures are fairly low and never exceed 91°C except at the highest loading condition (3103 kPa, 450 psi) , where temperatures reached 100 °C. The maximum predicted bearing temperatures rose with speed at approximately the same rate as the measured results but were commonly 10 to 15 degrees Celsius lower.

Power loss was shown to be dependent exclusively on speed and the maximum power loss was shown to be approximately 14 kW at the highest speed condition.. The theory was able to predict the power loss to a high degree of accuracy in the LOP condition but significantly over-predicted the loss for the LBP configuration.

REFERENCES

[1] A. Al-Ghasem, 2004, "Measurement of Rotordynamic Coefficients for a High Speed Flexure-Pivot Tilting-Pad Bearing (Load Between Pad) Configuration," Master's Thesis, Texas A&M University, College Station.

[2] L. Rodriguez, 2004, "Experimental Frequency-Dependent Rotordynamic Coefficients for a Load-on-Pad, High Speed, Flexible-Pivot Tilting-Pad Bearing," Master's Thesis, Texas A&M University, College Station.

[3] S. DeCamillo, 2006, "Test Results Comparing the Effect of Reverse Rotation on Offset Pivot Journal Bearing Pad Temperatures," Tribology Transactions **49**, pp. 305-314.

[4] R. G. Kirk, Reedy, S.W., 1988, "Evaluation of Pivot Stiffness for Typical Tilting-Pad Journal Bearing Designs," ASME Journal of Vibration, Acoustics, and Reliability in Design, **110**, pp. 165-171.

[5] L. Barret, and Allaire, P., 1988, "The Eigenvalue Dependance of Reduced Tilting Pad Bearing Stiffness and Damping Coefficients," Tribology Transactions, **31**, pp. 411-419.

[6] C. Carter, Kyoungtaek, K., Kim, T., Jafri, S., Toram, K., 2004, "The Analysis of a Flexible Rotor Supported by Two Plain Journal Bearings," MEEN 626 Assignment 3, Fall 2004, Texas A&M University.

[7] J. H. Ball, and Byrne, T.R., 1998, Tilting Pad Hydrodynamic Bearing for Rotating Machinery, Patent Number 5,795,076, Orion Corporation, Grafton, Wisconsin

[8] J. W. Lund, 1964, "Spring and Damping Coefficients for the Tilting-Pad Journal Bearing," ASLE Transactions, **7**, pp. 342-352.

[9] W. Shapiro, and Colsher, R., 1977, "Dynamic Characteristics of Fluid Film Bearings," in *Proceedings of the Sixth Turbomachinery Symposium*, Houston, TX pp. 39-53.

[10] J. C. Nicholas, Gunter, E.J., and Barrett, L.E., 1978, "The influence of Tilting Pad Bearing Characteristics on the Stability of High Speed Rotor-Bearing Systems," ASME.

[11] J. C. Nicholas, 2001, "Lund's Pad Assembly Method for Tilting Pad Journal Bearings," in Proc. of *ASME 2001 Design Engineering Technical Conference and Computers and information in Engineering Conference* Pittsburgh, PA: ASME.

[12] J. K. Parsell, Allaire, P.E., and Barrett, L.E., 1983, "Frequency Effects in Tilting-Pad Journal Bearing Dynamic Coefficients," ASLE Tran, **26**, pp. 222-227.

[13] H. C. Ha, and Yang, Seong Heon, 1999, "Excitation Frequency Effects on the Stiffness and Damping Coefficients of a Five-Pad Tilting Pad Journal Bearing," ASME J. of Tribology, **121**, pp. 517-522.

[14] K. Ikeda, Hirano, T., Yamashita, T., Mikami, M., Sakakida, H., 2004, "An Experimental Study of Static and Dynamic Characteristics of a 580MM (22.8IN) Diamter Direct Lubrication Tilting Pad Journal Bearing," in Proc. of *ASME/STLE International Joint Tribology Conference*, Long Beach, CA.

[15] L. Rodriguez, and Childs, D., 2004, "Experimental Rotordynamic Coefficient Results for a Load-on-Pad Flexible-Pivot Tilting-Pad Bearing With Comparison to Predictions From Bulk-Flow and Reynolds Equation Models," in Proc. of *Joint Tribology Conference* Long Beach, CA: ASME J. of Tribology, vol. **128**, pp 896-906.

[16] K. Wygant, 2001, "The Influence of Negative Preload and Non-Synchronous Excitations on the Performance of Tilting Pad Journal Bearings," Ph.D. Dissertation, University of Virginia, Charlottesville.

[17] W. Dmochowski, 2006, "Dynamic Properties of Tilting-Pad Journal Bearings: Experimental and Theoretical Investigation of Frequency Effects Due to Pivot Flexibility," in Proc. of *ASME Turbo Expo 2006: Power for Land, Sea and Air* Barcelona, Spain: ASME.

[18] B. Al-Jughaiman, 2006, "Static and Dynamic Characteristics for a Two-Axial-Groove Bearing and a Pressure Dam Bearing," Master's Thesis, Texas A&M University, College Station.

[19] M. Graviss, 2005, "The Influence of a Central Groove on Static and Dynamic Characteristics of an Annular Liquid Seal with Laminar Flow," Master's Thesis, Texas A&M University, College Station.

[20] D. Childs, Hale, K., and Elrod, D., 1989, "Annular Honeycomb Seals: Test Results for Leakage and Rotordynamic Coefficients: Comparison to Labyrinth and Smooth Configuration," ASME J. of Tribology, **111**, pp. 293-301.

[21] E. Reinhardt, and Lund, J., 1975, "The influence of Fluid Inertia on the Dynamic Properties of Journal Bearings," Journal of Lubrication Technology, **97**, pp. 159-167.

[22] S. Edney, and Mellinger, F., 1998, "Advances in Tilting Pad Journal Bearing Design," Dresser-Rand, Wellsville, NY.

[23] A. Kaul, 1999, "Design and Development of a Test Setup for the Experimental Determination of the Rotordynamic and Leakage Characteristics of Annular Bushing Oil Seals," Master's Thesis, Texas A&M University, College Station.

[24] V. Culatta, 2004, "Theory Versus Experiment of the Rotordynamic and Leakage Characteristics of Smooth Annular Bushing Breakdown Oil-Seals," Master's Thesis, Texas A&M University, College Station.

[25] D. Childs, and Hale, K., 1994, "A Test Apparatus and Facility to Identify the Rotordynamic Coefficients of High-Speed Hydrostatic Bearings," ASME J. of Tribology, **116**, pp. 337-344.

[26] C. Rouvas, and Childs, D., 1993, "A Parameter Identification Method for the Rotordynamic Coefficients of a High Reynolds Number Hydrostatic Bearing," ASME J. of Vibration and Acoustics, **115**, pp. 264-270.

[27] L. A. San Andres, 2004, "Turbulence in Fluid Film Bearings," in *Class Notes for MEEN 626*: Texas A&M University, p. 2.

[28] L. A. San Andres, 2004, "A thermohydrodynamic bulk-flow model for fluid film bearings," in *Class Notes for MEEN 626*: Texas A&M University, p. 5.

[29] L. A. San Andres, 1991, "Effect of Eccentricity on the Force Response of a Hybrid Bearing," STLE Tribology Transactions, **34**, pp. 537-544.

APPENDIX A

LBP CONFIGURATION

Table 5 LBP Static Test Data

ω (RPM)	W (kN)	p (kPa)	e_x (μm)	e_y (μm)	ε	Φ (degree)	Tin (°C)	Tout (°C)	Q (*lit / min*)	P (kW)
4000	2.17	353.3	-2.3	-5.0	0.07	-24.5	39.0	37.2	19.6	-0.95
4000	6.22	1013.8	-5.6	-25.7	0.33	-12.3	41.2	39.3	19.1	-1.00
4000	10.51	1712.0	-8.2	-40.5	0.52	-11.4	40.2	38.4	19.3	-0.96
4000	14.64	2385.2	-0.7	-53.6	0.68	-0.7	40.2	39.5	19.0	-0.40
7000	2.15	351.1	-0.8	-2.7	0.04	-15.7	39.2	39.9	23.5	0.47
7000	6.28	1023.1	-2.9	-18.6	0.24	-8.7	42.0	42.6	24.1	0.42
7000	10.29	1676.3	-3.6	-33.4	0.42	-6.2	39.5	40.2	23.6	0.45
7000	14.87	2423.2	-9.3	-64.2	0.82	-8.2	40.1	39.2	19.1	-0.49
7000	18.83	3068.3	4.8	-63.7	0.81	4.3	38.8	40.1	24.2	0.86
10000	2.22	362.3	1.5	-1.9	0.03	37.8	42.4	48.0	23.0	3.62
10000	6.54	1066.2	3.1	-17.4	0.22	10.0	39.0	45.3	21.0	3.69
10000	10.62	1730.2	1.7	-28.7	0.36	3.4	42.3	48.4	21.3	3.62
10000	14.87	2423.0	-1.9	-37.5	0.47	-3.0	39.7	45.8	21.8	3.75
10000	18.85	3071.8	9.3	-61.9	0.79	8.5	42.2	48.3	23.4	3.98
13000	2.27	369.7	2.6	-0.2	0.03	85.6	41.3	49.6	28.6	6.60
13000	6.65	1083.7	1.7	-12.0	0.15	8.2	40.5	49.2	26.5	6.40
13000	10.15	1653.7	1.6	-22.9	0.29	4.1	39.3	48.2	25.1	6.24
13000	14.97	2439.3	0.3	-34.7	0.44	0.5	38.3	46.9	26.0	6.25
13000	18.89	3077.3	10.8	-57.4	0.74	10.6	42.1	50.5	28.8	6.76

Table 6 LBP Pad Temperatures

		Pad 1					Pad 2				Pad 3		Pad 4		Pad 5				Pad 1	Pad 2
	Thermocouple number	1	2	3	4	5	6	7	8	9	10	11	12	13	14	15	16	17	18 (radial)	19(radial)
	% Of Pad Arc Length	NA	34	60	75	NA	NA	60	75	95	NA	75	NA	75	NA	60	75	95	NA	84
	Degree (from 1st probe)	NA	16	31	39	NA	NA	103	111	122	NA	183	NA	255	NA	319	327	338	NA	117
ω (RPM)	W (kN)	T1(°C)	T2(°C)	T3(°C)	T4(°C)	T5(°C)	T6(°C)	T7(°C)	T8(°C)	T9(°C)	T10(°C)	T11(°C)	T12(°C)	T13(°C)	T14(°C)	T15(°C)	T16(°C)	T17(°C)	T18(°C)	T19(°C)
4000	2.17	NA	50.04	53.13	55.45	NA	NA	46.41	47.91	50.10	NA	49.67	NA	50.19	NA	53.04	54.21	56.07	NA	53.78
4000	6.22	NA	54.59	58.28	61.27	NA	NA	46.79	47.94	49.63	NA	48.19	NA	50.99	NA	57.99	59.54	61.52	NA	58.77
4000	10.51	NA	57.31	61.84	65.51	NA	NA	47.25	48.17	49.43	NA	47.52	NA	51.11	NA	61.21	62.98	65.07	NA	62.16
4000	14.64	NA	59.51	64.68	68.42	NA	NA	47.81	48.72	50.22	NA	47.73	NA	52.13	NA	66.06	67.54	68.62	NA	66.06
7000	2.15	NA	51.09	55.48	59.39	NA	NA	48.52	50.87	54.71	NA	52.82	NA	53.69	NA	55.46	57.85	61.75	NA	58.27
7000	6.28	NA	58.21	63.34	68.16	NA	NA	52.49	54.31	57.27	NA	54.20	NA	57.59	NA	62.56	65.76	70.09	NA	66.19
7000	10.29	NA	59.13	66.21	72.50	NA	NA	48.87	50.73	53.81	NA	49.96	NA	55.17	NA	65.11	69.21	74.28	NA	69.29
7000	14.87	NA	61.60	70.19	77.33	NA	NA	47.18	49.08	52.29	NA	47.76	NA	54.39	NA	69.31	73.36	78.05	NA	72.69
10000	2.22	NA	59.41	63.78	68.47	NA	NA	57.25	59.88	64.49	NA	61.57	NA	63.94	NA	63.35	66.50	71.35	NA	67.25
10000	6.54	NA	58.21	64.91	71.45	NA	NA	52.40	55.14	59.66	NA	54.50	NA	59.30	NA	63.30	67.64	73.57	NA	68.24
10000	10.62	NA	64.28	72.14	79.87	NA	NA	55.33	57.66	61.42	NA	56.36	NA	61.90	NA	69.00	73.91	80.45	NA	74.42
10000	14.87	NA	66.31	76.35	85.73	NA	NA	52.25	54.63	58.39	NA	52.31	NA	59.59	NA	71.95	77.84	84.80	NA	77.82
13000	2.27	NA	57.25	63.63	70.39	NA	NA	56.75	60.63	67.75	NA	61.83	NA	64.58	NA	64.39	68.88	75.95	NA	68.69
13000	6.65	NA	59.66	67.52	75.56	NA	NA	56.22	59.92	66.60	NA	58.93	NA	64.37	NA	67.12	72.41	80.14	NA	69.86
13000	10.15	NA	61.03	70.61	79.88	NA	NA	54.22	57.59	63.64	NA	55.67	NA	62.52	NA	68.81	74.88	82.95	NA	70.13
13000	14.97	NA	69.23	79.44	89.97	NA	NA	58.78	61.83	67.00	NA	60.65	NA	67.10	NA	75.60	82.41	91.04	NA	73.41

Table 7 LBP Experimental Rotordynamic Coefficients

RPM	kPa	K_{xx}	K_{xy}	K_{yx}	K_{yy}	C_{xx}	C_{xy}	C_{yx}	C_{yy}	M_{xx}	M_{xy}	M_{yx}	M_{yy}
		(MN/m)				(kN.s/m)				(kg)			
4000	345	123.54	5.06	5.90	168.11	229.12	40.74	19.94	271.58	-8.99	-1.79	-16.58	12.20
4000	1034	172.45	13.70	-1.60	274.47	211.91	25.21	147.73	306.50	-15.53	-5.91	-8.37	-25.92
4000	1723	215.40	9.74	2.14	425.78	242.78	28.11	1.48	274.38	-37.53	-20.54	-29.53	-34.52
4000	2412	285.49	70.61	38.58	570.53	200.32	19.64	-8.90	306.90	-26.86	-7.43	-34.91	-46.55
7000	345	187.82	-8.91	12.65	256.96	221.67	37.86	27.24	256.54	7.13	-9.14	-16.12	31.62
7000	1034	212.12	0.21	13.57	303.03	214.94	23.96	56.11	260.58	2.39	-8.35	-18.83	14.24
7000	1723	253.33	6.70	7.51	419.51	240.39	26.35	5.35	258.42	-1.90	-11.59	-22.03	14.89
7000	2412	273.45	6.80	-19.45	597.06	219.99	30.99	0.04	353.27	-36.44	-15.00	-32.66	-31.82
7000	3101	370.94	5.91	-25.30	695.28	214.59	24.34	54.81	336.57	0.07	-8.53	-13.44	10.65
10000	345	230.59	-33.13	31.96	325.39	218.42	35.30	-1.91	256.94	-4.56	-19.99	-5.40	33.91
10000	1034	250.42	-21.70	31.48	352.67	216.59	22.86	8.80	231.34	2.01	-16.62	-8.51	20.21
10000	1723	283.04	-9.70	29.62	438.94	215.87	24.67	-5.55	234.85	-1.65	-15.24	-9.85	27.79
10000	2412	336.77	-4.55	14.61	573.62	222.36	18.15	-13.78	265.66	-0.08	-15.40	-16.75	35.56
10000	3101	396.70	-34.02	-43.27	670.30	200.31	15.53	19.04	299.03	15.33	-15.61	-26.83	11.39
13000	345	322.66	-49.97	38.20	420.11	191.13	12.36	11.13	263.96	34.42	-21.22	-16.53	68.87
13000	1034	321.89	-39.75	37.03	430.18	230.07	39.12	9.86	237.55	4.57	-16.00	-17.19	31.85
13000	1723	344.58	-30.36	32.99	477.79	249.37	36.75	16.38	244.89	21.38	-16.18	-9.21	37.06
13000	2412	378.14	-18.64	26.38	592.36	204.36	32.27	-1.37	239.47	29.85	-15.61	-7.14	66.80
13000	3101	429.89	-53.82	0.00	688.91	256.94	34.33	0.00	285.19	15.63	-15.12	0.00	34.94

Table 8 LBP Uncertainties of Experimental Rotordynamic Coefficients

RPM	kPa	Uncertainties												Coefficient of Determination							
		K_{xx}	K_{xy}	K_{yx}	K_{yy}	C_{xx}	C_{xy}	C_{yx}	C_{yy}	M_{xx}	M_{xy}	M_{yx}	M_{yy}								
		(MN/m)				(kN.s/m)				(kg)				R^2_{kxx}	R^2_{kxy}	R^2_{kyx}	R^2_{kyy}	R^2_{cxx}	R^2_{cxy}	R^2_{cyx}	R^2_{cyy}
4000	345	4.05	3.65	4.55	7.27	8.93	12.32	7.52	16.69	3.59	3.23	3.53	4.59	0.57	0.08	0.82	0.63	0.99	0.66	0.54	0.98
4000	1034	7.03	11.56	48.02	12.32	4.83	7.72	60.82	23.52	4.55	6.16	26.43	8.77	0.66	0.12	0.02	0.66	1.00	0.63	0.47	0.97
4000	1723	7.43	6.93	9.02	13.03	9.28	10.37	15.23	39.18	5.60	3.73	4.95	7.78	0.90	0.84	0.86	0.79	0.99	0.55	0.00	0.90
4000	2412	10.88	4.69	5.88	18.25	9.77	9.29	13.95	41.05	5.84	2.48	3.10	11.94	0.79	0.63	0.96	0.75	0.99	0.45	0.08	0.93
7000	345	4.79	3.85	9.98	7.62	13.37	10.86	12.37	20.13	4.15	2.56	6.45	4.98	0.40	0.74	0.89	0.89	0.98	0.67	0.47	0.97
7000	1034	2.55	3.58	4.44	13.24	12.06	5.94	20.67	28.34	2.65	2.16	2.74	6.82	0.17	0.73	0.90	0.41	0.98	0.72	0.54	0.93
7000	1723	2.17	5.11	5.68	10.22	8.09	9.76	12.00	15.05	2.26	2.58	3.17	6.64	0.15	0.78	0.91	0.50	0.99	0.54	0.04	0.98
7000	2412	5.92	3.92	6.50	16.92	8.57	9.10	17.19	32.95	4.37	2.55	3.98	9.98	0.93	0.88	0.94	0.65	0.99	0.66	0.00	0.97
7000	3101	5.32	4.99	12.87	14.78	8.23	10.19	25.37	22.15	3.03	2.64	7.18	9.62	0.00	0.63	0.44	0.21	0.99	0.48	0.49	0.98
10000	345	8.13	2.26	10.08	8.50	9.51	7.80	8.41	12.59	6.75	1.67	6.81	5.66	0.09	0.97	0.24	0.88	0.99	0.78	0.01	0.99
10000	1034	7.95	2.82	3.40	8.31	5.43	4.46	14.89	15.00	6.41	1.52	1.97	4.38	0.02	0.96	0.79	0.80	1.00	0.81	0.06	0.98
10000	1723	7.61	4.02	3.47	10.89	6.05	4.72	12.44	14.33	5.64	2.20	1.69	6.24	0.02	0.91	0.87	0.78	1.00	0.82	0.04	0.98
10000	2412	7.83	3.76	4.03	8.74	6.97	4.90	15.19	16.02	5.37	2.11	2.07	6.16	0.00	0.92	0.93	0.88	0.99	0.70	0.14	0.98
10000	3101	7.13	10.38	10.59	15.05	13.89	9.52	25.63	17.48	4.05	4.82	5.18	8.54	0.74	0.89	0.85	0.27	0.97	0.34	0.11	0.98
13000	345	7.45	8.44	4.24	11.18	12.65	10.87	14.02	19.09	9.90	11.23	5.41	8.39	0.76	0.48	0.73	0.93	0.98	0.21	0.12	0.98
13000	1034	4.97	2.37	4.49	10.25	9.91	8.66	18.51	13.80	4.69	1.52	2.78	5.49	0.21	0.96	0.89	0.87	0.99	0.78	0.06	0.98
13000	1723	3.95	2.31	4.52	11.01	8.56	8.75	22.65	15.53	6.77	1.60	3.38	6.47	0.76	0.96	0.67	0.87	0.99	0.77	0.09	0.98
13000	2412	9.28	4.49	4.86	7.40	9.94	7.24	18.54	19.27	7.40	2.69	3.23	4.78	0.80	0.88	0.54	0.98	0.99	0.79	0.00	0.97
13000	3101	18.20	33.26	0.00	36.80	43.74	30.60	0.00	79.13	9.34	17.40	0.00	17.85	0.34	0.10	0.00	0.45	0.84	0.16	0.00	0.66

Table 9 LBP Predicted Rotordynamic Coefficients

RPM	kPa	K_{xx}	K_{xy}	K_{yx}	K_{yy}	C_{xx}	C_{xy}	C_{yx}	C_{yy}	M_{xx}	M_{xy}	M_{yx}	M_{yy}
		(MN/m)				(kN.s/m)				(kg)			
4000	345	160.78	-0.41	0.29	174.28	378.76	1.68	-1.84	407.07	4.25	0.42	-0.45	4.72
4000	1034	173.23	-0.67	0.02	292.30	403.64	1.25	-2.27	648.15	5.48	0.35	-0.51	9.90
4000	1723	194.23	-0.93	-0.24	497.18	448.70	0.80	-2.69	1067.83	6.03	0.29	-0.55	15.36
4000	2412	207.97	-1.13	-0.44	734.64	477.79	0.49	-2.98	1559.72	6.57	0.23	-0.59	18.11
7000	345	237.97	-0.39	0.26	246.19	342.49	1.99	-2.07	352.34	7.90	0.98	-1.00	8.22
7000	1034	245.89	-0.74	-0.09	323.29	349.40	1.71	-2.39	441.25	8.96	0.94	-1.04	12.26
7000	1723	277.96	-1.06	-0.40	466.73	391.27	1.46	-2.64	616.99	9.45	0.88	-1.07	17.70
7000	2412	300.08	-1.44	-0.78	672.93	418.25	1.18	-2.96	869.34	10.33	0.83	-1.09	26.90
7000	3101	316.68	-1.67	-1.00	874.19	438.54	1.03	-3.13	1127.47	10.97	0.79	-1.11	35.63
10000	345	302.00	-0.28	0.16	308.66	305.74	1.83	-1.89	311.09	14.19	1.40	-1.41	14.51
10000	1034	338.55	-0.62	-0.17	394.44	339.51	1.65	-2.10	384.86	15.11	1.36	-1.41	17.88
10000	1723	337.55	-1.01	-0.58	499.81	334.08	1.45	-2.33	464.04	15.97	1.35	-1.47	24.15
10000	2412	376.14	-1.42	-0.98	663.93	369.20	1.21	-2.61	604.03	17.11	1.31	-1.48	32.36
10000	3101	380.62	-1.69	-1.26	848.89	369.65	1.08	-2.78	754.23	17.88	1.31	-1.51	43.30
13000	345	370.44	-0.19	0.07	375.84	285.39	1.54	-1.57	288.62	17.62	1.65	-1.66	17.86
13000	1034	391.62	-0.54	-0.28	439.14	299.19	1.39	-1.74	327.88	18.34	1.63	-1.68	20.35
13000	1723	418.33	-0.89	-0.62	526.42	317.05	1.25	-1.89	382.66	19.22	1.60	-1.70	23.95
13000	2412	455.95	-1.35	-1.09	678.46	342.16	1.06	-2.11	479.22	20.50	1.59	-1.70	30.71
13000	3101	445.84	-1.71	-1.48	830.31	330.78	0.89	-2.27	566.58	20.78	1.60	-1.77	38.55

Table 10 LBP Experimental Dynamic Stiffnesses at 4000 RPM and 345 kPa

	Dynamic stiffness								Uncertainty							
f(Hz)	$Re(H_{xx})$	$Im(H_{xx})$	$Re(H_{xy})$	$Im(H_{xy})$	$Re(H_{yx})$	$Im(H_{yx})$	$Re(H_{yy})$	$Im(H_{yy})$	$Re(U_{xx})$	$Im(U_{xx})$	$Re(U_{xy})$	$Im(U_{xy})$	$Re(U_{yx})$	$Im(U_{yx})$	$Re(U_{yy})$	$Im(U_{yy})$
20.00	128.7	33.3	-1.2	-0.7	7.1	-1.3	175.9	45.7	12.99	3.76	5.16	2.92	3.58	3.26	19.73	3.71
30.00	130.2	49.8	-0.3	0.8	9.3	-1.7	178.1	67.1	13.22	4.01	3.24	5.19	3.68	2.26	18.95	5.45
40.00	131.0	63.5	1.7	0.6	8.2	-3.1	178.0	90.1	14.14	4.30	5.81	3.07	2.42	2.36	19.70	6.09
50.00	130.4	80.6	13.3	5.8	7.3	-4.1	174.8	119.3	15.42	4.12	19.99	11.49	5.09	2.94	27.12	15.93
60.00	131.7	93.9	10.7	69.5	3.0	-5.1	95.7	144.1	76.41	82.08	186.56	195.84	34.91	49.76	201.41	55.63
70.00	125.6	103.7	-13.2	175.9	15.7	-8.9	-14.5	155.4	24.43	12.23	53.94	82.80	19.17	23.32	89.17	44.12
80.00	125.1	130.5	14.7	29.2	2.4	-17.5	79.3	206.1	14.39	7.67	8.92	40.06	3.18	2.73	36.84	10.29
90.00	136.1	134.3	9.0	12.0	10.2	-3.7	173.6	180.5	14.53	9.06	11.56	16.57	3.34	2.63	30.47	8.93
100.00	135.2	148.6	6.2	7.2	13.4	-5.7	173.7	204.4	12.80	9.87	4.45	15.06	2.63	3.07	25.59	13.38
110.00	132.1	160.2	6.2	4.7	17.8	-5.4	178.1	221.8	14.85	12.72	3.96	9.39	2.50	3.32	21.11	10.14
120.00	139.8	180.7	11.8	6.5	17.7	3.9	179.1	242.6	29.79	26.31	29.72	56.14	29.10	29.98	58.39	72.69
130.00	126.1	184.8	16.3	-12.9	23.4	2.1	148.4	267.1	36.91	78.07	71.15	172.98	37.13	88.80	68.19	213.29
140.00	144.9	211.7	18.2	9.8	8.5	-14.3	139.8	257.0	71.04	70.82	39.43	30.99	60.66	75.66	31.68	36.68
150.00	136.9	210.6	6.4	4.7	15.5	10.3	135.8	287.7	12.50	15.22	4.74	8.21	3.82	3.29	15.07	13.39
160.00	134.6	218.9	4.6	3.7	30.0	9.5	168.0	319.0	13.09	18.68	2.48	9.36	3.75	3.98	16.83	22.02
170.00	134.7	241.8	4.2	5.1	27.9	2.9	166.9	337.6	14.33	19.16	4.08	7.14	5.00	3.77	16.33	22.56
180.00	132.1	249.7	13.4	18.6	39.3	-3.7	188.3	355.3	50.89	34.10	44.74	48.96	90.00	68.21	107.55	93.52
190.00	136.4	260.9	4.1	12.0	35.1	11.8	165.9	350.2	14.96	28.18	4.07	6.42	13.32	8.90	15.41	23.44
200.00	144.3	281.1	3.4	19.3	32.5	12.8	155.4	361.4	11.70	22.92	7.19	7.26	6.26	2.85	16.17	23.61
210.00	131.9	303.2	3.7	22.4	50.7	5.7	147.7	364.6	11.66	33.98	10.52	5.84	22.60	6.25	14.50	27.23
220.00	139.4	321.9	8.3	36.0	53.4	-6.1	86.6	342.9	13.87	26.53	7.73	4.42	5.96	3.25	15.73	22.79
230.00	161.5	334.4	12.0	25.0	47.9	13.1	143.1	448.8	15.58	30.23	7.99	7.75	12.75	3.81	24.01	29.99
240.00	146.4	342.4	7.9	32.8	48.4	10.6	128.7	421.6	28.51	37.54	21.85	11.85	22.13	16.44	21.24	28.27
250.00	172.6	377.5	-8.7	14.0	56.6	8.4	63.6	438.6	28.99	43.15	159.35	199.11	30.17	32.65	143.26	227.48
260.00	118.8	402.4	-35.0	60.5	-27.1	7.2	75.0	395.4	376.41	64.78	273.72	47.71	306.95	35.80	226.96	71.21
270.00	238.9	398.2	44.6	69.2	7.9	35.2	-79.4	444.1	29.82	39.75	72.26	34.04	18.25	39.23	35.19	52.05
280.00	253.3	418.5	33.5	67.5	39.5	30.0	131.5	504.5	68.13	136.85	30.11	34.59	47.54	133.84	34.42	36.40
290.00	301.0	446.4	76.3	72.2	2.8	20.5	5.8	638.2	24.30	35.44	22.63	10.74	12.31	19.92	28.73	61.68
300.00	377.5	469.2	98.3	85.9	21.8	34.1	65.5	666.8	45.77	43.56	33.34	28.32	18.00	23.90	30.88	63.21
310.00	445.7	549.7	120.3	101.3	39.7	3.2	72.7	615.7	41.20	38.35	22.16	36.11	15.77	21.96	18.12	65.10
320.00	635.2	448.9	170.9	140.4	91.5	111.9	185.9	618.8	63.69	61.73	29.19	12.26	40.33	30.33	34.96	46.57

Table 11 LBP Experimental Dynamic Stiffnesses at 4000 RPM and 1034 kPa

	Dynamic stiffness								Uncertainty							
f(Hz)	$Re(H_{xx})$	$Im(H_{xx})$	$Re(H_{xy})$	$Im(H_{xy})$	$Re(H_{yx})$	$Im(H_{yx})$	$Re(H_{yy})$	$Im(H_{yy})$	$Re(U_{xx})$	$Im(U_{xx})$	$Re(U_{xy})$	$Im(U_{xy})$	$Re(U_{yx})$	$Im(U_{yx})$	$Re(U_{yy})$	$Im(U_{yy})$
20	170.8	35.5	4.1	0.5	-205.7	41.7	284.7	57.7	9.61	8.06	18.69	11.73	564.55	143.55	49.91	31.44
30	171.2	58.0	6.9	2.2	66.4	15.0	285.1	86.6	7.83	5.06	6.94	10.30	161.12	214.64	6.02	9.72
40	173.5	74.4	11.9	1.4	154.7	-13.5	297.8	115.9	3.73	3.74	11.06	10.58	397.81	70.86	12.46	12.46
50	174.4	90.3	34.6	7.7	-10.4	53.7	279.3	180.7	6.32	5.77	30.59	15.81	177.51	237.98	44.91	61.53
60	179.3	93.2	60.9	165.0	175.0	-105.1	292.6	330.1	48.63	71.65	164.71	273.49	404.75	202.41	384.59	192.63
70	187.9	106.6	-57.4	287.4	119.6	-145.2	129.0	277.5	8.74	11.66	11.72	12.30	134.80	441.12	638.58	205.88
80	177.1	135.8	67.4	63.3	-209.8	-98.0	134.7	210.5	3.77	4.99	31.91	59.63	598.86	326.51	228.38	269.58
90	183.1	151.0	30.0	21.7	11.5	44.3	282.3	253.9	6.47	4.02	18.74	23.96	194.64	184.61	40.30	39.41
100	185.0	165.8	22.0	16.5	110.7	-139.2	285.6	250.4	6.15	2.36	8.17	9.79	271.69	183.16	34.20	20.74
110	182.2	179.6	17.2	10.9	87.4	-39.7	279.9	283.3	4.35	3.72	10.97	11.33	344.24	65.15	26.78	31.35
120	183.3	192.4	21.0	9.0	-159.2	29.1	293.6	334.2	33.41	29.45	71.91	102.83	386.78	69.67	59.29	148.47
130	188.0	206.1	41.5	13.3	-109.9	-132.0	208.7	321.8	9.60	6.54	39.80	22.68	312.65	123.04	98.38	51.61
140	188.6	220.2	24.3	13.3	72.2	20.3	266.4	347.0	8.28	6.26	23.47	12.46	135.18	113.47	27.85	30.37
150	192.4	230.8	15.8	11.4	63.8	-97.9	296.4	358.6	6.34	3.18	7.01	5.29	155.61	528.24	18.90	31.28
160	188.8	238.9	17.6	-4.7	-117.1	328.3	395.6	585.4	7.03	5.48	7.06	11.83	697.26	566.42	30.46	29.48
170	189.0	259.1	13.0	12.5	-138.9	-37.2	306.5	423.5	3.56	4.60	3.74	4.97	403.27	92.93	21.82	8.95
180	186.6	268.7	25.6	9.1	-59.9	236.8	313.5	449.9	21.26	25.92	50.94	31.97	394.80	509.32	39.53	40.97
190	190.2	278.8	14.7	18.7	167.9	-48.6	334.2	444.1	4.44	5.44	5.74	7.70	311.99	411.72	24.72	30.60
200	188.8	294.4	19.2	29.3	-72.5	-18.3	321.1	455.0	28.63	14.91	34.31	40.80	293.52	305.64	54.76	46.64
210	179.0	304.3	16.2	26.5	274.6	96.1	340.8	484.1	4.23	4.87	6.53	9.08	276.39	132.32	24.38	9.76
220	184.2	324.8	21.1	33.1	-153.2	-71.4	271.5	468.3	4.49	7.22	9.49	3.94	620.72	240.16	75.57	19.42
230	193.5	336.1	29.0	23.2	-7.4	434.6	343.3	675.9	4.36	4.96	8.16	9.82	240.91	1102.70	97.39	104.36
240	184.9	342.1	14.4	27.8	-270.8	312.1	287.9	593.8	13.44	7.36	18.16	19.92	1196.05	635.16	96.03	116.42
250	192.9	360.3	23.7	38.4	50.9	275.1	338.8	600.1	3.99	9.26	11.22	11.88	243.18	559.51	60.65	54.92
260	204.3	376.3	24.1	44.1	-93.0	240.8	334.3	586.0	18.57	13.36	14.55	31.88	595.10	260.32	51.96	60.31
270	191.9	354.4	41.4	34.1	67.8	105.2	370.8	550.1	350.12	84.00	81.37	67.48	550.55	267.34	209.56	138.57
280	225.1	390.6	35.9	14.4	60.5	262.0	445.7	785.4	8.35	6.07	35.80	31.41	300.93	506.49	91.01	114.23
290	240.9	411.8	24.6	48.3	170.1	330.6	456.2	616.0	10.74	6.05	10.47	9.20	238.55	429.52	103.28	40.31
300	278.9	424.4	31.4	62.1	142.5	176.8	383.2	567.2	24.12	25.30	16.43	20.35	356.39	493.45	111.75	70.39
310	303.3	435.6	32.5	69.8	-281.4	557.8	473.7	654.7	23.62	11.15	6.10	6.50	814.80	1191.11	108.51	89.97
320	395.7	434.7	49.8	52.2	298.2	111.3	441.3	815.9	53.95	27.38	16.90	10.98	1397.47	539.90	50.87	185.77

Table 12 LBP Experimental Dynamic Stiffnesses at 4000 RPM and 1723 kPa

	Dynamic stiffness								Uncertainty							
f(Hz)	$Re(H_{xx})$	$Im(H_{xx})$	$Re(H_{xy})$	$Im(H_{xy})$	$Re(H_{yx})$	$Im(H_{yx})$	$Re(H_{yy})$	$Im(H_{yy})$	$Re(U_{xx})$	$Im(U_{xx})$	$Re(U_{xy})$	$Im(U_{xy})$	$Re(U_{yx})$	$Im(U_{yx})$	$Re(U_{yy})$	$Im(U_{yy})$
20	215.5	41.6	8.9	3.7	-12.5	4.7	416.4	75.8	17.66	29.17	18.60	20.88	8.73	13.94	9.35	6.80
30	213.4	62.5	10.2	2.2	-11.6	-3.3	426.1	106.9	11.94	7.14	15.29	18.43	16.84	9.94	8.45	6.83
40	216.3	84.9	13.1	5.7	-4.8	-0.2	432.0	138.1	7.64	6.57	13.77	12.38	9.68	6.29	10.31	7.53
50	219.1	106.7	27.7	5.3	-11.1	-19.5	435.6	186.8	7.92	7.10	15.08	9.86	14.84	8.45	14.76	25.50
60	218.9	138.1	44.6	84.9	-33.0	-37.9	224.0	313.4	130.79	117.57	253.80	270.99	65.93	124.96	237.35	105.33
70	196.5	119.2	8.6	313.4	21.1	-69.6	-24.7	285.7	18.39	13.38	40.54	23.97	17.35	22.89	31.57	64.68
80	226.8	153.3	65.4	33.2	5.3	-25.2	406.0	338.3	4.27	6.22	19.97	16.15	9.66	5.60	19.79	30.51
90	238.5	170.2	26.3	12.8	7.7	-19.2	448.5	285.2	3.84	4.28	11.36	16.15	9.56	4.24	15.29	16.94
100	241.0	178.6	27.3	4.8	11.5	-25.7	434.4	315.2	3.72	4.72	8.96	11.34	6.81	2.87	6.65	17.09
110	238.5	192.5	20.9	9.5	32.1	-42.5	446.8	328.1	5.96	5.92	7.98	11.60	7.09	4.81	7.22	11.23
120	252.1	206.8	18.2	-0.1	24.4	-13.8	468.8	355.2	39.21	39.53	54.95	69.05	66.95	75.31	100.82	124.87
130	240.3	229.0	36.5	-5.2	38.7	-33.6	408.0	417.2	69.71	33.25	31.98	26.16	133.90	39.43	53.87	51.23
140	251.9	236.2	25.3	10.7	24.7	-14.5	431.1	430.0	10.78	6.80	11.22	9.84	12.14	14.97	18.25	17.56
150	255.2	249.4	21.5	15.4	25.8	-8.1	469.0	417.1	4.17	6.13	5.65	4.75	8.09	5.55	9.77	9.90
160	256.0	256.0	35.3	-6.4	60.2	0.2	487.0	699.9	6.22	8.35	7.68	6.43	7.18	5.36	14.67	30.01
170	256.7	277.1	25.5	12.6	29.1	-23.3	487.6	490.7	2.83	6.28	8.57	5.43	5.11	4.72	8.92	10.92
180	250.0	278.6	28.7	10.2	43.3	-35.8	513.6	489.8	43.09	42.72	51.65	51.38	112.91	110.61	117.08	138.55
190	264.5	299.5	29.3	20.9	60.0	-9.6	516.3	496.0	6.13	6.82	8.70	3.59	5.38	4.63	7.92	7.57
200	270.7	311.9	34.0	25.0	48.2	-4.2	508.9	502.5	9.39	12.88	9.72	14.65	11.69	15.29	24.24	17.09
210	262.7	327.0	32.3	27.0	73.5	-23.7	499.7	519.1	5.05	7.13	8.11	4.59	4.98	5.94	8.86	7.34
220	275.5	345.0	40.3	29.4	79.4	-33.3	468.4	516.4	6.86	8.55	7.92	4.55	6.85	3.75	8.34	8.93
230	284.8	359.7	55.9	14.7	48.6	-7.4	395.7	742.7	5.43	10.13	8.18	6.38	6.54	7.86	10.78	23.24
240	286.4	368.9	37.4	26.0	73.3	-15.8	495.0	585.0	14.83	13.03	13.84	11.74	15.90	17.64	20.57	14.37
250	302.3	388.8	47.3	36.4	69.2	-16.8	479.1	630.3	10.98	8.76	15.44	12.73	10.94	9.49	18.19	24.13
260	331.2	369.2	49.8	42.9	68.5	-56.7	498.8	529.8	46.03	194.27	42.55	38.12	80.78	230.66	44.16	46.77
270	386.1	441.1	-51.2	22.3	123.1	45.0	342.6	541.0	325.80	838.24	492.80	481.81	420.22	960.28	613.30	548.16
280	386.0	440.2	99.4	15.3	55.2	80.5	378.0	928.2	12.51	12.54	25.61	14.05	8.87	11.71	31.82	29.58
290	425.0	467.4	68.7	58.6	95.2	39.4	512.8	572.8	5.12	8.62	7.25	10.19	7.89	4.59	12.47	9.33
300	484.1	492.1	86.9	73.4	97.3	72.2	454.8	562.1	17.64	25.04	17.27	18.84	7.38	9.07	11.02	9.92
310	556.3	518.3	105.5	74.3	103.4	106.0	398.6	587.8	13.99	9.98	9.08	6.98	6.62	7.67	11.80	6.84
320	656.9	547.3	93.8	68.7	140.0	135.5	522.2	611.7	22.68	19.44	9.40	8.86	18.41	15.17	12.43	10.29

Table 13 LBP Experimental Dynamic Stiffnesses at 4000 RPM and 2413 kPa

	Dynamic stiffness								Uncertainty							
f(Hz)	$Re(H_{xx})$	$Im(H_{xx})$	$Re(H_{xy})$	$Im(H_{xy})$	$Re(H_{yx})$	$Im(H_{yx})$	$Re(H_{yy})$	$Im(H_{yy})$	$Re(U_{xx})$	$Im(U_{xx})$	$Re(U_{xy})$	$Im(U_{xy})$	$Re(U_{yx})$	$Im(U_{yx})$	$Re(U_{yy})$	$Im(U_{yy})$
20	283.9	44.0	65.1	-0.2	18.8	6.1	543.1	84.2	29.64	32.27	18.53	19.49	14.78	12.59	9.75	9.56
30	277.5	65.7	60.0	2.9	28.6	-9.6	570.9	106.5	12.41	10.38	9.67	9.33	10.82	7.47	11.37	5.49
40	284.8	83.5	61.1	-1.2	41.3	0.3	576.7	138.6	10.93	17.64	11.07	7.93	9.66	10.79	8.28	8.73
50	293.3	102.3	68.7	1.2	35.9	-21.3	567.6	152.7	10.09	8.74	8.77	6.72	8.22	6.77	14.45	8.21
60	289.5	130.3	61.3	14.1	27.9	-14.6	555.0	209.7	53.13	82.97	157.46	126.38	34.19	26.77	23.05	64.80
70	174.2	124.7	150.3	367.6	-17.3	-188.2	165.3	456.2	72.26	117.94	142.70	151.48	138.56	110.68	142.02	240.53
80	302.7	155.6	75.1	1.1	52.0	-13.9	577.9	312.2	8.99	11.47	22.22	22.17	16.68	11.41	14.22	41.18
90	300.3	168.2	67.8	3.9	55.4	-32.7	612.7	244.3	7.60	8.55	10.67	11.44	7.25	6.04	13.52	17.88
100	308.6	186.1	78.8	2.4	50.1	-28.7	568.9	307.1	6.28	5.84	6.60	6.68	4.10	4.69	12.78	9.09
110	313.2	197.6	72.4	2.6	70.6	-42.8	612.9	307.7	4.19	10.23	9.13	7.29	6.31	6.26	13.40	8.53
120	316.2	193.3	81.7	0.6	49.3	-66.5	642.7	329.6	58.53	49.97	58.74	47.53	90.45	74.59	106.16	84.27
130	318.1	225.6	82.1	-0.2	64.3	-33.5	570.0	404.2	7.08	15.90	7.57	10.11	10.57	26.39	11.77	15.84
140	293.9	251.8	75.2	2.2	124.0	-45.4	577.1	452.9	124.91	50.38	78.74	23.95	224.94	145.60	141.77	73.14
150	321.0	249.6	78.9	7.5	72.4	-24.6	619.2	401.3	7.18	6.36	5.46	6.63	5.37	6.61	10.93	7.49
160	316.2	261.5	98.6	-21.0	115.7	-48.8	638.4	775.8	6.28	10.42	4.17	6.11	6.19	9.49	13.17	29.74
170	318.0	274.6	78.9	3.1	76.7	-41.1	648.0	476.1	4.88	9.38	6.16	4.01	4.24	3.94	12.63	8.07
180	308.5	284.3	77.4	-2.8	97.6	-40.1	684.2	485.2	40.03	68.10	63.27	55.55	13.82	10.78	20.23	6.54
190	323.2	302.5	90.4	16.2	99.3	-34.7	669.6	466.0	3.46	10.02	7.16	6.22	5.88	5.11	14.08	2.98
200	316.1	306.7	87.1	12.2	94.8	-21.3	680.0	498.9	8.40	7.31	6.47	8.34	6.45	6.16	15.99	4.67
210	317.4	320.3	85.1	18.4	123.8	-41.2	675.4	490.5	29.94	20.28	9.45	13.29	41.45	26.91	31.75	4.28
220	312.6	327.9	92.5	14.4	140.1	-50.3	632.8	512.1	15.60	9.99	7.12	3.51	10.85	7.70	13.04	5.63
230	326.1	340.1	99.1	-9.3	128.6	-12.8	601.7	767.0	5.79	6.64	4.86	4.83	5.82	4.57	19.91	8.23
240	327.5	345.8	93.1	11.5	115.1	-30.1	654.4	577.5	10.38	8.61	9.93	6.71	14.18	19.12	23.42	15.62
250	325.5	354.0	87.0	11.6	126.7	-24.9	650.9	626.6	8.62	12.66	2.91	7.54	6.29	8.09	15.52	10.76
260	330.8	371.3	94.7	30.6	130.3	-33.0	662.4	496.0	7.94	13.30	7.53	7.36	14.94	11.43	18.27	11.78
270	345.3	426.9	98.1	50.7	154.0	78.0	679.1	605.2	75.62	277.52	71.39	83.40	158.81	405.05	131.05	114.01
280	329.3	359.8	113.5	26.1	99.1	5.8	471.3	560.1	100.62	100.58	33.62	61.96	123.75	132.17	48.22	78.67
290	341.0	401.4	84.3	39.3	145.1	7.5	741.2	574.7	8.21	12.31	7.94	6.36	10.86	9.53	18.24	8.82
300	366.4	406.2	91.8	41.9	154.7	45.8	700.6	575.2	18.07	25.91	20.73	19.30	7.27	10.19	18.92	6.85
310	376.8	425.8	99.3	59.5	162.6	53.7	633.2	520.6	8.28	14.72	8.41	10.64	6.91	5.97	15.32	11.93
320	409.5	429.7	87.1	26.2	181.0	61.4	773.3	574.4	7.92	12.24	9.51	12.62	3.87	5.87	16.15	6.48

Table 14 LBP Experimental Dynamic Stiffnesses at 7000 RPM and 345 kPa

f(Hz)	Dynamic stiffness								Uncertainty							
	$Re(H_{xx})$	$Im(H_{xx})$	$Re(H_{xy})$	$Im(H_{xy})$	$Re(H_{yx})$	$Im(H_{yx})$	$Re(H_{yy})$	$Im(H_{yy})$	$Re(U_{xx})$	$Im(U_{xx})$	$Re(U_{xy})$	$Im(U_{xy})$	$Re(U_{yx})$	$Im(U_{yx})$	$Re(U_{yy})$	$Im(U_{yy})$
20	187.2	30.1	-16.1	0.4	18.2	-3.3	256.1	40.9	14.10	6.78	2.97	3.72	3.97	4.91	14.92	3.93
30	190.2	43.1	-14.8	1.1	20.2	-4.4	259.9	60.1	15.26	7.04	3.40	3.96	6.09	4.23	15.75	4.69
40	186.9	55.1	-14.2	2.4	21.4	-6.4	258.7	78.1	14.73	4.74	3.64	3.66	3.07	3.62	14.71	6.80
50	185.7	71.2	-14.4	2.6	19.5	-8.5	258.6	95.2	13.68	5.69	4.20	5.68	3.22	3.36	16.41	8.81
60	208.7	73.3	10.1	7.9	31.3	-3.1	288.5	115.4	88.56	99.08	175.57	172.30	77.24	70.74	104.94	116.52
70	182.4	98.2	-5.8	5.4	22.3	-9.6	250.4	130.8	12.41	7.74	6.98	3.87	2.65	2.42	17.58	10.72
80	181.4	123.8	2.4	2.6	6.4	-18.4	223.1	255.2	13.73	8.50	9.97	4.32	5.84	3.74	9.01	28.67
90	186.1	126.0	-0.6	9.8	16.0	-12.7	248.1	168.7	12.08	9.49	5.97	6.51	3.50	4.22	17.36	10.88
100	183.3	143.2	22.3	25.4	12.8	-17.0	231.1	217.2	17.12	11.19	12.41	10.52	4.40	5.74	27.78	16.74
110	113.8	159.0	-2.0	111.3	4.4	-88.5	131.2	215.3	103.31	26.57	60.14	74.37	18.65	106.65	88.48	74.19
120	110.5	168.9	-24.8	136.4	1.9	-95.5	102.3	208.0	67.70	32.03	51.63	89.30	36.89	97.33	96.58	44.31
130	175.1	180.4	10.0	28.8	17.3	-18.1	218.6	253.7	10.80	12.84	6.99	11.54	4.24	8.79	19.68	20.11
140	175.9	187.7	0.3	11.3	18.5	-15.1	228.7	248.8	15.85	12.63	3.19	5.26	4.50	5.37	18.94	13.35
150	183.6	196.9	3.3	11.4	21.0	-6.1	210.2	265.2	16.90	12.21	4.24	2.92	3.15	5.64	11.30	10.15
160	177.2	206.8	2.5	7.7	28.7	-9.5	229.8	293.2	15.29	12.01	3.04	4.97	3.23	3.53	24.43	21.66
170	183.7	223.8	3.2	7.3	25.7	-5.1	240.8	302.3	16.59	13.24	3.94	3.06	3.24	3.54	15.57	17.41
180	169.1	230.9	5.2	10.7	18.9	-14.1	231.0	305.5	32.49	13.90	27.44	16.45	38.06	43.59	44.79	36.25
190	179.8	248.2	5.9	12.6	31.8	0.7	221.4	312.2	12.83	15.25	2.49	3.77	3.81	2.81	14.75	17.67
200	181.9	259.8	9.0	15.3	28.8	4.9	204.4	321.0	14.37	14.65	4.46	2.08	3.38	4.13	16.97	17.08
210	173.4	274.6	7.6	15.5	46.3	1.0	199.1	323.8	17.10	15.92	2.72	4.49	3.16	3.86	13.75	17.21
220	164.1	291.8	13.1	27.9	59.0	2.4	120.6	322.1	37.56	18.06	5.14	5.18	23.75	15.50	15.05	12.85
230	141.9	258.7	29.1	41.9	101.3	82.3	186.3	376.5	68.83	95.04	42.43	86.81	82.68	97.85	66.28	80.44
240	178.5	283.0	9.6	26.1	62.2	55.8	171.5	381.7	29.22	59.14	6.41	12.12	36.86	71.41	27.04	24.25
250	222.2	339.9	10.6	30.5	53.8	13.6	172.2	426.6	21.64	15.49	6.73	1.79	14.15	7.72	8.90	29.55
260	236.8	365.2	6.0	51.1	46.5	15.8	143.1	366.3	20.56	14.66	2.68	2.55	6.88	7.11	17.52	18.86
270	305.7	398.9	38.5	69.4	-15.2	34.4	4.7	401.3	27.38	20.92	4.41	4.47	6.77	8.07	10.05	5.73
280	326.4	404.7	22.4	64.0	62.9	58.6	188.9	493.2	28.34	13.61	4.13	4.19	12.59	6.88	19.90	27.40
290	356.8	431.6	69.8	63.4	16.8	7.3	53.1	558.9	32.47	12.75	10.37	6.57	11.34	9.84	6.15	50.95
300	462.3	432.4	103.3	78.0	43.5	24.2	70.6	591.7	36.27	26.45	19.75	22.43	13.42	13.12	25.42	62.47
310	554.4	504.8	131.6	87.6	83.8	3.3	95.5	529.7	41.21	21.99	9.97	10.61	15.99	20.88	15.13	43.96
320	869.8	299.4	262.1	122.3	146.6	125.9	229.1	586.5	56.71	37.52	15.63	18.11	21.92	17.32	19.55	26.20

Table 15 LBP Experimental Dynamic Stiffnesses at 7000 RPM and 1034 kPa

	Dynamic stiffness								Uncertainty							
f(Hz)	$Re(H_{xx})$	$Im(H_{xx})$	$Re(H_{xy})$	$Im(H_{xy})$	$Re(H_{yx})$	$Im(H_{yx})$	$Re(H_{yy})$	$Im(H_{yy})$	$Re(U_{xx})$	$Im(U_{xx})$	$Re(U_{xy})$	$Im(U_{xy})$	$Re(U_{yx})$	$Im(U_{yx})$	$Re(U_{yy})$	$Im(U_{yy})$
20	212.2	30.8	-6.8	0.2	13.9	-1.8	303.9	50.3	12.02	10.87	6.39	4.47	5.75	5.96	5.67	3.35
30	216.0	45.8	-5.4	0.1	11.4	-4.8	308.7	69.0	6.13	8.73	5.51	5.21	3.24	4.46	6.85	6.00
40	213.8	58.2	-7.8	2.4	19.6	-4.2	313.0	84.2	3.55	7.07	6.28	4.09	2.86	3.75	8.34	3.87
50	212.5	74.1	-6.3	2.1	16.8	-11.9	308.4	101.8	5.49	3.94	5.83	4.32	4.23	3.11	10.01	5.94
60	225.5	92.1	-6.3	5.3	16.6	5.4	315.4	114.4	80.23	116.75	207.30	180.96	76.21	96.37	157.58	132.68
70	210.9	102.9	1.4	6.1	22.6	-16.4	300.7	135.9	5.96	3.04	5.97	5.79	2.99	3.10	5.12	9.65
80	209.4	115.6	7.5	6.9	24.6	-11.9	286.8	164.3	5.17	5.14	6.86	5.00	3.43	2.37	4.28	6.38
90	214.8	133.4	5.1	8.8	12.8	-18.3	311.9	173.6	7.63	4.42	10.50	7.64	5.20	4.12	5.71	12.84
100	209.2	147.9	14.6	11.6	14.1	-14.4	289.7	234.5	9.35	8.79	22.57	13.52	7.40	6.99	22.33	24.65
110	167.0	181.6	29.7	75.6	-4.0	-66.2	237.1	267.8	53.90	22.25	27.71	81.20	29.77	60.97	97.03	32.25
120	104.7	171.5	-51.4	169.3	5.9	-147.2	116.4	199.6	32.94	62.29	49.60	37.53	26.90	33.80	20.40	37.55
130	201.3	190.9	20.1	26.3	18.5	-24.5	271.9	282.9	10.93	6.47	11.53	15.47	6.82	6.03	24.08	14.64
140	205.4	199.4	7.1	12.3	22.4	-16.9	285.0	275.0	5.21	11.54	5.65	7.50	9.04	4.40	10.07	7.23
150	210.4	206.8	8.6	10.2	28.0	-8.7	287.1	273.3	5.60	3.85	4.49	4.46	4.40	3.74	9.05	7.68
160	207.6	220.1	10.4	2.5	36.5	-10.4	336.9	383.0	6.04	10.10	5.66	4.74	4.80	4.10	12.45	12.34
170	211.0	236.0	10.8	10.5	28.0	-8.6	299.3	321.1	4.20	8.11	3.28	4.27	3.52	3.58	12.13	8.83
180	196.4	253.8	4.1	16.4	24.6	1.5	285.5	343.2	51.30	35.19	36.15	51.61	106.64	81.22	72.03	99.37
190	210.7	261.8	12.2	13.4	43.9	-2.3	292.5	337.4	6.25	7.01	3.10	3.04	3.11	3.49	6.76	9.65
200	212.3	274.3	15.8	14.4	38.3	3.5	280.0	347.6	5.52	7.41	2.11	5.16	3.39	2.38	7.99	8.71
210	204.0	288.7	15.7	15.9	56.0	-2.8	273.7	357.2	3.17	5.86	3.47	4.62	7.11	2.48	4.08	8.39
220	208.8	313.5	20.2	20.5	62.1	-8.0	230.4	361.1	7.34	12.51	3.77	4.07	7.84	5.18	9.92	8.48
230	134.9	303.9	27.5	23.1	157.2	80.6	238.2	475.0	75.58	22.38	19.43	16.78	84.12	50.23	28.59	23.53
240	154.4	306.4	18.1	26.1	119.8	72.8	253.4	415.5	78.72	67.05	12.75	15.77	74.92	77.39	18.47	25.20
250	246.1	359.4	19.5	26.6	65.6	29.0	242.8	446.1	6.44	9.42	7.30	7.27	7.27	4.30	10.00	11.47
260	273.3	385.7	16.7	32.1	59.4	26.6	245.5	412.5	7.30	8.36	5.62	2.78	3.16	4.45	8.18	9.97
270	317.5	412.2	24.1	39.4	54.4	42.4	219.9	423.4	5.62	9.34	3.57	5.42	5.40	3.80	5.10	7.62
280	375.0	448.5	23.3	19.3	64.5	104.0	282.3	594.6	4.05	7.36	6.49	4.84	3.00	2.90	6.62	11.36
290	461.7	488.4	30.2	60.7	86.9	94.2	242.5	460.9	7.01	8.20	3.59	4.52	4.37	3.37	8.11	8.46
300	672.6	537.4	60.3	82.5	114.3	184.5	190.3	452.7	58.55	84.91	23.14	28.16	30.46	62.96	16.76	13.28
310	737.5	401.4	83.8	52.0	188.1	80.9	197.9	605.5	24.19	29.14	14.30	19.42	45.04	15.83	44.08	68.59
320	1047.8	-113.9	113.3	47.4	344.8	140.3	231.8	501.2	85.67	55.42	6.53	8.18	18.84	32.91	8.42	14.48

Table 16 LBP Experimental Dynamic Stiffnesses at 7000 RPM and 1723 kPa

	Dynamic stiffness								Uncertainty							
f(Hz)	$Re(H_{xx})$	$Im(H_{xx})$	$Re(H_{xy})$	$Im(H_{xy})$	$Re(H_{yx})$	$Im(H_{yx})$	$Re(H_{yy})$	$Im(H_{yy})$	$Re(U_{xx})$	$Im(U_{xx})$	$Re(U_{xy})$	$Im(U_{xy})$	$Re(U_{yx})$	$Im(U_{yx})$	$Re(U_{yy})$	$Im(U_{yy})$
20	252.0	30.7	5.2	1.9	6.2	-1.4	407.6	61.4	20.43	11.43	12.25	15.94	5.41	9.09	12.87	6.24
30	251.5	49.7	2.3	-2.5	1.2	-6.7	416.5	83.5	12.87	12.43	12.08	9.95	8.51	7.77	6.28	5.57
40	250.7	64.2	-0.2	2.1	15.2	-3.5	422.3	100.6	11.18	8.81	5.69	10.09	4.16	5.00	12.90	5.71
50	251.4	82.8	4.2	6.5	9.5	-20.5	415.6	119.9	7.15	9.80	11.55	9.57	4.23	4.34	8.92	6.36
60	266.5	74.1	5.1	69.9	24.0	-28.2	401.4	199.1	140.26	136.33	238.72	248.02	161.17	114.28	242.78	222.79
70	251.8	109.3	13.3	5.4	19.1	-23.3	410.2	156.8	9.50	7.68	11.79	15.60	6.02	3.32	9.97	10.13
80	249.3	123.4	16.0	0.5	20.0	-21.1	407.0	200.8	11.64	4.73	14.99	10.71	5.20	5.17	12.54	12.28
90	255.6	144.0	18.8	5.6	11.6	-28.9	429.0	206.4	11.14	8.01	21.85	15.38	8.61	3.39	9.62	14.78
100	253.0	160.3	29.6	13.1	8.6	-30.7	399.1	253.8	11.84	11.27	26.47	26.29	11.06	7.19	38.77	35.71
110	208.7	195.6	43.4	91.4	-14.2	-95.1	299.2	297.7	82.29	43.44	92.86	137.98	46.44	93.38	186.66	122.12
120	128.7	159.7	-21.9	162.8	9.9	-182.2	172.4	222.1	75.49	38.78	83.93	153.77	37.04	61.29	202.78	76.38
130	248.4	205.0	33.7	17.8	13.7	-28.8	387.7	328.9	13.95	9.49	21.25	10.78	12.36	12.25	17.33	24.81
140	251.0	215.9	16.1	6.9	17.1	-24.8	396.8	324.7	14.21	11.61	7.16	8.67	10.75	8.37	14.64	10.61
150	257.6	222.6	16.7	5.0	24.0	-13.7	405.4	315.1	11.76	9.75	6.71	5.04	6.79	4.16	8.73	7.74
160	252.2	235.5	24.6	-14.6	50.2	-21.4	446.3	560.6	11.54	7.77	6.36	13.62	8.58	12.10	17.97	19.97
170	256.7	248.1	17.6	2.8	25.5	-22.5	415.8	367.3	7.95	12.03	6.96	6.52	3.99	5.45	9.27	9.46
180	233.6	253.3	11.7	7.4	6.4	-36.7	405.2	389.6	38.66	45.40	26.47	56.06	74.47	112.17	53.22	119.86
190	258.6	277.1	19.4	7.9	45.3	-10.0	409.7	385.0	10.04	9.60	8.24	5.71	7.15	4.51	9.31	6.86
200	256.4	288.8	22.1	9.7	41.7	-4.7	396.4	394.4	12.84	9.67	5.21	5.14	6.29	2.66	7.65	6.25
210	249.4	302.3	21.9	10.6	66.7	-17.0	388.8	408.3	10.46	12.57	3.16	5.41	7.17	7.05	8.30	8.98
220	253.8	328.8	31.3	16.9	73.2	-29.4	346.5	409.5	18.16	32.54	34.94	15.76	20.70	33.09	44.15	24.11
230	217.8	379.7	46.3	29.0	139.6	-47.4	307.1	544.9	68.35	78.62	17.07	51.93	143.79	96.39	31.04	87.70
240	133.7	381.2	22.8	38.1	236.2	-20.4	373.7	445.3	177.81	63.78	19.71	20.24	236.21	112.93	24.58	40.90
250	274.7	371.7	27.6	25.0	72.2	-3.2	355.6	512.6	7.78	15.48	5.73	5.29	8.44	7.40	5.97	14.41
260	289.4	396.7	27.0	31.5	65.2	-2.5	365.4	461.2	8.68	14.85	6.80	3.56	7.54	6.46	6.42	11.80
270	313.5	398.7	32.2	35.2	67.1	28.5	339.5	488.4	8.23	17.44	5.43	7.22	7.49	3.79	7.22	9.37
280	346.0	425.7	60.1	7.1	53.5	77.6	276.6	767.4	8.39	17.52	4.24	13.89	7.08	5.24	14.12	20.79
290	382.6	455.3	35.9	47.3	84.9	45.1	368.3	511.6	11.54	19.74	6.39	3.52	5.22	2.67	6.65	9.34
300	435.5	495.1	48.6	61.6	83.5	73.3	310.7	501.6	22.74	26.30	16.64	20.96	10.66	8.35	11.91	7.86
310	509.0	529.7	61.3	69.7	92.3	102.6	286.6	536.8	16.99	17.07	3.43	7.71	4.19	6.77	7.29	8.87
320	620.3	564.1	56.0	67.9	122.1	128.2	366.2	567.6	15.75	20.33	2.98	6.38	6.05	8.52	6.87	11.16

Table 17 LBP Experimental Dynamic Stiffnesses at 7000 RPM and 2413 kPa

	Dynamic stiffness								Uncertainty							
f(Hz)	$Re(H_{xx})$	$Im(H_{xx})$	$Re(H_{xy})$	$Im(H_{xy})$	$Re(H_{yx})$	$Im(H_{yx})$	$Re(H_{yy})$	$Im(H_{yy})$	$Re(U_{xx})$	$Im(U_{xx})$	$Re(U_{xy})$	$Im(U_{xy})$	$Re(U_{yx})$	$Im(U_{yx})$	$Re(U_{yy})$	$Im(U_{yy})$
20	271.9	43.9	4.4	0.0	-30.5	2.4	574.9	83.3	49.65	29.52	23.50	27.99	19.15	19.41	14.22	10.74
30	262.5	59.7	-0.9	-1.6	-27.2	-9.1	589.5	115.2	10.23	23.34	20.38	10.68	16.72	17.58	12.21	5.97
40	267.9	89.1	-0.3	-2.5	-18.5	-10.4	602.8	147.2	8.95	12.01	14.78	18.74	11.31	6.17	14.34	13.13
50	272.7	104.3	13.0	2.9	-26.2	-29.5	593.5	187.4	9.39	14.61	15.41	12.00	15.29	7.50	16.07	27.55
60	215.1	136.8	144.8	-35.2	-133.4	-98.9	692.8	298.6	197.00	278.15	316.71	317.78	335.87	207.26	420.45	448.74
70	193.6	124.7	61.9	346.7	-8.4	-185.4	29.8	385.4	57.54	24.87	76.68	79.38	42.53	84.48	122.23	135.92
80	282.6	155.9	39.9	-2.1	-16.4	-38.2	591.2	346.3	12.57	5.48	29.45	20.33	14.24	14.52	28.39	41.07
90	288.6	171.9	15.1	-2.3	-1.5	-35.1	619.9	289.1	5.82	11.02	15.88	15.44	11.94	7.35	17.16	20.35
100	295.3	182.0	14.0	0.0	-7.4	-43.2	599.5	339.5	7.84	9.07	15.96	15.34	9.59	4.15	12.15	18.14
110	295.4	196.2	12.6	-3.5	12.1	-60.7	627.9	354.1	7.04	6.30	8.52	7.52	5.88	9.71	11.14	6.73
120	301.2	198.3	8.0	26.0	-29.6	-77.4	654.0	414.3	48.19	50.91	57.99	52.23	91.85	92.03	109.22	102.09
130	310.2	222.5	21.9	0.1	-6.6	-39.6	586.3	432.9	12.90	34.31	28.15	14.42	18.00	83.67	34.49	19.88
140	320.4	248.7	14.9	-5.9	-8.4	-68.3	612.8	479.6	19.58	21.10	9.51	13.27	36.18	48.22	25.32	24.52
150	314.2	250.0	15.7	3.6	6.2	-28.4	639.5	446.0	7.46	9.65	11.30	6.81	11.75	7.96	16.18	9.01
160	315.1	260.1	32.8	-15.6	38.0	-28.9	602.3	714.9	5.85	9.07	6.95	4.84	8.98	6.81	16.94	7.80
170	315.9	273.3	17.0	0.0	11.8	-48.9	678.8	526.5	4.13	10.56	7.63	5.45	6.15	6.82	16.49	8.06
180	288.7	275.2	16.1	-9.9	-44.2	-47.4	690.1	486.6	40.58	62.10	52.47	42.99	102.10	159.31	138.46	110.78
190	323.1	298.3	22.9	11.4	39.3	-38.6	695.8	508.1	5.56	11.06	5.11	4.35	14.31	10.91	9.43	11.74
200	328.3	301.3	15.1	17.5	26.2	-27.9	695.4	537.6	20.19	52.62	73.67	22.72	84.46	22.60	66.54	118.23
210	323.6	317.7	28.8	18.6	52.4	-40.0	677.2	526.9	7.83	8.78	6.05	4.19	9.35	10.61	9.43	8.97
220	337.8	336.9	37.4	18.0	59.6	-51.6	638.8	531.6	8.89	12.51	9.14	6.47	7.09	7.05	11.88	10.30
230	340.6	341.1	44.9	-1.3	53.7	-38.4	600.0	772.8	7.13	11.40	10.46	9.76	10.76	8.91	15.34	16.60
240	339.2	358.7	29.5	14.9	47.3	-49.8	676.4	600.2	10.88	14.47	13.20	9.44	20.96	28.36	26.26	16.14
250	356.3	378.6	39.0	26.3	55.2	-37.8	648.7	630.8	10.24	24.24	14.07	9.42	18.49	21.11	25.36	13.02
260	377.2	426.1	47.5	37.1	79.1	22.0	669.6	539.0	48.84	208.35	27.62	26.72	111.91	258.48	42.54	40.87
270	519.6	448.2	97.7	86.1	243.6	40.6	707.7	623.8	672.78	452.26	303.67	121.28	859.76	613.64	392.01	166.96
280	417.4	419.9	106.7	47.2	35.4	11.3	295.8	674.9	11.39	16.19	14.41	18.11	14.73	9.85	14.43	18.57
290	446.6	431.2	55.5	47.1	86.2	8.3	679.1	576.5	9.07	17.34	10.91	10.12	7.59	11.47	13.43	11.61
300	498.1	459.5	76.9	62.8	87.9	40.8	602.2	558.1	19.57	29.80	17.01	19.25	13.07	9.64	15.28	7.96
310	550.0	486.9	105.2	71.1	88.2	58.8	503.1	569.1	10.29	18.71	6.53	4.31	7.05	5.69	10.52	7.43
320	619.1	492.5	83.6	51.4	137.1	83.1	666.4	616.3	6.81	60.54	24.32	11.96	55.45	11.62	9.89	16.84

Table 18 LBP Experimental Dynamic Stiffnesses at 7000 RPM and 3103 kPa

	Dynamic stiffness								Uncertainty							
f(Hz)	$Re(H_{xx})$	$Im(H_{xx})$	$Re(H_{xy})$	$Im(H_{xy})$	$Re(H_{yx})$	$Im(H_{yx})$	$Re(H_{yy})$	$Im(H_{yy})$	$Re(U_{xx})$	$Im(U_{xx})$	$Re(U_{xy})$	$Im(U_{xy})$	$Re(U_{yx})$	$Im(U_{yx})$	$Re(U_{yy})$	$Im(U_{yy})$
20	370.2	41.1	5.5	-10.1	-21.1	-265.9	681.8	65.0	43.94	56.00	23.96	14.99	107.53	438.52	22.90	34.13
30	378.2	63.0	-2.7	-5.7	-113.3	-23.8	729.7	74.9	26.50	25.44	8.13	23.35	78.12	100.28	11.32	19.69
40	365.8	76.8	8.2	-5.9	-50.0	10.2	704.1	97.4	22.38	18.79	12.47	12.63	126.04	74.08	15.22	17.37
50	366.5	98.3	14.2	-8.7	-33.2	-25.0	710.9	132.3	18.13	13.41	21.15	19.21	78.35	98.43	20.06	15.82
60	360.8	97.8	-12.7	9.5	59.6	-80.0	696.4	120.5	51.92	75.64	157.13	126.42	193.94	112.67	26.14	24.93
70	370.5	128.8	2.5	-12.4	143.5	-166.6	699.5	139.8	13.33	13.23	22.66	13.72	277.05	174.38	31.26	21.70
80	372.2	145.1	16.7	-9.4	77.3	-164.6	653.0	210.8	9.66	9.07	20.11	15.55	219.92	210.25	23.53	19.33
90	366.7	162.7	16.7	-7.4	-219.9	-75.5	643.1	168.1	12.17	13.02	18.02	15.15	306.36	97.38	30.85	25.64
100	370.4	181.2	12.7	-11.7	-72.0	-75.3	696.2	248.5	9.00	8.97	16.43	13.16	133.87	93.80	19.59	21.51
110	370.9	215.0	18.6	-18.8	-29.7	-156.1	709.4	278.1	23.91	31.14	25.71	19.86	58.41	153.39	17.25	31.51
120	95.6	221.7	2.3	179.3	-62.4	-438.3	467.5	333.8	94.55	528.06	105.43	202.45	706.15	169.39	194.76	190.87
130	376.4	222.7	17.3	-19.4	-6.5	-94.3	674.8	364.0	19.27	13.98	17.75	12.93	43.57	139.69	19.99	31.89
140	375.8	241.3	12.8	-17.3	-92.1	-80.5	679.1	371.9	15.34	12.48	9.19	7.82	237.53	76.12	11.93	13.65
150	377.4	252.9	11.7	-16.9	-94.0	66.6	683.8	360.2	11.53	11.49	4.87	5.40	206.34	264.61	16.65	10.18
160	374.0	264.7	46.9	-34.0	137.6	70.1	500.8	625.1	8.35	11.25	6.27	5.06	277.52	317.68	34.45	25.36
170	374.2	282.6	8.3	-18.1	-64.7	21.4	716.0	422.7	5.76	8.96	4.24	6.77	158.36	268.01	21.21	9.17
180	367.1	279.8	5.3	-18.2	-105.0	-0.8	711.2	425.0	15.94	17.77	20.23	17.75	242.48	116.64	9.14	10.03
190	377.2	308.0	10.9	-8.0	-54.2	-17.2	704.7	416.2	13.67	12.79	5.97	6.32	170.44	159.91	19.43	16.32
200	369.4	309.9	12.8	-6.6	-8.1	-98.7	663.2	422.9	8.58	11.15	5.01	4.20	99.59	94.61	13.55	18.58
210	358.4	323.8	16.0	-2.3	-27.2	-232.4	681.1	443.4	8.79	8.99	3.73	4.91	187.84	303.51	18.61	8.22
220	358.0	341.7	37.0	-5.6	-113.5	-217.7	535.0	553.2	7.02	11.12	5.15	3.40	283.57	274.94	44.53	28.55
230	358.0	356.3	36.5	-2.4	-53.8	216.8	539.4	614.8	14.45	45.40	7.46	5.98	212.12	491.14	39.89	45.30
240	288.3	550.3	32.2	3.0	-35.8	-790.6	591.5	530.2	346.76	337.08	59.82	54.35	789.33	1220.54	144.92	129.38
250	349.2	378.5	24.4	4.1	-179.4	-36.8	627.7	626.2	8.25	11.45	6.32	3.80	392.59	257.79	16.27	29.01
260	352.5	387.3	21.2	17.2	96.2	17.3	638.6	525.8	8.16	11.90	2.98	4.83	198.03	278.03	12.49	24.16
270	352.5	387.5	25.4	16.9	28.4	-29.4	633.4	571.8	4.11	6.88	3.09	3.55	139.33	119.56	14.06	13.52
280	357.2	401.0	47.0	30.4	-81.7	-21.0	443.4	649.0	5.77	8.94	2.99	3.24	216.89	100.66	24.10	29.35
290	354.4	413.0	25.1	29.2	100.9	-25.9	728.4	646.1	4.97	4.80	3.31	2.28	133.62	55.60	20.72	18.14
300	367.1	427.7	37.6	40.2	-45.5	118.4	659.7	643.6	17.49	23.98	14.16	17.09	237.81	220.50	25.94	35.45
310	366.3	452.4	43.0	53.2	-105.4	10.3	633.6	599.5	7.29	6.98	1.49	2.09	275.57	38.74	52.46	20.56
320	379.3	462.2	38.0	39.1	-47.9	81.6	774.3	724.5	4.13	7.87	3.43	3.36	228.64	111.67	38.85	61.48

Table 19 LBP Experimental Dynamic Stiffnesses at 10000 RPM and 345 kPa

	Dynamic stiffness								Uncertainty							
f(Hz)	$Re(H_{xx})$	$Im(H_{xx})$	$Re(H_{xy})$	$Im(H_{xy})$	$Re(H_{yx})$	$Im(H_{yx})$	$Re(H_{yy})$	$Im(H_{yy})$	$Re(U_{xx})$	$Im(U_{xx})$	$Re(U_{xy})$	$Im(U_{xy})$	$Re(U_{yx})$	$Im(U_{yx})$	$Re(U_{yy})$	$Im(U_{yy})$
20	236.6	24.5	-34.6	0.4	33.2	-4.2	333.7	35.9	16.04	17.02	10.62	6.45	12.10	11.09	17.96	6.65
30	239.8	35.8	-31.2	3.5	38.2	-3.7	335.6	53.6	12.03	20.81	10.13	9.27	9.55	14.04	17.57	6.96
40	238.0	49.0	-31.3	0.7	38.5	-7.9	332.3	69.3	8.66	8.54	9.60	7.50	5.32	4.25	12.68	6.83
50	238.1	65.7	-33.1	1.0	39.1	-11.4	331.2	88.5	13.70	7.39	12.38	7.37	9.38	5.42	9.22	9.49
60	255.0	51.4	-42.4	21.7	48.3	-27.8	331.6	97.7	103.77	104.34	219.45	192.47	110.96	91.79	147.09	193.74
70	234.1	91.3	-27.1	4.5	39.8	-15.0	319.7	118.2	7.80	5.09	12.30	9.74	7.22	5.35	13.28	8.76
80	232.3	118.6	-27.2	-0.4	19.2	-14.1	300.8	211.2	11.51	3.90	12.22	10.51	5.56	7.43	13.80	7.50
90	236.5	117.3	-28.5	4.9	36.9	-17.7	324.9	154.0	10.01	9.15	8.73	5.77	6.53	4.45	10.19	8.84
100	236.3	132.1	-25.1	5.3	36.1	-20.8	322.4	180.0	9.81	6.24	7.85	11.03	5.41	5.10	13.02	11.18
110	233.9	148.4	-23.1	8.2	37.9	-25.1	320.7	191.6	10.70	5.91	9.26	6.25	6.10	3.36	17.76	8.46
120	231.7	160.0	-31.9	9.5	28.6	-20.0	300.3	211.8	37.42	39.68	29.88	49.17	56.17	42.93	49.23	68.03
130	233.2	168.1	-18.2	13.1	31.5	-16.4	304.0	222.5	9.29	7.26	4.91	8.24	3.11	8.56	12.19	5.14
140	222.8	184.9	-19.6	16.7	27.1	-24.6	293.3	236.2	21.74	8.17	6.36	6.33	10.21	12.85	12.66	8.58
150	213.8	202.3	-10.3	21.6	24.2	-33.3	266.5	257.8	42.12	13.48	7.22	17.94	24.14	30.28	27.00	6.06
160	105.6	197.1	-28.0	51.7	34.3	-150.8	249.9	266.9	205.42	67.77	50.17	40.71	43.40	213.55	54.95	72.62
170	-11.4	158.1	-113.6	88.7	91.3	-281.3	211.3	189.1	50.74	35.64	40.56	34.15	95.92	64.45	41.31	38.42
180	172.5	241.5	-3.2	47.4	0.2	-62.3	288.5	294.9	74.75	74.23	53.20	42.91	110.55	74.67	73.30	71.93
190	200.9	246.9	-7.4	29.3	37.1	-47.2	277.1	299.4	45.22	11.32	4.93	9.54	18.27	33.74	19.07	10.70
200	228.9	251.3	-4.7	30.6	39.7	-17.9	264.0	304.0	19.67	9.18	5.75	9.47	6.48	8.70	19.95	12.05
210	217.3	268.7	-2.7	29.1	45.2	-29.8	260.8	308.4	17.31	12.00	4.25	4.18	6.55	9.03	14.46	7.75
220	230.8	290.5	4.8	37.7	42.8	-32.6	188.5	305.9	21.05	9.68	5.57	6.17	6.47	5.56	10.45	8.93
230	239.7	295.0	0.6	27.7	61.2	-9.7	278.4	396.4	18.72	10.89	8.30	11.57	7.43	5.95	20.49	13.11
240	241.0	308.0	13.4	33.1	43.8	-7.4	238.0	356.9	21.41	13.53	10.39	12.89	14.77	14.15	18.17	10.04
250	268.3	328.0	19.4	39.1	45.4	-5.0	246.1	407.4	12.23	10.97	7.17	6.76	5.60	9.82	15.87	22.42
260	282.2	357.9	26.9	61.7	35.0	-9.0	206.4	345.7	9.90	10.94	6.05	4.60	4.31	5.08	8.16	8.38
270	347.9	378.3	78.6	78.4	-36.3	-7.7	55.7	364.8	17.08	11.10	6.35	7.32	16.77	7.81	7.08	12.59
280	379.2	401.4	66.7	63.3	47.9	42.5	262.9	467.1	11.17	7.80	7.88	9.98	4.66	8.69	13.29	10.50
290	435.6	429.7	106.9	28.7	-25.6	75.2	99.7	558.3	19.19	7.24	9.26	9.74	5.98	15.49	5.00	24.10
300	521.5	403.7	145.3	-9.7	83.9	91.2	168.9	605.3	31.67	33.68	29.87	25.52	27.51	40.24	26.96	32.02
310	611.0	398.0	159.5	-14.2	102.1	85.6	167.6	532.7	38.50	27.13	19.00	17.47	16.60	31.33	15.89	22.17
320	898.4	307.3	360.1	-41.8	149.4	111.1	318.4	536.5	81.27	98.49	35.03	55.07	28.84	30.16	12.38	11.00

Table 20 LBP Experimental Dynamic Stiffnesses at 10000 RPM and 1034 kPa

	Dynamic stiffness								Uncertainty							
f(Hz)	$Re(H_{xx})$	$Im(H_{xx})$	$Re(H_{xy})$	$Im(H_{xy})$	$Re(H_{yx})$	$Im(H_{yx})$	$Re(H_{yy})$	$Im(H_{yy})$	$Re(U_{xx})$	$Im(U_{xx})$	$Re(U_{xy})$	$Im(U_{xy})$	$Re(U_{yx})$	$Im(U_{yx})$	$Re(U_{yy})$	$Im(U_{yy})$
20	252.4	29.0	-28.1	1.2	32.4	-7.5	356.6	41.7	27.08	14.11	15.07	15.21	14.45	12.63	15.98	11.35
30	256.1	39.9	-23.1	5.8	28.5	-9.3	361.3	60.2	13.74	10.88	11.93	15.17	15.18	14.66	19.78	7.07
40	252.3	58.2	-20.1	4.1	32.6	-7.4	362.5	76.7	15.18	7.09	10.38	9.18	8.35	7.60	21.00	11.50
50	252.9	69.7	-25.1	3.3	34.0	-15.2	358.8	96.0	14.44	6.04	7.83	10.73	7.52	7.37	18.80	9.05
60	283.4	65.9	-4.3	8.6	57.4	-21.2	387.5	112.6	124.14	132.84	230.63	216.00	136.50	123.06	205.56	193.32
70	251.9	98.3	-15.7	8.3	37.1	-21.2	349.2	125.6	17.06	5.57	11.01	16.23	7.48	6.67	19.91	14.30
80	245.9	111.5	-14.8	10.0	39.5	-19.6	334.3	153.7	13.17	8.56	14.18	10.07	3.78	4.14	16.18	11.28
90	254.1	129.4	-21.0	4.8	33.1	-22.6	364.8	158.6	14.88	6.98	9.18	11.26	4.39	6.42	19.87	19.70
100	252.2	144.1	-14.4	8.4	32.8	-28.3	350.3	190.3	15.57	11.73	8.37	9.79	6.11	6.23	16.44	13.02
110	254.0	156.2	-12.4	9.7	41.3	-32.6	354.6	206.8	18.09	9.78	8.89	7.87	8.77	6.95	19.60	7.79
120	249.0	160.4	1.4	12.6	23.7	-37.9	362.8	214.8	43.06	36.28	46.79	43.12	50.36	51.15	45.11	58.38
130	252.6	180.1	-5.0	16.0	31.5	-24.2	320.5	244.0	10.57	12.51	9.35	8.49	4.74	5.03	13.68	17.41
140	241.5	197.1	-3.0	17.1	30.0	-25.8	315.9	276.6	11.55	13.12	15.04	7.43	10.14	11.71	20.50	17.30
150	226.2	221.0	3.5	29.7	20.4	-44.5	315.3	281.6	27.49	36.13	17.53	27.25	29.05	29.84	23.85	32.42
160	19.7	179.0	-82.0	80.2	106.5	-323.5	295.9	255.1	164.86	71.19	74.36	85.55	101.73	218.56	119.29	149.22
170	100.6	215.1	-52.2	107.2	43.9	-200.9	236.0	257.0	125.49	47.55	83.03	103.66	52.37	156.46	104.71	81.33
180	204.2	255.6	-0.5	37.3	6.8	-62.6	305.8	329.9	60.53	55.18	45.83	64.88	93.94	75.73	48.66	65.58
190	224.4	270.0	5.0	27.8	29.3	-50.5	328.4	327.9	26.94	27.21	10.05	13.78	18.19	29.60	14.13	18.79
200	247.0	269.2	12.2	25.7	41.4	-19.7	314.9	332.9	7.52	13.04	9.72	9.00	6.93	8.04	14.12	13.22
210	235.9	280.1	11.5	24.1	54.9	-31.9	312.8	342.7	14.61	16.32	9.76	4.25	7.74	16.59	15.64	11.76
220	249.7	295.2	13.7	27.3	55.4	-26.7	274.7	343.0	21.34	16.30	5.12	7.95	6.53	8.79	13.31	8.87
230	249.6	303.0	13.6	22.0	55.2	-17.7	291.3	456.2	13.26	15.77	5.89	10.64	9.82	11.36	32.17	22.58
240	242.3	326.8	9.9	28.4	47.0	-27.1	296.2	393.0	17.12	19.60	4.21	12.32	12.80	24.53	18.83	14.26
250	256.8	343.9	17.7	32.5	51.4	-19.4	287.3	417.6	13.72	20.47	10.54	3.43	6.09	8.03	10.69	14.44
260	275.7	357.4	16.8	36.8	50.8	-9.7	283.0	389.9	17.97	12.33	5.60	4.10	7.01	6.52	11.48	13.55
270	283.7	365.0	24.4	40.1	50.5	3.8	257.0	397.4	13.83	18.05	4.66	2.85	7.65	7.34	14.38	12.05
280	313.1	387.7	25.2	18.7	61.3	33.9	345.7	583.1	13.20	14.73	9.27	9.58	9.92	5.86	29.53	24.43
290	344.5	411.5	31.1	49.7	58.0	21.6	273.6	419.5	13.64	16.76	8.30	5.29	5.93	4.78	13.71	12.50
300	382.4	444.1	38.2	63.0	54.7	43.3	208.2	402.8	25.60	27.92	14.18	17.66	8.34	11.50	14.86	11.13
310	429.4	476.1	41.8	48.8	71.9	58.4	251.2	514.9	15.96	16.89	7.83	8.08	18.64	9.37	10.91	50.26
320	568.7	478.7	55.5	64.9	37.0	91.5	225.9	460.9	297.02	224.46	165.72	37.89	181.88	108.09	102.90	13.04

Table 21 LBP Experimental Dynamic Stiffnesses at 10000 RPM and 1723 kPa

	Dynamic stiffness								Uncertainty							
f(Hz)	$Re(H_{xx})$	$Im(H_{xx})$	$Re(H_{xy})$	$Im(H_{xy})$	$Re(H_{yx})$	$Im(H_{yx})$	$Re(H_{yy})$	$Im(H_{yy})$	$Re(U_{xx})$	$Im(U_{xx})$	$Re(U_{xy})$	$Im(U_{xy})$	$Re(U_{yx})$	$Im(U_{yx})$	$Re(U_{yy})$	$Im(U_{yy})$
20	280.5	18.9	-14.0	0.7	23.7	-0.5	438.9	50.4	40.95	39.57	24.31	16.40	27.94	22.08	13.55	11.84
30	287.6	45.2	-20.7	4.5	20.9	-8.5	447.2	72.1	16.78	14.01	14.08	20.41	17.58	16.75	15.06	13.16
40	289.1	61.6	-13.2	4.0	35.8	-6.0	447.0	76.4	19.55	22.24	17.74	17.81	11.58	13.63	16.28	14.97
50	288.0	69.6	-12.7	6.1	31.1	-20.0	444.3	100.8	19.96	16.77	22.42	20.75	6.23	8.10	13.28	13.22
60	332.0	76.9	-33.0	49.1	73.7	-10.6	421.2	151.5	141.40	132.55	256.18	278.67	183.74	137.83	266.11	300.92
70	284.2	96.6	-12.3	3.4	34.6	-24.7	436.3	131.4	12.50	14.43	28.63	21.78	8.08	7.58	16.21	15.65
80	282.1	113.3	1.4	9.5	36.4	-24.6	423.7	173.3	11.62	9.77	13.34	13.05	7.61	5.73	17.92	9.52
90	288.6	132.2	-12.0	6.4	32.8	-31.4	454.4	167.9	12.67	9.26	17.98	18.67	5.34	7.71	10.68	14.23
100	290.4	142.9	-2.2	11.4	29.8	-32.1	431.9	200.4	12.98	11.29	20.37	15.58	3.70	5.69	10.51	12.45
110	291.2	153.2	0.1	10.3	38.7	-42.4	440.0	211.8	12.35	8.12	17.98	15.51	5.17	8.22	6.28	10.77
120	281.8	163.4	-4.7	12.7	15.7	-40.8	434.8	223.6	29.01	48.97	64.31	67.88	46.86	73.84	87.40	83.29
130	287.2	177.1	4.5	16.4	33.8	-33.3	412.7	256.3	13.15	8.65	7.49	8.79	5.49	5.05	8.97	14.08
140	276.7	200.7	7.6	20.6	24.6	-35.7	397.9	276.7	15.68	8.35	10.21	15.64	15.96	11.55	16.64	6.90
150	268.9	217.3	15.5	32.8	13.4	-40.2	378.4	296.9	29.67	18.92	21.27	17.75	27.29	29.46	19.63	15.46
160	111.8	243.0	-31.2	86.2	34.4	-292.0	352.0	389.3	196.65	52.15	93.40	79.47	99.55	290.17	119.57	153.99
170	52.7	198.1	-111.1	140.6	53.4	-326.4	258.8	191.7	66.49	42.57	80.90	53.92	55.35	82.07	55.63	99.32
180	247.9	256.4	19.1	61.0	-8.5	-93.8	385.5	356.6	70.74	87.41	82.34	61.62	68.07	126.32	97.58	79.51
190	259.7	272.5	22.0	35.4	24.0	-57.0	398.8	353.2	32.90	18.06	8.98	13.23	28.11	26.38	19.61	13.19
200	281.3	270.6	21.2	27.3	36.6	-24.4	396.9	351.5	14.26	7.94	10.63	14.45	13.45	7.69	21.38	8.32
210	271.8	281.3	21.7	27.3	54.4	-38.1	388.6	362.9	8.56	14.12	9.22	4.26	14.33	7.67	10.40	7.80
220	284.3	294.1	23.3	25.2	61.0	-37.5	358.1	368.6	8.18	12.31	9.96	8.62	6.90	8.70	14.33	9.82
230	283.4	300.2	25.3	20.3	55.1	-29.9	334.4	503.5	13.11	9.50	10.10	9.75	7.65	6.47	22.01	11.55
240	271.0	332.0	16.9	28.5	49.9	-46.1	375.6	414.2	20.77	25.05	10.05	15.37	18.39	27.06	22.10	17.36
250	289.5	337.1	26.9	32.9	57.0	-35.8	357.9	447.9	14.31	17.91	14.90	10.02	7.52	9.58	12.58	7.73
260	304.3	346.8	25.9	36.6	57.7	-16.5	363.4	407.5	16.68	9.19	7.11	8.86	5.31	9.76	11.01	6.90
270	304.1	362.4	30.1	39.3	57.2	-10.7	337.9	423.3	10.92	13.19	4.73	7.35	6.12	7.72	10.59	6.82
280	335.5	377.7	69.2	20.3	46.8	34.9	191.4	744.8	12.16	11.95	11.77	11.26	5.87	6.80	16.32	11.41
290	351.3	390.9	37.2	46.2	65.5	4.6	360.1	442.5	6.22	12.39	4.17	5.36	6.45	7.39	7.11	6.66
300	382.7	425.1	53.8	61.1	60.2	24.9	300.3	431.6	25.27	26.06	15.66	19.28	10.42	10.62	6.13	8.51
310	421.4	448.7	61.0	52.9	63.5	43.7	295.5	495.7	10.46	12.52	5.37	8.60	7.49	10.77	6.55	12.11
320	474.0	475.4	55.6	55.2	75.7	56.9	343.9	493.8	11.84	14.44	10.37	9.47	9.47	6.92	3.72	6.86

Table 22 LBP Experimental Dynamic Stiffnesses at 10000 RPM and 2413 kPa

	Dynamic stiffness								Uncertainty							
f(Hz)	$Re(H_{xx})$	$Im(H_{xx})$	$Re(H_{xy})$	$Im(H_{xy})$	$Re(H_{yx})$	$Im(H_{yx})$	$Re(H_{yy})$	$Im(H_{yy})$	$Re(U_{xx})$	$Im(U_{xx})$	$Re(U_{xy})$	$Im(U_{xy})$	$Re(U_{yx})$	$Im(U_{yx})$	$Re(U_{yy})$	$Im(U_{yy})$
20	343.7	37.6	-19.9	6.7	6.1	6.6	569.1	52.1	53.76	57.35	43.90	41.07	23.08	12.36	26.34	31.86
30	334.1	40.4	-9.5	3.3	12.9	-2.9	577.4	81.6	36.48	36.19	29.67	32.48	20.07	25.76	26.34	15.02
40	343.0	62.8	-3.7	0.5	18.4	-12.4	578.8	91.8	22.87	18.24	33.03	21.47	23.62	16.63	18.33	18.38
50	337.8	80.6	-2.7	4.3	13.8	-32.1	570.7	114.8	16.17	18.30	24.74	35.28	14.26	13.38	18.01	28.96
60	385.3	88.7	24.3	-45.0	73.6	-8.9	634.7	79.0	246.81	167.37	458.63	252.60	311.89	215.81	624.86	292.33
70	337.6	105.4	-1.7	-4.4	22.5	-38.5	568.4	143.5	10.69	17.35	31.74	29.89	13.51	10.30	28.16	20.72
80	335.1	124.3	0.5	4.3	24.3	-35.1	557.0	196.7	14.68	8.78	33.23	20.63	12.71	8.26	24.11	17.92
90	339.0	143.9	1.0	9.0	25.2	-46.4	582.1	180.3	11.84	18.86	30.24	27.79	10.91	7.39	26.63	15.71
100	343.0	155.5	6.7	3.2	14.7	-43.0	560.4	229.5	15.60	6.20	25.98	24.64	6.23	6.84	17.64	26.89
110	343.3	165.4	4.9	4.1	27.9	-56.0	577.5	234.8	21.42	16.62	21.67	19.95	10.70	12.44	21.72	13.87
120	339.5	173.1	26.2	27.9	16.2	-59.2	607.4	278.6	81.97	44.64	67.68	71.01	108.24	81.20	120.39	112.56
130	335.7	192.2	12.2	3.8	25.9	-46.8	542.8	292.0	8.49	10.32	11.69	15.77	7.95	10.49	8.22	12.80
140	332.2	209.0	14.9	5.1	23.4	-50.4	531.9	316.4	16.85	22.25	19.86	15.90	22.40	9.50	13.55	13.67
150	329.1	239.5	22.3	15.0	0.2	-49.6	515.4	311.9	19.75	17.56	16.86	27.05	18.40	18.22	21.07	16.43
160	185.4	289.2	15.2	86.7	9.6	-261.7	381.3	500.7	184.66	32.73	76.21	65.71	67.71	252.05	78.63	120.73
170	48.0	209.2	-150.4	153.9	44.9	-428.2	343.5	155.3	36.07	27.28	46.74	30.59	41.12	50.58	39.59	61.95
180	273.5	290.7	27.7	33.0	-46.2	-90.9	489.3	387.8	57.68	54.30	56.67	61.45	76.46	126.94	109.29	118.87
190	319.0	298.6	25.9	21.2	5.8	-62.3	511.5	392.8	29.57	21.74	15.28	22.18	25.95	27.11	21.04	11.37
200	329.9	288.2	26.6	14.5	37.7	-36.9	520.0	394.5	18.19	16.36	10.30	11.24	18.51	12.77	10.13	10.83
210	325.8	302.1	26.3	12.6	51.4	-62.1	514.0	395.4	15.89	10.95	13.38	15.78	14.66	8.65	12.51	9.72
220	329.5	315.6	28.3	10.4	58.1	-59.1	498.4	430.4	13.73	15.93	8.28	14.67	17.26	16.81	6.92	8.77
230	333.5	319.5	46.9	15.2	56.1	-42.0	342.0	527.5	15.03	8.55	15.56	12.93	11.14	11.13	9.04	19.65
240	323.5	355.3	26.9	13.4	54.9	-62.4	496.4	464.8	28.66	20.18	14.87	12.36	31.35	19.03	18.12	15.87
250	338.8	357.5	35.6	21.0	57.2	-55.7	480.5	483.3	11.01	12.24	9.64	11.62	8.71	7.55	6.38	9.71
260	350.4	366.5	32.3	23.5	59.4	-29.6	478.4	444.0	8.74	11.07	8.92	15.05	10.47	10.50	8.17	6.02
270	343.5	379.3	38.5	27.7	65.6	-23.3	456.8	461.8	11.46	7.31	9.78	8.14	10.09	7.85	7.13	5.11
280	380.8	398.0	80.2	37.8	41.1	-1.6	168.7	558.4	5.08	9.49	5.73	8.15	3.46	4.20	4.83	10.99
290	387.0	405.2	40.7	37.0	74.7	-10.7	474.3	482.1	12.79	9.93	12.58	7.67	6.62	2.61	7.20	6.58
300	419.3	438.9	51.5	47.4	67.1	12.3	415.7	477.0	21.08	29.83	15.71	24.01	12.73	11.33	11.61	7.63
310	441.9	449.8	68.3	41.3	65.6	37.1	356.4	543.6	14.67	21.37	7.09	5.81	9.36	11.96	4.38	13.82
320	490.4	468.6	51.8	33.7	86.9	54.2	476.5	557.5	12.56	18.95	5.73	7.79	11.74	12.92	4.36	7.23

Table 23 LBP Experimental Dynamic Stiffnesses at 10000 RPM and 3103 kPa

	Dynamic stiffness								Uncertainty							
f(Hz)	$Re(H_{xx})$	$Im(H_{xx})$	$Re(H_{xy})$	$Im(H_{xy})$	$Re(H_{yx})$	$Im(H_{yx})$	$Re(H_{yy})$	$Im(H_{yy})$	$Re(U_{xx})$	$Im(U_{xx})$	$Re(U_{xy})$	$Im(U_{xy})$	$Re(U_{yx})$	$Im(U_{yx})$	$Re(U_{yy})$	$Im(U_{yy})$
20	-13.7	-114.3	10.7	8.3	91.1	18.9	646.5	63.1	548.39	295.87	59.30	53.40	746.10	637.79	95.54	61.94
30	362.6	-88.4	-46.6	11.1	-195.8	200.3	731.5	45.6	342.27	349.52	84.87	48.94	497.73	437.12	108.75	47.63
40	398.8	56.1	-32.7	11.7	-22.4	15.2	701.5	84.1	59.22	51.07	33.88	32.00	112.63	177.65	24.79	22.86
50	403.4	66.2	-37.4	16.9	-10.7	28.9	694.6	112.7	50.84	51.24	57.69	26.21	79.27	185.06	20.25	17.62
60	423.2	74.9	-52.7	29.1	39.7	0.6	678.7	124.1	104.88	105.28	166.14	138.21	255.14	125.69	22.24	26.18
70	390.8	111.0	-17.9	12.7	58.8	-75.1	669.7	114.2	23.62	26.32	42.68	43.99	363.33	169.35	19.38	25.38
80	400.0	139.1	-18.0	13.4	11.3	-129.2	662.3	194.5	39.04	51.38	50.46	28.60	239.17	213.97	19.87	20.45
90	391.7	145.2	-22.8	9.6	-105.3	-45.6	634.6	166.1	26.58	31.99	51.98	36.48	287.94	110.02	32.72	27.35
100	397.7	164.4	-19.3	10.3	-51.2	-54.3	672.8	223.9	35.49	17.88	48.26	21.21	125.51	109.30	24.55	16.18
110	394.6	170.8	-16.4	7.2	-65.8	-81.5	690.8	210.6	26.88	25.49	40.71	19.42	146.88	164.41	24.13	32.11
120	420.7	179.5	-18.0	2.3	85.8	-71.0	697.6	218.6	90.54	85.25	66.22	53.80	245.23	173.76	94.64	88.76
130	392.4	194.0	-5.5	1.7	-12.2	-74.0	654.7	304.0	25.66	16.82	40.18	16.91	124.98	80.71	20.60	16.38
140	388.5	216.8	-6.6	-0.5	-101.7	-59.0	644.6	318.3	16.30	18.36	29.87	8.14	222.15	81.61	23.56	8.71
150	383.4	237.7	-4.5	5.6	-77.0	16.2	653.9	304.0	26.17	28.95	26.15	17.19	75.32	324.33	22.89	13.66
160	256.9	344.2	29.8	-0.7	26.1	-249.1	460.3	574.8	216.94	142.19	30.02	53.70	518.77	522.75	90.83	59.50
170	-143.4	-0.6	-63.6	-51.5	326.7	-852.3	735.7	243.8	221.44	433.12	135.36	255.83	572.75	655.14	324.59	454.71
180	357.8	320.1	-6.9	14.0	-105.7	-21.7	673.6	369.2	53.85	76.30	34.03	24.98	115.22	332.04	20.84	24.64
190	367.6	300.0	0.9	2.8	-62.3	-69.1	661.5	367.7	27.79	31.33	29.85	11.80	149.10	87.67	19.89	13.95
200	372.5	301.6	-3.6	7.4	-44.0	-95.8	650.3	375.0	18.41	18.81	29.49	7.12	80.97	209.61	19.07	17.71
210	357.9	304.0	0.7	7.6	-14.2	-130.8	639.1	388.7	19.91	15.92	26.21	11.38	193.84	252.44	21.77	17.78
220	366.6	316.3	17.2	2.6	-58.8	-109.0	523.7	506.4	14.82	13.00	30.03	10.41	223.58	172.91	31.12	14.22
230	357.5	336.1	15.4	10.0	62.6	81.4	512.5	512.6	25.46	27.80	33.96	11.28	153.66	470.66	43.02	41.18
240	353.8	348.5	0.3	13.4	-110.4	-80.1	611.5	484.6	18.99	27.12	35.88	13.08	520.64	181.36	48.34	38.02
250	345.1	348.5	8.0	16.5	30.8	9.2	614.4	518.5	24.92	17.44	27.07	11.79	145.94	423.48	17.54	34.89
260	350.4	346.1	4.9	23.9	36.0	-139.5	609.8	446.8	24.73	25.03	25.75	11.42	48.52	296.44	31.42	23.81
270	347.9	373.4	10.4	27.2	-4.0	-7.4	595.7	498.9	16.48	16.21	27.58	10.77	182.68	238.91	16.84	27.25
280	353.4	372.7	31.8	37.2	-20.4	-9.2	444.9	557.7	17.47	13.96	24.48	9.00	143.72	61.83	24.04	22.99
290	354.3	370.3	15.7	33.6	81.3	11.4	666.4	540.3	13.26	23.22	25.61	10.39	111.57	118.78	8.83	17.70
300	373.5	395.6	30.2	45.4	42.6	42.4	612.5	543.8	20.17	29.63	22.83	20.51	93.27	248.88	16.75	37.35
310	375.1	410.4	33.4	51.8	3.8	20.7	592.3	522.3	16.31	19.92	18.02	7.15	168.59	59.06	32.14	24.13
320	388.7	431.6	29.3	46.1	66.6	68.6	706.3	619.4	17.03	14.72	15.79	13.21	72.04	167.67	15.23	37.30

Table 24 LBP Experimental Dynamic Stiffnesses at 13000 RPM and 345 kPa

	Dynamic stiffness								Uncertainty							
f(Hz)	$Re(H_{xx})$	$Im(H_{xx})$	$Re(H_{xy})$	$Im(H_{xy})$	$Re(H_{yx})$	$Im(H_{yx})$	$Re(H_{yy})$	$Im(H_{yy})$	$Re(U_{xx})$	$Im(U_{xx})$	$Re(U_{xy})$	$Im(U_{xy})$	$Re(U_{yx})$	$Im(U_{yx})$	$Re(U_{yy})$	$Im(U_{yy})$
20	317.8	16.3	-54.0	-4.3	32.4	-5.4	413.6	40.4	35.52	39.41	19.66	10.15	20.92	11.86	18.25	6.90
30	317.3	45.8	-46.2	-5.6	36.8	-5.7	415.3	56.8	17.17	15.46	13.24	13.71	8.69	9.41	15.58	7.76
40	314.4	55.8	-52.5	-1.4	42.5	-11.4	412.6	71.4	22.40	10.91	14.66	9.68	12.38	9.04	12.85	8.52
50	313.7	73.3	-50.6	0.9	37.5	-16.6	412.6	89.7	17.80	13.44	10.72	11.93	9.47	9.70	21.12	9.74
60	299.9	72.1	-93.8	-53.7	14.2	-19.5	387.1	22.2	120.60	130.31	180.44	210.69	124.40	142.60	148.42	212.30
70	305.0	96.4	-45.3	0.7	48.6	-18.9	399.4	115.2	19.18	11.64	11.18	9.03	4.55	7.75	20.76	15.59
80	320.7	132.0	-45.8	-4.5	22.1	-1.4	373.8	234.7	10.93	8.57	12.20	14.41	20.25	9.15	24.63	18.40
90	310.3	127.6	-40.8	8.7	37.0	-20.8	390.1	153.3	15.47	8.27	10.37	11.15	4.79	5.36	20.36	8.72
100	308.6	133.7	-31.8	-8.6	38.7	-5.2	376.6	213.2	17.44	11.37	7.71	16.48	4.86	6.70	22.21	11.22
110	306.1	155.8	-47.1	-1.1	52.4	-25.9	406.0	207.8	17.35	9.26	7.32	10.48	6.40	4.83	19.07	13.89
120	306.7	159.7	-48.1	-12.1	59.1	-29.3	382.3	207.8	32.73	38.84	43.96	28.79	46.52	48.10	61.53	41.37
130	300.3	178.7	-42.2	6.7	51.5	-26.4	387.2	234.1	12.04	10.57	9.24	9.55	4.20	6.43	19.82	16.86
140	298.8	186.5	-37.0	13.1	46.4	-21.0	364.1	234.8	18.04	9.19	8.54	8.51	7.70	7.71	14.54	15.85
150	299.1	203.9	-30.5	11.2	41.3	-15.7	330.2	253.5	19.42	10.09	6.61	6.55	11.67	7.18	17.34	23.83
160	296.8	215.7	-29.9	9.4	56.3	-19.8	365.7	301.6	17.47	13.62	9.46	7.34	6.33	9.19	6.70	18.71
170	291.8	228.9	-36.2	9.9	51.0	-23.5	380.8	290.8	20.64	12.48	7.86	7.59	9.39	9.16	21.44	12.02
180	267.3	231.4	-14.2	18.9	24.5	-38.3	366.7	287.0	29.93	39.15	42.24	30.12	47.34	50.39	55.80	59.44
190	243.1	214.6	-25.2	21.3	65.6	-75.9	340.1	302.7	82.14	38.16	6.95	14.22	15.62	64.13	20.68	18.00
200	213.9	211.9	-19.9	55.0	69.3	-95.9	292.7	325.4	138.34	107.93	26.07	47.79	25.52	135.95	49.82	10.08
210	429.3	-2.7	-114.7	327.8	304.5	-53.0	98.7	343.8	687.76	815.13	856.92	518.11	500.92	578.78	508.90	522.61
220	485.9	514.6	-823.1	25.0	64.2	181.8	-2.0	-185.7	2130.16	1321.13	354.34	1088.61	1277.92	1120.98	650.95	401.52
230	416.5	124.0	-87.4	139.1	283.7	-25.3	225.4	434.5	66.95	201.23	73.83	88.50	215.75	54.15	84.66	46.37
240	386.2	275.5	-15.8	28.1	141.1	17.0	271.8	367.4	25.76	97.50	19.94	20.88	81.59	24.42	15.27	34.46
250	405.1	302.7	29.9	14.5	149.8	-8.9	306.2	436.1	16.20	48.20	22.43	21.59	56.01	12.39	29.41	14.07
260	485.0	382.2	70.3	76.3	88.5	25.0	230.4	348.8	34.86	24.46	17.81	13.97	26.82	18.34	12.03	14.80
270	1077.6	-188.3	458.2	-302.0	-5.9	292.2	18.2	547.4	374.13	912.21	238.08	548.71	226.04	208.09	135.76	120.23
280	462.3	-364.5	-49.8	-330.7	323.7	-200.9	382.0	326.5	467.86	252.92	261.81	76.52	54.77	232.56	76.05	130.17
290	668.8	212.9	82.9	-111.4	354.9	14.0	143.9	507.3	65.27	48.57	27.97	31.21	60.81	51.03	52.90	60.04
300	555.7	90.2	37.9	-253.4	170.1	-72.9	28.4	665.3	50.02	85.44	59.28	73.61	76.63	49.39	85.50	32.85
310	537.3	48.2	-72.9	-8.6	132.2	-102.1	42.8	568.5	58.43	32.77	84.25	47.24	42.75	24.27	26.87	28.41
320	461.9	-29.8	-159.3	-320.1	143.8	-53.1	321.5	400.0	118.15	83.29	136.24	101.87	16.59	26.84	18.47	37.27

Table 25 LBP Experimental Dynamic Stiffnesses at 13000 RPM and 1034 kPa

	Dynamic stiffness								Uncertainty							
f(Hz)	$Re(H_{xx})$	$Im(H_{xx})$	$Re(H_{xy})$	$Im(H_{xy})$	$Re(H_{yx})$	$Im(H_{yx})$	$Re(H_{yy})$	$Im(H_{yy})$	$Re(U_{xx})$	$Im(U_{xx})$	$Re(U_{xy})$	$Im(U_{xy})$	$Re(U_{yx})$	$Im(U_{yx})$	$Re(U_{yy})$	$Im(U_{yy})$
20	327.2	24.4	-42.6	4.2	38.8	-7.6	434.9	44.3	24.83	18.94	17.60	20.94	20.31	15.25	17.30	7.90
30	329.5	45.7	-40.0	-4.3	31.3	-4.1	437.7	62.1	32.34	19.13	20.64	12.98	13.06	12.88	19.59	5.88
40	324.6	55.5	-42.4	-3.0	41.2	-7.4	440.6	74.5	20.69	11.27	18.01	12.25	9.67	9.15	19.76	5.04
50	326.5	71.4	-38.7	-0.9	38.0	-14.8	435.1	90.4	15.41	15.73	23.56	20.38	7.16	10.08	15.60	12.10
60	325.6	42.5	-51.1	29.2	30.7	-54.4	424.8	125.2	113.01	166.49	233.47	275.83	115.46	196.48	196.65	292.18
70	322.0	98.6	-40.7	2.7	45.0	-21.0	424.1	125.3	17.54	9.83	12.41	13.99	9.60	7.27	16.85	13.20
80	317.1	115.0	-31.5	6.0	48.8	-21.9	402.9	148.4	17.20	9.25	8.92	15.60	6.20	7.75	10.47	15.84
90	324.9	127.5	-35.9	6.9	41.5	-26.3	437.9	156.0	12.12	8.01	9.66	13.70	4.70	4.51	21.24	10.61
100	322.6	142.6	-34.4	3.0	42.0	-28.1	415.6	182.5	16.90	8.46	14.16	10.64	8.01	5.85	18.86	14.13
110	318.5	156.0	-30.5	0.8	46.9	-36.1	413.8	195.8	19.21	11.09	12.14	7.62	5.51	5.56	19.27	15.97
120	323.1	178.8	-39.3	-5.9	43.7	-13.0	373.2	198.1	43.36	40.51	38.86	50.84	51.93	48.88	57.68	63.08
130	312.1	181.0	-31.5	5.7	52.0	-24.4	404.5	266.0	17.57	12.04	7.49	7.04	5.97	8.15	21.20	15.74
140	310.1	195.4	-25.6	10.5	43.7	-30.3	408.7	255.6	13.70	10.57	7.56	6.00	10.94	10.05	21.67	12.23
150	313.7	209.9	-23.3	11.1	43.6	-23.1	392.8	255.5	20.03	13.22	4.54	4.84	10.71	9.13	17.19	15.50
160	309.3	223.1	-22.6	2.1	56.2	-27.3	442.7	367.3	20.66	13.59	8.54	9.86	16.88	8.35	8.71	15.94
170	304.6	240.1	-23.1	13.9	43.7	-26.7	405.8	304.0	20.21	9.49	4.79	10.17	7.22	5.33	21.14	14.04
180	293.6	260.1	-13.3	30.8	42.8	-22.8	410.5	336.2	56.76	45.42	43.21	33.76	99.49	92.00	64.56	69.09
190	233.9	288.6	-11.3	24.3	13.7	-72.4	379.1	326.1	90.39	32.67	6.69	18.65	72.28	50.65	25.72	18.68
200	193.5	289.5	-16.7	49.8	3.6	-113.0	341.6	337.4	149.75	14.70	12.28	51.51	70.33	117.91	61.48	10.78
210	-17.3	36.6	-117.8	19.0	180.6	-401.2	328.5	251.8	318.65	360.22	143.91	105.45	225.82	377.20	57.95	164.30
220	-143.6	-23.9	-251.4	-114.0	213.9	-496.2	360.8	106.2	235.33	331.44	290.22	138.51	273.62	236.85	134.11	232.05
230	43.6	264.0	-77.7	73.4	48.6	-314.2	266.2	402.5	232.10	115.25	68.39	37.24	50.64	270.19	60.81	72.49
240	134.7	279.7	-27.0	45.5	66.2	-204.2	321.6	382.7	182.17	71.55	27.90	17.33	18.48	182.49	39.57	28.56
250	299.5	339.0	-6.5	52.1	84.3	-51.1	328.5	419.8	55.41	35.20	11.48	17.50	10.65	45.67	33.11	19.14
260	319.3	348.5	1.2	48.7	85.7	-46.1	323.4	391.1	39.43	39.48	8.37	7.61	14.91	36.73	19.34	18.16
270	362.8	373.2	9.2	49.0	83.8	-2.8	294.4	396.1	13.90	26.65	9.84	6.93	15.72	12.15	21.86	14.27
280	415.0	414.8	2.8	24.4	101.7	50.3	396.7	610.5	11.42	15.93	11.27	17.40	5.05	8.38	28.14	15.71
290	486.0	448.5	19.0	68.8	96.0	37.9	315.2	426.7	17.45	18.94	5.82	10.72	7.90	4.57	19.92	10.50
300	576.3	483.8	46.4	86.4	104.1	80.4	256.3	414.9	23.22	28.28	15.34	19.82	8.17	11.57	16.76	14.05
310	710.6	468.7	68.0	68.8	173.3	79.2	294.7	525.5	32.00	31.36	5.51	12.39	27.77	19.91	26.71	25.13
320	933.0	431.2	82.7	85.0	186.4	157.9	282.7	476.8	25.38	31.58	11.10	5.74	17.49	14.38	7.62	26.57

Table 26 LBP Experimental Dynamic Stiffnesses at 13000 RPM and 1723 kPa

	Dynamic stiffness								Uncertainty							
f(Hz)	$Re(H_{xx})$	$Im(H_{xx})$	$Re(H_{xy})$	$Im(H_{xy})$	$Re(H_{yx})$	$Im(H_{yx})$	$Re(H_{yy})$	$Im(H_{yy})$	$Re(U_{xx})$	$Im(U_{xx})$	$Re(U_{xy})$	$Im(U_{xy})$	$Re(U_{yx})$	$Im(U_{yx})$	$Re(U_{yy})$	$Im(U_{yy})$
20	341.9	21.1	-33.5	5.8	22.3	-6.7	484.0	50.2	52.24	37.83	20.21	32.05	22.19	15.95	12.73	10.56
30	354.8	45.1	-32.2	-7.0	27.2	-10.5	483.0	65.6	44.01	14.14	23.79	11.48	21.27	9.71	11.64	7.32
40	339.0	62.3	-32.5	1.6	34.8	-13.1	484.7	78.2	21.62	14.54	18.01	16.35	14.39	11.08	15.32	9.49
50	344.7	75.3	-27.7	-2.6	33.3	-21.5	479.6	94.4	9.83	13.60	14.62	14.95	11.06	9.88	10.79	18.58
60	356.6	72.4	-87.0	-19.2	45.0	-23.5	426.9	75.4	155.49	172.92	282.56	235.38	190.39	191.67	340.38	200.83
70	338.4	98.0	-30.2	5.5	41.8	-26.8	466.7	124.5	10.02	7.50	16.42	17.45	5.09	8.63	17.90	17.76
80	334.2	114.9	-17.7	0.9	42.1	-27.6	455.8	166.0	15.19	9.68	9.59	15.56	8.71	7.36	16.62	21.59
90	341.1	131.0	-26.5	1.9	36.5	-33.1	489.1	165.6	11.58	12.84	13.60	12.47	7.45	5.72	17.75	14.24
100	337.0	145.1	-21.3	-0.7	39.6	-32.7	466.9	197.1	16.21	15.19	16.38	13.88	8.44	10.32	10.05	15.70
110	332.0	156.7	-24.5	2.2	47.4	-40.8	470.5	207.2	5.44	12.96	8.60	8.32	5.45	7.36	10.98	18.18
120	339.1	164.4	-11.0	3.2	44.2	-54.7	485.7	217.2	53.74	51.87	60.74	67.47	80.04	84.94	85.80	91.06
130	333.2	185.0	-19.1	11.0	41.7	-37.7	444.3	248.9	12.46	14.79	10.21	10.81	3.43	8.30	15.21	19.53
140	327.6	197.3	-17.6	9.8	38.8	-36.5	432.6	277.7	10.63	11.80	11.08	10.16	5.76	7.59	17.80	21.36
150	329.6	214.9	-14.4	8.6	37.9	-28.1	439.1	278.0	13.08	13.57	5.06	8.34	8.87	7.70	13.93	21.66
160	322.9	227.2	-13.8	-6.9	60.2	-35.3	507.9	437.6	11.09	14.65	13.92	12.61	10.90	15.67	18.26	32.73
170	321.1	243.6	-10.4	11.3	40.2	-41.6	454.5	320.5	13.18	19.81	11.79	7.67	8.11	10.64	12.54	15.16
180	319.3	249.2	-3.4	-0.2	44.2	-63.1	436.1	310.3	56.93	74.12	59.19	39.71	117.16	97.45	99.09	68.53
190	267.6	295.7	-1.8	31.4	11.0	-74.4	422.5	351.7	45.14	24.07	10.14	23.15	43.91	18.63	32.03	15.78
200	209.8	322.3	-2.8	65.2	-22.7	-114.5	376.6	364.8	103.68	27.02	18.23	51.95	64.33	87.94	59.10	23.83
210	-201.5	156.5	-218.9	-69.0	23.0	-574.0	420.0	134.2	307.23	280.25	279.95	314.04	261.34	324.15	222.36	360.23
220	-147.7	159.8	-302.6	-77.2	81.4	-508.8	378.0	80.7	265.60	181.68	213.45	265.75	146.08	233.62	207.55	200.09
230	107.3	354.8	-72.6	110.1	-22.2	-257.8	235.9	426.4	124.44	48.27	55.81	25.57	42.26	134.12	39.19	70.45
240	163.5	364.0	-16.6	67.5	1.2	-180.7	355.6	417.8	85.37	35.34	11.42	26.05	39.94	80.42	32.71	27.73
250	290.8	376.5	2.6	58.9	41.4	-68.2	351.2	443.2	32.97	14.74	14.25	15.24	17.11	25.56	29.79	16.20
260	312.7	385.1	9.7	49.6	52.3	-59.3	371.4	407.6	26.46	18.10	11.23	13.31	13.77	20.84	20.40	17.65
270	337.6	388.2	20.4	45.6	61.1	-28.0	346.0	421.1	25.50	14.20	11.82	9.44	9.11	11.61	14.72	17.13
280	377.9	407.9	51.8	15.7	66.5	21.8	221.2	754.8	19.97	23.98	15.41	10.48	7.19	11.10	17.29	24.88
290	408.6	429.5	22.9	57.1	83.5	-9.8	371.4	443.6	24.97	27.30	13.13	7.54	8.67	8.28	15.34	19.68
300	460.4	462.8	40.8	67.9	82.9	19.4	313.3	429.2	28.84	35.04	14.86	18.93	9.36	8.14	13.78	15.75
310	525.9	491.8	58.9	61.7	89.2	50.9	311.0	497.8	25.36	30.29	6.73	8.43	6.12	5.68	20.55	14.42
320	594.6	515.7	53.9	62.7	109.8	59.1	361.0	499.4	29.91	22.62	11.99	9.02	3.18	6.48	16.01	16.54

Table 27 LBP Experimental Dynamic Stiffnesses at 13000 RPM and 2413 kPa

f(Hz)	Dynamic stiffness								Uncertainty							
	$Re(H_{xx})$	$Im(H_{xx})$	$Re(H_{xy})$	$Im(H_{xy})$	$Re(H_{yx})$	$Im(H_{yx})$	$Re(H_{yy})$	$Im(H_{yy})$	$Re(U_{xx})$	$Im(U_{xx})$	$Re(U_{xy})$	$Im(U_{xy})$	$Re(U_{yx})$	$Im(U_{yx})$	$Re(U_{yy})$	$Im(U_{yy})$
20	377.6	43.1	-12.7	-7.0	19.8	-9.6	584.8	59.2	58.98	52.17	25.21	33.06	32.75	27.05	26.91	19.45
30	388.4	47.2	-19.7	-4.5	13.6	-10.7	597.5	69.3	43.71	30.68	18.38	18.35	20.40	26.73	19.66	10.55
40	391.8	66.2	-28.4	-4.3	20.8	-12.7	599.7	90.7	32.74	22.78	24.84	21.61	22.36	9.53	21.53	10.14
50	387.4	75.5	-22.9	2.8	20.2	-26.9	589.5	107.6	16.95	14.97	33.22	16.14	10.90	11.52	32.94	14.52
60	376.7	50.9	12.4	-31.2	17.0	-56.0	645.4	84.3	242.84	241.26	401.96	438.48	293.06	315.02	539.39	537.18
70	376.9	103.5	-17.1	-2.7	29.7	-35.2	578.6	144.0	14.91	15.36	27.47	24.76	9.64	11.61	26.00	16.24
80	381.4	115.0	-3.9	1.4	31.4	-30.8	571.6	183.3	14.48	11.64	23.17	23.84	11.00	14.71	29.06	21.94
90	377.6	141.3	-19.9	-2.2	29.8	-50.4	592.8	181.9	18.49	16.45	27.86	17.29	13.90	11.60	35.08	21.31
100	377.5	149.2	-13.0	-0.3	26.7	-43.2	571.8	216.0	13.12	13.76	21.77	13.24	7.26	5.95	12.73	13.99
110	372.1	166.8	-9.9	-3.7	39.7	-54.3	576.3	219.7	11.08	15.39	18.25	11.31	8.44	12.42	26.54	12.91
120	371.3	195.7	-12.4	-8.0	37.3	-15.2	578.1	220.2	72.66	73.59	96.79	92.48	105.78	96.15	148.28	145.42
130	367.6	191.1	-11.3	5.4	34.9	-49.0	550.5	269.0	16.01	12.00	12.28	11.75	7.71	8.27	17.73	14.26
140	357.9	206.7	-6.0	0.2	33.6	-53.5	544.6	292.8	15.93	13.19	8.27	11.98	9.57	10.94	21.22	11.99
150	360.5	218.8	-1.8	-0.2	29.3	-41.6	525.1	282.9	19.65	12.59	9.06	6.45	8.67	8.14	20.22	15.15
160	354.9	233.8	13.9	-20.3	48.0	-41.9	524.4	529.3	24.51	15.30	12.18	12.92	18.40	17.15	21.96	26.14
170	346.3	250.4	-3.3	7.4	23.3	-52.2	535.4	345.2	18.12	14.77	8.27	14.23	17.08	9.80	25.74	12.41
180	328.0	262.2	-3.6	14.8	3.9	-47.5	511.9	368.0	81.75	87.03	83.18	77.58	149.77	138.01	119.66	140.00
190	295.1	307.1	13.1	25.9	-9.9	-77.0	498.8	379.2	35.03	25.75	15.23	25.61	43.89	33.58	24.94	26.34
200	229.1	366.0	14.4	72.8	-96.0	-118.2	441.1	398.4	92.66	53.33	29.03	47.45	91.50	75.84	75.54	24.56
210	-111.5	136.4	-169.8	10.9	15.2	-600.7	429.2	167.3	113.59	265.22	209.30	128.10	234.74	241.54	141.58	294.65
220	-123.4	164.5	-275.6	-47.4	40.6	-555.5	408.9	82.5	314.02	211.88	207.79	303.14	239.59	333.97	271.31	209.60
230	86.3	363.6	-52.5	122.4	-23.5	-295.8	213.5	429.0	131.85	27.25	60.13	40.38	23.51	137.64	55.39	61.75
240	164.5	386.9	-2.1	66.5	-64.9	-205.5	414.1	438.4	76.36	37.62	18.60	27.48	49.37	96.67	28.94	18.30
250	286.7	375.1	27.3	49.6	11.8	-84.1	428.9	451.1	26.09	28.02	20.26	21.01	40.23	26.31	29.59	10.11
260	295.2	366.3	21.0	38.5	34.0	-72.1	431.7	413.6	25.44	21.45	9.19	17.75	21.63	13.41	17.67	16.52
270	308.5	366.2	25.6	38.1	48.4	-49.2	405.1	418.8	19.88	23.74	7.18	9.52	13.06	18.42	19.22	12.09
280	334.4	370.8	62.7	45.1	48.3	-15.8	114.0	501.2	14.98	19.35	13.72	6.63	5.54	10.09	7.04	18.07
290	334.4	380.6	27.6	41.5	58.5	-40.4	414.3	436.1	19.03	19.95	8.84	15.88	13.77	12.47	17.76	11.89
300	366.9	398.6	41.4	51.3	65.5	-8.7	351.4	420.5	23.99	30.18	21.67	19.10	11.40	14.62	16.03	12.00
310	387.1	408.7	59.9	46.1	78.2	9.0	290.6	489.8	21.49	21.91	8.69	5.74	6.52	7.01	13.16	20.50
320	419.4	424.1	46.6	40.4	97.6	16.6	399.2	489.9	19.52	17.87	9.09	7.20	4.18	4.45	16.93	14.23

Table 28 LBP Experimental Dynamic Stiffnesses at 13000 RPM and 3103 kPa

	Dynamic stiffness								Uncertainty							
f(Hz)	$Re(H_{xx})$	$Im(H_{xx})$	$Re(H_{xy})$	$Im(H_{xy})$	$Re(H_{yx})$	$Im(H_{yx})$	$Re(H_{yy})$	$Im(H_{yy})$	$Re(U_{xx})$	$Im(U_{xx})$	$Re(U_{xy})$	$Im(U_{xy})$	$Re(U_{yx})$	$Im(U_{yx})$	$Re(U_{yy})$	$Im(U_{yy})$
20	277.5	-190.3	-36.7	25.0	842.4	-692.1	399.6	195.2	599.59	477.35	103.15	50.13	3270.80	9757.72	956.56	1178.81
30	455.6	33.8	-57.5	-7.8	1243.9	2111.4	588.4	-171.3	115.36	95.89	45.04	37.11	1283.25	1327.09	119.00	286.65
40	439.3	65.6	-39.1	1.0	-292.0	710.3	692.2	40.5	42.28	34.77	30.22	35.35	695.03	1157.95	66.02	92.26
50	438.4	89.7	-43.0	2.5	-223.8	1067.6	699.7	18.6	38.70	33.57	15.27	35.81	899.81	1168.83	109.63	70.04
60	422.7	112.4	-69.2	2.2	620.9	625.3	624.7	87.4	69.12	107.51	169.18	141.72	699.22	791.62	66.72	101.04
70	430.8	103.4	-46.6	3.6	683.0	-72.2	625.6	151.1	25.48	31.31	27.70	36.45	271.41	366.69	37.79	67.33
80	425.0	141.1	-36.0	-9.2	-263.8	-542.0	693.2	219.7	33.39	37.79	29.12	35.55	1830.52	1147.72	110.38	98.18
90	429.3	140.6	-35.6	-3.3	-1822.4	794.9	760.3	98.9	13.37	11.99	23.50	18.04	1152.79	736.87	157.54	99.59
100	427.6	157.4	-38.0	0.9	-27.5	-486.8	694.2	243.0	16.10	31.10	17.99	21.15	936.12	431.00	52.88	49.94
110	428.2	174.6	-36.7	0.6	-853.7	-221.4	746.8	205.1	15.90	19.18	22.76	16.71	758.56	498.68	60.40	44.62
120	445.0	197.6	-45.4	26.1	843.2	210.7	631.7	305.1	128.08	101.61	79.29	79.57	478.98	580.91	272.93	261.38
130	425.7	202.3	-33.3	2.0	-442.6	541.1	659.8	236.6	17.54	8.72	20.04	12.33	976.49	793.19	68.77	65.84
140	424.6	214.0	-28.4	3.1	-761.3	418.0	674.7	261.9	12.08	21.26	13.78	11.27	875.91	601.47	58.39	54.20
150	424.3	228.4	-31.1	4.3	137.3	403.7	633.5	267.7	15.46	18.99	12.46	11.84	259.64	416.31	38.17	28.30
160	416.9	243.5	12.0	-17.6	281.8	-545.4	404.1	538.9	11.82	22.32	8.80	10.91	415.80	274.65	25.83	40.09
170	385.3	296.8	-27.0	-1.0	639.6	-2185.6	714.6	447.9	57.09	73.11	13.04	13.57	1491.27	2362.55	128.82	141.83
180	406.6	266.7	-20.5	-1.0	330.1	1020.5	622.0	311.3	20.89	32.51	30.64	23.69	508.61	1049.49	59.25	69.18
190	397.6	299.4	-16.1	4.8	290.7	1048.3	607.6	337.3	18.03	42.32	14.38	12.70	762.68	458.99	35.18	63.32
200	397.6	314.4	-10.6	20.1	-571.9	892.3	581.2	352.2	33.41	40.55	26.75	21.79	432.57	911.57	31.44	134.92
210	224.7	308.7	-41.8	85.2	-273.0	-530.6	604.8	358.7	410.34	176.64	159.72	206.54	1215.28	443.71	406.11	189.04
220	117.6	353.3	-278.7	235.6	67.4	-240.3	132.5	370.6	513.90	455.10	442.70	191.60	1074.68	1354.98	909.10	1030.78
230	254.0	434.9	-4.5	48.6	966.4	2545.9	418.4	723.5	243.20	182.84	37.14	66.74	1103.61	1827.21	192.30	305.36
240	342.2	381.0	-11.5	19.7	-601.3	622.1	569.4	459.8	49.98	43.15	28.96	33.65	516.75	583.32	84.37	107.20
250	331.0	377.5	1.8	20.1	588.4	1149.5	570.0	505.6	32.64	57.87	15.98	14.00	703.91	547.38	44.81	42.25
260	324.1	369.6	-1.9	23.8	-935.7	130.6	598.7	410.9	27.66	47.52	6.07	11.65	986.35	1176.88	35.47	35.30
270	363.1	411.9	-1.7	27.8	251.3	964.9	545.1	486.4	12.68	17.31	10.07	12.64	376.74	856.86	43.55	45.66
280	359.2	397.7	17.6	31.3	118.4	948.3	436.6	572.1	11.60	21.37	7.08	5.46	682.41	430.71	29.01	26.31
290	381.9	376.4	5.6	34.8	397.8	559.8	613.1	538.6	8.81	18.93	7.18	5.42	363.92	425.96	32.09	23.97
300	373.7	411.2	18.5	46.0	-115.8	661.3	560.4	510.1	21.31	26.34	15.64	17.83	295.87	452.99	43.43	15.93
310	394.6	417.4	26.4	53.5	-230.9	680.0	537.5	495.2	11.36	14.38	3.72	3.57	269.52	414.04	38.91	26.09
320	392.0	439.6	25.5	46.5	156.9	726.0	604.8	570.4	8.54	14.54	5.24	3.89	178.18	284.67	43.03	25.27

APPENDIX B

LOP CONFIGURATION

Table 29 LOP Static Test Data

ω (RPM)	W (kN)	p (kPa)	e_x (μm)	e_y (μm)	ε	Φ (degree)	Tin (°C)	Tout (°C)	Q (*lit / min*)	P (kW)
4000	2.17	353.8	2.5	-15.3	0.20	9.5	41.6	45.3	11.7	1.21
4000	6.40	1042.0	2.1	-35.8	0.45	3.3	42.3	46.0	11.4	1.17
4000	10.30	1678.6	0.5	-47.3	0.60	0.6	42.3	46.5	11.6	1.36
4000	14.98	2440.8	-1.9	-57.1	0.72	-1.9	42.5	47.1	11.6	1.50
7000	2.05	334.3	0.1	-9.7	0.12	0.8	40.9	48.9	20.7	4.64
7000	6.35	1034.9	-1.2	-26.6	0.34	-2.7	42.6	50.0	21.2	4.40
7000	10.61	1728.2	-1.4	-38.7	0.49	-2.0	41.5	50.9	21.0	5.54
7000	14.76	2405.0	-3.4	-47.3	0.60	-4.1	42.5	51.8	21.0	5.47
7000	19.09	3110.9	-4.6	-54.6	0.69	-4.8	42.3	52.6	21.3	6.14
10000	2.15	350.1	1.3	-8.7	0.11	8.5	43.4	54.8	21.2	6.77
10000	6.34	1033.5	2.1	-22.0	0.28	5.4	43.5	56.1	21.2	7.52
10000	10.50	1710.2	1.8	-32.9	0.42	3.1	43.8	56.8	21.2	7.77
10000	14.65	2386.8	0.2	-41.0	0.52	0.3	43.5	57.2	21.3	8.23
10000	19.01	3097.4	-1.7	-48.2	0.61	-2.0	44.0	57.0	21.2	7.79
13000	2.39	389.5	0.3	-8.0	0.10	2.1	43.7	58.3	30.3	12.38
13000	6.07	988.4	1.5	-18.2	0.23	4.8	43.9	59.7	30.5	13.65
13000	10.36	1687.1	2.3	-28.6	0.36	4.5	44.1	61.0	30.6	14.54
13000	14.68	2391.8	1.4	-37.2	0.47	2.1	44.1	61.1	30.6	14.64
13000	19.24	3134.0	0.2	-44.9	0.57	0.3	43.5	59.1	30.5	13.46

Table 30 LOP Pad Temperatures

		Pad 1					Pad 2				Pad 3		Pad 4		Pad 5				Pad 1	Pad 2
	Thermocouple number	1	2	3	4	5	6	7	8	9	10	11	12	13	14	15	16	17	18 (radial)	19(radial)
	% Of Pad Arc Length	6	34	60	75	95	6	60	75	95	6	75	6	75	6	60	75	95	84	84
	Degree (from 1st probe)	0	16	31	39	50	72	103	111	122	144	183	216	255	288	319	327	**338**	45	117
ω (RPM)	*W* (kN)	T1(℃)	T2(℃)	T3(℃)	T4(℃)	T5(℃)	T6(℃)	T7(℃)	T8(℃)	T9(℃)	T10(℃)	T11(℃)	T12(℃)	T13(℃)	T14(℃)	T15(℃)	T16(℃)	T17(℃)	T18(℃)	T19(℃)
4000	2.17	47.34	50.07	52.89	55.60	58.55	45.43	47.62	49.38	51.61	45.78	50.46	45.91	50.70	48.51	53.94	55.65	55.11	55.39	48.44
4000	6.40	50.92	55.42	58.96	62.09	65.09	46.07	49.01	50.85	52.95	45.70	48.74	46.16	49.27	49.89	55.78	57.40	56.89	61.94	50.11
4000	10.30	53.75	59.23	63.20	66.63	69.38	46.69	50.05	52.07	54.22	46.06	48.22	46.65	48.84	50.63	57.09	58.71	58.17	66.22	51.61
4000	14.98	55.84	62.38	66.80	70.60	73.11	46.77	50.78	53.13	55.50	45.99	47.90	46.68	48.38	51.11	58.33	60.16	59.89	69.83	52.72
7000	2.05	49.06	52.29	56.42	60.19	65.38	48.38	52.17	54.53	57.97	48.75	55.56	48.34	54.63	50.49	58.29	61.09	59.50	61.06	54.39
7000	6.35	51.28	56.69	62.37	67.53	73.59	48.61	53.28	56.07	59.77	48.52	53.49	48.47	52.73	51.35	59.66	62.61	61.06	67.89	56.28
7000	10.61	54.84	62.54	69.50	75.76	81.84	49.24	54.76	57.95	62.04	48.92	52.98	49.08	52.33	52.51	61.59	64.72	63.06	75.44	69.67
7000	14.76	57.77	67.28	75.19	82.37	88.12	49.68	55.82	59.41	63.91	49.12	52.76	49.45	52.18	53.29	63.18	66.54	65.33	81.44	59.94
7000	19.09	60.65	71.91	80.50	88.28	92.91	50.17	57.00	60.99	65.82	49.45	52.76	49.82	52.14	54.05	64.96	68.56	67.33	86.56	61.72
10000	2.15	52.65	55.60	59.78	64.34	71.75	52.27	56.61	59.62	64.78	52.57	60.73	52.32	59.76	53.95	63.00	66.48	60.39	66.11	60.44
10000	6.34	53.42	57.92	64.02	70.21	78.82	52.07	57.29	60.68	66.11	52.17	58.60	52.12	57.68	54.07	63.53	67.16	61.28	72.00	61.61
10000	10.50	55.89	62.68	70.80	78.87	88.63	52.81	58.84	62.83	69.07	53.02	58.55	53.22	57.77	55.55	65.44	69.53	65.50	80.44	64.39
10000	14.65	57.87	67.06	77.00	86.62	96.17	52.86	59.70	64.15	70.74	52.97	58.02	53.31	57.24	55.93	66.58	70.91	66.89	87.11	65.44
10000	19.01	60.05	71.82	82.92	93.36	100.98	52.70	60.21	64.96	71.35	52.50	57.08	52.90	56.27	55.82	67.33	71.79	66.94	92.67	66.11
13000	2.39	54.44	57.47	61.80	66.88	74.93	54.10	59.08	62.58	68.69	54.25	63.82	54.33	63.18	55.41	65.51	69.19	39.78	99.50	63.28
13000	6.07	55.74	59.81	65.51	71.85	81.14	55.11	60.58	64.35	70.47	54.88	62.95	54.97	62.22	56.30	66.82	70.73	41.83	117.89	64.72
13000	10.36	56.52	62.12	69.76	77.82	88.11	55.21	61.30	65.45	71.56	54.83	61.94	54.91	61.11	56.39	67.56	71.66	42.83	165.56	65.83
13000	14.68	55.26	63.86	74.74	85.38	97.32	53.13	61.75	67.46	74.78	52.46	59.75	52.72	58.68	54.55	66.69	71.16	47.17	148.06	68.83

Table 31 LOP Experimental Rotordynamic Coefficients

RPM	kPa	K_{xx}	K_{xy}	K_{yx}	K_{yy}	C_{xx}	C_{xy}	C_{yx}	C_{yy}	M_{xx}	M_{xy}	M_{yx}	M_{yy}
		(MN/m)				(kN.s/m)				(kg)			
4000	345	134.24	-22.99	-27.99	171.07	231.57	-4.98	-31.08	296.38	9.00	0.89	-28.43	20.28
4000	1034	143.52	-2.97	-3.78	338.32	232.02	30.22	20.41	334.94	-17.44	4.11	-20.69	-29.70
4000	1723	172.46	-0.58	-9.55	522.10	235.61	23.87	-0.04	318.59	-18.33	-5.23	-23.46	-38.97
4000	2412	199.78	1.17	-24.14	775.27	245.02	37.35	-35.48	366.25	-23.65	-17.75	-26.99	-9.74
7000	345	198.85	-25.46	-23.22	268.12	187.30	13.23	5.32	224.53	5.97	3.28	-42.27	32.10
7000	1034	214.98	-15.17	-12.98	355.89	213.03	10.69	15.51	238.80	3.00	6.63	-19.86	7.24
7000	1723	245.02	-5.46	-25.73	530.64	226.63	18.36	10.72	269.09	-0.06	5.90	-31.83	29.44
7000	2412	269.89	-2.07	-36.63	706.14	234.26	36.57	30.13	287.73	-4.92	4.01	-31.91	39.45
7000	3101	303.44	3.41	-57.87	888.23	246.28	44.85	12.45	293.25	-4.91	3.47	-35.63	51.86
10000	345	252.99	-65.15	-3.15	334.03	190.70	17.85	2.29	222.47	10.59	-13.29	-16.29	53.36
10000	1034	270.84	-52.21	-3.67	397.70	205.27	10.85	-8.02	231.23	9.98	-12.20	-13.73	24.50
10000	1723	296.11	-36.73	-12.99	524.76	216.91	19.83	-7.48	262.07	7.88	-8.92	-17.47	27.48
10000	2412	320.26	-18.69	-26.46	692.94	230.07	24.41	-5.94	265.76	4.14	-3.32	-23.03	45.26
10000	3101	349.74	-9.46	-45.43	864.95	243.64	26.21	-9.79	319.76	-0.66	-2.48	-26.06	56.74
13000	345	322.91	-91.46	-0.53	412.75	196.70	34.56	-1.94	226.46	19.45	-18.27	-24.69	60.10
13000	1034	332.49	-80.52	-1.56	453.38	204.51	26.66	-7.35	226.66	15.02	-12.80	-17.97	36.68
13000	1723	356.47	-70.77	-5.89	553.37	209.36	30.40	-18.12	263.62	17.13	-13.42	-17.00	37.33
13000	2412	384.55	-57.63	-20.89	702.88	220.79	29.38	-17.76	300.52	16.80	-13.46	-21.28	50.58
13000	3101	413.61	-43.64	-42.19	857.64	232.21	37.19	-26.33	269.57	16.09	-11.74	-27.33	60.12

Table 32 LOP Uncertainties of Experimental Rotordynamic Coefficients

RPM	kPa	Uncertainties												Coefficient of Determination							
		K_{xx}	K_{xy}	K_{yx}	K_{yy}	C_{xx}	C_{xy}	C_{yx}	C_{yy}	M_{xx}	M_{xy}	M_{yx}	M_{yy}								
		(MN/m)				(kN.s/m)				(kg)				R^2_{kxx}	R^2_{kxy}	R^2_{kyx}	R^2_{kyy}	R^2_{cxx}	R^2_{cxy}	R^2_{cyx}	R^2_{cyy}
4000	345	6.80	2.41	6.93	6.91	5.32	8.98	5.50	17.84	4.44	1.39	3.74	4.73	0.44	0.07	0.91	0.82	1.00	0.06	0.85	0.98
4000	1034	7.34	2.50	4.26	13.04	8.42	9.11	12.78	22.44	4.54	1.26	2.51	7.04	0.73	0.66	0.94	0.80	0.99	0.67	0.31	0.98
4000	1723	5.45	3.00	4.82	14.32	10.98	9.87	14.40	37.18	3.53	1.56	2.48	7.62	0.82	0.73	0.95	0.85	0.99	0.52	0.00	0.95
4000	2412	10.91	6.95	5.57	17.86	14.83	15.88	14.70	28.66	6.25	3.46	2.94	11.34	0.69	0.86	0.94	0.14	0.98	0.48	0.53	0.97
7000	345	5.13	5.96	10.88	8.93	12.79	10.42	12.83	15.60	4.33	3.67	6.66	6.46	0.28	0.12	0.88	0.85	0.98	0.24	0.03	0.98
7000	1034	6.67	4.22	5.05	15.50	9.17	10.18	14.22	21.60	5.63	2.20	3.12	9.25	0.05	0.61	0.89	0.11	0.99	0.17	0.19	0.96
7000	1723	3.88	2.29	7.89	13.80	11.10	12.38	16.21	20.46	2.96	1.19	4.17	9.52	0.00	0.83	0.92	0.71	0.99	0.30	0.08	0.98
7000	2412	5.69	4.06	6.04	17.71	10.88	12.07	14.03	19.94	3.52	2.10	3.14	12.49	0.24	0.42	0.95	0.71	0.99	0.63	0.42	0.98
7000	3101	4.87	5.05	5.82	13.45	12.48	11.75	17.33	21.02	3.02	2.82	3.10	8.33	0.32	0.24	0.96	0.90	0.98	0.72	0.09	0.98
10000	345	5.01	3.09	2.76	11.68	7.88	6.56	7.54	16.20	3.83	2.12	1.82	7.68	0.60	0.89	0.94	0.92	0.99	0.56	0.02	0.98
10000	1034	2.82	2.32	2.83	6.88	8.01	5.77	8.56	16.12	2.14	1.59	1.63	4.68	0.82	0.92	0.94	0.86	0.99	0.37	0.14	0.97
10000	1723	3.10	2.94	4.22	9.64	8.45	5.76	10.96	16.17	2.17	1.58	2.21	6.87	0.72	0.84	0.92	0.76	0.99	0.66	0.08	0.98
10000	2412	4.72	2.58	4.53	11.44	9.22	7.56	12.38	17.72	2.86	1.34	2.34	7.66	0.27	0.53	0.95	0.88	0.99	0.63	0.04	0.98
10000	3101	6.49	3.06	6.79	13.76	9.85	8.78	14.17	18.25	3.42	1.58	3.53	8.61	0.01	0.31	0.90	0.90	0.99	0.62	0.08	0.98
13000	345	6.50	4.00	3.42	16.03	10.19	9.99	12.91	16.23	5.14	2.28	2.92	12.67	0.75	0.92	0.94	0.83	0.99	0.70	0.00	0.98
13000	1034	6.71	3.28	3.04	8.28	7.98	9.61	12.22	19.34	4.54	1.89	2.03	6.24	0.67	0.89	0.93	0.88	0.99	0.58	0.06	0.96
13000	1723	4.97	3.81	3.18	10.52	8.18	9.19	11.95	16.65	3.36	2.06	1.69	7.76	0.83	0.88	0.94	0.84	0.99	0.64	0.30	0.98
13000	2412	6.98	4.11	4.37	10.83	9.10	9.51	12.90	17.70	4.33	2.24	2.28	7.78	0.72	0.87	0.94	0.91	0.99	0.61	0.25	0.99
13000	3101	5.60	3.48	4.30	18.82	8.25	9.06	14.85	12.87	3.47	1.82	2.26	11.98	0.78	0.87	0.96	0.84	0.99	0.75	0.34	0.99

Table 33 LOP Predicted Rotordynamic Coefficients

RPM	kPa	K_{xx}	K_{xy}	K_{yx}	K_{yy}	C_{xx}	C_{xy}	C_{yx}	C_{yy}	M_{xx}	M_{xy}	M_{yx}	M_{yy}
		(MN/m)				(kN.s/m)				(kg)			
4000	345	152.47	-0.46	0.24	163.76	358.80	1.60	-1.94	382.58	4.94	0.42	-0.46	5.36
4000	1034	200.56	-1.50	-0.80	271.91	456.69	0.15	-3.37	605.83	7.24	0.21	-0.64	9.98
4000	1723	274.87	-4.12	-3.43	421.25	606.62	-3.23	-6.73	908.94	10.04	-0.17	-1.00	15.52
4000	2412	382.10	-10.64	-9.94	631.17	822.45	-12.62	-16.10	1333.27	13.13	-0.96	-1.75	21.48
7000	345	225.98	-0.39	0.25	232.69	324.98	2.01	-2.07	333.05	8.24	0.99	-1.01	8.51
7000	1034	259.08	-1.23	-0.58	310.89	364.04	1.37	-2.74	426.19	9.72	0.88	-1.10	11.84
7000	1723	322.04	-2.96	-2.30	438.39	440.11	0.18	-3.95	579.75	12.13	0.70	-1.25	17.01
7000	2412	394.05	-6.43	-5.77	589.06	523.57	-2.24	-6.42	756.74	15.82	0.41	-1.52	24.14
7000	3101	480.54	-10.36	-9.71	758.69	628.19	-5.21	-9.36	962.56	13.99	0.23	-1.70	21.80
10000	345	291.95	-0.29	0.14	297.63	295.64	1.82	-1.90	300.24	14.13	1.40	-1.42	14.38
10000	1034	316.81	-0.96	-0.53	359.22	315.28	1.50	-2.25	349.55	15.38	1.36	-1.47	17.35
10000	1723	362.78	-2.34	-1.91	462.18	351.45	0.81	-2.98	431.77	17.73	1.27	-1.57	22.40
10000	2412	427.16	-4.86	-4.43	594.47	403.26	-0.39	-4.23	538.49	20.99	1.13	-1.71	29.02
10000	3101	504.84	-8.29	-7.87	753.73	465.35	-2.10	-6.00	666.99	25.26	0.95	-1.90	37.46
13000	345	352.83	-0.20	0.06	358.53	271.99	1.51	-1.57	275.43	17.37	1.66	-1.68	17.61
13000	1034	370.02	-0.70	-0.45	402.90	282.15	1.33	-1.76	301.95	18.11	1.64	-1.71	19.45
13000	1723	408.07	-1.96	-1.72	491.98	304.57	0.80	-2.30	355.10	19.77	1.59	-1.78	23.21
13000	2412	464.20	-3.99	-3.76	612.09	338.16	0.04	-3.09	427.40	22.21	1.52	-1.87	28.33
13000	3101	539.01	-6.54	-6.32	761.08	384.51	-0.98	-4.14	519.46	25.48	1.39	-2.01	34.92

Table 34 LOP Experimental Dynamic Stiffnesses at 4000 RPM and 345 kPa

	Dynamic stiffness								Uncertainty							
f(Hz)	$Re(H_{xx})$	$Im(H_{xx})$	$Re(H_{xy})$	$Im(H_{xy})$	$Re(H_{yx})$	$Im(H_{yx})$	$Re(H_{yy})$	$Im(H_{yy})$	$Re(U_{xx})$	$Im(U_{xx})$	$Re(U_{xy})$	$Im(U_{xy})$	$Re(U_{yx})$	$Im(U_{yx})$	$Re(U_{yy})$	$Im(U_{yy})$
20.00	142.9	30.6	-23.7	-4.9	-29.7	-6.8	171.8	44.1	4.01	2.71	1.91	1.04	11.84	6.07	7.74	2.96
30.00	143.6	48.0	-23.1	-7.0	-23.8	-8.6	172.2	63.9	5.66	2.69	1.74	1.03	4.82	8.49	7.23	1.96
40.00	137.6	62.3	-23.5	-9.7	-22.3	-9.5	174.0	83.5	4.42	1.88	3.36	1.05	1.85	3.12	6.62	4.24
50.00	137.0	84.8	-18.5	-9.5	-21.4	-13.6	166.5	102.8	5.12	2.95	5.65	4.87	2.91	2.45	9.78	4.80
60.00	138.3	89.1	14.9	23.2	-14.6	-25.5	121.3	132.3	74.52	67.70	97.82	89.20	25.39	39.28	56.77	47.91
70.00	120.0	108.9	-12.6	87.2	-7.0	-29.4	47.6	121.5	4.81	5.68	32.54	35.52	5.41	6.39	26.79	41.68
80.00	136.3	130.6	-15.7	-4.3	-31.4	-5.2	101.0	259.5	4.98	2.44	8.32	6.71	3.40	2.62	17.99	12.41
90.00	136.3	137.9	-21.5	-16.5	-14.1	-21.7	167.8	175.9	4.60	1.23	4.76	2.77	1.35	1.98	10.62	6.63
100.00	134.3	156.3	-23.4	-19.0	-12.0	-25.4	163.8	193.3	4.47	1.59	2.82	2.48	1.82	1.30	10.45	5.12
110.00	125.2	169.3	-23.3	-23.4	-10.0	-25.8	168.1	208.1	4.39	1.19	2.85	2.47	1.28	1.38	6.75	2.58
120.00	133.4	186.9	-23.7	-26.6	-11.3	-27.9	159.5	223.3	21.18	16.26	33.08	19.72	27.18	18.40	43.24	25.37
130.00	109.1	214.2	-8.7	-35.5	17.9	-44.9	134.7	251.9	77.41	138.90	158.21	211.45	84.55	144.49	174.52	222.98
140.00	127.9	210.9	-25.5	-30.6	-5.5	-30.4	145.0	259.7	6.14	3.42	9.25	8.14	4.89	4.65	12.96	7.77
150.00	129.7	222.3	-24.1	-28.5	-6.3	-32.3	136.3	265.0	2.48	3.69	2.15	3.43	3.08	2.51	5.45	4.60
160.00	119.6	236.6	-20.7	-35.5	8.2	-29.1	159.7	352.4	5.76	2.82	2.55	2.68	1.48	3.19	7.04	4.21
170.00	129.2	265.6	-24.8	-33.9	6.7	-40.3	148.4	316.4	6.29	6.56	2.86	4.48	1.71	2.97	6.25	3.41
180.00	52.7	269.7	-23.4	-61.3	23.2	-50.4	147.2	337.1	686.33	588.97	308.89	343.09	22.83	100.38	62.38	37.64
190.00	111.2	282.9	-28.2	-32.1	11.0	-42.5	147.7	346.9	5.25	3.09	3.43	5.06	1.60	2.14	4.96	2.64
200.00	121.3	286.3	-30.4	-26.5	7.0	-45.1	134.3	353.7	4.22	5.07	5.40	2.80	5.25	5.47	10.50	6.75
210.00	104.2	315.4	-32.1	-30.4	9.7	-48.9	133.0	355.9	4.72	4.49	3.32	2.16	3.46	3.45	4.35	2.62
220.00	95.5	331.8	-27.0	-18.5	2.3	-57.8	46.5	344.0	5.70	4.04	1.15	2.85	3.31	3.44	6.15	2.05
230.00	119.2	347.0	-28.8	-33.1	34.8	-45.5	139.4	475.4	3.98	4.11	2.03	4.28	4.38	3.61	4.95	6.87
240.00	101.8	357.5	-25.3	-28.2	29.6	-51.8	125.8	440.0	9.22	5.68	6.45	4.74	7.92	2.79	7.96	4.60
250.00	93.3	381.8	-25.9	-16.9	26.3	-57.4	95.6	445.6	9.84	6.41	6.27	4.79	7.91	4.08	13.70	7.77
260.00	170.9	429.4	12.8	6.7	92.4	-19.5	169.1	459.0	493.85	359.78	366.59	222.90	527.94	265.16	375.45	183.42
270.00	108.9	378.0	-35.5	16.0	-18.7	-63.0	-89.4	520.5	86.02	135.98	166.41	135.09	94.58	118.91	182.30	104.00
280.00	128.1	390.0	1.1	-25.1	59.1	-49.4	146.6	597.6	9.57	9.79	8.77	9.39	6.86	6.94	11.82	14.50
290.00	101.1	434.1	-16.5	-47.8	99.1	-15.7	99.0	655.9	27.67	12.13	33.23	34.57	11.28	13.81	34.79	44.15
300.00	1836.6	-2178.5	3203.5	-1395.3	71.6	113.3	-133.5	801.3	6184.10	5591.23	13448.03	5016.64	196.45	412.10	540.55	561.56
310.00	158.1	463.5	7.9	5.0	74.4	-78.5	94.7	531.7	13.11	8.51	12.96	21.15	4.63	10.22	24.25	10.61
320.00	189.7	472.4	18.2	46.0	118.5	-48.7	237.7	664.6	12.61	12.48	13.33	18.62	13.57	6.27	27.99	16.71

Table 35 LOP Experimental Dynamic Stiffnesses at 4000 RPM and 1034 kPa

	Dynamic stiffness								Uncertainty							
f(Hz)	$Re(H_{xx})$	$Im(H_{xx})$	$Re(H_{xy})$	$Im(H_{xy})$	$Re(H_{yx})$	$Im(H_{yx})$	$Re(H_{yy})$	$Im(H_{yy})$	$Re(U_{xx})$	$Im(U_{xx})$	$Re(U_{xy})$	$Im(U_{xy})$	$Re(U_{yx})$	$Im(U_{yx})$	$Re(U_{yy})$	$Im(U_{yy})$
20	148.3	34.2	-4.9	-3.9	-11.2	-10.1	334.3	79.3	17.10	15.62	8.03	4.07	8.60	6.62	3.88	3.84
30	146.1	57.2	-3.8	-11.3	-9.4	-10.5	346.8	101.3	9.67	7.82	6.09	11.09	4.68	3.97	4.90	3.49
40	151.7	77.3	-4.9	-14.9	-5.5	-13.0	354.4	128.1	6.59	4.13	8.85	13.32	3.73	4.13	4.78	7.81
50	147.7	92.3	4.7	-6.7	-3.1	-18.4	344.6	156.4	6.98	5.24	7.31	7.61	4.22	4.56	7.76	7.16
60	158.5	108.5	78.3	79.5	-15.0	-42.6	259.2	315.6	119.12	93.84	149.78	164.06	120.88	70.56	118.16	159.65
70	146.6	120.6	29.0	195.0	11.6	-42.0	24.8	282.1	11.01	8.03	28.96	28.76	7.22	16.98	44.45	49.96
80	162.5	131.5	5.3	19.1	2.0	-33.8	271.7	301.3	17.96	34.83	19.80	24.13	4.84	3.17	14.31	16.07
90	153.9	161.3	-9.2	-7.8	1.7	-25.6	363.7	241.0	8.36	6.53	19.04	8.74	2.74	3.68	8.59	13.97
100	156.6	171.7	-10.7	-9.3	6.3	-29.6	347.2	273.7	8.47	6.34	9.85	11.06	2.69	2.65	6.59	7.57
110	161.1	190.2	-12.7	-11.5	12.3	-28.4	356.8	295.4	3.30	7.53	14.84	9.23	2.11	3.02	6.18	12.27
120	159.3	209.0	-10.6	-11.1	7.0	-43.1	366.0	301.5	31.60	38.96	21.55	47.32	49.71	62.86	78.64	71.47
130	152.8	232.0	48.3	-11.6	22.3	-43.8	221.9	391.5	95.06	49.37	296.59	149.31	162.05	84.85	511.48	252.87
140	160.2	243.1	-12.2	-4.9	12.0	-30.8	332.0	392.5	19.49	10.02	12.00	9.09	23.33	10.91	9.17	14.94
150	158.6	258.9	-9.3	-2.8	14.9	-25.3	357.2	379.5	8.74	8.91	13.00	11.70	3.21	2.64	4.76	7.60
160	150.2	269.0	-9.7	-9.7	23.3	-35.1	413.3	478.9	12.08	10.91	14.88	11.77	3.48	3.85	10.50	11.12
170	156.3	289.7	-12.5	2.4	17.4	-38.3	370.3	439.0	10.77	27.01	12.27	14.50	2.54	4.65	4.11	11.35
180	305.4	271.1	-3.1	80.1	68.8	-119.4	429.9	460.1	623.33	568.51	343.37	321.19	126.66	131.22	84.13	93.57
190	166.5	316.1	-4.3	8.1	34.5	-26.4	391.9	467.3	12.43	14.37	9.18	11.20	2.09	3.88	5.71	7.76
200	157.0	328.4	-4.1	9.4	26.1	-16.9	383.6	465.9	7.32	20.61	9.15	13.89	4.94	4.57	20.26	15.09
210	156.4	327.4	-10.4	12.6	46.8	-26.5	404.9	475.8	13.40	7.67	8.26	9.52	2.23	3.65	8.06	7.56
220	167.6	360.5	-7.6	21.5	51.6	-21.7	320.4	471.4	9.88	19.31	5.79	10.04	2.77	3.08	4.29	8.63
230	166.1	371.3	-6.1	9.5	41.2	-23.4	328.9	633.1	5.51	24.27	8.76	12.57	2.42	3.05	9.27	8.48
240	174.3	381.4	-11.2	18.5	38.5	-19.9	372.4	548.1	15.51	14.96	18.25	11.41	9.79	8.22	13.79	12.07
250	175.8	387.2	-11.4	31.0	49.8	-11.6	381.1	585.1	15.75	23.90	19.48	15.58	6.61	6.82	13.11	15.92
260	168.3	463.3	-32.5	27.4	51.9	69.2	345.8	510.2	57.84	110.47	260.72	35.88	63.33	131.34	299.69	119.38
270	184.7	423.7	7.9	40.1	40.8	16.1	350.5	543.2	15.44	22.90	28.81	27.55	8.84	19.97	9.87	31.53
280	208.2	413.7	5.5	-4.3	10.5	25.1	401.2	816.2	44.11	14.75	28.69	16.74	66.92	9.10	17.88	19.46
290	218.8	440.9	-17.5	30.6	69.2	39.9	433.2	490.5	29.88	17.79	39.51	37.04	7.44	11.35	36.33	44.27
300	1946.3	-2189.5	3202.5	-1309.3	56.6	265.3	167.4	690.4	6184.13	5591.36	13447.93	5016.10	197.78	411.19	534.76	560.46
310	300.3	457.1	4.9	85.6	94.1	111.7	380.1	506.9	20.88	30.01	32.89	26.75	8.51	10.33	19.79	10.99
320	312.7	476.6	-6.2	83.7	147.0	20.2	307.3	818.0	21.52	44.06	34.37	21.55	57.38	13.80	62.90	28.57

Table 36 LOP Experimental Dynamic Stiffnesses at 4000 RPM and 1723 kPa

	Dynamic stiffness								Uncertainty							
f(Hz)	$Re(H_{xx})$	$Im(H_{xx})$	$Re(H_{xy})$	$Im(H_{xy})$	$Re(H_{yx})$	$Im(H_{yx})$	$Re(H_{yy})$	$Im(H_{yy})$	$Re(U_{xx})$	$Im(U_{xx})$	$Re(U_{xy})$	$Im(U_{xy})$	$Re(U_{yx})$	$Im(U_{yx})$	$Re(U_{yy})$	$Im(U_{yy})$
20	168.6	47.0	-0.6	-2.8	-13.5	-8.4	517.1	93.2	14.46	15.49	14.70	11.52	19.63	12.07	13.42	10.19
30	173.3	62.1	-2.1	-8.8	-11.9	-15.8	535.0	118.6	11.39	6.81	8.59	6.70	11.43	9.13	13.54	10.31
40	174.8	80.3	0.9	-9.8	-9.4	-14.7	542.6	148.7	6.33	5.45	11.68	13.20	10.08	8.92	14.23	12.87
50	172.5	102.8	12.1	-10.8	-8.9	-22.9	535.4	176.1	6.69	6.06	9.44	9.45	11.06	7.47	23.90	19.74
60	186.9	109.9	27.5	59.0	8.0	-51.4	415.6	364.3	153.03	59.66	252.02	171.58	221.52	104.85	408.52	344.59
70	179.0	127.7	-31.1	254.9	16.8	-47.7	-23.9	283.6	11.94	14.69	96.78	163.72	27.49	25.85	352.16	183.66
80	163.8	150.0	28.5	10.2	-2.8	-44.6	453.1	348.7	13.13	22.24	19.85	16.34	11.80	9.64	18.68	28.63
90	193.6	175.1	-0.9	-7.0	-1.3	-37.4	561.3	284.7	14.01	5.87	11.66	12.44	3.32	7.37	15.40	12.67
100	188.5	186.5	-0.4	-11.3	4.0	-42.1	536.9	316.3	9.03	7.22	8.51	6.76	6.88	4.59	14.37	15.76
110	192.5	204.4	-5.5	-16.7	10.6	-42.8	547.5	336.2	9.32	6.41	6.52	11.12	5.52	3.36	14.30	19.45
120	196.9	231.0	-2.1	5.7	22.0	-47.3	563.8	365.7	42.54	32.21	61.73	56.46	78.94	81.67	132.00	94.26
130	190.8	245.5	-5.0	7.9	17.2	-33.7	513.2	392.4	19.07	17.49	27.43	50.69	35.94	35.28	62.00	93.92
140	189.4	252.0	-9.3	7.5	12.9	-34.2	532.4	433.8	21.02	16.26	30.42	19.13	50.87	27.83	57.13	25.99
150	197.0	282.6	5.6	-7.2	11.1	-41.2	542.8	439.9	12.80	11.57	8.37	8.01	5.45	10.26	18.48	18.91
160	197.6	289.3	12.5	-18.1	32.9	-49.8	586.3	645.9	12.75	14.05	6.80	4.96	7.02	6.96	14.80	26.25
170	189.3	295.5	5.0	-2.7	11.0	-59.9	569.1	504.0	11.73	12.72	8.32	10.54	6.38	9.59	17.78	17.33
180	134.9	380.4	88.4	-84.6	81.6	-76.9	579.8	475.6	870.01	578.25	352.12	315.57	127.04	317.35	108.83	151.46
190	199.4	330.7	5.9	4.8	30.3	-43.8	593.6	524.4	8.70	12.32	9.48	5.64	12.37	19.72	17.86	14.43
200	180.2	350.1	10.9	6.7	22.0	-29.8	591.8	516.3	7.96	11.45	7.39	10.08	9.09	8.02	25.08	12.75
210	202.0	353.3	1.7	18.8	44.9	-43.6	600.7	529.5	10.25	10.06	5.27	6.30	3.38	8.52	16.93	10.55
220	216.8	380.6	8.0	26.4	48.1	-40.9	514.8	507.7	10.56	9.54	3.96	6.90	1.89	5.50	18.80	11.83
230	216.4	395.3	8.7	11.2	43.3	-49.7	563.2	705.6	18.77	10.82	8.76	6.21	5.33	8.95	21.56	16.53
240	203.8	386.4	19.7	18.3	41.8	-48.2	584.2	595.7	16.17	16.03	13.08	11.37	12.73	9.72	27.61	17.59
250	210.7	402.6	43.0	18.9	47.1	-45.8	610.8	590.8	12.65	15.25	176.49	112.02	10.07	28.92	198.72	263.46
260	203.5	419.3	7.2	33.5	50.8	-23.0	572.9	552.1	13.61	23.03	35.32	21.52	13.07	19.45	53.33	18.77
270	208.7	433.2	65.5	-5.7	41.9	-15.0	529.2	504.7	94.00	161.27	101.66	217.75	186.44	165.78	191.74	257.76
280	238.1	435.2	92.8	-10.7	53.9	3.5	282.7	1056.9	44.93	11.10	23.58	15.91	84.36	27.07	34.27	41.90
290	232.1	464.0	22.2	23.6	74.7	7.9	653.5	573.1	27.96	14.28	34.54	34.94	6.80	12.77	40.72	45.32
300	1958.6	-2147.6	3254.0	-1331.2	70.3	209.9	317.5	852.5	6184.01	5590.98	13447.91	5016.02	192.80	410.97	534.82	560.65
310	290.9	477.8	52.3	73.9	87.9	52.3	588.0	539.2	17.41	10.83	19.75	23.29	6.29	10.12	26.71	15.60
320	307.9	477.6	36.8	98.8	86.4	84.0	552.1	611.5	17.13	17.69	17.94	12.52	6.24	8.19	24.25	11.73

Table 37 LOP Experimental Dynamic Stiffnesses at 4000 RPM and 2413 kPa

	Dynamic stiffness								Uncertainty							
f(Hz)	$Re(H_{xx})$	$Im(H_{xx})$	$Re(H_{xy})$	$Im(H_{xy})$	$Re(H_{yx})$	$Im(H_{yx})$	$Re(H_{yy})$	$Im(H_{yy})$	$Re(U_{xx})$	$Im(U_{xx})$	$Re(U_{xy})$	$Im(U_{xy})$	$Re(U_{yx})$	$Im(U_{yx})$	$Re(U_{yy})$	$Im(U_{yy})$
20	227.7	47.6	12.9	-15.9	-37.5	-4.9	754.4	104.9	31.90	17.36	39.31	28.04	27.51	26.30	25.36	20.85
30	198.5	64.1	-9.2	-12.6	-34.8	-15.2	774.5	133.9	20.69	19.79	20.04	12.10	17.39	16.79	14.00	17.93
40	202.7	95.0	2.2	9.9	-24.2	-19.8	790.5	169.5	8.98	8.39	15.16	15.05	9.93	17.69	28.37	33.14
50	205.3	110.1	27.8	-27.6	-30.3	-32.7	793.4	226.4	12.95	13.75	15.78	20.76	17.14	17.40	33.60	52.03
60	197.6	107.3	14.2	177.2	-53.6	-144.5	229.1	596.1	136.76	144.47	265.85	424.90	242.58	240.51	923.38	739.20
70	206.8	147.6	-94.3	342.9	33.0	-62.4	-227.1	309.6	20.20	20.67	153.29	61.36	19.23	30.23	160.58	377.67
80	172.0	150.2	121.8	21.9	-21.5	-53.2	740.9	443.1	29.29	24.73	57.62	49.03	28.46	14.13	73.73	157.92
90	234.1	206.6	48.8	7.6	-17.5	-54.9	819.5	355.3	32.43	19.19	37.44	33.20	8.58	9.44	34.38	62.81
100	225.4	209.4	25.6	-26.6	-11.3	-60.8	775.2	364.1	14.92	9.53	18.68	20.14	9.73	7.03	27.26	25.01
110	229.8	228.2	12.7	-14.2	-1.8	-62.7	786.1	374.6	16.65	16.40	27.30	24.27	8.83	7.42	40.30	30.98
120	226.7	253.1	23.7	-25.9	-9.5	-55.3	769.9	386.7	32.82	31.78	54.01	67.29	67.80	74.99	139.49	183.51
130	195.8	266.5	66.2	22.5	105.6	-66.9	557.4	447.7	79.42	159.53	238.60	99.12	186.45	414.02	630.48	203.09
140	237.1	293.4	24.5	22.5	10.7	-85.0	722.2	514.2	38.05	28.73	22.53	43.53	51.77	65.76	71.17	51.56
150	213.7	309.6	25.3	-24.8	-5.3	-69.2	769.9	457.7	20.09	10.07	25.02	22.31	42.07	20.74	18.93	14.83
160	255.9	332.8	29.9	-49.1	10.8	-89.2	980.3	676.7	20.19	13.49	34.68	28.12	10.54	6.58	36.14	40.51
170	231.1	322.7	33.7	-17.8	0.8	-90.7	784.2	532.9	18.23	43.87	39.20	32.79	7.75	5.22	18.29	19.55
180	406.0	380.0	64.0	-35.9	74.4	-200.8	795.0	540.8	489.96	444.59	150.19	302.23	70.01	143.26	132.82	83.99
190	218.2	351.2	30.5	-15.6	23.3	-74.4	803.0	577.5	12.50	41.86	33.59	24.14	7.14	7.18	29.30	16.13
200	230.8	380.9	19.8	-15.4	15.8	-53.3	811.3	564.4	14.16	21.04	10.41	25.86	12.91	7.95	27.28	14.02
210	242.9	376.2	19.2	15.0	28.2	-72.4	809.1	561.8	16.61	17.92	12.03	17.64	5.61	6.25	29.01	18.96
220	252.2	403.4	29.9	26.0	42.7	-70.6	737.1	565.5	14.54	17.45	22.07	15.40	3.12	8.49	22.16	8.90
230	275.2	426.4	52.3	-23.0	40.3	-73.2	802.3	791.9	37.17	17.12	32.00	46.27	4.91	8.20	26.29	9.06
240	242.6	397.7	24.9	12.6	33.4	-86.9	797.7	620.7	28.08	41.64	16.21	15.90	6.54	12.54	30.67	20.98
250	249.2	411.1	57.4	62.5	40.5	-80.3	782.5	662.6	15.62	55.67	34.95	26.72	17.53	13.82	27.60	22.28
260	223.3	382.7	-15.6	-23.6	2.2	-112.3	656.1	544.1	43.65	172.45	267.31	263.50	155.85	211.16	560.94	209.74
270	250.3	448.1	86.3	60.6	32.8	-51.1	745.8	607.5	24.73	45.22	96.49	29.81	50.38	50.09	121.82	62.07
280	264.6	457.4	153.7	-6.5	41.7	-32.9	344.1	978.0	21.15	41.93	53.06	40.05	15.21	17.62	25.27	35.43
290	290.8	469.0	72.9	12.2	92.0	-58.1	825.8	558.7	111.80	115.62	49.57	47.57	98.87	187.70	37.31	60.01
300	2009.3	-2107.2	3311.6	-1318.0	72.0	158.3	551.4	756.9	6184.05	5590.97	13447.96	5016.04	193.07	411.72	534.65	560.81
310	328.2	491.1	117.4	68.2	88.3	26.2	560.9	579.3	16.80	21.76	41.31	23.58	18.20	14.63	30.18	44.04
320	346.7	503.3	112.8	90.8	90.4	41.4	774.3	667.3	27.45	31.61	56.63	20.38	15.57	16.99	29.38	18.69

Table 38 LOP Experimental Dynamic Stiffnesses at 7000 RPM and 345 kPa

	Dynamic stiffness								Uncertainty							
f(Hz)	$Re(H_{xx})$	$Im(H_{xx})$	$Re(H_{xy})$	$Im(H_{xy})$	$Re(H_{yx})$	$Im(H_{yx})$	$Re(H_{yy})$	$Im(H_{yy})$	$Re(U_{xx})$	$Im(U_{xx})$	$Re(U_{xy})$	$Im(U_{xy})$	$Re(U_{yx})$	$Im(U_{yx})$	$Re(U_{yy})$	$Im(U_{yy})$
20	195.1	29.1	-39.5	-1.0	-8.0	-9.5	269.4	52.7	7.21	4.11	4.59	4.08	4.66	4.96	4.63	4.24
30	202.7	48.6	-39.2	-4.9	-5.8	-12.9	271.3	67.1	4.25	3.12	3.59	3.44	3.75	3.89	4.77	2.49
40	204.7	64.0	-39.1	-7.3	-5.8	-15.0	273.8	87.6	5.21	3.49	6.12	2.90	2.27	3.06	5.69	4.29
50	198.2	79.9	-36.5	-6.8	-5.4	-17.1	268.4	99.0	2.90	3.31	2.91	2.64	2.63	1.54	6.87	3.16
60	200.2	90.1	-41.9	11.0	-12.1	-19.9	247.8	128.9	50.23	57.92	63.42	98.39	40.05	42.01	42.87	93.13
70	204.6	108.4	-29.4	-10.9	-0.3	-30.3	257.2	141.5	4.89	4.27	8.98	6.85	2.31	2.57	7.86	5.70
80	207.6	129.6	-29.4	-9.8	-10.8	-23.2	273.1	226.6	4.36	5.06	9.43	8.37	8.03	3.43	15.62	18.98
90	203.9	138.6	-27.8	-9.7	-4.3	-27.9	258.2	180.3	4.01	3.52	7.90	11.02	3.18	2.15	16.09	8.94
100	198.7	150.3	-23.5	-2.1	-4.4	-31.8	251.6	207.9	5.22	4.15	11.97	13.67	3.05	3.20	19.57	12.25
110	192.6	158.0	-4.9	96.5	7.6	-41.1	137.4	223.2	10.13	16.58	42.79	121.69	18.34	8.17	142.46	47.24
120	173.5	171.6	-22.2	123.1	12.0	-60.7	101.3	211.5	25.19	22.66	44.02	72.57	39.96	19.07	74.88	47.67
130	196.2	196.0	-25.4	6.7	-0.8	-36.5	225.9	249.2	7.05	6.61	13.11	20.57	4.63	3.61	27.07	11.95
140	193.2	208.2	-27.2	-8.5	1.9	-32.6	229.2	259.4	4.25	3.95	5.35	4.97	4.86	3.60	8.70	7.44
150	194.5	224.6	-24.4	-15.8	2.1	-27.8	224.1	258.9	5.70	5.49	2.51	4.50	3.31	1.85	7.16	3.87
160	192.4	230.1	-18.6	-24.7	5.7	-44.5	241.7	360.6	4.52	5.73	2.71	3.06	3.39	4.17	4.82	5.97
170	187.3	249.2	-25.9	-22.6	5.2	-34.9	249.0	299.8	5.56	7.24	4.42	4.65	2.16	4.03	7.99	4.80
180	88.9	277.3	-24.3	-29.7	27.2	-34.7	245.8	316.6	486.97	441.04	188.89	166.72	15.85	19.77	22.94	30.52
190	185.8	266.4	-24.4	-17.2	14.8	-22.0	237.6	326.9	6.59	5.79	2.31	3.65	3.01	2.15	5.16	5.88
200	181.5	278.5	-26.3	-12.9	15.3	-12.6	214.6	327.3	6.80	4.64	2.61	2.65	3.29	3.72	4.94	5.78
210	181.7	283.8	-26.7	-12.5	29.5	-19.4	210.4	323.9	5.02	6.00	3.33	3.87	3.23	3.21	4.88	4.50
220	186.8	302.5	-16.7	-5.4	55.4	-19.1	107.8	333.4	5.51	5.38	8.41	10.83	9.31	7.54	10.34	9.44
230	82.9	262.9	126.8	44.6	155.7	59.3	45.6	351.7	95.92	112.08	182.75	272.55	120.19	151.49	242.14	334.93
240	166.6	310.9	-6.7	-17.9	55.4	-9.4	171.9	408.2	40.09	30.77	102.13	56.03	46.76	33.80	116.83	44.89
250	178.5	315.0	-23.7	-3.8	73.2	0.0	155.5	449.7	6.65	5.95	8.37	6.72	11.87	9.61	11.41	10.33
260	195.6	326.5	-33.8	16.1	42.2	9.3	187.6	389.7	4.92	6.06	4.07	4.08	7.06	3.55	6.94	8.57
270	210.7	329.2	-15.9	18.7	66.2	-11.2	57.0	434.0	6.51	7.82	6.15	5.55	9.95	12.04	9.25	13.60
280	211.2	297.5	-49.7	13.5	57.2	53.0	300.5	532.3	12.51	14.23	6.54	7.49	10.19	15.12	14.66	11.53
290	224.2	331.5	-50.7	0.6	41.0	-37.9	156.7	663.3	27.76	13.40	32.50	34.28	8.39	14.70	42.67	45.56
300	1963.0	-2314.6	3159.6	-1325.5	94.4	181.0	-279.1	762.9	6184.05	5591.30	13447.91	5016.10	197.62	411.13	535.46	562.17
310	282.1	293.3	-16.0	64.6	180.4	1.8	-72.7	478.1	19.21	20.13	14.90	25.90	44.43	45.80	37.49	27.17
320	318.1	200.9	-82.0	135.8	188.4	80.4	314.7	491.0	31.73	34.26	16.52	29.40	38.76	26.31	37.96	20.29

Table 39 LOP Experimental Dynamic Stiffnesses at 7000 RPM and 1034 kPa

	Dynamic stiffness								Uncertainty							
f(Hz)	$Re(H_{xx})$	$Im(H_{xx})$	$Re(H_{xy})$	$Im(H_{xy})$	$Re(H_{yx})$	$Im(H_{yx})$	$Re(H_{yy})$	$Im(H_{yy})$	$Re(U_{xx})$	$Im(U_{xx})$	$Re(U_{xy})$	$Im(U_{xy})$	$Re(U_{yx})$	$Im(U_{yx})$	$Re(U_{yy})$	$Im(U_{yy})$
20	210.4	29.5	-25.5	-1.9	-16.5	-6.2	362.3	63.7	7.23	6.94	5.19	4.24	7.97	5.36	6.81	8.05
30	216.2	55.1	-24.1	-6.4	-16.0	-12.5	375.2	80.2	5.05	3.75	4.60	3.55	4.38	4.65	8.06	4.27
40	221.9	70.7	-24.8	-9.9	-9.1	-11.5	379.5	93.1	5.93	3.40	6.26	5.95	2.77	3.05	5.33	2.85
50	217.1	82.6	-24.2	-8.3	-8.6	-22.3	370.2	116.1	5.56	3.96	4.55	3.34	2.62	1.67	6.30	4.86
60	236.9	85.1	-17.8	-9.2	6.8	-30.8	358.5	132.0	56.23	73.12	104.92	140.14	54.90	77.62	124.41	159.32
70	225.8	112.5	-20.6	-11.4	0.4	-29.9	349.3	156.8	6.57	4.54	11.10	5.79	1.85	2.60	13.53	11.70
80	224.2	138.4	-17.7	-13.6	-9.9	-36.5	324.4	217.5	5.46	3.52	8.08	6.77	2.73	3.20	14.51	9.88
90	221.5	145.7	-21.1	-14.8	-7.2	-30.1	374.5	189.5	7.55	5.14	15.49	9.28	2.42	3.85	13.06	23.82
100	216.5	158.3	-13.1	-10.0	-4.6	-40.2	349.3	231.3	6.19	6.62	13.96	12.42	4.11	4.00	16.40	22.22
110	212.1	166.2	16.6	96.4	16.0	-48.4	214.0	275.9	15.70	19.50	86.03	159.86	27.78	14.07	214.35	111.47
120	175.8	179.7	9.7	121.4	5.2	-93.1	192.5	270.0	34.66	22.86	74.12	83.00	28.80	42.54	101.49	109.21
130	211.9	207.5	-11.3	1.6	1.2	-43.4	319.9	314.8	10.79	7.94	17.94	16.75	6.35	10.18	22.19	24.89
140	212.7	223.2	-16.4	-10.6	1.8	-35.6	333.0	306.3	6.71	6.12	4.44	4.41	2.32	4.17	5.84	10.00
150	213.5	239.8	-15.8	-15.4	-0.3	-29.2	335.3	294.2	6.34	6.32	4.64	4.62	2.76	3.80	6.52	9.02
160	216.6	246.7	-15.1	-24.7	5.5	-39.6	390.6	369.8	6.64	5.89	3.98	4.71	3.53	4.98	6.97	9.37
170	206.9	268.1	-17.0	-19.1	-3.0	-38.6	347.8	345.8	7.21	8.57	6.60	6.31	3.44	3.80	5.67	8.22
180	85.9	257.8	-5.8	-56.9	27.3	-43.2	360.8	352.1	495.33	444.31	267.45	230.56	24.05	33.88	54.49	56.05
190	208.2	286.3	-17.7	-16.1	15.6	-25.7	349.8	369.8	5.27	5.83	3.67	5.12	3.42	2.67	5.50	8.50
200	203.0	303.0	-19.2	-12.1	13.3	-12.9	330.5	369.7	6.16	5.67	4.35	4.21	3.84	3.19	3.45	8.33
210	203.6	306.6	-23.2	-10.2	30.6	-24.1	342.3	375.1	6.16	7.22	5.91	4.82	4.43	3.17	7.14	10.67
220	215.4	328.0	-20.2	-6.3	39.6	-19.3	266.1	388.4	6.95	7.82	7.55	11.37	12.00	8.52	7.46	9.77
230	185.4	102.8	-358.6	182.2	-7.5	337.7	834.3	327.8	378.41	560.90	1032.81	484.59	659.80	863.59	1605.18	856.64
240	204.5	190.8	-175.0	179.3	14.2	198.5	537.2	218.6	418.18	514.16	1081.50	560.38	593.83	668.92	1471.03	722.14
250	206.3	360.2	-30.6	-5.4	40.9	-11.7	318.4	478.5	13.64	10.94	9.54	22.44	14.86	20.11	11.63	26.57
260	209.5	367.7	-25.3	8.3	43.4	-4.4	292.5	434.5	4.80	7.71	4.27	6.93	3.79	7.63	8.69	8.68
270	216.4	373.7	-11.0	15.8	45.2	13.8	259.8	465.8	5.26	7.22	7.24	4.88	3.91	5.35	7.24	8.12
280	238.3	369.8	-17.3	-27.7	26.1	24.8	354.5	740.3	9.52	10.06	7.57	9.26	7.12	5.84	11.39	11.66
290	245.8	398.8	-35.3	13.7	70.7	50.8	343.1	426.5	27.22	12.39	32.21	34.29	6.74	13.92	34.50	45.06
300	1975.5	-2239.4	3187.1	-1337.2	79.7	296.8	76.5	616.1	6184.03	5590.97	13447.89	5016.01	193.21	411.48	534.36	560.32
310	324.8	384.7	-12.7	74.7	121.8	135.4	278.6	445.6	15.81	14.87	13.12	21.16	18.64	22.80	18.63	13.16
320	341.3	348.1	-40.1	86.0	68.5	108.7	330.2	709.6	13.33	34.62	8.67	15.35	26.30	62.82	26.58	28.65

Table 40 LOP Experimental Dynamic Stiffnesses at 7000 RPM and 1723 kPa

	Dynamic stiffness								Uncertainty							
f(Hz)	$Re(H_{xx})$	$Im(H_{xx})$	$Re(H_{xy})$	$Im(H_{xy})$	$Re(H_{yx})$	$Im(H_{yx})$	$Re(H_{yy})$	$Im(H_{yy})$	$Re(U_{xx})$	$Im(U_{xx})$	$Re(U_{xy})$	$Im(U_{xy})$	$Re(U_{yx})$	$Im(U_{yx})$	$Re(U_{yy})$	$Im(U_{yy})$
20	234.9	30.2	-10.6	-6.7	-22.8	0.4	527.0	79.3	6.62	6.52	8.10	8.33	7.59	7.86	12.52	12.93
30	239.4	64.7	-7.4	-10.9	-32.5	-16.1	536.7	95.0	4.66	3.65	7.94	6.22	4.61	5.25	6.57	8.29
40	247.2	80.4	-6.8	-15.3	-17.5	-11.4	542.7	110.7	6.02	3.12	6.33	5.56	2.43	2.79	9.79	9.47
50	244.4	91.9	-9.4	-13.8	-17.0	-31.6	531.7	132.3	5.99	3.21	7.00	7.11	2.68	2.69	4.68	6.05
60	259.9	108.1	-4.5	33.3	-8.5	-27.0	501.2	227.1	62.46	73.28	198.12	171.84	92.68	87.53	289.35	250.10
70	254.8	124.6	-3.9	-16.8	-5.1	-39.9	508.4	185.1	4.51	3.13	9.77	9.09	3.50	2.75	9.37	18.44
80	245.5	153.6	0.4	-23.1	-14.5	-44.5	466.6	302.9	6.17	2.95	14.84	10.19	3.16	3.06	14.96	13.19
90	252.3	159.3	-6.2	-21.6	-12.0	-40.5	544.4	228.4	7.35	3.54	17.89	7.92	3.59	3.11	12.15	20.63
100	247.6	173.8	7.2	-19.1	-6.6	-50.3	511.5	278.2	6.30	3.77	23.24	13.75	2.71	4.31	14.90	30.23
110	255.1	181.3	82.7	143.1	20.1	-49.4	296.1	423.5	11.99	12.45	68.06	232.94	18.81	14.58	331.91	115.56
120	237.2	196.3	41.3	283.7	12.3	-81.8	97.3	381.8	16.79	45.42	98.16	109.00	24.54	26.93	167.32	119.91
130	246.8	229.9	15.7	9.4	-9.3	-52.4	446.5	375.2	5.21	8.20	24.06	21.20	6.32	3.99	29.47	31.00
140	243.8	248.9	-5.8	-16.8	-4.8	-45.8	483.5	374.0	5.33	4.42	7.16	8.74	3.05	3.97	9.83	13.05
150	246.6	267.6	-9.7	-19.1	-6.4	-34.1	491.8	344.9	5.68	5.33	6.60	5.30	3.59	2.83	8.83	7.79
160	250.9	273.1	-7.0	-37.3	11.7	-51.1	566.3	495.8	5.57	4.56	4.69	3.84	2.74	2.13	8.28	9.99
170	237.2	296.1	-11.6	-23.9	-14.4	-52.6	506.5	404.7	6.03	7.38	6.25	4.46	2.33	3.76	7.81	6.72
180	133.6	262.2	-69.1	-83.0	21.5	-68.8	513.2	425.2	487.02	456.62	291.19	221.68	50.88	30.55	69.97	92.17
190	244.6	316.7	-16.3	-18.9	19.1	-35.5	505.5	419.9	5.74	3.29	4.98	5.38	2.32	2.71	7.17	9.02
200	235.0	334.4	-17.9	-10.3	8.1	-20.0	483.8	415.0	4.85	3.58	4.37	4.93	2.01	3.07	6.22	6.59
210	238.8	332.8	-20.8	-8.5	37.3	-38.5	494.6	431.3	4.97	5.60	8.37	5.00	3.29	3.43	10.09	9.80
220	246.7	353.9	-18.7	5.5	47.5	-29.2	417.9	419.7	4.78	5.56	10.67	8.40	3.13	6.86	12.43	11.03
230	270.4	297.9	-75.0	-2.6	-32.2	87.6	563.5	600.9	281.73	256.89	130.72	202.69	459.30	443.07	223.17	321.09
240	224.7	351.5	-60.7	36.9	59.4	21.8	528.1	458.1	54.45	75.67	95.21	116.71	78.93	109.26	139.09	162.93
250	239.3	388.0	-24.1	12.2	46.8	-15.3	473.9	534.2	6.09	8.86	20.36	9.02	6.72	12.37	25.66	12.29
260	241.7	399.7	-18.2	15.6	43.7	-16.0	451.7	493.5	7.61	3.76	7.48	6.17	5.65	6.24	5.46	7.47
270	246.9	412.4	1.1	23.8	45.7	4.4	404.3	517.8	6.71	3.28	6.80	4.16	3.20	2.93	7.72	7.94
280	271.7	408.7	39.1	-32.2	31.7	14.1	241.5	952.1	10.13	7.07	8.54	8.44	4.00	4.92	21.98	11.99
290	273.2	436.8	-21.4	11.1	85.3	37.9	510.8	518.4	27.52	10.42	32.23	34.11	6.31	11.67	34.56	44.18
300	2012.5	-2186.0	3213.3	-1341.2	65.7	253.5	142.9	766.6	6184.01	5590.97	13447.90	5016.00	192.84	410.79	534.40	560.31
310	354.3	439.3	3.0	65.6	124.3	130.2	467.8	528.7	14.28	8.42	12.37	20.56	11.87	14.59	17.61	10.59
320	358.9	427.7	-10.0	100.4	127.0	153.2	444.1	598.6	12.75	12.92	7.94	9.52	13.46	15.37	12.67	9.93

Table 41 LOP Experimental Dynamic Stiffnesses at 7000 RPM and 2413 kPa

	Dynamic stiffness								Uncertainty							
f(Hz)	$Re(H_{xx})$	$Im(H_{xx})$	$Re(H_{xy})$	$Im(H_{xy})$	$Re(H_{yx})$	$Im(H_{yx})$	$Re(H_{yy})$	$Im(H_{yy})$	$Re(U_{xx})$	$Im(U_{xx})$	$Re(U_{xy})$	$Im(U_{xy})$	$Re(U_{yx})$	$Im(U_{yx})$	$Re(U_{yy})$	$Im(U_{yy})$
20	265.8	35.6	-0.2	-11.0	-42.8	3.6	711.8	81.2	7.91	4.34	14.05	13.10	7.67	11.53	17.66	16.82
30	264.4	70.2	2.6	-10.9	-50.8	-26.6	724.0	99.6	5.28	4.51	9.76	11.33	5.09	6.76	9.21	13.05
40	273.4	86.8	3.9	-17.6	-29.5	-15.0	726.9	114.5	5.59	4.33	7.94	8.56	4.81	6.63	18.34	12.15
50	271.2	98.7	0.6	-14.6	-34.8	-40.3	713.1	141.9	3.58	5.37	11.28	7.37	4.18	4.02	14.67	12.84
60	294.2	113.8	23.6	60.8	-7.0	-38.1	720.3	322.2	79.02	104.68	238.48	318.46	124.28	177.09	405.69	583.96
70	282.6	133.6	2.4	-23.5	-18.4	-47.4	683.9	204.0	4.98	5.20	15.00	11.99	4.13	2.60	20.42	27.58
80	273.8	157.9	8.0	-20.1	-24.9	-54.1	615.7	227.8	5.28	5.52	13.39	13.03	3.56	3.32	12.47	28.44
90	280.3	172.3	5.0	-28.8	-24.3	-51.3	727.0	250.8	4.21	6.68	19.30	15.02	4.54	5.17	22.97	39.28
100	276.6	186.9	17.4	-23.2	-19.6	-61.1	692.5	311.7	6.97	7.52	36.83	10.09	7.70	6.49	21.16	60.66
110	286.3	198.1	94.2	156.4	10.0	-59.7	421.7	503.4	12.83	10.18	132.38	311.64	19.16	28.74	529.02	207.15
120	248.2	203.2	27.4	348.0	1.0	-96.3	59.3	438.9	41.83	30.37	151.85	118.53	56.68	34.93	224.19	149.81
130	274.5	244.8	27.4	7.7	-20.2	-67.3	618.1	427.0	5.04	10.03	44.14	41.57	11.21	7.37	63.12	73.28
140	273.6	264.7	-0.2	-20.9	-16.6	-62.8	656.8	400.9	5.19	8.66	13.04	11.92	5.84	6.05	11.93	27.00
150	275.3	285.2	-8.4	-21.9	-22.1	-47.9	650.7	366.1	5.78	7.70	8.02	7.30	4.76	2.98	12.25	14.20
160	283.9	296.7	-14.6	-42.4	-4.2	-59.7	810.0	510.6	3.41	7.89	6.30	6.32	3.65	4.76	19.89	11.79
170	268.7	314.6	-14.0	-24.0	-30.3	-72.5	669.5	431.6	5.00	9.64	9.48	9.55	3.81	5.29	9.61	19.10
180	187.5	291.6	-49.5	34.4	18.1	-93.3	711.6	461.9	487.53	453.24	238.65	321.89	57.04	35.05	122.56	87.19
190	275.1	341.9	-17.5	-15.4	5.9	-44.0	667.7	453.3	7.83	9.52	7.11	9.78	3.13	3.61	8.15	7.60
200	270.1	354.5	-15.5	-6.9	-1.0	-31.8	647.4	446.6	6.82	8.02	8.59	5.45	3.82	3.54	8.60	12.57
210	275.2	352.3	-19.5	-3.9	34.1	-51.9	641.9	459.8	6.04	8.87	6.87	4.61	5.19	3.29	8.70	5.95
220	283.3	376.8	-15.6	15.3	43.4	-51.6	584.6	449.9	5.64	7.92	12.90	7.89	5.15	4.12	17.01	16.77
230	263.6	361.4	-73.6	57.1	32.2	0.1	726.1	516.0	46.90	31.28	142.56	118.52	80.11	61.41	264.11	206.91
240	260.5	389.8	-62.3	61.3	47.6	-17.8	683.6	446.9	39.96	35.40	86.58	129.33	69.00	48.23	139.07	222.24
250	271.0	414.7	-14.1	18.1	42.3	-43.0	624.5	579.4	8.49	11.92	11.81	9.20	7.31	6.54	22.04	16.62
260	270.7	422.0	-9.8	22.1	43.4	-40.0	602.5	535.8	4.21	9.97	6.42	3.66	2.80	3.48	10.92	10.25
270	277.6	441.8	12.6	28.1	39.1	-11.7	563.0	562.8	6.15	8.63	6.99	6.05	4.30	2.78	9.15	12.14
280	295.4	436.8	61.3	-3.5	24.9	-17.0	262.6	876.9	9.79	9.78	8.59	7.62	3.76	5.06	20.35	20.68
290	291.9	464.6	-5.2	22.2	75.6	4.9	639.3	521.6	27.34	13.08	32.38	34.06	5.03	10.71	34.49	45.09
300	2023.7	-2154.8	3220.2	-1339.1	68.7	208.3	367.7	763.7	6184.01	5590.95	13447.89	5016.01	192.41	410.74	534.54	560.34
310	350.1	475.2	17.7	53.5	101.0	65.2	655.8	597.9	12.19	10.80	12.62	20.60	2.65	6.87	17.95	13.08
320	347.2	476.7	2.5	91.3	104.3	83.4	608.6	651.0	11.78	11.72	8.17	9.55	3.96	4.69	12.99	12.40

Table 42 LOP Experimental Dynamic Stiffnesses at 7000 RPM and 3103 kPa

	Dynamic stiffness								Uncertainty							
f(Hz)	$Re(H_{xx})$	$Im(H_{xx})$	$Re(H_{xy})$	$Im(H_{xy})$	$Re(H_{yx})$	$Im(H_{yx})$	$Re(H_{yy})$	$Im(H_{yy})$	$Re(U_{xx})$	$Im(U_{xx})$	$Re(U_{xy})$	$Im(U_{xy})$	$Re(U_{yx})$	$Im(U_{yx})$	$Re(U_{yy})$	$Im(U_{yy})$
20	295.5	40.4	7.1	-9.6	-62.9	3.7	893.6	81.2	10.61	9.72	15.69	24.27	15.25	16.80	25.09	25.24
30	295.4	71.2	6.8	-10.5	-72.2	-27.7	905.0	100.2	4.65	3.54	10.49	12.46	9.06	9.04	11.02	17.62
40	304.8	90.6	9.9	-16.7	-48.7	-18.6	905.7	126.1	5.25	5.95	17.41	16.19	2.19	6.42	22.16	21.66
50	301.7	105.5	5.3	-22.2	-56.6	-49.9	894.1	153.3	4.16	3.39	8.45	12.79	4.80	4.22	10.93	18.95
60	300.2	123.8	34.0	-87.0	-77.0	-43.2	938.0	48.0	109.54	105.90	408.85	475.72	214.75	193.44	831.71	946.86
70	314.1	142.5	9.4	-27.1	-39.8	-56.8	865.0	207.2	3.00	5.06	27.00	13.96	4.37	3.22	25.40	27.87
80	307.5	167.0	9.4	-24.3	-45.0	-63.1	805.5	235.5	4.24	5.83	17.47	20.53	4.90	5.91	11.94	26.37
90	310.9	182.9	12.7	-28.9	-42.0	-62.4	905.9	271.4	3.81	7.41	29.88	15.12	7.42	5.09	25.85	50.61
100	308.2	199.7	13.5	-24.9	-40.0	-72.2	865.4	320.7	7.63	5.95	33.35	16.75	5.23	9.14	37.15	60.78
110	312.9	209.5	133.2	135.5	-2.9	-83.9	621.1	610.0	19.74	15.52	145.87	253.49	29.14	38.14	429.18	351.28
120	290.2	206.7	-58.1	418.3	-0.9	-107.4	20.9	376.8	65.88	68.06	103.37	151.95	45.89	41.76	138.00	160.78
130	306.8	259.1	37.3	8.0	-41.6	-80.2	794.1	460.3	9.40	11.37	50.67	45.88	10.00	18.40	84.48	93.06
140	307.1	280.6	-2.1	-21.2	-31.6	-71.7	825.0	391.7	6.07	7.76	15.69	11.33	8.44	9.19	16.89	30.38
150	307.4	300.6	-7.3	-22.5	-38.0	-60.9	826.7	373.7	5.64	8.92	7.07	9.11	4.81	5.75	20.34	11.20
160	310.9	317.3	4.5	-89.4	-3.9	-98.4	1064.1	949.3	6.12	7.78	14.00	12.70	8.01	11.43	40.92	26.61
170	302.7	330.7	-11.8	-21.4	-44.8	-94.8	830.9	431.5	5.39	10.39	7.73	8.81	4.01	6.24	18.81	11.32
180	179.4	260.6	58.3	-93.6	-26.8	-91.5	799.2	413.6	533.40	487.84	515.95	693.32	110.10	113.43	331.95	243.52
190	308.0	363.6	-13.3	-14.0	-6.7	-60.4	826.7	471.6	6.19	8.60	8.62	5.69	5.15	4.52	8.72	14.52
200	305.4	375.6	-15.3	-2.9	-14.8	-38.8	798.1	456.3	6.91	8.26	9.37	4.75	3.56	4.66	12.94	8.58
210	310.1	375.0	-16.0	-1.5	14.7	-61.6	789.9	471.0	5.00	7.16	8.01	5.55	4.62	4.42	12.62	12.05
220	320.7	395.9	-8.5	21.2	37.8	-56.1	704.9	463.4	4.37	5.53	9.44	12.78	6.67	8.86	9.31	14.37
230	296.7	374.1	-35.8	26.2	25.7	-2.9	662.6	669.6	29.17	49.57	47.02	62.97	43.98	105.89	96.20	111.60
240	280.7	383.0	-85.3	91.4	66.1	10.8	880.5	394.1	53.18	67.52	132.41	100.97	95.60	109.70	230.05	216.37
250	305.1	434.4	-7.6	24.0	29.9	-64.8	765.2	596.9	7.26	9.83	18.51	9.04	8.53	13.74	35.30	15.28
260	305.2	442.4	-0.8	27.6	37.7	-50.1	740.6	547.6	6.25	8.48	7.73	4.60	6.55	4.06	14.15	12.24
270	310.9	466.4	18.8	33.5	32.4	-30.7	697.0	583.2	5.38	6.04	7.46	9.00	3.67	2.82	10.31	12.10
280	325.3	458.2	51.8	40.3	29.2	-31.3	397.9	556.8	9.41	8.62	7.45	9.11	4.66	4.60	11.01	7.81
290	319.2	487.2	3.2	23.5	67.2	-20.5	787.4	550.8	27.38	11.92	32.59	34.14	5.26	10.76	34.47	45.98
300	2056.0	-2134.1	3233.9	-1320.5	53.4	178.5	530.4	739.1	6184.06	5591.00	13448.06	5016.55	194.33	411.36	541.23	563.45
310	366.2	499.3	49.8	72.2	90.0	24.4	603.5	550.1	11.94	8.92	12.46	20.44	4.23	6.47	18.30	15.87
320	364.1	502.6	17.3	83.0	97.4	44.9	764.5	685.6	11.61	11.31	8.20	10.30	4.51	3.69	13.01	11.54

Table 43 LOP Experimental Dynamic Stiffnesses at 10000 RPM and 345 kPa

	Dynamic stiffness								Uncertainty							
f(Hz)	$Re(H_{xx})$	$Im(H_{xx})$	$Re(H_{xy})$	$Im(H_{xy})$	$Re(H_{yx})$	$Im(H_{yx})$	$Re(H_{yy})$	$Im(H_{yy})$	$Re(U_{xx})$	$Im(U_{xx})$	$Re(U_{xy})$	$Im(U_{xy})$	$Re(U_{yx})$	$Im(U_{yx})$	$Re(U_{yy})$	$Im(U_{yy})$
20	249.1	29.8	-69.1	1.3	1.8	-9.6	332.7	40.7	10.64	9.51	12.56	12.59	10.05	12.26	12.58	12.38
30	263.9	41.5	-72.8	-2.1	-5.5	-13.9	333.6	58.1	8.22	6.55	10.48	8.17	7.11	8.13	6.81	7.33
40	258.3	53.0	-68.7	-1.8	0.6	-14.4	329.4	76.3	7.59	5.33	5.89	9.71	4.03	3.94	7.78	8.47
50	249.4	76.0	-65.0	-3.7	0.2	-18.1	322.3	86.2	5.10	3.71	4.51	6.17	3.43	3.71	6.96	6.64
60	274.8	96.3	-65.6	0.0	11.3	-1.7	305.2	106.8	61.26	52.19	103.95	111.72	49.99	43.24	109.24	117.66
70	255.7	102.6	-61.6	-2.8	6.2	-32.7	312.3	125.2	5.51	4.37	11.14	10.40	1.92	4.38	9.38	9.11
80	260.1	120.4	-60.8	-10.7	-7.6	-14.2	328.8	226.8	6.21	3.28	12.53	13.35	5.50	4.06	20.76	16.34
90	251.7	131.9	-60.2	-9.8	3.1	-30.2	316.7	163.9	6.10	4.95	10.02	11.40	2.82	1.89	9.01	7.37
100	248.5	144.9	-60.7	-10.2	4.2	-34.6	311.7	186.8	5.34	3.80	11.59	4.17	3.19	2.64	8.39	6.07
110	251.9	160.6	-58.1	-13.0	3.6	-39.4	318.8	200.6	4.53	5.94	9.52	7.53	2.97	2.28	8.72	5.45
120	247.0	177.7	-56.3	-14.1	1.4	-31.7	305.6	211.8	13.16	15.85	30.23	22.32	18.67	19.17	47.61	33.96
130	249.1	186.6	-53.1	-6.1	5.2	-33.7	297.4	234.7	4.43	3.23	10.43	7.02	3.22	2.83	8.03	8.32
140	243.4	201.4	-53.5	-2.6	8.5	-36.0	284.8	240.4	5.45	5.19	5.44	4.68	3.27	3.18	9.32	7.64
150	239.3	212.8	-48.3	0.0	6.4	-35.1	263.8	243.4	7.74	4.41	8.05	8.57	3.73	4.31	13.11	5.24
160	223.5	212.6	-57.0	57.2	28.4	-72.5	216.0	304.7	29.48	12.71	31.85	78.94	20.08	29.79	92.92	62.82
170	206.7	215.3	-89.2	132.7	50.3	-76.4	139.8	225.1	30.50	10.37	52.54	72.72	10.46	38.78	81.89	62.60
180	119.1	224.2	-70.9	8.2	29.2	-59.0	274.5	293.7	488.09	443.68	200.95	198.56	20.28	18.13	31.17	25.25
190	232.4	257.9	-44.8	1.2	23.6	-37.6	277.0	303.6	6.52	3.31	6.85	5.04	3.57	3.79	6.64	7.22
200	229.0	269.0	-43.2	0.0	22.5	-30.8	259.4	303.1	4.39	5.61	3.50	2.50	2.79	1.97	5.54	3.32
210	231.4	275.4	-43.3	3.7	26.0	-33.5	265.0	300.5	4.10	5.96	2.77	3.78	2.40	2.61	4.80	6.11
220	231.9	291.2	-31.3	7.1	53.4	-39.9	164.5	314.0	2.72	4.99	3.11	4.50	4.96	6.13	11.97	9.71
230	228.9	297.2	-48.0	0.4	32.7	-28.4	291.5	433.4	3.25	4.49	4.48	5.13	1.77	4.39	4.27	9.23
240	226.2	302.6	-42.6	9.9	37.1	-23.0	249.5	373.0	3.44	4.50	4.55	4.51	3.16	3.66	4.07	6.76
250	226.5	314.4	-26.4	17.1	56.3	-20.0	196.3	408.9	5.05	4.75	6.20	8.70	7.55	13.43	17.29	24.37
260	237.2	327.5	-29.8	24.1	39.2	-8.6	221.7	369.5	3.71	4.50	3.51	2.66	6.24	4.61	7.66	7.03
270	265.2	325.3	-10.0	19.2	51.9	-30.2	106.8	421.2	8.98	9.30	7.16	4.75	9.52	5.71	7.16	13.03
280	304.6	339.6	-38.3	16.5	-10.3	76.2	318.7	489.7	17.49	13.31	8.08	9.18	14.92	22.10	23.53	9.79
290	315.7	361.7	-33.3	3.9	54.5	-20.2	182.5	623.1	28.44	14.46	32.92	34.99	12.02	14.88	81.47	51.34
300	2012.8	-2338.8	3180.5	-1328.9	120.1	150.2	-189.8	710.2	6184.02	5591.02	13447.89	5016.02	193.06	415.06	535.81	564.91
310	353.7	249.4	40.8	73.7	250.7	-17.2	27.1	544.5	21.20	17.98	15.49	23.24	45.92	72.62	31.42	41.58
320	301.0	126.0	-6.9	149.5	191.7	1.9	310.2	583.3	40.91	28.84	17.57	16.46	29.54	24.08	15.29	22.99

Table 44 LOP Experimental Dynamic Stiffnesses at 10000 RPM and 1034 kPa

	Dynamic stiffness								Uncertainty							
f(Hz)	$Re(H_{xx})$	$Im(H_{xx})$	$Re(H_{xy})$	$Im(H_{xy})$	$Re(H_{yx})$	$Im(H_{yx})$	$Re(H_{yy})$	$Im(H_{yy})$	$Re(U_{xx})$	$Im(U_{xx})$	$Re(U_{xy})$	$Im(U_{xy})$	$Re(U_{yx})$	$Im(U_{yx})$	$Re(U_{yy})$	$Im(U_{yy})$
20	261.4	20.1	-53.8	-0.2	-5.3	-14.1	395.7	55.4	14.03	10.22	12.20	10.67	13.43	11.88	13.80	14.87
30	272.5	54.8	-52.9	-1.6	-15.2	-14.0	407.3	66.3	6.57	10.24	8.94	6.27	5.63	8.58	7.10	12.26
40	274.7	64.2	-54.4	-0.9	-3.4	-10.3	404.8	77.6	5.92	5.80	8.63	10.26	3.51	4.88	10.20	10.30
50	269.5	75.6	-52.5	-4.2	0.3	-21.7	400.2	103.1	3.87	3.64	6.80	7.91	5.60	3.51	6.06	8.55
60	281.3	89.8	-41.7	-21.8	4.5	-21.2	401.2	97.4	61.76	75.55	144.22	116.99	66.51	79.90	160.42	140.74
70	274.0	104.5	-51.9	-5.8	7.0	-31.8	382.6	141.0	4.04	4.40	11.81	16.37	2.81	4.70	10.08	11.89
80	275.1	127.3	-44.1	-8.1	-7.4	-38.7	354.0	196.4	3.75	6.04	11.56	10.85	4.52	3.67	9.33	12.29
90	269.7	137.4	-49.4	-8.9	2.9	-36.7	402.7	173.9	4.58	4.45	8.34	6.94	4.00	2.79	9.25	9.07
100	267.2	152.5	-49.2	-9.8	3.2	-41.2	392.3	202.9	3.64	4.31	4.75	9.42	4.26	1.92	6.60	9.61
110	270.5	167.6	-49.0	-11.4	8.9	-44.6	389.3	211.8	4.04	4.37	12.77	7.83	2.51	3.36	10.02	9.13
120	265.2	184.7	-43.2	-7.1	0.3	-42.8	391.1	225.2	18.37	17.71	31.04	40.88	27.61	21.61	46.97	57.52
130	264.5	198.0	-44.0	-3.3	5.7	-44.3	371.0	282.6	3.15	6.26	8.05	6.63	3.17	1.91	5.19	9.58
140	262.8	212.9	-41.4	-2.9	7.8	-43.8	367.0	284.1	4.75	5.15	9.09	4.68	2.79	3.88	8.36	10.97
150	261.5	228.7	-34.0	-2.5	6.1	-39.6	358.0	277.2	5.94	7.91	9.37	9.45	3.82	4.65	11.27	14.80
160	244.8	233.8	-14.3	42.0	18.1	-81.8	336.6	368.9	27.48	11.84	28.12	84.07	19.49	36.71	111.37	30.01
170	231.0	233.5	-49.3	194.4	30.9	-74.4	114.0	292.8	31.04	19.17	44.81	78.03	20.46	38.04	101.42	61.08
180	123.1	239.0	8.0	-36.0	31.2	-59.4	361.3	331.2	509.33	440.40	215.35	216.06	20.48	39.12	48.56	45.59
190	254.6	274.4	-29.9	0.5	19.9	-42.4	366.6	348.7	5.12	7.50	9.70	7.89	3.93	4.44	9.65	10.93
200	248.7	288.1	-30.3	-2.3	19.0	-37.7	357.3	345.6	3.85	5.09	6.10	7.00	2.66	2.87	5.82	6.11
210	249.0	291.2	-31.5	0.7	34.1	-44.4	364.6	354.4	4.19	6.07	6.22	7.06	2.47	3.42	7.10	11.57
220	256.6	311.7	-25.0	9.0	37.8	-38.7	295.5	354.0	3.51	3.43	5.76	4.00	2.31	2.59	5.79	7.24
230	246.8	317.3	-25.2	-4.1	29.0	-40.4	330.4	480.9	4.37	5.23	4.35	3.10	2.74	2.91	5.44	8.73
240	246.1	331.5	-28.9	3.9	24.9	-36.0	340.8	413.7	2.12	5.31	7.84	5.21	2.87	4.85	6.51	7.31
250	244.3	341.5	-22.1	9.9	32.5	-31.6	343.7	437.6	3.15	5.69	5.91	6.96	2.66	1.78	3.52	7.94
260	245.7	350.1	-19.2	9.2	30.6	-30.1	322.4	407.1	3.81	5.39	3.97	4.04	2.22	3.34	6.14	7.57
270	252.8	361.0	-2.2	8.6	32.3	-21.3	292.7	444.4	4.72	5.19	7.04	6.07	2.41	3.92	6.36	7.35
280	273.2	356.9	-11.8	-28.0	18.5	-7.6	380.8	649.4	8.91	8.21	9.48	9.98	3.81	5.72	12.89	14.74
290	271.3	382.0	-24.2	2.8	50.5	5.6	367.1	400.7	27.24	11.79	32.31	34.07	5.85	11.14	34.34	44.70
300	2007.6	-2245.9	3201.3	-1354.7	36.9	212.2	107.2	604.1	6184.01	5590.96	13447.90	5016.00	192.56	410.84	534.32	560.20
310	334.5	378.3	3.7	37.6	56.7	55.2	306.6	429.9	12.06	7.90	12.41	20.48	5.38	8.23	17.78	11.18
320	336.9	379.3	-22.9	37.2	35.1	31.5	354.4	668.0	12.17	10.58	9.34	11.22	5.26	10.24	15.95	29.99

Table 45 LOP Experimental Dynamic Stiffnesses at 10000 RPM and 1723 kPa

	Dynamic stiffness								Uncertainty							
f(Hz)	$Re(H_{xx})$	$Im(H_{xx})$	$Re(H_{xy})$	$Im(H_{xy})$	$Re(H_{yx})$	$Im(H_{yx})$	$Re(H_{yy})$	$Im(H_{yy})$	$Re(U_{xx})$	$Im(U_{xx})$	$Re(U_{xy})$	$Im(U_{xy})$	$Re(U_{yx})$	$Im(U_{yx})$	$Re(U_{yy})$	$Im(U_{yy})$
20	290.1	26.8	-40.7	-2.7	-16.4	-9.5	524.6	66.2	16.82	9.57	14.46	17.24	21.09	16.49	29.71	28.73
30	291.1	60.0	-34.8	-3.8	-27.6	-15.7	540.0	71.9	8.33	10.89	11.08	22.44	16.98	14.01	16.40	14.30
40	299.9	71.8	-36.8	-2.3	-11.7	-11.3	538.8	85.5	7.40	6.73	12.43	17.60	5.07	12.14	11.18	19.18
50	293.7	81.5	-39.5	-3.2	-9.6	-26.1	530.2	111.8	5.04	3.92	12.05	13.33	4.55	5.34	20.97	15.74
60	289.0	86.2	-13.8	-15.6	-23.9	-44.5	546.0	124.6	59.06	75.68	206.74	127.28	68.31	94.48	282.49	170.78
70	300.3	111.3	-37.3	-12.0	-0.9	-37.4	516.6	160.6	5.13	3.66	16.90	19.12	3.67	3.77	18.05	11.50
80	297.3	138.8	-30.7	-10.3	-10.4	-52.2	472.0	250.8	5.12	4.27	10.93	18.23	4.36	4.16	15.47	13.74
90	298.2	147.2	-38.6	-16.3	-3.9	-41.0	538.5	189.9	5.82	3.43	14.92	11.10	3.55	4.42	12.64	10.61
100	293.1	162.4	-35.6	-13.6	-0.9	-47.7	516.1	222.4	5.07	4.06	8.58	9.99	3.64	5.13	13.26	9.40
110	298.7	177.7	-34.8	-12.2	9.1	-49.4	515.6	236.7	5.59	4.16	13.98	12.56	4.18	3.92	14.30	22.81
120	289.6	195.9	-31.7	-16.3	-13.1	-54.6	517.2	242.0	9.13	12.51	25.47	34.53	17.27	18.17	44.92	53.21
130	291.7	212.3	-30.1	-7.8	0.5	-50.4	491.7	307.5	5.04	5.96	9.92	8.92	5.34	4.90	15.23	12.80
140	290.1	229.1	-28.6	-3.1	2.5	-53.7	487.3	316.5	4.60	5.19	6.07	7.25	5.54	5.67	9.58	16.53
150	287.7	245.5	-18.3	-4.0	-3.2	-48.2	482.4	316.9	11.05	7.22	15.90	16.68	10.28	7.23	18.85	24.15
160	271.3	255.5	2.5	92.8	23.0	-95.1	365.7	487.6	33.48	22.63	71.49	149.92	39.36	52.78	232.44	107.46
170	259.9	241.1	-62.2	276.4	35.4	-92.0	85.1	315.8	46.35	36.96	105.58	116.47	56.00	61.40	176.79	135.93
180	169.3	246.0	8.3	4.9	24.5	-76.5	475.7	394.8	489.10	436.93	151.62	206.37	26.21	34.81	34.25	34.15
190	280.0	297.6	-18.8	1.6	13.3	-45.4	486.8	387.2	5.72	6.10	9.71	10.46	5.53	5.40	9.83	19.77
200	276.1	310.2	-19.8	4.0	13.5	-39.1	474.4	380.0	8.13	5.47	8.03	6.14	3.41	5.23	10.23	11.57
210	278.3	310.5	-21.1	4.4	32.5	-49.4	488.9	391.3	3.85	6.27	5.45	6.60	4.44	3.04	10.15	7.48
220	287.3	329.7	-17.0	13.7	39.1	-43.7	414.7	383.3	7.08	5.67	7.31	4.75	2.71	4.78	6.98	12.60
230	273.3	338.1	-16.2	-2.8	26.2	-54.9	462.2	544.5	4.68	3.75	9.30	6.90	3.42	2.28	10.78	15.61
240	272.2	351.9	-18.8	9.1	25.0	-46.0	459.2	455.2	3.84	4.61	9.09	8.53	3.11	2.36	5.53	9.10
250	270.9	362.3	-8.8	14.0	33.5	-42.3	459.2	486.1	4.97	5.76	9.48	7.18	2.96	2.82	8.57	10.18
260	270.6	370.4	-8.4	11.3	34.8	-39.4	446.5	448.6	5.96	5.10	4.36	5.45	2.12	2.59	5.19	7.50
270	277.6	388.4	12.5	14.2	29.5	-24.9	401.7	475.6	5.33	5.61	6.92	6.68	2.31	2.89	7.67	7.89
280	292.9	382.1	39.7	-40.2	20.6	-22.0	282.8	863.5	9.88	8.64	9.34	9.85	4.21	5.28	17.49	20.26
290	287.8	405.7	-8.9	-3.6	53.9	-6.3	504.8	472.7	27.70	12.66	32.44	34.22	5.19	10.74	34.50	44.69
300	2016.4	-2217.0	3226.8	-1363.9	44.5	186.5	158.8	724.4	6184.00	5590.95	13447.89	5016.00	192.32	410.74	534.39	560.23
310	333.0	408.5	17.3	30.5	66.5	27.8	451.4	477.1	12.72	9.40	12.51	20.57	3.64	7.65	18.07	11.48
320	323.8	412.3	-3.5	55.9	64.3	42.6	425.4	551.6	12.01	10.89	9.34	9.51	4.95	4.95	14.56	11.43

Table 46 LOP Experimental Dynamic Stiffnesses at 10000 RPM and 2413 kPa

	Dynamic stiffness								Uncertainty							
f(Hz)	$Re(H_{xx})$	$Im(H_{xx})$	$Re(H_{xy})$	$Im(H_{xy})$	$Re(H_{yx})$	$Im(H_{yx})$	$Re(H_{yy})$	$Im(H_{yy})$	$Re(U_{xx})$	$Im(U_{xx})$	$Re(U_{xy})$	$Im(U_{xy})$	$Re(U_{yx})$	$Im(U_{yx})$	$Re(U_{yy})$	$Im(U_{yy})$
20	142.9	30.6	-23.7	-4.9	-29.7	-6.8	171.8	44.1	4.01	2.71	1.91	1.04	11.84	6.07	7.74	2.96
30	143.6	48.0	-23.1	-7.0	-23.8	-8.6	172.2	63.9	5.66	2.69	1.74	1.03	4.82	8.49	7.23	1.96
40	137.6	62.3	-23.5	-9.7	-22.3	-9.5	174.0	83.5	4.42	1.88	3.36	1.05	1.85	3.12	6.62	4.24
50	137.0	84.8	-18.5	-9.5	-21.4	-13.6	166.5	102.8	5.12	2.95	5.65	4.87	2.91	2.45	9.78	4.80
60	138.3	89.1	14.9	23.2	-14.6	-25.5	121.3	132.3	74.52	67.70	97.82	89.20	25.39	39.28	56.77	47.91
70	120.0	108.9	-12.6	87.2	-7.0	-29.4	47.6	121.5	4.81	5.68	32.54	35.52	5.41	6.39	26.79	41.68
80	136.3	130.6	-15.7	-4.3	-31.4	-5.2	101.0	259.5	4.98	2.44	8.32	6.71	3.40	2.62	17.99	12.41
90	136.3	137.9	-21.5	-16.5	-14.1	-21.7	167.8	175.9	4.60	1.23	4.76	2.77	1.35	1.98	10.62	6.63
100	134.3	156.3	-23.4	-19.0	-12.0	-25.4	163.8	193.3	4.47	1.59	2.82	2.48	1.82	1.30	10.45	5.12
110	125.2	169.3	-23.3	-23.4	-10.0	-25.8	168.1	208.1	4.39	1.19	2.85	2.47	1.28	1.38	6.75	2.58
120	133.4	186.9	-23.7	-26.6	-11.3	-27.9	159.5	223.3	21.18	16.26	33.08	19.72	27.18	18.40	43.24	25.37
130	109.1	214.2	-8.7	-35.5	17.9	-44.9	134.7	251.9	77.41	138.90	158.21	211.45	84.55	144.49	174.52	222.98
140	127.9	210.9	-25.5	-30.6	-5.5	-30.4	145.0	259.7	6.14	3.42	9.25	8.14	4.89	4.65	12.96	7.77
150	129.7	222.3	-24.1	-28.5	-6.3	-32.3	136.3	265.0	2.48	3.69	2.15	3.43	3.08	2.51	5.45	4.60
160	119.6	236.6	-20.7	-35.5	8.2	-29.1	159.7	352.4	5.76	2.82	2.55	2.68	1.48	3.19	7.04	4.21
170	129.2	265.6	-24.8	-33.9	6.7	-40.3	148.4	316.4	6.29	6.56	2.86	4.48	1.71	2.97	6.25	3.41
180	52.7	269.7	-23.4	-61.3	23.2	-50.4	147.2	337.1	686.33	588.97	308.89	343.09	22.83	100.38	62.38	37.64
190	111.2	282.9	-28.2	-32.1	11.0	-42.5	147.7	346.9	5.25	3.09	3.43	5.06	1.60	2.14	4.96	2.64
200	121.3	286.3	-30.4	-26.5	7.0	-45.1	134.3	353.7	4.22	5.07	5.40	2.80	5.25	5.47	10.50	6.75
210	104.2	315.4	-32.1	-30.4	9.7	-48.9	133.0	355.9	4.72	4.49	3.32	2.16	3.46	3.45	4.35	2.62
220	95.5	331.8	-27.0	-18.5	2.3	-57.8	46.5	344.0	5.70	4.04	1.15	2.85	3.31	3.44	6.15	2.05
230	119.2	347.0	-28.8	-33.1	34.8	-45.5	139.4	475.4	3.98	4.11	2.03	4.28	4.38	3.61	4.95	6.87
240	101.8	357.5	-25.3	-28.2	29.6	-51.8	125.8	440.0	9.22	5.68	6.45	4.74	7.92	2.79	7.96	4.60
250	93.3	381.8	-25.9	-16.9	26.3	-57.4	95.6	445.6	9.84	6.41	6.27	4.79	7.91	4.08	13.70	7.77
260	170.9	429.4	12.8	6.7	92.4	-19.5	169.1	459.0	493.85	359.78	366.59	222.90	527.94	265.16	375.45	183.42
270	108.9	378.0	-35.5	16.0	-18.7	-63.0	-89.4	520.5	86.02	135.98	166.41	135.09	94.58	118.91	182.30	104.00
280	128.1	390.0	1.1	-25.1	59.1	-49.4	146.6	597.6	9.57	9.79	8.77	9.39	6.86	6.94	11.82	14.50
290	101.1	434.1	-16.5	-47.8	99.1	-15.7	99.0	655.9	27.67	12.13	33.23	34.57	11.28	13.81	34.79	44.15
300	1836.6	-2178.5	3203.5	-1395.3	71.6	113.3	-133.5	801.3	6184.10	5591.23	13448.03	5016.64	196.45	412.10	540.55	561.56
310	158.1	463.5	7.9	5.0	74.4	-78.5	94.7	531.7	13.11	8.51	12.96	21.15	4.63	10.22	24.25	10.61
320	189.7	472.4	18.2	46.0	118.5	-48.7	237.7	664.6	12.61	12.48	13.33	18.62	13.57	6.27	27.99	16.71

Table 47 LOP Experimental Dynamic Stiffnesses at 10000 RPM and 3103 kPa

	Dynamic stiffness								Uncertainty							
f(Hz)	$Re(H_{xx})$	$Im(H_{xx})$	$Re(H_{xy})$	$Im(H_{xy})$	$Re(H_{yx})$	$Im(H_{yx})$	$Re(H_{yy})$	$Im(H_{yy})$	$Re(U_{xx})$	$Im(U_{xx})$	$Re(U_{xy})$	$Im(U_{xy})$	$Re(U_{yx})$	$Im(U_{yx})$	$Re(U_{yy})$	$Im(U_{yy})$
20	142.9	30.6	-23.7	-4.9	-29.7	-6.8	171.8	44.1	4.01	2.71	1.91	1.04	11.84	6.07	7.74	2.96
30	143.6	48.0	-23.1	-7.0	-23.8	-8.6	172.2	63.9	5.66	2.69	1.74	1.03	4.82	8.49	7.23	1.96
40	137.6	62.3	-23.5	-9.7	-22.3	-9.5	174.0	83.5	4.42	1.88	3.36	1.05	1.85	3.12	6.62	4.24
50	137.0	84.8	-18.5	-9.5	-21.4	-13.6	166.5	102.8	5.12	2.95	5.65	4.87	2.91	2.45	9.78	4.80
60	138.3	89.1	14.9	23.2	-14.6	-25.5	121.3	132.3	74.52	67.70	97.82	89.20	25.39	39.28	56.77	47.91
70	120.0	108.9	-12.6	87.2	-7.0	-29.4	47.6	121.5	4.81	5.68	32.54	35.52	5.41	6.39	26.79	41.68
80	136.3	130.6	-15.7	-4.3	-31.4	-5.2	101.0	259.5	4.98	2.44	8.32	6.71	3.40	2.62	17.99	12.41
90	136.3	137.9	-21.5	-16.5	-14.1	-21.7	167.8	175.9	4.60	1.23	4.76	2.77	1.35	1.98	10.62	6.63
100	134.3	156.3	-23.4	-19.0	-12.0	-25.4	163.8	193.3	4.47	1.59	2.82	2.48	1.82	1.30	10.45	5.12
110	125.2	169.3	-23.3	-23.4	-10.0	-25.8	168.1	208.1	4.39	1.19	2.85	2.47	1.28	1.38	6.75	2.58
120	133.4	186.9	-23.7	-26.6	-11.3	-27.9	159.5	223.3	21.18	16.26	33.08	19.72	27.18	18.40	43.24	25.37
130	109.1	214.2	-8.7	-35.5	17.9	-44.9	134.7	251.9	77.41	138.90	158.21	211.45	84.55	144.49	174.52	222.98
140	127.9	210.9	-25.5	-30.6	-5.5	-30.4	145.0	259.7	6.14	3.42	9.25	8.14	4.89	4.65	12.96	7.77
150	129.7	222.3	-24.1	-28.5	-6.3	-32.3	136.3	265.0	2.48	3.69	2.15	3.43	3.08	2.51	5.45	4.60
160	119.6	236.6	-20.7	-35.5	8.2	-29.1	159.7	352.4	5.76	2.82	2.55	2.68	1.48	3.19	7.04	4.21
170	129.2	265.6	-24.8	-33.9	6.7	-40.3	148.4	316.4	6.29	6.56	2.86	4.48	1.71	2.97	6.25	3.41
180	52.7	269.7	-23.4	-61.3	23.2	-50.4	147.2	337.1	686.33	588.97	308.89	343.09	22.83	100.38	62.38	37.64
190	111.2	282.9	-28.2	-32.1	11.0	-42.5	147.7	346.9	5.25	3.09	3.43	5.06	1.60	2.14	4.96	2.64
200	121.3	286.3	-30.4	-26.5	7.0	-45.1	134.3	353.7	4.22	5.07	5.40	2.80	5.25	5.47	10.50	6.75
210	104.2	315.4	-32.1	-30.4	9.7	-48.9	133.0	355.9	4.72	4.49	3.32	2.16	3.46	3.45	4.35	2.62
220	95.5	331.8	-27.0	-18.5	2.3	-57.8	46.5	344.0	5.70	4.04	1.15	2.85	3.31	3.44	6.15	2.05
230	119.2	347.0	-28.8	-33.1	34.8	-45.5	139.4	475.4	3.98	4.11	2.03	4.28	4.38	3.61	4.95	6.87
240	101.8	357.5	-25.3	-28.2	29.6	-51.8	125.8	440.0	9.22	5.68	6.45	4.74	7.92	2.79	7.96	4.60
250	93.3	381.8	-25.9	-16.9	26.3	-57.4	95.6	445.6	9.84	6.41	6.27	4.79	7.91	4.08	13.70	7.77
260	170.9	429.4	12.8	6.7	92.4	-19.5	169.1	459.0	493.85	359.78	366.59	222.90	527.94	265.16	375.45	183.42
270	108.9	378.0	-35.5	16.0	-18.7	-63.0	-89.4	520.5	86.02	135.98	166.41	135.09	94.58	118.91	182.30	104.00
280	128.1	390.0	1.1	-25.1	59.1	-49.4	146.6	597.6	9.57	9.79	8.77	9.39	6.86	6.94	11.82	14.50
290	101.1	434.1	-16.5	-47.8	99.1	-15.7	99.0	655.9	27.67	12.13	33.23	34.57	11.28	13.81	34.79	44.15
300	1836.6	-2178.5	3203.5	-1395.3	71.6	113.3	-133.5	801.3	6184.10	5591.23	13448.03	5016.64	196.45	412.10	540.55	561.56
310	158.1	463.5	7.9	5.0	74.4	-78.5	94.7	531.7	13.11	8.51	12.96	21.15	4.63	10.22	24.25	10.61
320	189.7	472.4	18.2	46.0	118.5	-48.7	237.7	664.6	12.61	12.48	13.33	18.62	13.57	6.27	27.99	16.71

Table 48 LOP Experimental Dynamic Stiffnesses at 13000 RPM and 345 kPa

	Dynamic stiffness								Uncertainty							
f(Hz)	$Re(H_{xx})$	$Im(H_{xx})$	$Re(H_{xy})$	$Im(H_{xy})$	$Re(H_{yx})$	$Im(H_{yx})$	$Re(H_{yy})$	$Im(H_{yy})$	$Re(U_{xx})$	$Im(U_{xx})$	$Re(U_{xy})$	$Im(U_{xy})$	$Re(U_{yx})$	$Im(U_{yx})$	$Re(U_{yy})$	$Im(U_{yy})$
20	310.3	28.0	-90.4	-0.3	2.2	-14.4	413.4	42.0	11.17	11.86	6.83	8.40	13.17	8.74	9.57	10.59
30	335.7	36.8	-95.4	2.4	-0.1	-12.4	413.4	59.1	8.81	10.61	4.35	6.75	9.95	10.80	9.64	10.18
40	327.7	54.8	-90.0	-1.0	-1.6	-16.9	412.4	75.2	8.38	6.17	10.82	10.53	5.01	6.26	8.95	7.90
50	321.3	76.8	-91.5	-5.5	-0.1	-18.5	404.4	91.7	3.95	3.44	5.50	7.15	4.05	4.93	8.47	6.03
60	327.6	84.2	-81.8	-5.0	-2.4	-18.3	391.8	112.4	82.34	70.13	143.72	163.54	93.68	74.13	180.98	178.13
70	320.2	103.2	-88.2	-16.9	15.2	-32.4	394.9	140.9	6.07	4.52	13.84	15.44	3.53	4.90	21.75	12.15
80	328.8	123.0	-88.8	-4.8	10.0	-19.1	407.0	202.0	4.84	2.58	13.40	16.75	3.28	6.84	13.61	19.59
90	317.6	135.2	-83.5	-4.0	8.4	-32.8	391.5	170.8	3.81	4.95	10.08	11.43	5.08	3.07	12.93	14.07
100	315.5	148.6	-82.3	-8.1	9.8	-40.7	398.4	197.1	3.66	3.44	9.82	7.11	4.60	2.11	10.11	7.59
110	316.6	162.6	-82.3	-16.0	7.4	-41.9	393.5	192.4	4.74	4.11	7.56	10.30	2.70	3.63	12.47	9.41
120	314.6	179.6	-69.6	-6.5	16.4	-35.4	397.3	229.4	24.81	24.79	41.65	32.58	33.39	32.41	55.80	48.56
130	311.8	190.2	-77.6	-8.9	14.8	-36.3	372.7	236.8	3.80	4.59	7.50	6.63	1.82	2.58	8.34	8.35
140	304.7	202.3	-72.9	-5.6	22.9	-41.1	354.6	239.5	5.38	5.04	4.49	4.97	4.02	4.72	5.92	7.52
150	301.6	217.5	-71.3	-8.0	12.4	-36.7	332.8	250.5	4.16	5.26	5.55	4.87	2.76	4.79	6.51	7.93
160	297.2	228.7	-67.0	-18.1	20.7	-62.9	370.8	358.3	6.46	5.59	4.93	6.70	3.03	7.73	5.45	13.29
170	296.0	243.5	-74.6	-3.9	20.4	-45.8	364.3	287.9	6.20	7.08	7.28	7.43	3.03	4.80	9.13	15.24
180	168.6	233.4	-58.6	1.5	39.4	-65.0	356.8	305.6	496.38	459.05	240.94	227.74	34.45	30.42	44.81	41.98
190	283.5	260.1	-72.7	15.8	33.9	-42.7	323.9	298.6	8.25	6.61	7.39	16.62	2.67	3.86	20.32	10.62
200	271.1	268.3	-66.8	56.7	43.0	-36.3	266.8	307.5	9.32	8.98	11.66	39.51	7.04	6.63	41.31	21.69
210	263.8	308.4	-268.5	279.2	18.2	-37.1	36.1	129.2	59.20	70.11	306.19	229.42	52.75	50.02	255.11	246.82
220	168.5	376.5	-537.0	-42.5	-19.9	-148.7	284.3	-98.7	201.62	236.20	272.07	323.14	158.55	137.99	162.89	213.74
230	300.1	298.2	-156.8	84.8	47.2	-10.0	277.1	359.5	6.32	11.44	37.55	38.65	10.11	6.67	46.52	38.31
240	264.8	320.3	-104.5	20.8	53.7	-34.5	326.4	327.5	5.81	12.68	29.59	15.50	7.68	5.04	17.35	22.44
250	274.9	311.5	-34.0	35.6	94.8	-17.7	220.8	400.7	7.75	5.02	10.74	8.66	14.44	8.01	11.34	13.76
260	279.6	330.1	-45.5	44.2	73.7	-6.3	262.5	340.0	6.41	7.45	4.49	5.35	13.68	8.89	14.75	6.88
270	324.4	285.3	-10.0	38.2	119.6	-23.8	95.2	432.1	13.98	25.56	15.28	6.09	37.76	16.90	14.60	9.66
280	398.6	343.5	-31.7	38.3	-111.2	246.2	456.0	521.8	46.54	40.61	7.97	9.69	151.94	88.44	22.59	16.00
290	355.7	293.3	-31.4	21.2	192.2	-104.3	274.4	700.7	36.19	23.83	33.05	36.00	26.10	89.25	54.74	49.84
300	2056.4	-2316.2	3178.0	-1281.4	117.2	137.0	-321.0	739.0	6184.02	5591.00	13447.90	5016.02	194.24	411.17	544.09	565.12
310	334.2	280.0	63.1	46.4	27.5	-170.1	189.7	651.3	23.95	13.25	23.75	30.99	56.35	63.10	31.42	41.43
320	279.8	214.8	7.9	169.6	248.9	-248.6	592.3	343.3	30.63	27.47	24.75	26.11	47.19	81.41	43.19	115.55

Table 49 LOP Experimental Dynamic Stiffnesses at 13000 RPM and 1034 kPa

	Dynamic stiffness								Uncertainty							
f(Hz)	$Re(H_{xx})$	$Im(H_{xx})$	$Re(H_{xy})$	$Im(H_{xy})$	$Re(H_{yx})$	$Im(H_{yx})$	$Re(H_{yy})$	$Im(H_{yy})$	$Re(U_{xx})$	$Im(U_{xx})$	$Re(U_{xy})$	$Im(U_{xy})$	$Re(U_{yx})$	$Im(U_{yx})$	$Re(U_{yy})$	$Im(U_{yy})$
20	142.9	30.6	-23.7	-4.9	-29.7	-6.8	171.8	44.1	4.01	2.71	1.91	1.04	11.84	6.07	7.74	2.96
30	143.6	48.0	-23.1	-7.0	-23.8	-8.6	172.2	63.9	5.66	2.69	1.74	1.03	4.82	8.49	7.23	1.96
40	137.6	62.3	-23.5	-9.7	-22.3	-9.5	174.0	83.5	4.42	1.88	3.36	1.05	1.85	3.12	6.62	4.24
50	137.0	84.8	-18.5	-9.5	-21.4	-13.6	166.5	102.8	5.12	2.95	5.65	4.87	2.91	2.45	9.78	4.80
60	138.3	89.1	14.9	23.2	-14.6	-25.5	121.3	132.3	74.52	67.70	97.82	89.20	25.39	39.28	56.77	47.91
70	120.0	108.9	-12.6	87.2	-7.0	-29.4	47.6	121.5	4.81	5.68	32.54	35.52	5.41	6.39	26.79	41.68
80	136.3	130.6	-15.7	-4.3	-31.4	-5.2	101.0	259.5	4.98	2.44	8.32	6.71	3.40	2.62	17.99	12.41
90	136.3	137.9	-21.5	-16.5	-14.1	-21.7	167.8	175.9	4.60	1.23	4.76	2.77	1.35	1.98	10.62	6.63
100	134.3	156.3	-23.4	-19.0	-12.0	-25.4	163.8	193.3	4.47	1.59	2.82	2.48	1.82	1.30	10.45	5.12
110	125.2	169.3	-23.3	-23.4	-10.0	-25.8	168.1	208.1	4.39	1.19	2.85	2.47	1.28	1.38	6.75	2.58
120	133.4	186.9	-23.7	-26.6	-11.3	-27.9	159.5	223.3	21.18	16.26	33.08	19.72	27.18	18.40	43.24	25.37
130	109.1	214.2	-8.7	-35.5	17.9	-44.9	134.7	251.9	77.41	138.90	158.21	211.45	84.55	144.49	174.52	222.98
140	127.9	210.9	-25.5	-30.6	-5.5	-30.4	145.0	259.7	6.14	3.42	9.25	8.14	4.89	4.65	12.96	7.77
150	129.7	222.3	-24.1	-28.5	-6.3	-32.3	136.3	265.0	2.48	3.69	2.15	3.43	3.08	2.51	5.45	4.60
160	119.6	236.6	-20.7	-35.5	8.2	-29.1	159.7	352.4	5.76	2.82	2.55	2.68	1.48	3.19	7.04	4.21
170	129.2	265.6	-24.8	-33.9	6.7	-40.3	148.4	316.4	6.29	6.56	2.86	4.48	1.71	2.97	6.25	3.41
180	52.7	269.7	-23.4	-61.3	23.2	-50.4	147.2	337.1	686.33	588.97	308.89	343.09	22.83	100.38	62.38	37.64
190	111.2	282.9	-28.2	-32.1	11.0	-42.5	147.7	346.9	5.25	3.09	3.43	5.06	1.60	2.14	4.96	2.64
200	121.3	286.3	-30.4	-26.5	7.0	-45.1	134.3	353.7	4.22	5.07	5.40	2.80	5.25	5.47	10.50	6.75
210	104.2	315.4	-32.1	-30.4	9.7	-48.9	133.0	355.9	4.72	4.49	3.32	2.16	3.46	3.45	4.35	2.62
220	95.5	331.8	-27.0	-18.5	2.3	-57.8	46.5	344.0	5.70	4.04	1.15	2.85	3.31	3.44	6.15	2.05
230	119.2	347.0	-28.8	-33.1	34.8	-45.5	139.4	475.4	3.98	4.11	2.03	4.28	4.38	3.61	4.95	6.87
240	101.8	357.5	-25.3	-28.2	29.6	-51.8	125.8	440.0	9.22	5.68	6.45	4.74	7.92	2.79	7.96	4.60
250	93.3	381.8	-25.9	-16.9	26.3	-57.4	95.6	445.6	9.84	6.41	6.27	4.79	7.91	4.08	13.70	7.77
260	170.9	429.4	12.8	6.7	92.4	-19.5	169.1	459.0	493.85	359.78	366.59	222.90	527.94	265.16	375.45	183.42
270	108.9	378.0	-35.5	16.0	-18.7	-63.0	-89.4	520.5	86.02	135.98	166.41	135.09	94.58	118.91	182.30	104.00
280	128.1	390.0	1.1	-25.1	59.1	-49.4	146.6	597.6	9.57	9.79	8.77	9.39	6.86	6.94	11.82	14.50
290	101.1	434.1	-16.5	-47.8	99.1	-15.7	99.0	655.9	27.67	12.13	33.23	34.57	11.28	13.81	34.79	44.15
300	1836.6	-2178.5	3203.5	-1395.3	71.6	113.3	-133.5	801.3	6184.10	5591.23	13448.03	5016.64	196.45	412.10	540.55	561.56
310	158.1	463.5	7.9	5.0	74.4	-78.5	94.7	531.7	13.11	8.51	12.96	21.15	4.63	10.22	24.25	10.61
320	189.7	472.4	18.2	46.0	118.5	-48.7	237.7	664.6	12.61	12.48	13.33	18.62	13.57	6.27	27.99	16.71

Table 50 LOP Experimental Dynamic Stiffnesses at 13000 RPM and 1723 kPa

	Dynamic stiffness								Uncertainty							
f(Hz)	$Re(H_{xx})$	$Im(H_{xx})$	$Re(H_{xy})$	$Im(H_{xy})$	$Re(H_{yx})$	$Im(H_{yx})$	$Re(H_{yy})$	$Im(H_{yy})$	$Re(U_{xx})$	$Im(U_{xx})$	$Re(U_{xy})$	$Im(U_{xy})$	$Re(U_{yx})$	$Im(U_{yx})$	$Re(U_{yy})$	$Im(U_{yy})$
20	142.9	30.6	-23.7	-4.9	-29.7	-6.8	171.8	44.1	4.01	2.71	1.91	1.04	11.84	6.07	7.74	2.96
30	143.6	48.0	-23.1	-7.0	-23.8	-8.6	172.2	63.9	5.66	2.69	1.74	1.03	4.82	8.49	7.23	1.96
40	137.6	62.3	-23.5	-9.7	-22.3	-9.5	174.0	83.5	4.42	1.88	3.36	1.05	1.85	3.12	6.62	4.24
50	137.0	84.8	-18.5	-9.5	-21.4	-13.6	166.5	102.8	5.12	2.95	5.65	4.87	2.91	2.45	9.78	4.80
60	138.3	89.1	14.9	23.2	-14.6	-25.5	121.3	132.3	74.52	67.70	97.82	89.20	25.39	39.28	56.77	47.91
70	120.0	108.9	-12.6	87.2	-7.0	-29.4	47.6	121.5	4.81	5.68	32.54	35.52	5.41	6.39	26.79	41.68
80	136.3	130.6	-15.7	-4.3	-31.4	-5.2	101.0	259.5	4.98	2.44	8.32	6.71	3.40	2.62	17.99	12.41
90	136.3	137.9	-21.5	-16.5	-14.1	-21.7	167.8	175.9	4.60	1.23	4.76	2.77	1.35	1.98	10.62	6.63
100	134.3	156.3	-23.4	-19.0	-12.0	-25.4	163.8	193.3	4.47	1.59	2.82	2.48	1.82	1.30	10.45	5.12
110	125.2	169.3	-23.3	-23.4	-10.0	-25.8	168.1	208.1	4.39	1.19	2.85	2.47	1.28	1.38	6.75	2.58
120	133.4	186.9	-23.7	-26.6	-11.3	-27.9	159.5	223.3	21.18	16.26	33.08	19.72	27.18	18.40	43.24	25.37
130	109.1	214.2	-8.7	-35.5	17.9	-44.9	134.7	251.9	77.41	138.90	158.21	211.45	84.55	144.49	174.52	222.98
140	127.9	210.9	-25.5	-30.6	-5.5	-30.4	145.0	259.7	6.14	3.42	9.25	8.14	4.89	4.65	12.96	7.77
150	129.7	222.3	-24.1	-28.5	-6.3	-32.3	136.3	265.0	2.48	3.69	2.15	3.43	3.08	2.51	5.45	4.60
160	119.6	236.6	-20.7	-35.5	8.2	-29.1	159.7	352.4	5.76	2.82	2.55	2.68	1.48	3.19	7.04	4.21
170	129.2	265.6	-24.8	-33.9	6.7	-40.3	148.4	316.4	6.29	6.56	2.86	4.48	1.71	2.97	6.25	3.41
180	52.7	269.7	-23.4	-61.3	23.2	-50.4	147.2	337.1	686.33	588.97	308.89	343.09	22.83	100.38	62.38	37.64
190	111.2	282.9	-28.2	-32.1	11.0	-42.5	147.7	346.9	5.25	3.09	3.43	5.06	1.60	2.14	4.96	2.64
200	121.3	286.3	-30.4	-26.5	7.0	-45.1	134.3	353.7	4.22	5.07	5.40	2.80	5.25	5.47	10.50	6.75
210	104.2	315.4	-32.1	-30.4	9.7	-48.9	133.0	355.9	4.72	4.49	3.32	2.16	3.46	3.45	4.35	2.62
220	95.5	331.8	-27.0	-18.5	2.3	-57.8	46.5	344.0	5.70	4.04	1.15	2.85	3.31	3.44	6.15	2.05
230	119.2	347.0	-28.8	-33.1	34.8	-45.5	139.4	475.4	3.98	4.11	2.03	4.28	4.38	3.61	4.95	6.87
240	101.8	357.5	-25.3	-28.2	29.6	-51.8	125.8	440.0	9.22	5.68	6.45	4.74	7.92	2.79	7.96	4.60
250	93.3	381.8	-25.9	-16.9	26.3	-57.4	95.6	445.6	9.84	6.41	6.27	4.79	7.91	4.08	13.70	7.77
260	170.9	429.4	12.8	6.7	92.4	-19.5	169.1	459.0	493.85	359.78	366.59	222.90	527.94	265.16	375.45	183.42
270	108.9	378.0	-35.5	16.0	-18.7	-63.0	-89.4	520.5	86.02	135.98	166.41	135.09	94.58	118.91	182.30	104.00
280	128.1	390.0	1.1	-25.1	59.1	-49.4	146.6	597.6	9.57	9.79	8.77	9.39	6.86	6.94	11.82	14.50
290	101.1	434.1	-16.5	-47.8	99.1	-15.7	99.0	655.9	27.67	12.13	33.23	34.57	11.28	13.81	34.79	44.15
300	1836.6	-2178.5	3203.5	-1395.3	71.6	113.3	-133.5	801.3	6184.10	5591.23	13448.03	5016.64	196.45	412.10	540.55	561.56
310	158.1	463.5	7.9	5.0	74.4	-78.5	94.7	531.7	13.11	8.51	12.96	21.15	4.63	10.22	24.25	10.61
320	189.7	472.4	18.2	46.0	118.5	-48.7	237.7	664.6	12.61	12.48	13.33	18.62	13.57	6.27	27.99	16.71

Table 51 LOP Experimental Dynamic Stiffness at 13000 RPM and 2413 kPa

	Dynamic stiffness								Uncertainty							
f(Hz)	$Re(H_{xx})$	$Im(H_{xx})$	$Re(H_{xy})$	$Im(H_{xy})$	$Re(H_{yx})$	$Im(H_{yx})$	$Re(H_{yy})$	$Im(H_{yy})$	$Re(U_{xx})$	$Im(U_{xx})$	$Re(U_{xy})$	$Im(U_{xy})$	$Re(U_{yx})$	$Im(U_{yx})$	$Re(U_{yy})$	$Im(U_{yy})$
20	142.9	30.6	-23.7	-4.9	-29.7	-6.8	171.8	44.1	4.01	2.71	1.91	1.04	11.84	6.07	7.74	2.96
30	143.6	48.0	-23.1	-7.0	-23.8	-8.6	172.2	63.9	5.66	2.69	1.74	1.03	4.82	8.49	7.23	1.96
40	137.6	62.3	-23.5	-9.7	-22.3	-9.5	174.0	83.5	4.42	1.88	3.36	1.05	1.85	3.12	6.62	4.24
50	137.0	84.8	-18.5	-9.5	-21.4	-13.6	166.5	102.8	5.12	2.95	5.65	4.87	2.91	2.45	9.78	4.80
60	138.3	89.1	14.9	23.2	-14.6	-25.5	121.3	132.3	74.52	67.70	97.82	89.20	25.39	39.28	56.77	47.91
70	120.0	108.9	-12.6	87.2	-7.0	-29.4	47.6	121.5	4.81	5.68	32.54	35.52	5.41	6.39	26.79	41.68
80	136.3	130.6	-15.7	-4.3	-31.4	-5.2	101.0	259.5	4.98	2.44	8.32	6.71	3.40	2.62	17.99	12.41
90	136.3	137.9	-21.5	-16.5	-14.1	-21.7	167.8	175.9	4.60	1.23	4.76	2.77	1.35	1.98	10.62	6.63
100	134.3	156.3	-23.4	-19.0	-12.0	-25.4	163.8	193.3	4.47	1.59	2.82	2.48	1.82	1.30	10.45	5.12
110	125.2	169.3	-23.3	-23.4	-10.0	-25.8	168.1	208.1	4.39	1.19	2.85	2.47	1.28	1.38	6.75	2.58
120	133.4	186.9	-23.7	-26.6	-11.3	-27.9	159.5	223.3	21.18	16.26	33.08	19.72	27.18	18.40	43.24	25.37
130	109.1	214.2	-8.7	-35.5	17.9	-44.9	134.7	251.9	77.41	138.90	158.21	211.45	84.55	144.49	174.52	222.98
140	127.9	210.9	-25.5	-30.6	-5.5	-30.4	145.0	259.7	6.14	3.42	9.25	8.14	4.89	4.65	12.96	7.77
150	129.7	222.3	-24.1	-28.5	-6.3	-32.3	136.3	265.0	2.48	3.69	2.15	3.43	3.08	2.51	5.45	4.60
160	119.6	236.6	-20.7	-35.5	8.2	-29.1	159.7	352.4	5.76	2.82	2.55	2.68	1.48	3.19	7.04	4.21
170	129.2	265.6	-24.8	-33.9	6.7	-40.3	148.4	316.4	6.29	6.56	2.86	4.48	1.71	2.97	6.25	3.41
180	52.7	269.7	-23.4	-61.3	23.2	-50.4	147.2	337.1	686.33	588.97	308.89	343.09	22.83	100.38	62.38	37.64
190	111.2	282.9	-28.2	-32.1	11.0	-42.5	147.7	346.9	5.25	3.09	3.43	5.06	1.60	2.14	4.96	2.64
200	121.3	286.3	-30.4	-26.5	7.0	-45.1	134.3	353.7	4.22	5.07	5.40	2.80	5.25	5.47	10.50	6.75
210	104.2	315.4	-32.1	-30.4	9.7	-48.9	133.0	355.9	4.72	4.49	3.32	2.16	3.46	3.45	4.35	2.62
220	95.5	331.8	-27.0	-18.5	2.3	-57.8	46.5	344.0	5.70	4.04	1.15	2.85	3.31	3.44	6.15	2.05
230	119.2	347.0	-28.8	-33.1	34.8	-45.5	139.4	475.4	3.98	4.11	2.03	4.28	4.38	3.61	4.95	6.87
240	101.8	357.5	-25.3	-28.2	29.6	-51.8	125.8	440.0	9.22	5.68	6.45	4.74	7.92	2.79	7.96	4.60
250	93.3	381.8	-25.9	-16.9	26.3	-57.4	95.6	445.6	9.84	6.41	6.27	4.79	7.91	4.08	13.70	7.77
260	170.9	429.4	12.8	6.7	92.4	-19.5	169.1	459.0	493.85	359.78	366.59	222.90	527.94	265.16	375.45	183.42
270	108.9	378.0	-35.5	16.0	-18.7	-63.0	-89.4	520.5	86.02	135.98	166.41	135.09	94.58	118.91	182.30	104.00
280	128.1	390.0	1.1	-25.1	59.1	-49.4	146.6	597.6	9.57	9.79	8.77	9.39	6.86	6.94	11.82	14.50
290	101.1	434.1	-16.5	-47.8	99.1	-15.7	99.0	655.9	27.67	12.13	33.23	34.57	11.28	13.81	34.79	44.15
300	1836.6	-2178.5	3203.5	-1395.3	71.6	113.3	-133.5	801.3	6184.10	5591.23	13448.03	5016.64	196.45	412.10	540.55	561.56
310	158.1	463.5	7.9	5.0	74.4	-78.5	94.7	531.7	13.11	8.51	12.96	21.15	4.63	10.22	24.25	10.61
320	189.7	472.4	18.2	46.0	118.5	-48.7	237.7	664.6	12.61	12.48	13.33	18.62	13.57	6.27	27.99	16.71

Table 52 LOP Experimental Dynamic Stiffnesses at 13000 RPM and 3103 kPa

	Dynamic stiffness								Uncertainty							
f(Hz)	$Re(H_{xx})$	$Im(H_{xx})$	$Re(H_{xy})$	$Im(H_{xy})$	$Re(H_{yx})$	$Im(H_{yx})$	$Re(H_{yy})$	$Im(H_{yy})$	$Re(U_{xx})$	$Im(U_{xx})$	$Re(U_{xy})$	$Im(U_{xy})$	$Re(U_{yx})$	$Im(U_{yx})$	$Re(U_{yy})$	$Im(U_{yy})$
20	405.1	42.2	-44.8	-3.1	-49.7	-6.3	872.4	62.2	18.37	7.87	12.81	29.15	26.84	20.63	13.04	39.44
30	404.2	62.6	-43.3	-8.8	-57.3	-21.8	895.8	78.4	14.46	16.94	15.82	15.34	14.71	15.34	23.10	20.22
40	419.9	73.7	-41.9	-9.4	-42.7	-7.6	886.9	85.6	11.28	7.82	15.57	17.65	9.58	11.11	31.64	29.60
50	412.1	87.4	-40.8	-9.8	-41.7	-35.7	863.1	122.6	10.19	7.80	18.68	13.56	7.49	8.05	15.85	17.37
60	408.4	109.2	75.2	-43.5	-62.9	-22.1	1046.9	100.3	154.77	169.20	378.66	510.40	278.86	292.45	671.62	960.37
70	420.9	119.3	-37.7	-24.2	-32.0	-46.7	844.5	161.0	10.37	4.68	14.96	37.27	9.00	7.41	37.25	49.88
80	413.7	141.8	-37.4	-7.3	-35.0	-53.1	784.4	187.5	8.33	4.37	32.56	23.54	7.98	4.98	27.54	18.44
90	418.6	158.9	-40.2	-7.7	-30.7	-55.7	864.8	193.6	7.73	5.80	15.48	18.19	8.44	4.17	14.54	22.58
100	412.1	174.0	-40.6	-16.8	-31.9	-59.4	844.7	234.0	6.55	4.15	13.04	14.17	7.01	5.67	14.43	21.51
110	415.9	187.6	-39.2	-20.7	-19.2	-67.2	835.6	236.9	7.80	6.78	23.99	25.51	7.71	3.47	17.89	19.90
120	406.6	209.4	-38.4	-30.1	-32.0	-70.1	836.3	236.7	32.20	29.90	98.27	91.15	70.61	41.46	183.15	183.88
130	407.2	226.4	-36.5	-17.4	-21.8	-67.3	809.0	313.6	7.00	5.41	15.78	12.37	6.45	5.12	25.45	12.27
140	404.8	246.6	-32.4	-16.0	-14.6	-64.9	800.1	311.6	8.51	5.76	14.76	17.74	6.22	6.09	10.60	16.41
150	401.7	264.4	-33.6	-18.7	-18.7	-64.8	792.4	306.9	5.45	5.14	10.39	14.28	4.82	7.01	13.16	12.01
160	405.2	275.5	-43.9	-68.4	-0.1	-87.0	1060.4	693.5	8.57	6.61	18.55	21.31	7.63	9.45	35.67	31.27
170	392.8	289.5	-37.9	-12.3	-21.1	-86.7	794.1	355.0	11.40	9.48	16.57	17.31	8.75	6.70	22.21	20.93
180	300.2	249.8	10.8	-3.5	-6.1	-111.0	797.1	348.5	490.50	458.31	305.16	240.39	72.27	44.82	97.74	120.56
190	390.7	317.3	-31.1	2.3	-3.4	-75.8	744.4	391.6	9.13	8.59	16.25	15.32	6.79	11.31	21.81	26.08
200	376.9	333.2	-23.3	23.6	-6.4	-65.2	693.3	417.9	16.59	13.11	24.91	44.45	13.36	18.23	62.81	36.65
210	363.9	334.7	-71.6	209.1	6.0	-89.9	402.0	448.2	32.43	38.28	128.20	226.39	50.35	55.58	363.61	117.09
220	381.7	358.2	-155.5	366.6	31.7	-68.4	146.7	380.6	50.96	69.58	194.22	259.71	77.90	88.92	402.49	177.42
230	373.0	372.6	-6.0	46.4	29.2	-64.3	489.4	607.6	14.23	10.77	20.88	53.21	17.79	14.33	83.96	32.92
240	368.4	386.9	-23.0	32.2	24.7	-78.3	698.1	500.9	5.51	7.47	21.38	37.47	13.83	10.42	47.39	21.66
250	363.9	396.6	-12.8	24.1	32.1	-84.7	710.9	528.3	6.07	9.77	17.16	11.58	7.04	8.68	20.11	19.76
260	363.4	409.0	-11.3	22.4	30.4	-65.0	696.4	480.7	8.28	7.08	12.31	8.12	6.04	6.59	9.27	13.57
270	368.5	427.0	13.6	27.0	29.9	-55.0	654.3	510.9	6.11	5.13	9.88	12.12	4.86	4.57	18.96	8.46
280	373.2	421.2	49.0	26.7	28.3	-46.9	348.4	510.4	10.99	8.46	8.60	10.00	5.71	5.16	11.71	10.09
290	360.4	447.4	-5.7	12.4	59.6	-51.6	737.9	475.2	27.63	11.75	32.90	34.51	5.54	11.24	35.54	44.86
300	2092.6	-2166.4	3224.9	-1345.7	46.5	134.2	470.5	683.1	6184.01	5590.95	13447.89	5016.01	192.34	410.74	534.36	560.18
310	393.3	460.4	41.2	52.2	73.3	-29.4	570.3	510.5	12.30	9.33	12.94	20.55	3.89	6.88	19.16	14.13
320	386.5	464.5	11.4	69.2	74.7	-16.4	701.3	600.9	12.17	9.99	8.98	10.52	3.83	3.72	14.20	10.16

VITA

Name: Clint Ryan Carter

Address: 1750 E League City Pkwy Apt 725, League City TX 77573

Email Address: carter989@aol.com

Education: B.S. Mechanical Engineering, Texas A&M University, College Station, 2002

M.S. Mechanical Engineering, Texas A&M University, College Station, 2007